UNIVERSITY OF GHANA

COLLEGE OF BASIC AND APPLIED SCIENCE

PALYNOLOGY, PALYNOFACIES AND ORGANIC GEOCHEMICAL ANALYSES OF CRETACEOUS AND EARLY PALEOGENE SEDIMENTS, OFFSHORE TANO BASIN, WESTERN GHANA

BY

CHRISTOPHER ALIRAH ACHAEGAKWO

(10193563)

THIS THESIS IS SUBMITTED TO THE UNIVERSITY OF GHANA IN PARTIAL FULFILMENT OF THE REQUIREMENT FOR THE AWARD OF DEGREE OF DOCTOR OF PHILOSOPHY IN EARTH SCIENCE

EARTH SCIENCE DEPARTMENT

SEPTEMBER, 2021.

DECLARATION

This is to certify that this thesis is the result of research carried out by Christopher A. Achaegakwo towards the award of Doctor of Philosophy Degree in Earth Science from the Department of Earth Science, University of Ghana, under the supervision of Prof. David Atta-Peters, Prof. Daniel K. Asiedu and Prof. Chris Y. Anani.

Signature: .... Date....01/01/2023..................

Christopher A. Achaegakwo (10193563)

(Student)

Signature: .... Date....05/01/2023..................

Prof. David Atta-Peters

(Principal Supervisor)

Signature: .... Date....05/01/2023..................

Prof. Daniel K. Asiedu

(Co-Supervisor)

Signature: .... Date.....05/01/2023..................

Prof. Chris Y. Anani

(Co-Supervisor)

ABSTRACT

Palynological analysis from two exploratory and one appraisal wells (Lynx-1X, Dzata-1 and Dzata-2A) and organic geochemical results from two wells (Dzata-1 and Dzata-2A) samples were obtained from the Middle Cretaceous-Early Tertiary of the Deepwater Cape Three Points offshore Tano Basin, Western Ghana. From the rich and well preserved palynomorphs recovered, the First Appearance Datum (FAD) and Last Appearance Datum (LAD) of stratigraphically significant species were used to propose four palynozones (PZ-I to PZ-IV) for the samples. Lynx-1X is Albian-Eocene, Dzata-1 and Dzata-2A wells are dated Albian-Maastrichtian, based on evidence of stratigraphically significant sporomorphs and dinocysts.

The sporomorph associations recovered from the three wells exhibit similarity to Cretaceous Phytogeographic Provinces of African-South America (ASA). Sporomorphs recorded are characteristic of Albian-Cenomanian Elaterate Province for the deeper intervals and of the Senonian Palmae Province for the shallower intervals in all the wells. The Late Cretaceous peridineacean assemblage has a lot of similarity with those of Malloy or Tropical/Subtropical suite of Lentin and Williams (1980).

Distribution of palynomorphs enabled the identification of two major sedimentary facies: the nearshore and open marine facies. The nearshore facies, concentrated at deeper intervals, are characterized by abundant sporomorphs and peridinoid dinocysts while the open marine facies are dominated by gonyaulacoid dinocysts and are restricted to the shallower intervals. This occurred as a result of marine transgression which flooded the area causing marine sedimentation.

Palynofacies analysis carried out under transmitted microscopy defined seven palynofacies associations (PF-1 to PF-7) for Lynx-1X, five palynofacies associations (PT-1 to PT-5) for Dzata-1 and six palynofacies associations (PT-A to PT-F) for Dzata-2A wells.

The first palynofacies assemblage in Lynx-1X well, PF-1, reflects deposition in a fluvio-deltaic/nearshore environment under a marginal dysoxic-anoxic basin condition with sediments typical of kerogen type III-IV (gas prone). PF-2 is deposited under a proximal suboxic-anoxic shelf conditions in a marginal marine/nearshore environment and sediments classified as kerogen type II/III (gas prone). PF-3 suggests deposition in a marginal marine to shallow marine environment under distal suboxic-anoxic conditions suggesting kerogen type II>I (highly oil prone). PF-4 is inferred to be deposited under a distal suboxic-anoxic basin condition in a shallow marine environment and sediments characterized by kerogen type II>I (highly oil prone). PF-5 indicates a deposition under a distal dysoxic-oxic shelf conditions in middle-outer neritic environment depicting kerogen type II>I (oil prone). PF-6 suggests a deposition in a shelf to basin transition condition in the inner-middle neritic environments indicating kerogen type III and II (oil prone). PF-7 reflects an outer neritic environment under distal mud-dominated oxic shelf conditions and characterized by kerogen type II/III (gas prone).

In Dzata-1 well, PT-1 suggests deposition in a nearshore environment under proximal suboxic-anoxic conditions with sediments typical of kerogen type II and III (oil prone). PT-2 indicates deposition in a dysoxic-suboxic conditions in a nearshore environment typifying kerogen type III (gas prone). PT-3 suggests deposition in a marginal dysoxic-anoxic basin condition in a fluvio-deltaic/nearshore environment typical of kerogen type III (gas prone). PF-4 represents inner-middle neritic to outer neritic environment deposited in distal dysoxic-oxic shelf conditions typifying kerogen type II>I (oil prone). PT-5 represents deposition in a nearshore environment under marginal dysoxic-anoxic basin conditions which is characterized by kerogen type III (gas prone).

PT-A of Dzata-2A well indicates deposition in a nearshore to shallow marine (inner neritic) environment under a proximal suboxic-anoxic shelf condition with typical type II/III kerogen (oil prone). PT-B infers an inner neritic/nearshore depositional environment under dysoxic-suboxic conditions with facies characterized by kerogen type III or II (gas prone). PT-C is deposited under a distal dysoxic-oxic shelf conditions in environments ranging from nearshore/inner neritic to middle-outer neritic characteristic of kerogen type II>I (oil prone). PT-D indicates a nearshore/inner neritic depositional environment under marginal dysoxic anoxic basin conditions and facies constituted by kerogen type III (gas prone). PT-E suggests deposition in inner-outer neritic environment under distal suboxic-anoxic basin condition characteristic of kerogen type II≥I (highly oil prone). PT-F suggests a deposition in a nearshore/shallow marine environment under a distal dysoxic-anoxic shelf environment with facies characterized by kerogen type II/III (oil prone).

Rock-Eval pyrolysis and TOC results for Lynx-1X and Dzata-2A wells indicates that most of the analyzed samples are thermally immature to marginally mature and have a good petroleum potential with the ?Turonian-Santonian age samples as a better potential source rocks than the Campanian-Eocene and Albian-Cenomanian source samples. Analyzed samples generally have low kerogen conversion.

DEDICATION

This work is dedicated to the Almighty God, my parents, siblings and all my friends.

ACKNOWLEDGEMENTS

I give thanks to the Almighty God for seeing me through this work. This thesis has been completed at the Department of Earth Science, University of Ghana, under the supervision of Prof. David Atta-Peters, Prof. Daniel K. Asiedu and Prof. Chris Y. Anani whose guidance and help are greatly appreciated. I am indebted particularly to Prof. David Atta-Peters who agreed to provide principal supervision of this work with his useful suggestions and continuous follow-up are a real push to this work. I am extremely grateful to my co-supervisors Prof. Daniel K. Asiedu and Prof. Chris Y. Anani for their close supervision and encouragement during the write up. Laboratory analysis of the palynological samples were undertaken at the Geolab, Faculty of Geoscience, Utrecht University, The Netherlands; the support of the staff at the Department of Earth Science, Utrecht University are deeply appreciated. I would also like to extend my gratitude to Prof. Bas van de Schootbrugge who supervised my work with valuable suggestions at the Department of Earth Science, Utrecht University. Special thanks to Prof. Patrick Asamoah Sakyi, Prof. Sandow Mark Yidana and Prof. Thomas MBA Akabzaa. I would like also to express my appreciation to all my friends and colleagues for their unlimited support at various occasions. The scholarship provided by the Ghana Education Trust Fund (GETFUND) is greatly acknowledged and made this work possible. Special thanks and gratitude to all the staff at the Department of Earth science, University of Ghana; Department of Earth Science, Utrecht University, The Netherlands; British Geological Survey (BGS), Keyworth, Nottingham, UK who contributed to the success of this work. I am deeply grateful to all staff of the Petroleum Commission of Ghana and Ghana National Petroleum Corporation (GNPC) for working together to provide me with the data for this successful work. Finally, this work would not be possible without the support and patience of my family and friends to whom I am particularly grateful.

TABLE OF CONTENT

DECLARATION ... i

ABSTRACT ... ii

DEDICATION ... v

ACKNOWLEDGEMENTS ... vi

LIST OF FIGURES ... xiv

LIST OF TABLES ... xx

CHAPTER ONE ... 1

INTRODUCTION ... 1

1.1 BACKGROUND ... 1

1.2 PROBLEM STATEMENT AND JUSTIFICATION ... 2

1.3 AIMS AND OBJECTIVES OF STUDY ... 3

1.3.1 General overview of the geology of Ghana ... 4

1.3.1.1 The Western units ... 4

1.3.1.2 The Pan-African Dahomeyide Belt ... 6

1.3.1.3 The Voltaian ... 7

1.3.1.4 The Coastal Sediments ... 9

1.4 STUDY AREA ... 10

1.5 GEOLOGY AND TECTONICS OF THE TANO BASIN ... 10

1.6 STRATIGRAPHY OF THE TANO BASIN ... 14

1.6.1 Lower Cretaceous Section ... 14

1.6.1.1 Lower Albian (Kobnaswaso Formation) 14

1.6.1.2 B-Shale (Bonyere Formation).. 15

1.6.1.3 Middle to Upper Albian 15

1.6.2 The Upper Cretaceous Section 16

1.6.2.1 Cenomanian Limestone 16

1.6.2.2 Turonian to Upper Santonian.. 16

1.6.2.3 Campanian 17

1.6.2.4 Maastrichtian... 17

1.6.3 The Tertiary Section 18

1.6.3.1 Paleocene, Eocene, Oligocene and Miocene 18

1.7 PETROLEUM EXPLORATION AND EXPLOITATION HISTORY IN THE TANO BASIN.. 18

CHAPTER TWO 22

LITERATURE REVIEW 22

2.1 PREVIOUS PALYNOLOGICAL WORK IN THE STUDY AREA. 22

2.2 PREVIOUS SOURCE ROCK EVALUATION AND HYDROCARBON POTENTIAL OF THE TANO BASIN. 26

CHAPTER THREE 28

MATERIALS AND METHODS.. 28

3.1 MATERIALS 28

3.1.1 The Lynx-1X well 28

3.1.1.1 Lithology of Lynx-1X. 28

3.1.2 Dzata-1 well......33

3.1.2.1 Lithology of Dzata-1......33

3.1.3 The Dzata-2A well......35

3.1.3.1 Lithology of Dzata-2A......35

3.2 METHODS......37

3.2.1 Sample preparation and palynological analysis......37

3.2.2 Sample Processing Techniques......38

3.2.2.1 Sample Crushing and Drying......38

3.2.2.2 Pre-Hydrofluoric Acid (HF) Treatment......38

3.2.2.3 (38-40%) Hydrofluoric acid (HF) treatment......39

3.2.2.4 Sieving, Ultrasonification and Centrifuging......40

3.2.2.5 Oxidation......40

3.2.2.6 Mounting......40

3.2.3 Microscopic Study and Photomicrography......41

3.2.4 Repository......42

3.2.5 Palynofacies and Palaeoenvironmental Analysis......42

3.2.6 Geochemical Analysis......43

CHAPTER FOUR......44

PALYNOSTRATIGRAPHY......44

4.1 INTRODUCTION......44

4.2 PALYNOZONATION (PZ) AND AGE ASSIGNMENT......45

4.2.1 Palynozone I (PZ-I): *Afropollis jardinus-Sofrepites legouxae-Elaterocolpites castelaini* Assemblage Zone 45

4.2.2 Palynozone II (PZ-II): *Cretaceaeiporites polygonalis-C. scabratus-Dinogymnium accuminatum* Assemblage Zone 56

4.2.3 Palynozone III (PZ-III): *Trichodinium castanea-Cerodinium diebelli-Dinogymnium acuminatum* Assemblage Zone 63

4.2.4 Palynozone IV (PZ-IV): *Cerodinium diebelli-Apectodinium homomorphum-Homotryblium tenuispinosum* Assemblage Zone 74

4.3 PALEOECOLOGY AND PALEOPROVINCES 81

4.3.1 Palaeoecological and paleoclimatic implications from sporomorphs 81

4.3.1.1 Paleofloral Provinces 83

4.3.1.1.1 The Pre-Albian Early Cretaceous Dicheiropollis etruscus/Afropollis Province.. 83

4.3.1.1.2 Albian-Cenomanian Elaterate Province 84

4.3.1.1.3 The Senonian Palmae Province.. 85

4.3.2 Paleoecological and paleoclimatic implications from dinoflagellates 85

4.3.2.2 Dinoflagellates Provincialism.. 94

CHAPTER FIVE 126

PALYNOFACIES ANALYSIS AND PALAEOENVIRONMENTAL INTERPRETATIONS 126

5.1 INTRODUCTION.. 126

5.1.1 Classification of Palynofacies Constituents 128

5.1.2 Structureless organic matter 132

5.1.3 Structured organic matter 135

5.1.3.1 Phytoclasts (Translucent and Opaques (black debris)):................................135

5.1.3.2 Palynomorphs 137

5.1.3.2.1. Marine palynomorphs: This includes dinoflagellate cysts, acritarchs and prasinophytes..137

5.1.3.2.2. Freshwater microplankton...139

5.1.3.2.3. Zoomorph 139

5.1.3.2.4. Sporomorph (Terrestrial Palynomorphs): 140

5.2 PALYNOFACIES ASSOCIATIONS AND PALAEOENVIRONMENTAL INTERPRETATIONS..142

5.2.1 Lynx-1X well...147

5.2.1.1 Palynofacies type 1 (PF-1) (Opaque phytoclasts) dominant with moderate AOM)...147

5.2.1.2 Palynofacies type 2 (PF-2) (Equal abundance of AOM and Opaque phytoclasts). 150

5.2.1.3 Palynofacies type 3 (PF-3) (AOM dominant with high opaques) 154

5.2.1.4 Palynofacies type 4 (PF-4) (AOM dominant with relatively equal abundance of opaques and phytoclasts...157

5.2.1.5 Palynofacies type 5 (PF-5) (AOM dominant with palynomorphs)................159

5.2.1.6 Palynofacies type 6 (PF-6) (AOM, phytoclasts and palynomorphs abundant). 164

5.2.1.7 Palynofacies type 7 (PF-7) (Palynomorphs with equal abundance of AOM and opaques). 167

5.2.2 Dzata-1 well 173

5.2.2.1 Palynofacies type 1 (PT-1) (AOM dominant with abundant Opaque phytoclasts) 173

5.2.2.2 Palynofacies type 2 (PT-2) (Relatively equal abundance of opaques phytoclasts and phytoclasts (non-opaques) with AOM and palynomorphs). 177

5.2.2.3 Palynofacies type 3 (PT-3) (Opaques dominant) 180

5.2.2.4 Palynofacies type 4 (PT-4) (AOM dominant with palynomorphs). 183

5.2.2.5 Palynofacies type 5 (PT-5) (Abundant opaque phytoclasts and AOM). 187

5.2.3 Dzata-2A 192

5.2.3.1 Palynofacies type 1 (PT-A) (AOM dominant with abundant opaque phytoclasts). 192

5.2.3.2 Palynofacies type 2 (PT-B) (Abundant AOM with relatively equal abundance of phytoclasts and palynomorphs) 196

5.2.3.3 Palynofacies type 3 (PT-C) (AOM dominant with high palynomorphs) 199

5.2.3.4 Palynofacies type 4 (PT-D) (Abundance of AOM and opaque phytoclasts with high translucent phytoclasts) 203

5.2.3.5 Palynofacies type 5 (PT-E) (AOM dominant) 206

5.2.3.6 Palynofacies type 6 (PT-F) (AOM dominant with relatively equal abundance of translucent phytoclasts and palynomorphs). 209

CHAPTER SIX 214

SOURCE ROCK EVALUATION 214

6.1 INTRODUCTION....214

6.2 METHODOLOGY....215

6.3 EVALUATION OF LYNX-1X AND DZATA-2A WELLS....218

6.3.1 Organic Carbon richness and Hydrocarbon Potential....218

6.3.2 Kerogen Types....224

6.3.3 Organic Matter Maturity....227

6.3.4 Expulsion Potential....232

CHAPTER SEVEN....234

CONCLUSION....234

RECOMMENDATION....240

REFERENCES....241

APPENDICES....296

LIST OF FIGURES

Figure 1.1. Simplified geological map of Ghana. 6

Figure 1.2: Map of the Dahomeyide orogen in southeastern Ghana and adjoining part of Togo. 8

Figure 1.3. Geological map of the Dahomeyide belt showing the Voltaian Supergroup. 9

Figure 1.4: Map of Study area showing studied wells Offshore Tano Basin (Lynx-1, Dzata-1 and Dzata-2A). 10

Figure.1.5 Tano Basin within the St. Paul and Romanche transform fault zones. 12

Figure 1.6. The General Stratigraphy of the Tano Basin. 19

Figure 3.1: Lithology of Lynx-1X, Dzata-1 and Dzata-2A wells. 37

Figure 4.1: Age, palynozone, lithological column and stratigraphical significant taxa from Lynx-1X well. 60

Figure 4.2: Age, palynozone, lithological column and stratigraphical significant taxa from Dzata-1 well. 61

Figure 4.3: Age, palynozone, lithological column and stratigraphical significant taxa from Dzata-2A well. 62

Figure 4.4: Relative percentage composition distribution chart of dinocysts (marine palynomorphs) with spores and pollen (terrestrial palynomorphs) in Palynozone III and IV from Lynx-1X well. 71

Figure 4.5: Relative percentage composition distribution chart of dinocysts (marine palynomorphs) with spores and pollen (terrestrial palynomorphs) of Palynozone III from Dzata-1 well. 72

Figure 4.6: Relative percentage composition distribution chart of dinocysts (marine palynomorphs) and spores and pollen (terrestrial palynomorphs) of Palynozone III from Dzata-2A well. 73

Figure 4.7: Relative percentage composition of Gonyaulacoids and Peridinoids abundance in palynozone III of Lynx-1X well. 89

Figure 4.8: Relative percentage composition of Gonyaulacoids and Peridinoids abundance in palynozone III of Dzata-1 well. 90

Figure 4.9: Relative percentage composition of Gonyaulacoids and Peridinoids abundance in palynozone III of Dzata-2A well. 91

Figure 4.10: Relative percentage composition of Gonyaulacoids and Peridinoids abundance in palynozone IV of Lynx-1X well. 92

Figure 4.11: Correlation of lithology, palynozones and depositional environments of Lynx-1X, Dzata-2A and Dzata-1 wells……………………………………………………93

Figure 5.1: AOM-Palynomorphs-Phytoclasts (APP) ternary plot showing environment of deposition and kerogen types. 145

Figure 5.2: Representative photograph of palynofacies association and pie chart of PF-1 from Lynx-1X well. 149

Figure 5.3: APP Ternary diagram for PF-1 samples from Lynx-1X well. 150

Figure 5.4: Representative photograph of palynofacies association and pie chart of PF-2 from Lynx-1X well. 152

Figure 5.5: APP Ternary diagram of studied samples from the Lynx-1X well 153

Figure 5.6: MSP Ternary plot for PF-2 samples from Lynx-1X well. 153

Figure 5.7: Representative photograph of palynofacies association and pie chart of PF-3 from Lynx-1X well. 155

Figure 5.8: APP Ternary diagram for PF-3 samples from Lynx-1X well. 156

Figure 5.9. MSP Ternary plot of studied samples from the Lynx-1X well. 156

Figure 5.10: Representative photograph of palynofacies association and pie chart of PF-4 from Lynx-1X well. 158

Figure 5.11. APP Ternary diagram for PF-4 samples from Lynx-1X well. 159

Figure 5.12: Representative photograph of palynofacies association and pie chart of PF-5 from Lynx-1X well. 162

Figure 5.13: APP Ternary diagram for PF-5 from Lynx-1X well. 163

Figure 5.14: MSP Ternary plot for PF-5 samples from Lynx-1X well. 163

Figure 5.15: Representative photograph of palynofacies association and pie chart of PF-6 from Lynx-1X well. 166

Figure 5.16: APP Ternary diagram for PF-6 samples from Lynx-1X well. 167

Figure 5.17: Representative photograph of palynofacies association and pie chart of PF-7 from Lynx-1X well. 169

Figure 5.18: APP Ternary diagram for PF-7 samples from Lynx-1X well 170

Figure 5.19: MSP Ternary plot for PF-7 samples from Lynx-1X well. 170

Figure 5.20: Relative percentage composition of Gonyaulacoids and Peridinoids of Lynx-1X well. 171

Figure 5.21: Palynofacies assemblages showing POM (%) from Lynx-1X well. 172

Figure 5.22: Representative photograph of palynofacies association and pie chart of PT-1 from Dzata-1 well. 175

Figure 5.23: APP Ternary diagram for PT-1 samples from Dzata-1 well. 176

Figure 5.24: MSP Ternary plot for PT-1 samples from Dzata-1 well. 176

Figure 5.25: Representative photograph of palynofacies association and pie chart of PT-2 from Dzata-1 well. 178

Figure 5.26: APP Ternary diagram for PT-2 samples from Dzata-1 well. 179

Figure 5.27: MSP Ternary plot for PT-2 samples from Dzata-1 well. 179

Figure 5.28: Representative photograph of palynofacies association and pie chart of PT-3 from Dzata-1 well. 181

Figure 5.29: APP Ternary diagram for PT-3 samples from Dzata-1 well. 182

Figure 5.30: MSP Ternary plot for PT-3 samples from Dzata-1 well. 182

Figure 5.31: Representative photograph of palynofacies association and pie chart of PT-4 from Dzata-1 well. 185

Figure 5.32: APP Ternary diagram for PT-4 samples from Dzata-1 well. 186

Figure 5.33: MSP Ternary plot for PT-4 samples from Dzata-1 well. 186

Figure 5.34: Relative percentage composition of Gonyaulacoids and Peridinoids of Dzata-1 well. 187

Figure 5.35: Representative photograph of palynofacies association and pie chart of PT-5 from Dzata-1 well. 189

Figure 5.36: APP Ternary diagram for PT-5 samples from Dzata-1 well. 190

Figure 5.37: MSP Ternary plot for PT-5 samples from Dzata-1 well. 190

Figure 5.38: Palynofacies associations showing POM (%) from Dzata-1 well. 191

Figure 5.39: Representative photograph of palynofacies association and pie chart of PT-A from Dzata-2A well. 194

Figure 5.40: APP Ternary diagram of studied samples from the Dzata-2A well. 195

Figure 5.41: MSP Ternary plot for PT-A samples from Dzata-2A well. 195

Figure 5.42: Representative palynofacies association and pie chart of PT-B from Dzata-2A well. 197

Figure 5.43: APP Ternary diagram for PT-B samples from Dzata-2A well. 198

Figure 5.44: MSP Ternary plot for PT-B samples from Dzata-2A well. 198

Figure 5.45: Representative photograph of palynofacies association and pie chart of PT-C from Dzata-2A well 201

Figure 5.46. APP Ternary diagram for PT-C samples from Dzata-2A well. 202

Figure 5.47: MSP Ternary plot for PT-C samples from Dzata-2A well. 202

Figure 5.48: Representative photograph of palynofacies association and pie chart of PT-D from Dzata-2A well. 204

Figure 5.49. APP Ternary diagram for PT-D samples from Dzata-2A well. 205

Figure 5.50: MSP Ternary plot for PT-D samples from Dzata-2A well...............................205

Figure 5.51: Representative photograph of palynofacies association and pie chart of PT-E from Dzata-2A well. 207

Figure 5.52: APP Ternary diagram for PT-E samples from Dzata-2A well. 208

Figure 5.53: MSP Ternary plot for PT-E samples from the Dzata-2A well. 208

Figure 5.54: Representative photograph of palynofacies association and pie chart of PT-F from Dzata-2A well. 210

Figure 5.55. APP Ternary diagram for PT-F samples from Dzata-2A well. 211

Figure 5.56: MSP Ternary plot for PT-F samples from Dzata-2A well. 211

Figure 5.57: Relative percentage composition of Gonyaulacoids and Peridinoids of Dzata-2A well...212

Figure 5.58: Palynofacies associations showing POM (%) from Dzata-2A well. 213

Figure 6.1: S_2 against TOC% showing the Hydrocarbon potentiality and source efficiency 220

Figure 6.2: S_2 against TOC% plot showing types of kerogens 221

Figure 6.3: Plot of Hydrogen Index against TOC% indicating kerogen types and generation potential...223

Figure 6.4: Plot of GP (S_1+S_2) against TOC% indicating hydrocarbon potentiality for the well samples...223

Figure 6.5: Types of kerogens indicated on a modified Van Krevelen diagram 226

Figure 6.6: Types of kerogen and levels of maturity shown by Hydrogen Index against Tmax 226

Figure 6.7: Types of kerogen and levels of maturity shown by Hydrogen Index against Tmax 227

Figure 6.8: Plot of Tmax versus Production Index showing hydrocarbon generation zone. .229

Figure 6.9: Plot of Production Index versus Tmax showing levels of kerogen conversion and maturity 230

Figure 6.10: Plot of Tmax versus Vitrinite reflectance (Ro) showing maturity levels..........230

Figure 6.11: Plot of depths versus vitrinite reflectance data ($R_{calculated}$) showing thermal maturity stages of Lynx-1X and Dzata-2A wells. 231

Figure 6.12: Vitrinite reflectance ($R_{calculated}$) versus the Hydrogen Index (HI) showing variation of organic matter quality from Lynx-1X and Dzata-2A wells...232

Figure 6.13: S_1 versus TOC as an indicator of indigenous and non-indigenous hydrocarbons...233

LIST OF TABLES

Table 5.1: Classification of the sedimentary organic matter. 130

Table 5.2: Organic Matter Classification in sediments. 132

Table 5.3: Phytoclast and Amorphous Groups. 134

Table 5.4: Major subdivisions of the Palynomorph Group. 143

Table 5.5: Palynofacies defined on the triangle -APP with kerogen type and generation potential 146

Table 5.6: Percentage composition of palynofacies associations of particulate organic matter (POM) in Lynx-1X well 147

Table 5.7: Percentage composition of palynofacies associations of particulate organic matter (POM) in Dzata-1 well 173

Table 5.8: Percentage composition of palynofacies associations of particulate organic matter (POM) in Dzata-2A well 192

Table 6.1. Guidelines for interpreting source rock quantity, quality and maturation, and commonly used Rock-Eval parameters. 217

CHAPTER ONE

INTRODUCTION

1.1 BACKGROUND

Ghana, in the last ten (10), years has made significant new hydrocarbon discoveries (mostly crude oil) which have been documented offshore in the Tano Basin in western Ghana, the current most important oil-producing area in Ghana. In 2010, Ghana started production of crude oil in commercial quantities from the Jubilee oil field with proposed production of 55,000 barrels per day. In 2018, Ghana National Petroleum Corporation (GNPC) continued to manage its interests in various petroleum licenses in Ghana's sedimentary basins specifically in the Tano basin and together with its upstream partners continued the production of crude oil and gas from the three producing fields (Greater Jubilee, Tweneboa-Enyenra-Ntomme (TEN) and Sankofa-Gye-Nyame (SGN)). Cumulative crude oil production achieved from the three producing fields totalled 46,024,211 million barrels from January to September 2018, translating into an average daily oil production of 196,177 barrels (Annual report on the petroleum funds, Ministry of Finance, 2018).

The Cretaceous source rocks have proved to be the most prolific oil and gas producing horizons in the Tano basin. The future of the Ghanaian oil and gas industry within the basin needs a holistic detailed study of both shallow and deep-water oil blocks. However, sediments within the deep-water settings have not been subjected to detailed biostratigraphic study or lithostratigraphic correlation. There is therefore the need for detailed biostratigraphic and lithostratigraphic correlations study as GNPC embarks on detailed geological and geophysical study on the Tano basin and other sedimentary basins in Ghana.

1.2 PROBLEM STATEMENT AND JUSTIFICATION

In the petroleum exploration history of Ghana, seismic data acquisition, processing and interpretation by GNPC and their partners in the Tano Basin have received tremendous attention. Seismic data analysis over the last decades have made tremendous improvements which have led to the discovery of numerous giant oil reservoirs in petroleum provinces around the world. The science of petroleum exploration and production is multi-tool based with each tool complementing the other. Comprehensive palaeontological and palynofacies analyses are rarely performed during petroleum exploration and only surfaces are picked for age assignment using index fossils. Biostratigraphy (e.g. palynology) is one of the most important tools used in petroleum exploration essentially as a stratigraphic tool in depositional settings such as continental, coastal and marginal marine environments. When integrated with other tools including wireline logs and seismic stratigraphy, it is useful mainly for chronostratigraphic correlation, palaeoenvironmental studies, evaluation of source, reservoir and sealing rocks (Copestake, 1993). For true representation of the subsurface by seismic and Sequence stratigraphy, there is the need of integrating tools such as well logs, biostratigraphy and geochemistry to be able to interpret seismic sections to provide information on facies, lithologies, stratigraphic ages, palaeowater depths, palaeoclimate, and palaeoenvironment.

Subsurface informative tools and techniques such as palynology and palynofacies are utilized to subdivide and correlate subsurface sedimentary sediments and in combination with organic geochemistry data, it is used to evaluate the hydrocarbon potential of basin. Regardless of the effectiveness of palynology as an important tool in sequence stratigraphic analysis and resolution, it is still being grossly under-utilized in petroleum exploration and production in Ghana partly due to how young the industry is. This project seeks to specifically investigate the Deep-Water Cape Three Points (DWCTP) block offshore Tano basin which was acquired by ExxonMobil Exploration and Production Ghana, in January 2018.

The PhD thesis seeks to study samples from three oil/gas wells out of the four wells within the DWCTP oil block which would provide detailed biostratigraphic interpretations based on palynology, depositional environments based on palynofacies analysis and evaluate the hydrocarbon potential based on palynofacies and rock eval pyrolysis data analysis. This would provide significant contributions to fully explore the basin and form basis for further studies in the basin and other sedimentary basins of interest in Ghana.

1.3 AIMS AND OBJECTIVES OF STUDY

This research aims for the following:

1. Provide independent age control for the studied intervals by means of palynological studies.
2. Interpret paleoenvironmental and paleoclimatic conditions at the time of deposition and the probable hydrocarbon product using palynofacies analysis.
3. To evaluate the organic richness and hydrocarbon potential of source rocks.

The objectives of this project carried out were as follows:

1. Standard acid maceration palynological preparation techniques were applied to studied samples to extract palynomorphs for biostratigraphic and other investigations.
2. Identification of all stratigraphically significant recorded taxa present in each well in order to establish a biostratigraphy for each of the three well successions.
3. The paleoenvironmental settings prevailing during the deposition of the studied sections were determined through study of the palynomorphs and palynofacies analyses.
4. Source rock analyses were used to determine source rocks potential for hydrocarbon generation, in addition to the determination of the different kerogen types in order to evaluate the hydrocarbon potential and quality of source rocks.

1.3.1 General overview of the geology of Ghana.

Ghana, based on age data, tectonics and lithology, can be divided into five main geological domains (Attoh et al, 1997) (Fig. 1.1):

A. The western Units found at the eastern margin of the West African Craton (Birimian and Tarkwaian).

B. The Precambrian mobile belt units found at south-eastern part of the country (the Dahomeyide: - the Dahomeyan, the Togo and the Buem).

C. The Voltaian sediments at the central part of the country (the largest sedimentary terrain).

D. The Coastal sedimentary basins.

E. Tertiary to Recent deposits.

1.3.1.1 The Western units

The western part of Ghana is characterized by supra crustal rocks of Paleoproterozoic ages, which can be sub-divided into the Birimian and Tarkwaian. The Birimian rocks comprise an assemblage of sedimentary/volcaniclastic rocks which separate a series of subparallel, roughly equal-spaced northeast trending volcanic belts of volcanic rocks. The sedimentary/volcaniclastic rocks were considered to be the lower members of the Birimian whereas the upper members consist of the volcanic belts, mainly metamorphosed basic and intermediate lavas and pyroclastic rocks (Junner, 1935). The lower Birimian rocks comprise an assemblage of fine-grained rocks with a large volcano clastic component. Typical lithologies include tuff, calcareous shale, phyllite, siltstone, greywacke and some chemical (Mn-rich) sediment. The upper Birimian rocks comprise mostly basalts with some interflow sediment (Eisenlohr and Hirdes, 1992). However, recent studies, have shown that the volcanics and the sedimentary rocks were deposited contemporaneously as lateral facies equivalents (Leube et al., 1990). The Birimian is intruded by different generations of granitoids.

Overlying the Birimian unit in a synclinal basin is the Tarkwaian unit of rocks (e.g., Junner et al., 1942; Kesse, 1985). The Tarkwaian rocks consists mainly of coarse clastic sediments, subdivided into four major units: (i) the Kawere Group, (ii) Banket Series, (iii) Tarkwa Phyllite, and (iv) Huni Sandstone (Junner et al., 1942; Kesse 1985). The basal Kawere Group consists of the units of sandstones, and polymictic, poorly sorted, large-pebble conglomerates and argillites. The Banket Series is mainly made up of sandstones and conglomerates with minor grits, breccias and argillites. The Tarkwa Phyllite is mainly made up of finely laminated and graded argillite with interbedded green sandstone, which is conformably overlain by the Huni Sandstone. The Huni sandstone consists of fine-grained green sandstone with thin, intercalated argillite layers.

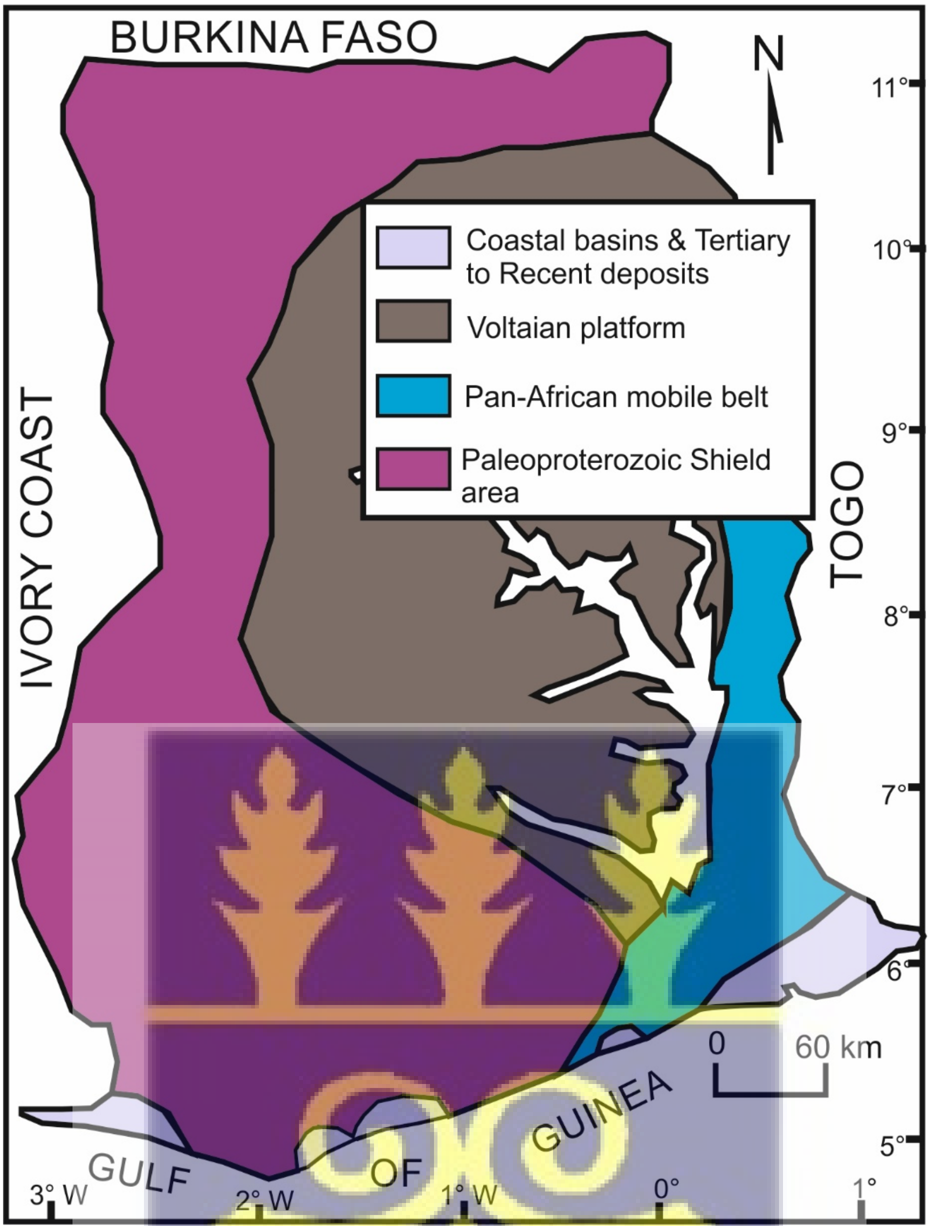

Figure 1.1. Simplified geological map of Ghana.

1.3.1.2 The Pan-African Dahomeyide Belt

The Dahomeyide orogeny of West Africa is a Pan African belt between the passive continental margin of the West African Craton (WAC) which is postulated to have resulted from the easterly subduction of the rifted margin of WAC (Affaton et al., 1991; Attoh and Nude, 2008) and the Saharan Meta Craton (SMC) and resulted in the assembly of northwest Gondwana (Hoffman, 1991). The Dahomeyide belt in Ghana is about 600Ma, exposed in the south-eastern part of the country and represents the southern extension of the Trans-Saharan mobile belt (Nude and Attoh, 2008). These rock units are also found in some parts of Benin and Togo. Its northern extension forms the Adrar des Iforas of Mali, the Gourma of Burkina Faso and Mali and the Western Hogger in Algeria which lies on the eastern margin of the West African Craton (Cordani et al., 2003, Tohen et al., 2006).

The Dahomeyide of Ghana (Fig.1.2), based on litho-tectonic unit and age can be subdivided into three structural units (Kesse, 1985). These include:

1. Buem structural units
2. Togo structural units
3. Dahomeyan structural units

Stratigraphically, the Dahomeyan forms the basement unit and is overlain by the Togo and Buem respectively. Due to thrust faulting, the Togo overlies the Buem as certain places and seen to be overlain by the Dahomeyan at some other places.

1.3.1.3 The Voltaian

The Voltaian which occupies a surface area of ~115,000 km² in Ghana as well as smaller areas in Togo, Burkina Faso, Niger and Benin consist of Neoproterozoic to early Paleozoic strata (Kalsbeek et al., 2008). The Voltaian (Fig. 1.3) is up to ~ 6 km thick succession of sandstones and mudstones with subordinate proportions of limestone (Junner and Hirdes, 1946; Bozhko, 1969; Affaton et al., 1980; Affaton, 1990). According to Leprun and Trompette, 1969; Sougy, 1971; Affaton (1975, 1990, 2008), the Voltaian is characterized by three surpergroups: (1) The Kwahu/Kintampo/Damongo/Gambaga/Bombouaka Supergroup, (2) the Oti/Afram/ Pendjari Supergroup, and (3) the Tamale Supergroup.

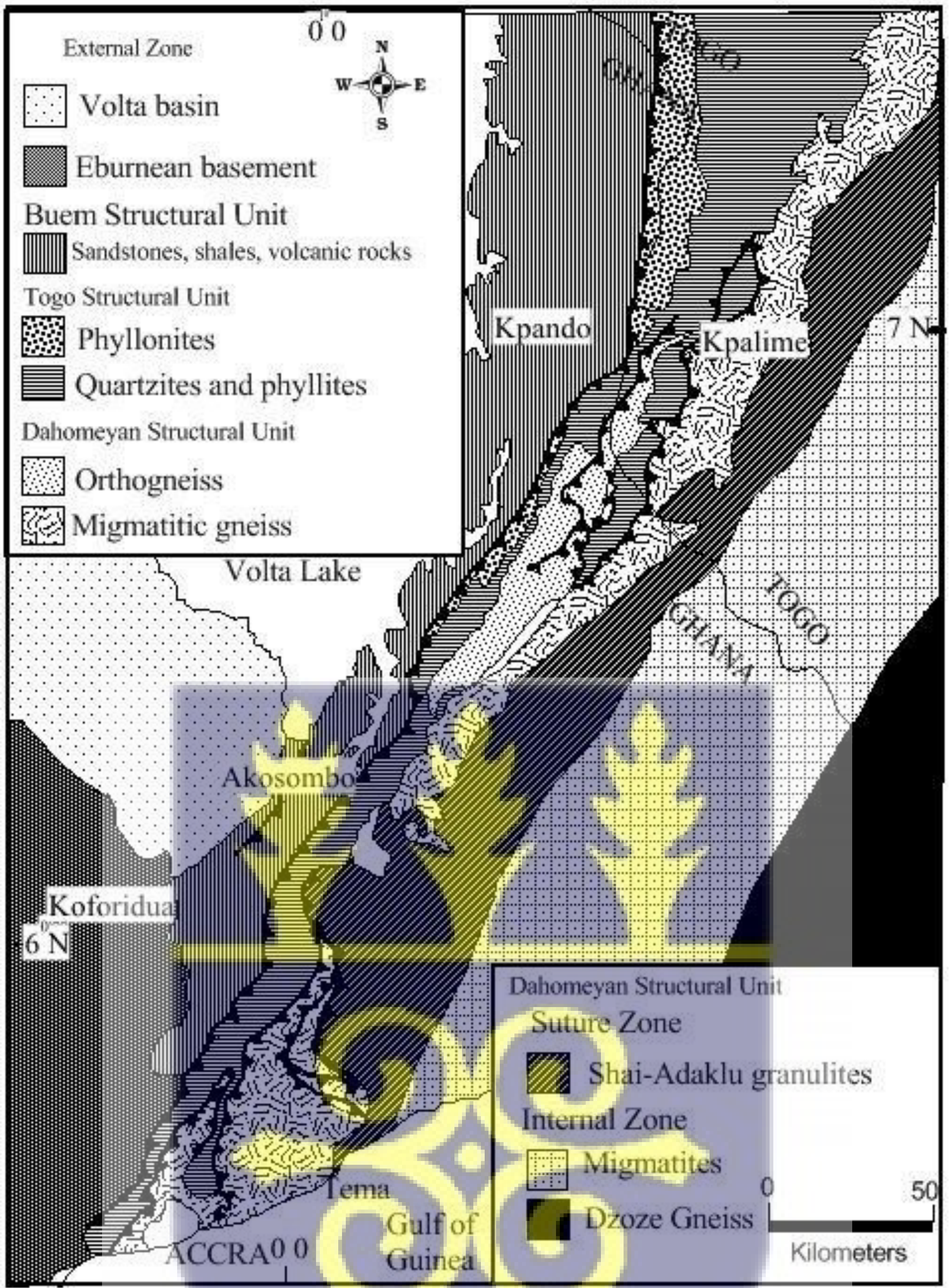

Figure 1.2: Map of the Dahomeyide orogen in southeastern Ghana and adjoining part of Togo (After Attoh, 1990).

These supergroups represent clearly different stratigraphic divisions than the lower, middle, and upper Voltaian subdivisions previously used in Ghana. Moreover, they consider the Volta basin as a composite basin, comprising a passive margin and a typical foreland basin (Geotect, 2009).

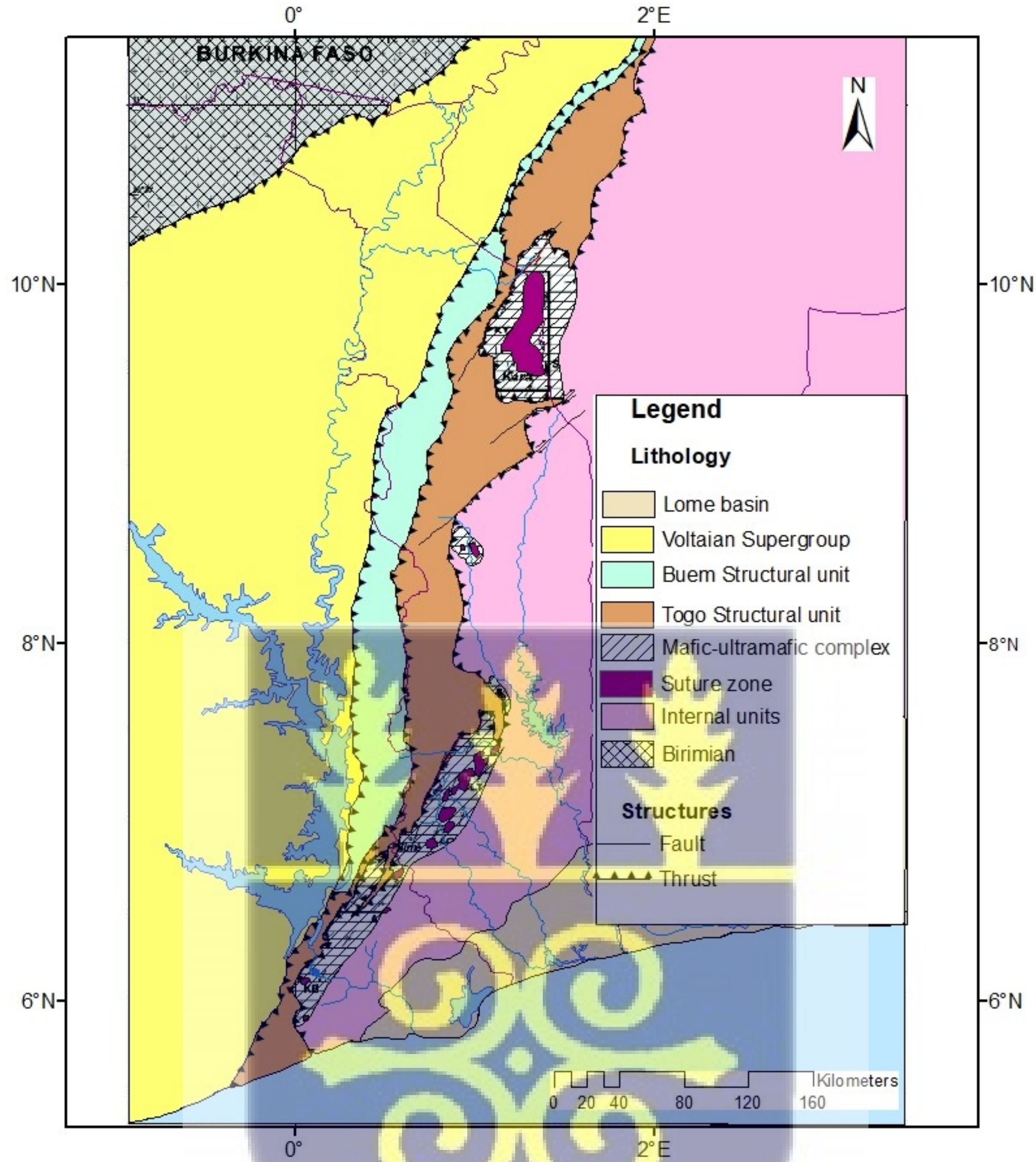

Figure 1.3. Geological map of the Dahomeyide belt showing the Voltaian Supergroup (after Duclaux et al., 2006).

1.3.1.4 The Coastal Sediments

The crustal evolution of Ghana in the Phanerozoic era was characterized by development of a series of spatially restricted shallow, mostly marine coastal basins along the present-day Ghanaian coast. Sedimentation began in the Ordovician (Sekondian Group), to the Devonian

(Accraian Group) to Upper Jurassic-Lower Cretaceous (Amissian Group) to Cretaceous (Apollonian Group) to the Tertiary and Quaternary (Kesse, 1985).

1.4 STUDY AREA

Selected cutting samples of rocks for this thesis was collected from three wells in the Deepwater Cape Three Points (DWCTP) Block offshore Tano basin, western Ghana, namely; Lynx-1X, Dzata-1 and Dzata-2A (Fig. 1.4). Samples were provided by the Core Laboratory of the Ghana National Petroleum Corporation (GNPC).

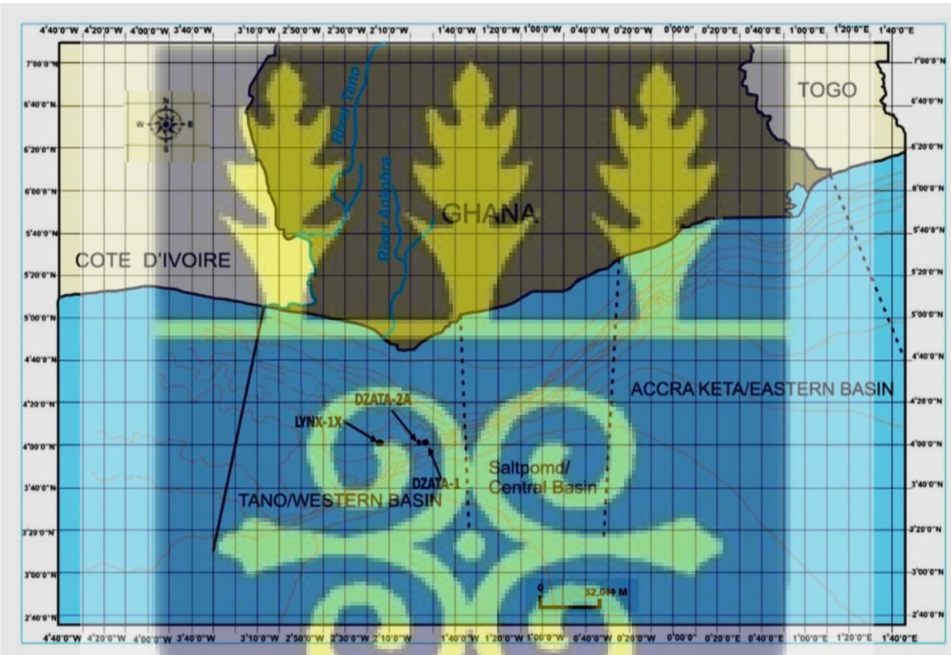

Figure 1.4: Map of Study area showing studied wells Offshore Tano Basin (Lynx-1, Dzata-1 and Dzata-2A).

1.5 GEOLOGY AND TECTONICS OF THE TANO BASIN

The Tano basin is located between the mouths of the Ankobra River in the east and the Tano River in the west (96 km). It is East-West onshore-offshore structural basin (Davies, 1986) occupying an area of about 3000 square kilometers offshore with an estimation onshore constituent to be approximately 1165 km^2 (Kesse, 1985). The Gulf of Guinea Province as defined by the U.S. Geological Survey (USGS) consists of the coastal and offshore areas of Côte d'Ivoire, Ghana, Togo, and Benin, and the western part of the coast of Nigeria, from the Liberian border east to the west edge of the Niger Delta. The province includes the Ivory Coast, Tano, Saltpond, Keta, and Benin Basins and the Dahomey Embayment. The Tano basin includes the narrow Mesozoic coastal strip of southwestern Ghana, the continental shelf, and steep submarine Ivory Coast-Ghana ridge which form the continental slope (Mah, 1987). The Tano Basin formed because of a complex series of pull apart and transforms movements which accompanied the opening of the South Atlantic Ocean due to the separation of the South American and African continents. Kesse (1985) described the Tano Basin as being a portion of the crescent shaped basin along the coast of the Atlantic Ocean. The St. Paul transform fault zone to the east and the Romanche transform fault zone to west mark the boundaries of the Tano basin (Fig. 1.5).

Rocks of the Tano Basin are part of the Apollonian System of Cretaceous age and consist mainly of limestones with alternating clays and sands (Kitson, 1928) and Junner (1940) in Cox (1952) articulated that, the limestones are fossiliferous and are inter bedded with clay and formed a continuous crest rising from the beach near the village of Kangan and run in a north-westward direction through a point one-and-a-half-mile north of Nauli and to the Tano river north of Edu. The Precambrian metasedimentary rocks of the Birimian supergroup form the basement rocks of the Apollonian rocks. These metasedimentary rocks are mostly schist, phyllite and greywacke.

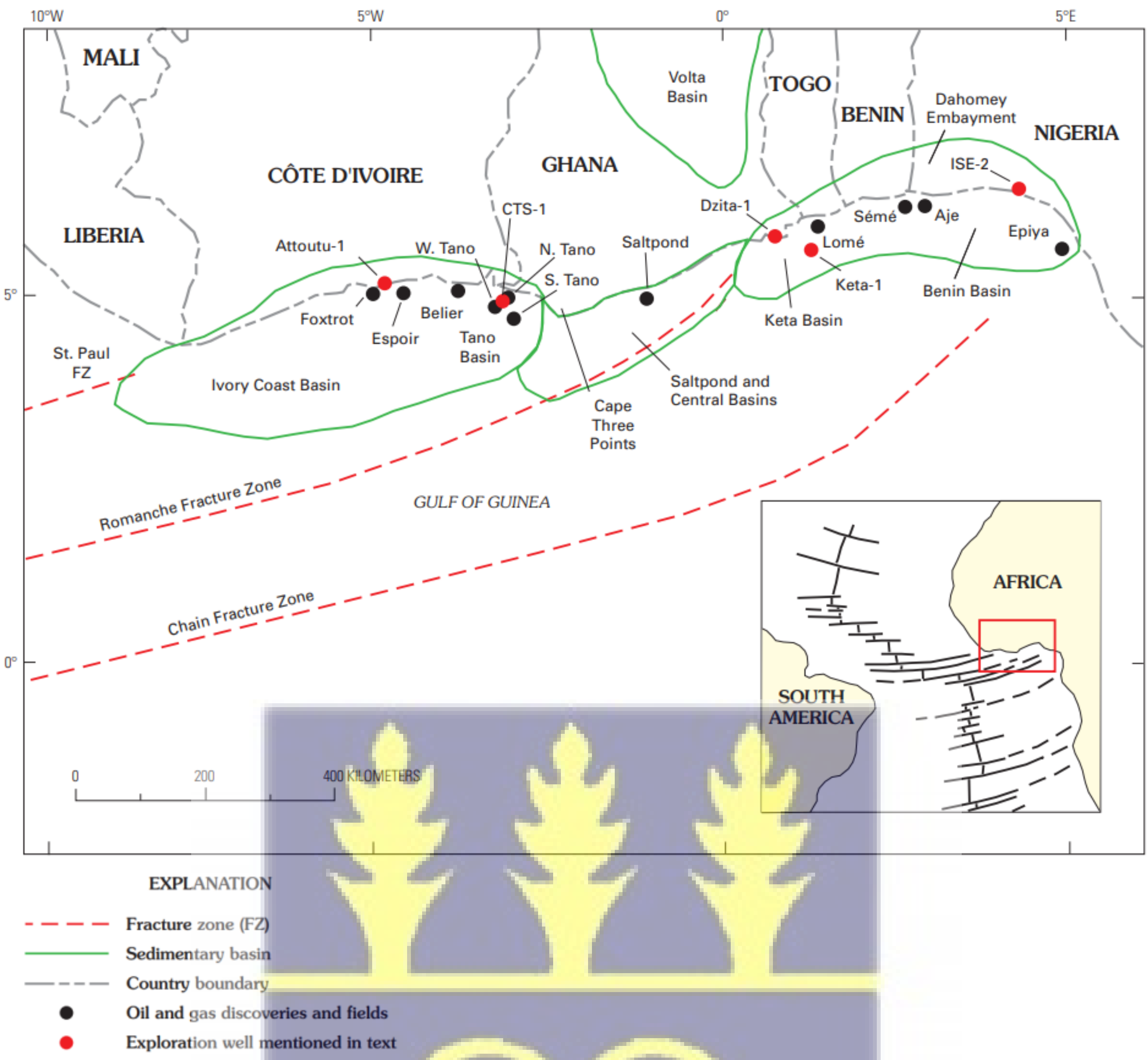

Figure.1.5 Tano Basin within the St. Paul and Romanche transform fault zones (after Brownfield and Charpentier, 2006).

The Tano Basin is underlain by Eocene and Cretaceous sediments and is the focus for deposition of a thick Upper Cretaceous, deep water clastic sequence which, in combination with a different Tertiary section, provided enough thickness to mature an early-mid Cretaceous source rock in the central part of the Tano basin. This distinct reservoir resulted in the formation of combination trapping geometries that create the Jubilee accumulations, and along which several other prospects are located. The early Albian tectonism resulted in the formation of the North Tano fault bounded by tilted structural block which are termed 'structural highs' in the Tano Sub-basin that influenced and controlled some of the sediment deposition in the basin whereas the creation of the South Tano Structural trend, faulting, uplift and erosion along the outer margin of the Tano basin resulted from the final separation of the West Africa and Northern Brazilian continental plates (Davies, 1989). The South Tano High creates focus of migration, concentrating oil generated in a large kitchen where the Jubilee fan drapes over high, on top of source rock and focuses charge up-dip.

Onshore of the Tano basin, is predominantly clays, sands and limestone with a general SSW dip direction and low dip angles. However, at depth, these sands and clays compact to form sandstones and shales. The limestones are extremely fossiliferous and are overlain by recent to Tertiary deposits of sands, clays and laterite.

As per Guiraud et al. (1997), three lithofacies creates the CIG sedimentary wedge which are yellowish siltstones, dark clays and interbedded greenish sandstone with grey coarse sandstones and micro conglomerates. Early Cretaceous age in a shallow marine deltaic environment of deposition was inferred for these synrift sediments.

The Tano Basin lies within the West African Transform Margin. Seismic surveys of the Ocean Drilling Programme (ODP) have shown that this margin has a distinctive feature of a NE-SW trending marginal ridge about 130 km long (Atta-Peters and Salami, 2004). This transform margin is associated with the (CIG) continental disintegration of the South America and Africa. The ridge within the CIG is bounded to the north by the deep Ivorian Rift Basin (Atta-Peters and Salami, 2004). Larmache et al., (1997) indicated that the ridge has a sedimentary sequence which bears a close resemblance with the syn-rift sediments of the Ivorian Basin.

The basin accumulated thick Upper Cretaceous, deepwater clastic succession in combination with a Tertiary section, gave adequate thickness to mature an early to mid-Cretaceous source rock in the focal part of the Tano Basin. This reservoir and charge fairway formed the play which, when draped over the large plunging South Tano high resulted in the formation of numerous trapping geometries that resulted in the Jubilee and Odum accumulations, and alongside different prospects (Daily et al., unpublished).

The three main tectonic phases of the Tano Basin are as follows:

- Pre-Rift represented by Precambrian to late Jurassic rocks.
- Syn-Rift phase with sediments of early Cretaceous age. The end of the syn-rift stage is delineated by a major unconformity which separates it from the marine post-transform rocks of the uppermost Albian and Cenomanian.
- Post-Rift phase of marine Cenomanian to present day.

Davies (1989) reported that "movement along a series of transform faults including major east-west oceanic transform faults in the Romanche Fault Zone and the St. Paul fracture zone during the continental separation led to the development of the large rift basin in the Tano area of Ghana". These movements brought about the formation of the rift basin around the Aptian-Early Albian time. Davies (1989) suggested the separation of the continents to have occurred in the late Albian.

1.6 STRATIGRAPHY OF THE TANO BASIN

GNPC (2004) describes the stratigraphy of the Tano Basin from the lower sections to the upper sections as represented below (Fig. 1.6):

1.6.1 Lower Cretaceous Section

1.6.1.1 Lower Albian (Kobnaswaso Formation)

The lower Albian rocks are called the Kobnaswaso Formation and comprises mainly sandstones and shales. The basement of this interval has never been penetrated even though deepest well drilled here is 4,270 m deep. Age proposed for these sediments is lower

Cretaceous (Albian) to Jurassic. There is evidence for two distinct megasequences within parts of the South Tano area. The lower part of the Kobnaswaso Formation consists of dark grey to green shales with occasional beds of very fine sandstone and siltstone.

According to Davies (1989), the upper megasequence on top of these shales is a series of upward coarsening sequences, often referred to as parasequences. There are also intrusives of Jurassic age that mark the onset of rifting in the Gulf of Guinea. Regional seismic surveys indicate thick and different sedimentary wedges within the Kobnaswaso interval which is a characteristic of rift basin deposits. The extremely thick sandstones which are characteristic of the Kobnaswaso sequence in the North Tano and onshore wells provide excellent potential reservoirs over this entire area.

1.6.1.2 B-Shale (Bonyere Formation)

This formation is 200 m thick and the most important strata within the Tano Basin because it can be correlated throughout the whole basin. B-Shale is a medium to dark grey, blocky, micromicaceous shale with a few siltstone and sandstone interbeds. The age of the B-Shale is inferred to be middle Albian (Davies 1989). The B-Shale is considered to record the first major marine transgression into the Tano Basin (Davies, 1989). These transgressive shales overlie the Kobnaswaso unconformably and provide a good seal and possibly, source rock of hydrocarbons within the Tano Basin (Khan, 1970).

1.6.1.3 Middle to Upper Albian

These are shallow marine deposits that mainly comprises of sandstones, shales and a little of limestones. These sediments presumably represent early breakup (transitional stage) deposits. In the South Tano area this interval comprises approximately 600 m of thick coarsening upward units which provide numerous thick reservoir sandstones. The mid Albian deposits are of a lacustrine depositional environment and are large source rocks for gas in North Tano Basin. A regional mid-Albian unconformity divides the mid-Albian interval into upper and lower sedimentary packages. An angular unconformity overlying tilted fault blocks is observed in the South Tano area. In the North Tano area, the mid-Albian unconformity is overlain by dark grey transgressive shales which truncates and seals the underlying Kobnaswaso sandstones. The Cenomanian strata represent a period of local shallow water shoaling which preceded the major transgressions of the Late Cretaceous and Tertiary times.

1.6.2 The Upper Cretaceous Section

1.6.2.1 Cenomanian Limestone

The upper Cenomanian section consists of the thickest limestone accumulations in the area interbedded with several shales, claystones, siltstone and fine sandstone beds. It is the most prominent reflector on the seismic data and appears to be laterally continuous across the area, found in every South Tano well. The limestone is partly mottled, slightly argillaceous and chalky. Although laterally continuous, this Cenomanian section does vary quite considerably in thickness (RRI, 1998; Davis, 1986). The Upper Cretaceous to recent sediments comprises of an offshore dipping sedimentary wedge which thickens from 1,500 m in the North Tano area to approximately 3,700 m offshore at South Dixcove.

1.6.2.2 Turonian to Upper Santonian

The Turonian to Upper Santonian section comprises medium brownish-grey shales and claystones, with occasional dolomite or limestone. It is generally thick, about 920 ft (280 m). The rate of deposition in this succession of fine-grained sediments was high, approximately 167 ft (51 m) per million years; which could only have taken place in a rapidly subsiding basin.

Most deepwater reservoirs of commercial importance are in the Turonian (Jubilee, Tweneboa, etc.). The Turonian also contains a significant portion of the source rock responsible for the Jubilee Field oil.

1.6.2.3 Campanian

The Campanian interval averages over 900 ft (276 m) over the South Tano area. This thick succession is known to have formed under conditions of rapid subsidence and was laid down in a relatively short period of time. This interval is shale-rich with occasional stringers of dolomite and limestone. In the deepwater area fields such as Teak, Odum have Campanian reservoirs.

1.6.2.4 Maastrichtian

The Maastrichtian section is relatively thin in comparison to the rest of the Upper Cretaceous sections. This interval is an indicator that during the late stages of the Upper Cretaceous, subsidence slowed. It is described as principally claystone with occasional sandstone and dolomite beds with the upper parts having significant fossils (Davies, 1986). The thick, highly porous Maastrichtian sandstones are of great interest. Although the Maastrichtian section appears to lie above the oil maturation window, numerous oil shows have been reported from these sandstones. It may be that either oil has migrated upward through faults into the Maastrichtian, or oil has been generated at very low maturation levels, or thirdly, that Maastrichtian sediments may be found in oil mature deep basinal areas that flank the southwest and northeast sides of the North Tano high.

1.6.3 The Tertiary Section

1.6.3.1 Paleocene, Eocene, Oligocene and Miocene

"The Middle and lower Eocene stratigraphic section consists of finely laminated dark grey/brown claystones with thin beds of fossiliferous dolomite and fine sandstone. Large portions of the Paleocene, Upper Eocene and Oligocene section are either only present as a thin bed or completely absent and attributed to extensive uplift and erosion associated with the Alpine Orogeny" (GNPC, 1998). In the south-eastern part of the area, seismic data show the presence of a number of Oligocene to Miocene submarine channels that have removed large amounts of the Eocene section. Miocene sedimentary rocks which were found are described as predominantly brown-grey coloured claystones, highly fossiliferous, glauconitic and sandy in part with stringers of dolomitic limestone. Unconsolidated marine sands with shell fragments and some clays grading to claystones and siltstones dominate the Middle Miocene to Recent section.

1.7 PETROLEUM EXPLORATION AND EXPLOITATION HISTORY IN THE TANO BASIN.

Searching for oil and gas in Ghana officially started in 1896 in the Tano area. Earlier explorationists discovered seepages of oil in the Tano areas which initiated the exploration for hydrocarbons in Ghana formerly called the Gold Coast.

The West Africa Oil and Fuel Company drilled wells between 1896 and 1903 (WAOFCO-1, 2, 3, 4 & 5). WAOFCO-2, the second well on the Takinta concession with a total depth of 35 m, was the first documented discovery well in the country, producing 5 bopd between 1896 and 1897. In the early part of the twentieth century, there was an influx of international oil companies on the shores of Ghana from 1909-1925. Between 1909 and 1913 the French oil company, Societe Francaise de Petrole (SFP) drilled a total of six onshore wells (SFP-1, 2, 3, 4, 5, & 6). SFP-1 struck oil at 10-17 m depth and produced 7 bopd. The wells SFP-3, 4, 5 & 6 all had very good oil indications and/or flowed at relatively shallow horizons, according to available records. Two wells were drilled by African and Eastern Trade Corporation (AETC) and named AETC-1&2 in onshore Tano between 1923 and 1925, progressively encountering heavy oil, light oil and gas at various depths.

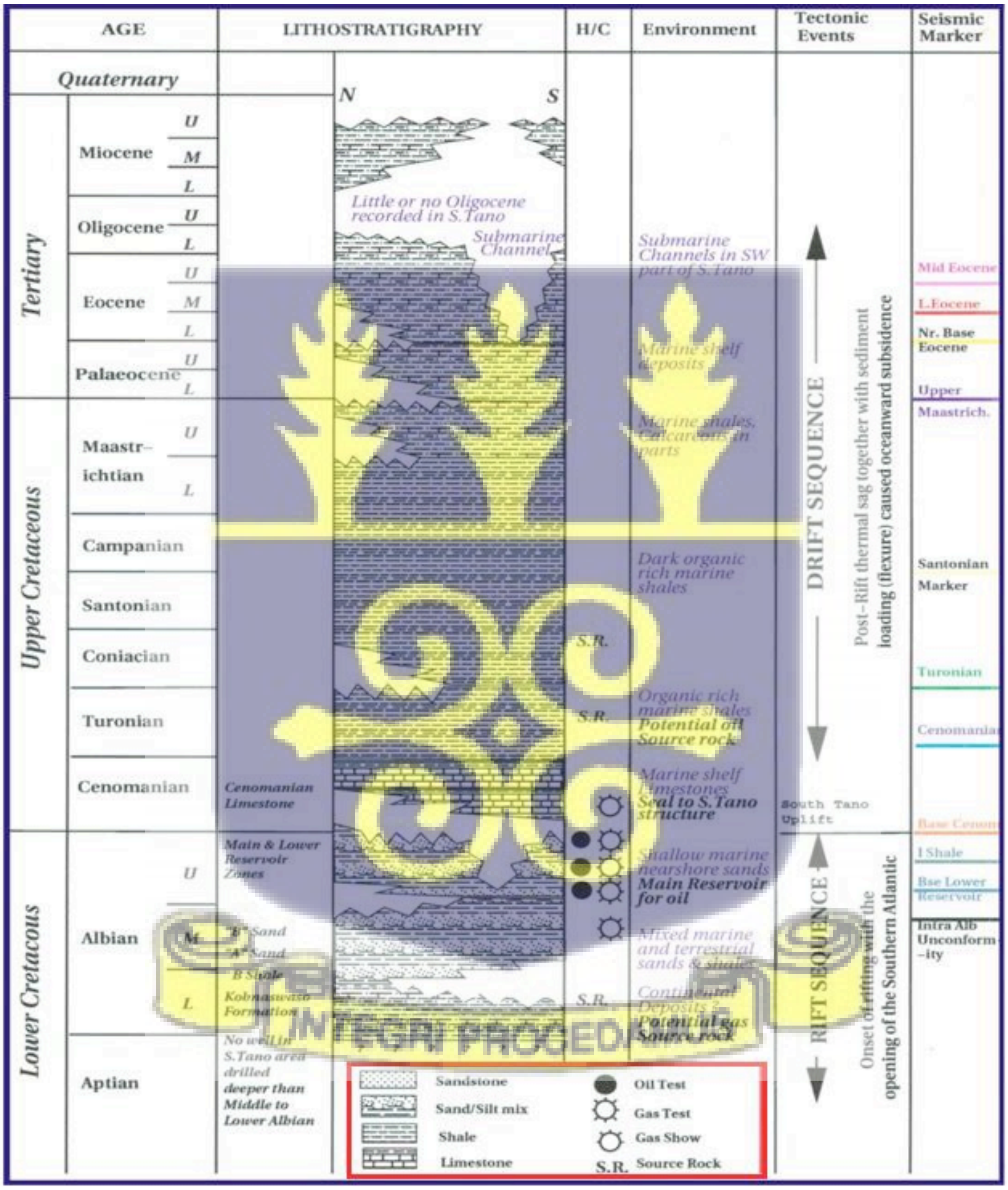

Figure 1.6. The General Stratigraphy of the Tano Basin (After GNPC, 2004).

After a period of inactivity in exploration in Ghana which lasted for almost 30years, Gulf Oil Company acquired the onshore Tano license and drilled four (4) wells at Bonyere, Epunsa, and Kobnaswaso from 1956 to 1957. Apart from well logs, there is very little information on these wells as the wells were drilled without the help of seismic data. From 1896 to 1957 a period of 61 years, 17 onshore wells had been drilled in the Onshore Tano basin.

Phillips Petroleum appraised the South Tano discovery in 1979 and made gas and condensate discovery on the satellite 1S-3AX structure down dip of the main field. They went ahead to further appraise the South Tano find by drilling IS-4X in 1981 and later declared the South Tano discovery sub-commercial and finally relinquished the block. Geophysical Services Incorporated (GSI) in 1982 entered into a Petroleum Agreement with the then Ministry of Fuel and Power to acquire a Non-Exclusive 2D seismic survey to accelerate the exploration and production of hydrocarbons offshore Ghana. The data was acquired in late 1982 to 1983 and covered the area from the Eastern border of Ghana to Cape Three Points.

The Canadian government, acting through Petro Canada International Assistance Corporation (P.C.I.A.C), expended considerable funds to support GNPC in acquiring extensive 2D seismic data in the offshore Tano/Cape Three Points Basin in 1984 (PCIAC-84 -97, 98 & 99 vintages). P.C.I.A.C also funded the drilling of two appraisal wells (ST-5) and ST-6) over the Tano field and the drilling of shallow wells in the Onshore Tano Basin.

The Government of Japan in a bilateral cooperation also assisted the Government of Ghana by acquiring offshore 2D seismic data for GNPC in 1987. This data covered the area from the Eastern border of Ghana to Cape Three Points and it was an infill to the 1982/83 GSI Speculative Survey. GNPC in 1989 funded the acquisition, processing and interpretation of first 3D seismic over the South Tano Field. Following interpretation of the 3D seismic data and subsequent commissioned studies to determine the viability of the Integrated Tano Fields

Development Project to use the gas for power generation, GNPC drilled three wells over the South Tano Field in 1994 using its acquired drillship (Discoverer 511) and three other rigs in addition to other infrastructure to help facilitate rapid development of the Tano Fields.

As part of the integrated Tano Fields development project, GNPC ordered a power barge to utilize the anticipated gas from the Tano Fields. The infrastructure for the power generation barge was built at Effasu-Mangyea and power transmission lines to link the national grid in the Jomoro district in the Western Region to Essiama and Elubo with funds that GNPC had secured.

From 2001-2007, commercial exploration for hydrocarbons intensified with some independent Oil Companies such as Kosmos Energy, Hess Corporation and Tullow Oil, acquiring exploration and production rights over areas in deep water. There was a shift of focus from shallow water to deepwater areas which was occasioned by other deepwater discoveries made in the region and by the results of four deepwater wells drilled in Ghana between 1999 and 2003. These wells proved the existence of an active petroleum system in the deepwater, a fact which hitherto was unknown. Hunt Oil's WCTP-2X well encountered 14 ft of light oil column. This effectively reduced the risk of petroleum generation in the deepwater areas of Ghana.

Kosmos Energy (block operator), Anadarko (technical operator), Tullow Oil and E. O. Group struck a significant (about 312 ft net) column of high-grade oil in the Mahogany prospect with the Mahogany-1 well in the West Cape Three Points Licence. This is the most significant discovery crowning years of concerted effort by all. From August 2007 to 2013, 23 discoveries (Odum, Ebony, Tweneboa, Sankofa, Dzata, Owo, Teak-1, Paradise-1, Banda-1, Gye Nyame, etc.) have been made. Except Ebony, all recent discoveries were made in deepwater (water depths ranging from 800 to 1600 m). The Mahogany and Hyedua discoveries have been appraised and put into production as Jubilee Field (Petroleum Commission of Ghana, n.d.).

CHAPTER TWO

LITERATURE REVIEW

2.1 PREVIOUS PALYNOLOGICAL WORK IN THE STUDY AREA.

Earlier recorded palynological study in the region was in the Cretaceous-Paleocene from the Côte D'Ivoire-Ghana transform margin, sites 959, 960, 961, and 962 by Mascle et al. (1998) as part of the proceedings of the Ocean Drilling Programme.

Total of 204 Cretaceous and Paleocene samples from Holes 959D, 960A, 960C, 961A, 961B, 962B, 962C (barren), and 962D of the Côte d'Ivoire-Ghana Transform Margin (Leg 159) were analyzed and revealed three main palynofacies types. "The first type indicates strong terrestrial depositional conditions and characterizes lithologic Unit V of Hole 959D, Subunit VB and most samples of Subunit VA of Hole 960A, and Unit III of Holes 961A and 961B" (Mascle et al., 1998). Stratigraphically significant spores and pollen grains present indicated a late Barremian-middle Albian age for Unit V of Holes 959D and 960A, and a middle Albian age for Unit III of Holes 961A and 961B. Palynofacies type two revealed mixed terrestrial and marine depositional conditions. "This type was observed in Subunit IIC of Hole 962B and Unit III of Hole 962D".

Stratigraphically significant spore, pollen grain, and dinoflagellate cyst species suggested a Cenomanian age for these units in Holes 962B and 962C. Palynofacies type three represented clearly marine environmental conditions which was found in Subunit IVA and Unit III of Hole 959D, which were of highly diversified dinocyst assemblages (Mascle et al., 1998). They inferred that Subunit IVA and the lowermost cores of Unit III were probably early Coniacian in age; subsequent cores of Unit III are Santonian, Campanian, Maastrichtian, Danian and at the top, Late Thanetian in age.

Atta-Peters and Salami (2004) recovered miospores dominated by angiospermic pollen with trilete and monolete pteridophytic spores from the ST-8 well, offshore Tano Basin. The monosulcate pollen recovered were *Spinizonocolpites*, *Proxapertites*, *Longapertites* and *Mauritiides* of late Cretaceous and Lower Tertiary pollen assemblage, which fit well into the palmae and belong to the tropical-subtropical Senonian Palmae Province of Africa, South America and India (Herngreen and Chlonova, 1981) which suggest a mangrove environment of warm and humid climate (Atta- Peters and Salami, 2004).

Atta-Peters and Salami (2006) recovered Cretaceous dinoflagellate cysts and miospores from the Tano 1-1 and 1S-3AX wells in Ghana. Based on maker palynomorphs recovered from the Tano 1-1 well, an Aptian-early Cenomanian age has been assigned to the sediments of this well. The palynomorphs observed were elements of the Albian-Cenomanian Elaterate Province and suggested a warm tropical climate. From the well 1S-3AX, Atta-Peters and Salami (2006) recovered the palynomorphs *Auriculiidites reticulatus*, *Spinizonocolpites echinatus*, *Buttinia andreevi*, *Longapertites spp*., and *Echitriporites trianguliformis*, which are typical elements for the Campanian-Maastrichtian. These palynomorphs fit into the late Cretaceous Senonian Palmae Province which also supports a warm tropical climate.

Atta-Peters et al. (2012) identified five palynofacies assemblages (I-V) based on the percentage relative abundances of the sedimentary organic matter from the Bonwire-1 well, Tano basin western Ghana. The revealed palynofacies reflected brackish, distal dysoxic-anoxic shelf, proximal dysoxic-suboxic, fluvio-deltaic/nearshore environments with high oxygen levels and low preservation rates respectively.

Atta-Peters (2013) worked on the elater bearing forms from the 1S-3AX well with sediments being assigned Albian-Cenomanian age based on the palynomorph assemblage and further suggested an arid to semi-arid paleo-climatic condition existing at the time of deposition based on recorded species and inferred that the elaterates were deposited in a fluvial/lacustrine environment and went extinct after the Cenomanian because of the sudden shift to a more open marine environment.

Data recovered by Atta-Peters and Kyorku (2013) assigned an Aptian to Cenomanian age based on recovered marker palynomorphs (*Afropollis jardinus*, *Ephedripites* spp, Elaterspores etc.) from palynofacies analysis carried out on fifty-eight (58) cutting samples from the Dixcove 4-2X well offshore Cape Three Points in the South Tano Basin. Atta-Peters and Kyorku (2013) identified five palynofacies types (P-I to P-V) with P-I and P-IV suggesting proximity to a fluvio-deltaic source in a moderately dysoxic environment, P-II reflecting a proximal (pro delta) dysoxic - suboxic environment, P-III being indicative of deposition in an oxidizing condition in proximity to terrestrial sources and P-V being attributed to deposition resulting from high preservation rate and low energy dysoxic- anoxic condition in marginal marine environment.

Atta -Peters et al. (2015) established five palynofacies associations (I-V) from samples of the ST-7H well, Offshore Tano basin, based on the percentage relative abundances of the sedimentary organic matter. Based on marker palynomorphs, Atta-Peters et al. (2015) identified an Aptian to Maastrichtian age for the sediments of the ST-7H well, with an unconformity between the Cenomanian and Campanian sediments.

Atta-Peters and Achaegakwo (2016) observed the presence of *Afropollis*, *Classopollis*, *Ephedripites*, elaterate pollen and pteridophytic fern spores from the sediments from the Epunsa-1 well, Onshore Tano basin. This assemblage suggested a paleoenvironment with parent plants inhabiting moist biotopes or wetlands in a humid, warm coastal plain in a semi-arid/arid climate. Based on biostratigraphically important elaterate pollen and associated taxa, they suggested an Albian-Cenomanian age for the sediments of the Epunsa-1 well succession.

Atta-Peters and Achaegakwo (2016) also adopted visual kerogen analysis and spore colour for the evaluation of hydrocarbon potential and thermal maturation respectively and suggested a mature oil prone to immature gas prone source rock in the Epunsa-1 well.

Achaegakwo and Atta-Peters (2021) carried out palynofacies analysis on 43 samples from the ST-9H well in the Tano Basin, with the aim of reconstructing the palaeoenvironment of the Upper Cretaceous sediments in the well. Their study defined four palynofacies units (PA-PD) which reflected a deposition in near shore/shallow marine (inner neritic) environment under distal dysoxic-anoxic shelf condition, an inner-middle neritic environment under mud-dominated oxic shelf conditions, an open marine (outer neritic) environment under distal suboxic-anoxic basin conditions, and in a proximal-marginal marine environment under dysoxic-anoxic basin conditions.

Achaegakwo and Atta-Peters (2021) recovered species that supported a Campanian-Maastrichtian age. The dinocysts contents recovered include *Dinogymnium euclaensis*, *D. longicornis*, *D. denticulatum*, *Cyclonephelium vannophorum*, *Oligosphaeridium complex*, *Cordosphaeridium inodes*, *Spiniferites ramosus*, *Andalusiella polymorpha*, *A. mauthei*, *A. rhomboides*, *Adnatosphaeridium multispinosum*, *Palaeocystodinium australinium*, *P. golzowense*, *Cerodinium obliquipes*, *C. boloniense*, C. *diebelli*, *Senegalinuim bicavatum*, *S. laevigatum*, *Phleodinium magnificum*, *P. tricuspis*, *Subtilisphaera* sp., *Xenascus ceratioides*, *Trichodinium castanea*, *Glaphyrocysta* sp., and *Odontochitina porifera*. Stratigraphic miospores they recorded from the well and used to support the Campanian-Maastrichtian age include abundant occurrences of *Auriculiidites* sp., *Proteacidites dehanni*, *Echimonocolpites* sp., *Spinizonocolpites echinatus*, *S. baculatus*, *Buttinia andreevi*, *Zlivisporis blanenesis*, *Retitricolpites* sp., *Echitriporites trianguliformis*, *Longapertites marginatus*, *L.*

vaneendenburgi, *Proxapertites cursus*, *P. operculatus*, *Mauriitidites crassibaculatus*, and *Foveotriletes margaritae.*

2.2 PREVIOUS SOURCE ROCK EVALUATION AND HYDROCARBON POTENTIAL OF THE TANO BASIN.

Sediments from three exploratory oil wells (ST-9H, WCTP-2X and WT-1X) from the Tano Basin, south-western Ghana were evaluated for their hydrocarbon generation potential by using geochemical data (TOC, Rock-Eval pyrolysis data) by Atta-Peters and Garrey (2014). The total organic carbon (TOC) contents of samples of these wells ranges from fair to good which indicated that conditions exist in the Basin that was favourable for organic matter production and preservation. Atta-Peters and Garrey (2014) further stated that sediments from oil wells (ST-9H, WCTP-2X and WT-1X) kerogen types variations were attributed to the relative stratigraphic positions of the outcrops within the basin and that the samples represented sufficient organic matter contents to produce oil and gas. ST-9H well yielded kerogen types II, IV and III whereas wells WCTP-2X and WT-1X was identified with kerogen types III and II.

Atta-Peters et al. (2015) performed a source rock evaluation on samples from ST-7H well offshore Tano basin in the western region of Ghana and geochemical data indicated that the samples from ST-7H well had fair to very good petroleum potential and most of the samples were out of the hydrocarbon generating zone due to the low (< 0.10) Production Index (PI)". Atta-Peters et al. (2015) revealed that, the kerogen types shown for the samples in ST-7H well were of type II, II/III and III which are oil prone, oil-gas prone and gas prone respectively. Thermal maturity of samples within ST-7H well indicated immature to early mature hydrocarbons.

Atta-Peters et al. (2016) studied 66 cuttings for source - rock potential of the lower cretaceous sediments in SD-1X well, offshore Tano basin, southwestern Ghana and inferred that the source rocks are of good to excellent organic matter with TOC values between 0.69-8.58 wt. % (average of 2.39 wt. %) which suggested that there might exist conditions in the basin that favour organic matter production and preservation. Atta-Peters et al. (2016) further stated that the thermal maturity of samples had Tmax values of 342-450℃ (average of 427℃), with majority of them indicating moderately immature to early mature source rocks, with good to excellent organic richness. "The organic matter contained in the samples with S_2 values of 0.2-44.39 (average 6.28 mg HC/g rock) indicated good to very good source rock of kerogen types II, II/III and III which are oil prone, oil-gas prone and gas prone respectively. The production index (PI) of between 0.02-0.53 (0.11) of SD-1X well indicates that most of the samples are indigenous hydrocarbons and with low levels of contamination.

CHAPTER THREE

MATERIALS AND METHODS

3.1 MATERIALS

3.1.1 The Lynx-1X well

Lynx-1X well is an exploratory oil well drilled in the year 2014 in the Deep-water Cape Three (DWCTP) block offshore Tano Basin which was operated by LukOil Overseas Ghana Ltd. It is represented by 140 well samples. Lynx-1X well is located geographically on these coordinates; Latitude 4° 04′ 52.8878″ N, and Longitude 2° 13′ 52.4221″ W (Fig. 1.4) and attained a total depth of 5300 m. End of well reports gives details of various lithologies below (GNPC, unpublished) (Fig 3.1).

3.1.1.1 Lithology of Lynx-1X.

Detailed lithology of the well from 2520 m to 5300 m is described below.

- 2520 – 2558 m: Claystone and Additives.

Claystone: Yellowish grey to pale yellowish brown, non-calcareous, firm, swelling, moderately hard, sub-blocky to fissile, slightly waxy, slightly micaceous. Additives, drilling mud coating the cuttings and casing cement.

- 2558 – 2580 m Claystone: Yellowish grey locally light brownish grey, non-calcareous, firm, non-swelling, moderately hard, sub-blocky to sub-fissile, slightly waxy, slightly micaceous.

- 2580 – 2600 m Claystone: light brownish grey, medium dark grey, white to yellowish grey, non-calcareous, firm, swelling, moderately hard, waxy, sub-fissile to fissile, slightly micaceous.

- 2600 – 2743 m Claystone: Medium dark grey to medium light grey, slightly calcareous to non-calcareous, firm, swelling, moderately hard, sub-fissile to fissile, waxy, slightly micaceous, trace pyrite.

- 2743 - 2813 m: Claystone: Dark grey to medium dark grey, brownish, non-calcareous, firm, non-swelling, moderately hard, sub-blocky to sub-fissile, slightly waxy, slightly micaceous.
- 2813 - 3100 m Claystone: Medium grey and dark medium grey to brownish grey and brownish black, non-calcareous to slightly calcareous, firm, non-swelling, moderately hard, sub-blocky to fissile, slightly waxy, micaceous to slightly micaceous, trace indeterminate biogenic debris.
- 3200 – 3262 m Claystone: Brownish grey to brownish black, slightly calcareous to calcareous, firm, non-swelling, moderately hard to hard, sub-blocky to blocky, silty, trace biogenic debris. Siltstone, trace, medium light grey to light brownish grey, noncalcareous, firm, non-swelling, moderately hard, blocky, speckled with black minerals. Additives, drilling mud coating cuttings.
- 3262 – 3300 m Claystone: Brownish grey, calcareous, firm, non-swelling, moderately hard, sub-blocky, silty. Marl, very light grey, speckled with dark brown to black minerals, firm, moderately hard, blocky, locally finely laminated.
- 3300 - 3340.50 m Claystone: Medium dark grey to brownish grey, slightly calcareous to calcareous, firm, swelling, moderately hard, sub-blocky to sub-fissile, slightly micaceous, slightly organic.
- 3340.50 – 3705 m Claystone: Medium dark grey to brownish grey, non-calcareous to slightly calcareous, firm, slightly swelling to swelling, moderately hard, sub-blocky to sub-fissile, slightly micaceous. Silty claystone, medium grey to brownish grey and brownish black, slightly calcareous to calcareous, firm, slightly swelling, moderately hard, sub-blocky to sub-fissile, slightly micaceous, slightly bituminous.

- 3705 – 3760 m Silty Claystone: Medium grey to brownish grey and brownish black, slightly calcareous to calcareous, firm, slightly swelling, moderately hard, sub-blocky to subfissile, slightly micaceous, slightly bituminous.

- 3760 – 3803 m Silty claystone grading to Siltstone: Light brownish grey to brownish grey, locally light olive grey, slightly calcareous, firm, moderately hard to hard, non-swelling, sub-blocky, indeterminate biogenic debris.

- 3803 – 3960 m Silty claystone grading to Siltstone: Light brownish grey to brownish grey, slightly calcareous to calcareous, firm, non-swelling, moderately hard to hard, subblocky, slightly micaceous, slightly bituminous, trace pyrite.

- 3960 – 3980 m Siltstone: Mottled yellowish grey, light olive grey, white to very light grey, slightly calcareous, firm, non-swelling, hard, blocky.

- 3980 -3991 m Silty claystone: Brownish grey to brownish black, calcareous, firm, nonswelling, sub-blocky to sub-fissile, slightly bituminous, slightly micaceous. Limestone, very pale orange to white, argillaceous, moderately hard, mudstone to wackestone, blocky. Siltstone, as above, slightly greenish grey.

- 3991 – 4000 m Silty Claystone: Brownish grey, slightly calcareous, firm, hard, nonswelling, slightly blocky, finely laminated with sandy stingers. Sandstone, light brownish grey, consolidated, slightly calcareous, hard, very fine sand grade, sugary, clast-supported, sub-angular.

- 4000 - 4100.80 m Silty claystone: Medium grey to brownish grey, slightly calcareous to calcareous, firm, non-swelling to slightly swelling, moderately hard, sub-blocky, slightly micaceous, gritty. Argillaceous silty limestone, yellowish grey to very light grey, firm, moderately hard, blocky.

- 4100.80 – 4120 m Siltstone: Brownish grey, calcareous, firm, non-swelling, hard, subblocky to sub-fissile, highly micaceous.

- 4120 – 4260 m Siltstone grading to Silty claystone: Brownish grey to medium dark grey, slightly calcareous to calcareous, firm, non-swelling to slightly swelling, moderately hard, sub-blocky, slightly micaceous to micaceous, slightly bituminous. Argillaceous silty limestone, yellowish grey to very pale orange, soft to moderately hard, blocky, speckled with black minerals.

- 4260 - 4333.20 m Claystone: Brownish grey to brownish black, non-calcareous, firm, no swelling, moderately hard to hard, sub-blocky, slightly micaceous, bituminous. Limestone, pale yellowish brown to very pale orange, moderately hard to hard, blocky, mudstone, oily shows. Silty Sandstone, light olive grey, non-calcareous, firm, non-swelling, hard, poorly sorted, silt to fine sand grade, sub-angular, translucent, biotite and dark glassy minerals. Silty claystone, brownish grey, calcareous, firm, non-swelling, moderately hard, sub-blocky to sub-fissile, micaceous, slightly bituminous.

- 4333.20 – 4340 m Sandstone: Pale yellowish brown to light grey, consolidated, hard to very hard, calcareous, moderately sorted, very fine to medium sand grade, translucent, subangular, sub-spherical, micaceous.

- 4340 – 4495 m Siltstone: Yellowish grey to very pale orange, non-calcareous, soft, swelling, blocky, massive, trace black minerals. Silty claystone, brownish grey to brownish black, non-calcareous, firm, moderately hard, blocky, micaceous. Sandy Siltstone grading to Sandstone, very pale orange to pale yellowish brown, non-calcareous to calcareous, firm, soft, swelling, blocky, massive, very fine to fine sand grade grains, trace black minerals. Additives, drilling mud coating cuttings.

- 4495 – 4500 m Siltstone: Brownish grey to brownish black, slightly calcareous, firm, moderately hard, non-swelling, finely laminated, sub-blocky to sub-fissile, micaceous.

- 4500 – 4578 m Siltstone: As above. Trace pyrite. Also, yellowish grey to light grey, calcareous, firm, slightly swelling, moderately hard, blocky, micaceous, trace pyrite. Silty claystone, brownish black to medium dark grey, non-calcareous, firm, swelling, hard, blocky, slightly micaceous, organic. Sandy siltstone, light grey to pale yellowish brown, non-calcareous, firm, swelling, moderately hard, blocky, gritty, contains very fine sand grade quartz grains. Limestone: white to very light grey, finely laminated with siltstone, mudstone texture, moderately hard, argillaceous.

- 4578 – 4600 m Silty claystone: Brownish grey, slightly calcareous, firm, swelling, moderately hard, sub-blocky to sub-fissile, slightly micaceous.
- 4600 – 4620 m Silty claystone: As above. Marl, yellowish grey to light grey, firm, swelling, moderately hard, blocky, contains trace black minerals. Trace sandy siltstone.
- 4620 – 4700 m Claystone: Medium light grey to light brownish grey, non-calcareous, firm, swelling, moderately hard, blocky, sticky, slightly waxy, micaceous. Siltstone, pale yellowish brown, calcareous, firm, swelling, moderately hard, blocky, micaceous.
- 4700 – 4780 m Claystone grading to Silty claystone: Light grey to pale yellowish brown, locally light brownish grey to brownish grey, slightly calcareous, firm, swelling, moderately hard, sub-blocky to sub-fissile.
- 4780 – 4860 m Claystone: Medium grey to brownish grey, non-calcareous, firm, swelling, moderately hard, sub-blocky to sub-fissile, micaceous, slightly silty, occasional strong hydrocarbon odour.
- 4860 – 4885 m Siltstone grading to silty sandstone: Yellowish grey to very pale brown, calcareous, firm, moderately hard, blocky, mottled. Siltstone, light brownish grey, slightly calcareous, firm, swelling, hard, blocky to sub-blocky, micaceous. Sandstone, yellowish grey, calcareous, consolidated, matrix supported, hard, blocky, well sorted, fine to medium, sub-angular, translucent grains, trace mica. Claystone, as above.
- 4885 – 4925 m Silty Claystone: Light brownish grey to light grey, non-calcareous, firm,

swelling, moderately hard, sub-blocky, slightly micaceous. Trace marl, white to very light grey, firm, swelling, soft, blocky. Trace basement, dark greenish grey, mottled with quartz and calcite veins, hard to very hard, massive.

- 4925 -5300 m: Silty claystone: Light brownish grey to light grey and medium grey,

non-calcareous, firm, swelling, moderately hard, sub-blocky to sub-fissile, slightly micaceous. Siltstone, yellowish grey to light grey, locally light brownish grey, calcareous, firm, swelling, soft, sub-blocky, slightly sandy. Contains? foraminifera bioclasts and locally contains? dolomite crystals. Trace anhydrite, white, soft, opaque, amorphous, massive, blocky.

3.1.2 Dzata-1 well.

Dzata-1 well is the first exploratory oil well drilled in the DWCTP block in the year 2009 offshore Tano Basin and was operated by Vanco Ghana Ltd. It is represented by 100 well cutting samples. Dzata-1 well is located geographically on these coordinates; Latitude 4° 04′ 52.4307″ N, and Longitude 1° 56′ 42.4541″ W (Fig. 1.4), which attained a total depth of 4433 m.

3.1.2.1 Lithology of Dzata-1.

Detailed lithology of the well from 2450 m to 4430. m is described below (Fig. 3.1);

- 2450 – 2690 m: Claystone and Casing Cement/Additive.

Claystone: Olive grey to olive black, non-calcareous, locally glauconitic, firm, amorphous. Casing Cement/Additive, very light grey, calcareous, firm, crumbly.

- 2690 - 2718.5 m: Claystone and Casing Cement/Additive.

Claystone: Olive grey, non-calcareous, firm, sub-blocky.

Casing Cement/Additive, very light grey, calcareous, firm and crumbly.

- 2718.5 – 2901 m: Claystone and Marl.

Claystone: Brownish grey to olive grey, slightly to highly calcareous, firm, sub-blocky.

Marl: brownish grey, firm, sub-blocky.

- 2901 – 2982 m: Claystone, Marl, ?Dolomitic Limestone and Calcite.

Claystone: Olive grey, slightly to highly calcareous, firm, amorphous to sub-blocky, locally glauconitic.

Marl: brownish grey, firm, sub-blocky.

Minor ?Dolomitic Limestone: light brownish grey, hard, blocky. Minor Calcite, whitish, blocky, loose grains.

- 2982 - 3502 m: Claystone, Marl, Silty Claystone, Sandstone and Casing Cement/Additive

Claystone: Light olive grey to olive grey to brownish grey, non-calcareous to very calcareous, fairly-firm, sub-rounded to sub-blocky.

Marl: light olive grey, silty, sub-blocky, fairly-soft.

Silty Claystone: olive grey to olive black, moderately to highly calcareous, fairly-firm, amorphous to sub-blocky.

Minor Sandstone: very fine grade, rounded, very well sorted, unconsolidated.

Casing Cement/Additive, very light grey, calcareous, firm, crumbly.

- 3502 – 4430 m: Claystone, Marl, Limestone and Sandstone.

Claystone: Olive grey, non-calcareous to very calcareous, fairly-firm, sub-blocky.

Marl: light olive grey, silty, fairly-soft, sub-blocky.

Limestone: yellowish grey, silty, soft, amorphous.

Minor Sandstone, light olive grey, medium grade, grain-supported, calcareous, firm.

3.1.3 The Dzata-2A well.

The Dzata-2A well is an appraisal oil well drilled in the Deep-Water Cape Three Points (DWCTP) block offshore Tano Basin formally operated by Vanco Ghana Ltd in 2011. It is represented by 101 well cutting samples. Dzata-2A well is located geographically on these coordinates; Latitude 4° 05′ 48.78″ N, and Longitude 1° 56′ 56.88″ W (Fig. 1.4), which attained a total depth of 4450 m.

3.1.3.1 Lithology of Dzata-2A.

Detailed lithology of the well from 2520 m to 4470 m is described below (Fig. 3.1);

- 2420 – 2649 m: Claystone and Casing Cement/Additive.

Claystone: Olive grey to olive black, non-calcareous, locally glauconitic and locally grading to Silty Clay, with very fine to no visible quartz grains. Blocky, firm and amorphous.

Casing Cement/Additive, very light grey, calcareous, firm, crumbly.

- 2649 – 2676 m: Claystone and Silty Clay.

Claystone: Olive black to black, medium firm to firm, blocky and amorphous, noncalcareous. Locally grading to Silty Clay.

- 2676 – 2915 m: Claystone and Siltstone.

Claystone: Brownish black to grayish black, highly calcareous, firm, blocky.

Siltstone: brownish black to black, blocky. Very fine to non-visible quartz grains, poorly sorted. Traces of glauconite and light brown calcite crystals. Casing Cement/Additive, very light grey, calcareous, firm, crumbly.

- 2901 – 2982 m: Claystone and Siltstone.

Claystone: Brownish black to grayish black, highly calcareous, firm, blocky.

Siltstone: brownish black to black, blocky. Very fine to non-visible quartz grains, poorly sorted. Traces of glauconite and light brown calcite crystals.

- 2963 – 3875 m: Siltstone, Sandstone and localized Dolomite.

Siltstone: Medium dark grey to dark grey, blocky, soft to firm, moderately argillaceous, grading to Sandstone in parts, very light grey, pepper texture due to phosphate as a secondary mineral, very fine to non-visible quartz grains, poorly sorted.

Localized Dolomite, dark grey to brownish black, micro-crystalline, non-visible porosity, very hard. Trace glauconite.

- 3875 – 4470 m: Siltstone and Sandstone.

Siltstone: Medium dark grey to dark grey, blocky, soft to firm, moderately argillaceous, grading to Sandstone in parts, very fine to non-visible quartz grains, poorly to moderately sorted.

Sandstone: transparent to localised off white quartz grains, very fine lower to fine lower. Localised Dolomite, dark grey to brownish black, micro-crystalline, non-visible porosity, very hard. Kaolin spots, off-white.

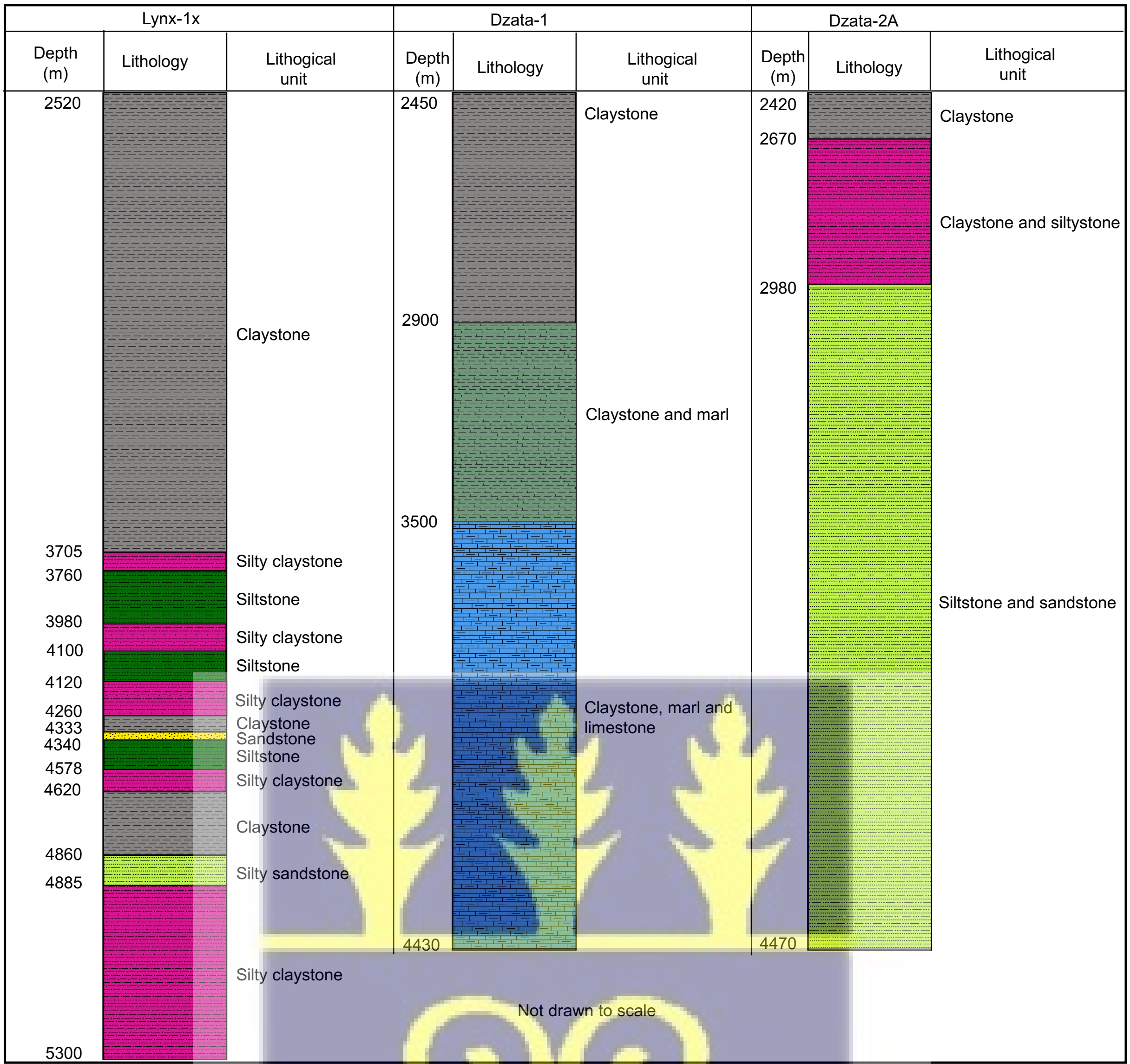

Figure 3.1: Lithology of Lynx-1X, Dzata-1 and Dzata-2A wells.

3.2 METHODS

3.2.1 Sample preparation and palynological analysis.

Total of 341 cutting samples from 3 wells (Lynx-1X, Dzata-1, Dzata-2A) in the Tano Basin were obtained from the Core laboratory of GNPC. The samples were processed in the Faculty of Geoscience GML laboratory, Utrecht University, Utrecht, the Netherlands, producing a total of 1,023 palynological slides (2 slides from unoxidized residues and 1 slide from oxidized residues samples for each analysed sample interval) for this study.

3.2.2 Sample Processing Techniques.

The standard palynological procedures of processing samples followed those outlined by Phipps and Playford (1984) which are described in detail in the following paragraphs.

3.2.2.1 Sample Crushing and Drying.

Sample Crushing

About 8 gm was processed from each sample interval. Sample code was written on the cover and container to be used for the treatments. Codes were generated for all the studied samples with labels indicating the well name, depth interval, country, weight and sieve used. Samples were crushed by selecting the biggest sample cutting and crushed with a clean crushing bowl and pestle to about 5 mm fragments and emptied into the nalgene container on the balance. The procedure was repeated until desired weight was obtained. The sample was covered and put aside. Crushing bowl and pestle were cleaned after each sample to prevent contamination from previous samples. Samples were then transferred into the oven for drying at 60 degrees Celsius and left overnight and then emptied into the labelled container.

3.2.2.2 Pre-Hydrofluoric Acid (HF) Treatment

Samples were transferred into fume chamber (FC) for first stage of HCl treatment. One tablet of Lycopodium with known amount of *Lycopodium clavatum* marker spores was added to each sample to enable quantification of the palynomorphs and their accumulation rates (ARs) to the sediment. Few drops of agepon (kind of soap solution) were added from the water bottle onto the Lycopodium in the sample to aid coating removal.

10% HCl solution was added to each sample slowly and swirled. The process was repeated till all the calcareous materials were out and then solution added to about half full of the container. This repeated process was very important because any carbonate left would form insoluble precipitates of secondary fluorides (Ca_2F, Mg_2F) upon treatment with HF. This took about 1-4 hrs depending on the type of samples analyzed and distilled water added to each sample to about 3/4th full of container. Samples were tightly closed and left in the fume chamber overnight on the sample shelf. Procedures were repeated for all the samples.

3.2.2.3 (38-40%) Hydrofluoric acid (HF) treatment

Step A.

Before HF treatment the acid solution on samples were decanted as far as possible and filled with distilled water. Samples were transferred to the HF laboratory for centrifuging and HF treatment. Samples were centrifuged at 2200 rpm, 5 mins, acc 9, break 6. Samples were carefully removed from the bucket one after the other. Each solution was carefully decanted and the process repeated for all the samples.

HF treatment was started by adding a little concentrated HF (38-40%) or five drops in each sample and swirled by holding the base stacked to the working area and put placed back to resting position. The procedure was repeated by adding more HF until half (½) full of sample container. All samples were closed and transferred to the shaking machine.

Step B: Shaking

Each sample was placed on the shaking machine with the timer set to 120 mins. 250 mot 1/min programme. Samples were then shook for 2 hours. After shaking, the samples were uncovered simultaneously and washed at the edges with water under a pressure from the water bottle and filled to about 4/5th full of the container and left overnight with tightly closed covers. Procedure was repeated for all the samples. HF treatment removed the silica and silicates content of the rock matrix with resultant release of organic material.

3.2.2.4 Sieving, Ultrasonification and Centrifuging.

Ultra-Sonic machine (USM) was filled with tap water to the operation level after it was cleaned, and polyester sieves were placed in for 5mins after switching on the USM. Sample was rinsed slowly from its container into the sieve using water and were transferred after sieving into the labelled test tubes and centrifuged for about 25 minutes. Sieving combined with 'sonification' produced exquisitely clean size-sorted residues. All centrifuged samples were decanted and the residues made loose by using the vortex and 6 drops of glycerin water was added. The mixed residue was carefully transferred into the small residue vials which were labeled based on sample codes. The procedure was repeated for all the samples. All samples were centrifuged and decanted and corked for making slides.

3.2.2.5 Oxidation.

Oxidation was carried on most of the samples for detailed palynological study. It was done using Schultze solution ($KClO_3$ in HNO_3) overnight and palynomorphs showed marked improvements. The concentration and appearance of palynomorphs were further enhanced when SOBO solution (SOBO S) was added to the residue and ultrasonified for few seconds. Organic residues were concentrated in cryogenic vials and preserved by adding two drops 10% hydrochloric acid to prevent algae and fungi growth.

3.2.2.6 Mounting.

Method A: Mounting before oxidation

Small amount of glycerin gel was placed on a slide and a drop of thoroughly mixed residue was place on slide to be mounted. The slide with the residue was heated immediately for few seconds to dissolve the glycerin gel using the lighted burner. Two slides were mounted for each sample code. The pointed needle was used to completely spread the residue uniformly on the slide. A cover slip was slightly heated and gently placed on the slide with the help of the hooked needle. The prepared slide was placed back in the heat for less than 7 seconds and removed. The prepared label was then fixed on the mounted slide according to its sample code. The procedures were repeated for all the samples. The mounted slides were dried (between 14-18 hrs) and later cleaned and polished using a razor and cover glass polish and placed in the various slide box. Two slides were prepared for each sample before oxidation process and one slide each after oxidation.

Method B: Mounting after oxidation

Few drops of a solution of Polyvinyl alcohol (PVA; 10 gms in 100 mls of water) was added to diluted residues for mounting permanent slides and mixed thoroughly for even distribution of the residue on cover slip and allowed to dry on a hot plate. Permanent slides using Glue 4 Glass (G4G) was applied to residues. Two drops of G4G were placed on glass slide and placed on the cover slip with dried residue on hot plate. Prepared slide was cured in visible light using a desk lamp containing fluorescent lamp and Slide washed with soap and water after bonding to remove excess mounting medium. The procedure was applied to all the residues and permanent slides were mounted.

3.2.3 Microscopic Study and Photomicrography.

The slides were studied using Olympus CK41 light microscope and Leica DM2500 LED microscope fitted with Leica MC170 HD digital camera connected to a monitor for photomicrography.

The slides were placed on the mechanical stage of the microscope with the label to the left of the observer and the co-ordinates quoted refers to the mechanical stage of this microscope with the horizontal scale given first followed by the vertical scale (e.g. 135.9/18.7). England Finder Slide was later used together with sample slide for photomicrography. Each slide was thoroughly scanned for complete coverage. Well preserved species on each slide was photographed.

3.2.4 Repository

All slides used in the project are deposited in the core laboratory of Ghana National Petroleum Corporation (GNPC) and with their permission duplicate slides prepared are deposited in the Research Laboratory of the Department of Earth Science, University of Ghana. Procedure adapted for labelling slides are (1) Well name (2) Country and year drilled (3) Company (4) Sample interval and size of sieve used (5) weight of sample (6) slide number prepared for a particular sample.

3.2.5 Palynofacies and Palaeoenvironmental Analysis.

Examination and study of palynomorphs were done using oxidized residue slides while palynofacies analysis was performed on the unoxidized residue slides. A total of 500 particulate organic matter (POM) were counted for each sample to determine the relative abundance in percentage of POM at each sample depth interval of all the wells. Based on the quantitative analysis from microscopic observations of the different POM which were assessed according to the pattern and organized relationship between them and established the differences in the studied succession using the palynofacies approach, palynofacies associations were revealed. Relationship and range charts were produced using Tilia version 2.6.1 (2019) and StrataBugs version 2.1.1.

AOM-Phytoclast-Palynomorphs (APP) ternary plot (Tyson, 1993 & 1995) were used to infer and determine the depositional environments and the relative proximity to terrestrial organic matter sources (Tyson 1995).

3.2.6 Geochemical Analysis

In Geochemical analysis, the purpose of geochemical logging and cross plots is to measure the following parameters relating to source rock evaluation in sedimentary rocks: quantity of organic matter, quality of the organic matter and the thermal maturation of the organic matter. The knowledge of these three parameters will permit accurate evaluation of the source rock geochemistry and hydrocarbon potential in the oil block.

CHAPTER FOUR

PALYNOSTRATIGRAPHY

4.1 INTRODUCTION

The processed samples from the wells (Lynx-1X, Dzata-1 and Dzata-2A) yielded well preserved and relatively diverse assemblages of dinoflagellate cysts and sporomorphs. Dinoflagellate cysts have been used for biostratigraphical purposes, with sporomorphs providing additional supporting evidence for the upper Late Cretaceous (Campanian-Maastrichtian) to Early Tertiary (Paleocene-Eocene) sediments and sporomorphs for the upper Early Cretaceous (Albian) to lower Late Cretaceous (Cenomanian). This is because many of the independently calibrated events for dinocyst were not recovered in the analyzed samples of study within the lower Cretaceous.

Dinoflagellate cysts and sporomorphs recognized in this study have been reported from the Cretaceous to Tertiary sediments of Africa (e.g. Cote D'Ivoire, Sudan, Nigeria, Egypt, Angola, Senegal) and different territories such as South America (e.g. Brazil, Venezuela, Peru). Four palynozones (palynozone I, II, III and IV) have been proposed for the sediments from the processed samples of the research. The results of the palynological analysis of the studied wells are displayed on distribution charts (Appendices 1-3).

Palynozonation (PZ) and age assignment of the samples studied were based on first appearance datum (FAD) and the last appearance datum (LAD) of index species and other associated species within the three wells studied (Lynx-1X, Dzata-1 and Dzata-2A) located in the Deepwater Cape Three Points oil Block, offshore Tano Basin. Correlation of lithology, palynozones and depositional environments of the three wells were also displayed (Fig. 4.11).

4.2 PALYNOZONATION (PZ) AND AGE ASSIGNMENT

4.2.1 Palynozone I (PZ-I): *Afropollis jardinus-Sofrepites legouxae-Elaterocolpites castelaini* Assemblage Zone

This palynozone is recognized at depth intervals between (3710 – 3720 m) - (5155 – 5160 m) for Lynx-1X, (3050 – 4390 m) for Dzata-1 and from 2943 m – 4426 m for Dzata-2A (Figs. 4.1-4.3).

Definition of zone: FAD of *Afropollis jardinus*, *Elaterocolpites castelaini* and LAD of *Sofrepites legouxae* and *Galaeocornea causea*.

Associated taxa group: *Ephedripites brasiliensis*, *E. barghoonii*, *Classopollis brasiliensis, Tricolpites*, *Triplanosporites*, *Cicatricosisporites*, *Cyathidites australis*, *Cyclonephelium brevispinatum, Spiniferites*, *Subtilisphaera pellucida*, *Florentina laciniata* and *F. cooksoniae.*

Remarks: Recovered palynological assemblages were dominated by terrestrial palynomorphs with little to no recovery of marine palynomorphs in some intervals of this zone. The derived taxa in PZ-I are similar in all the studied wells. The sporomorphs are dominated by gymnosperm pollen grains with few pteridophyte spores and angiosperm pollen grains. This palynozone is characterized by the first and last occurrences of several other index sporomorph species such as *Elaterosporites klaszii*, *Elateroplicites africaensis* and *Afropollis kahramanensis* which were recovered in all the three wells. Palynozone I is subdivided into four subzones 1-4 which are detailed below;

Subzone 1: *Afropollis jardinus-Elaterosporites klaszii* Interval Zone

Definition of subzone: FAD of *Afropollis jardinus* and *Elaterosporites klaszii*.

Discussions and Age assessments of subzone:

Afropollis jardinus reported in subzone 1 recorded its FAD at level 5135 m – 5140 m, 4390 m and 4363 m for Lynx-1X, Dzata-1 and Dzata-2A wells respectively. *A. jardinus* is widely accepted as entering the stratigraphical record in the Early Albian in the Elaterates Phytogeographical Province (Doyle et al. 1982; Hochuli and Kelts 1980; Jardiné and Magloire 1965; Muller 1966; Regali et al., 1974). *A. jardinus* was documented in Egypt in the Aptian (Ibrahim 1996), Albian-Cenomanian (El-Beialy et al., 2010; Ibrahim, 1996), Albian-Early Cenomanian (Schrank, 2001), Early Aptian (Sultan, 1986), Aptian-Early Cenomanian (Mahmoud et al., 2000), Aptian-Albian in Egypt (Ibrahim et al., 2001). In Sudan, *A. jardinus* was recorded from the Aptian-Albian (Ibrahim, 2002), Late Albian-Early Cenomanian (Schrank, 2001), Albian-Cenomanian (Cole et al., 2017), Late Aptian-Late Cenomanian (Schrank, 1990) and in Libya from the Albian-Cenomanian (Batten and Uwins, 1985) and Early Cenomanian (Keegan and Stead 2007).

A. jardinus was documented in Nigeria from Late Albian-Early Cenomanian (Lawal and Moullade, 1986), Early-Middle Cenomanian (Abubakar et al., 2011) and Late Aptian-Cenomanian (Salard-Cheboldaeff, 1991). *A. jardinus* was also reported in Brazil from Early Albian-Early Cenomanian sediments (Herngreen, 1973, 1975), Barremian-Aptian (Muller et al., 1987), Aptian-Early Cenomanian (Regali et al., 1985) and Aptian-Albian (de Lima and Boltenhagen, 1981). *A. jardinus* was documented in the Late Albian in Senegal (Jardinè and Magloire, 1965), Albian (Brenner, 1968) and Aptian-Albian in Peru (Ibrahim, 2002) and in Gabon (Wood et al., 1997).

Elaterosporites klaszii observed in this subzone first appeared at level at 4580 m, 3950 m and 3850 m for Lynx-1X, Dzata-1 and Dzata-2A wells respectively. The first occurrence of *E. klaszii* is accepted to document the base of the Middle Albian in the Elaterates Phytogeographical Province (Muller, 1966; Hochuli, 1981; Jardiné, 1967; Jardiné and

Magloire, 1965; Schrank and Ibrahim, 1995; Deaf et al., 2014). *Elaterosporites klaszii* was observed in Senegal in the Cenomanian (Kotova,1978), Early Cenomanian (Babinot et al., 1988) and from Late Albian-Early Cenomanian (Salard-Cheboldaeff,1991). In Peru, *E. klaszii* was documented from the Albian-Cenomanian (Brenner, 1968), Late Albian (Brenner, 1976) and in the Albian (Volkheimer,1980). In Brazil, *E. klaszii* was reported from the Late Albian-Cenomanian (Herngreen, 1973; Dino et al., 1999), Early Albian-Late Cenomanian (Herngreen,1974; de Lima, 1978; Kherngrin and Chlonova 1983), Middle Albian-Cenomanian Brazil (Regali, et al., 1974), Albian (Regali,1989), Early Cenomanian (Carvalho and Pedrao, 1998), Aptian-Albian (Beurlen and Regali, 1987), Albian (de Lima and Boltenhagen, 1981) and Late Albian-Early Cenomanian (Herngreen and Jimenez, 1990).

E. klaszii was also documented in Egypt from the Albian-Early Cenomanian (Saad, 1974; Sultan,1987; Ibrahim, 1996; Mahmoud et al., 1999), Cenomanian (Urban, et al., 1976), Albian (Sultan,1978; Abdel-Kireem et al., 1996), Aptian-Early Albian (Saad,1978), Middle Albian (Penny,1991), Albian-Early Cenomanian (Aboul Ela and Mahrous, 1992; El-Beialy, 1994), Early Cenomanian (El-Beialy, 1993), Late Aptian-Early Albian (El-Beialy et al., 1990), Late Albian-Early Cenomanian (Mahmoud et al. 2000), Albian-Cenomanian (Schrank and Ibrahim, 1995) and Late Albian-Late Albian/Early Cenomanian (El Beialy et al., 2008).

In Sudan, *E. klaszii* was documented from the Aptian-Cenomanian (Kaska,1989), Late Albian-Early Cenomanian (Schrank,1990, 1994) and Aptian-Cenomanian (Christopher et al., 1996). *E. klaszii* was reported from the Late Albian-Turonian in Venezuela (Helenes and Somoza, 1999) and Albian-Cenomanian in Tanzania (Srivastava and Msaky, 1999). *E. klaszii* was also documented from Late Albian-Early Cenomanian (Doukaga, 1980) in Gabon, Middle Albian-Lower Cenomanian age in Ghana (Atta-Peters, 2013; Atta-Peters and Achaegakwo, 2016), Cenomanian in the Atlantic Ocean (East) from the Cote D'Ivoire-Ghana transform margin, Sites 959, 960, 961 and 962 (Masure, et al., 1998) and in Ivory Coast from the Late Albian-Cenomanian (Jardiné,1967) and Late Albian-Early Cenomanian (Salard-Cheboldaeff, 1991). *Elaterosporites klaszii* was recorded in Libya in the Albian (Thusu et al., 1985) and from the Albian-Cenomanian (Batten and Uwins, 1985).

Elaterosporites protensus was recognized together with *E. klaszii* and *E. verrucatus* in this subzone. In Lynx-1X, Dzata-1 and Dzta-2A wells, *Elaterosporites protensus* made its first appearance at depth 4580 m, 3950 m and 3850 m respectively. Jardinè (1967) and Jardinè and Magloire (1965) reported *Elaterosporites protensus* first in sequence followed by other *Elaterosporites* forms in Senegal, Ivory Coast and Gabon from Middle-Late Albian/Early Cenomanian sediments. *E. protensus* was later observed in Brazil from the Early-Middle Albian (Mũller, 1966), Late Albian (Herngreen, 1973), Early-Late Albian (Herngreen, 1974, 1975), Middle-late Albian (Regali et al., 1974), Albian-Cenomanian (Daemon, 1975; de Lima, 1978; de Lima and Boltenhagen, 1980; Herngreen & Chlonova, 1981; Kherngrin and Chlonova, 1983; Batten, 1996), Late Albian-Cenomanian (Dino et al., 1999). I

n Senegal, *E. protensus* was recovered in the Early Cenomanian (Babinot et al., 1988) and Albian-Early Cenomanian in Senegal and Ivory Coast (Salard-Cheboldaeff, 1991). *E. protensus* was documented in Sudan from Aptian-Cenomanian (Kaska, 1989; Christopher et al., 1996) and Albian-Cenomanian in Tanzanian (Srivastava and Msaky, 1999). In Egypt, *E. protensus* was reported in the Early Cenomanian (Mahmoud et al., 1999) and from the Late Albian-Early Cenomanian (Deaf et al., 2014). In Morocco, *E. protensus* was recovered from the Albian (Bettar and Meon, 2006) and from Late Albian in Nigeria (Abubakar et al., 2006 and 2011). *E. protensus* was later recovered in Ghana from the middle Albian-Early Cenomanian from the Tano Basin (Atta-Peters and Salami 2006; Atta-Peters 2013; Atta-Peters and Achaegakwo 2016).

Elaterosporites verrucatus observed in this palynozone first appeared at depths 4580 m, 3950 m and 3770 m for Lynx-1X, Dzata-1 and Dzata-2A wells respectively. In Egypt, Schrank and Ibrahim (1995), Sultan (1987) observed *Elaterosporites verrucatus* from the Albian-Early Cenomanian and from the Middle Albian-Early Cenomanian (Aboul Ela and Mahrous, 1992). *E. verrucatus* was reported in Senegal in the Middle Cenomanian (Babinot et al., 1988), Albian-Early Cenomanian (Salard-Cheboldaeff, 1991), Late Albian-Early Cenomanian (Jardiné, 1967; Potonie, 1970), Late Albian-Early Cenomanian and in Sudan from the Aptian-Cenomanian (Christopher and Goodman,1996; Kaska, 1989).

E. verrucatus was documented Brazil in the Late Albian (Herngreen, 1973), Early Albian-Late Cenomanian (Herngreen,1974; Herngreen, 1975), Middle Albian-Late Albian (Regali et al., 1974), Albian-Early Cenomanian (Lima, 1975), Albian-Cenomanian (de Lima, 1978; de Lima and Boltenhagen, 1981; Batten, 1996), Early Albian-Middle Albian (Volkheimer, 1980) and Albian (Regali et al., 1985). *E. verrucatus* was also observed from Late Albian-Cenomanian in Ecuador (Dino et al., 1999), Late Albian-Turonian in Venezuela (Helenes and Somoza, 1999), Albian-Cenomanian in Tanzania (Srivastava and Msaky, 1999), Albian in Gabon (Boltenhagen, 1980), Albian-Cenomanian in Ivory Coast (Jardiné, 1967), Albian in Morocco (Bettar and Meon, 2006) and from the Late Albian-Early Cenomanian in Ghana (Atta-Peters, 2013).

Masure et al. (1988) recovered *Elaterosporites verrucatus*, *E. klaszii* and *E. protensus* and intimated they were confined to the Middle-Late Albian of Holes 961A and 961B of the Cote D'Ivoire Ghana (CIG) transform margin.

Based on the FAD of *A. jardinus* and *E klaszii*, subzone 1 of palynozone I range from the Early-Middle Albian from (5155 – 5160 m) - 4580 m in Lynx-1X well, 4390 m-3950 m for Dzata-1 well and 4426 m – 3850 m for Dzata-2A well.

Age of subzone 1: Early-Middle Albian

Subzone 2: *Elaterocolpites castelaini* Interval Zone

Definition of subzone: FAD of *Elaterocolpites castelaini* and LAD of *Sofrepites legouxae*

Discussions and Age assessments of subzone:

In this study, *Elaterocolpites castelaini* was first recognized in Lynx-1X, Dzata-1 and Dzata-2A wells at depths 4580 m, 3930 m and 3830 m respectively. *E. castelaini* is an index species in this interval used to document the base of the Late Albian and top of the Middle Cenomanian in the Elaterates Province in Brazil (Herngreen 1973; Herngreen and Jimenez, 1990) and in Senegal (Jardiné and Magloire 1965; Jardiné 1967). Batten and Uwins (1985) observed *Elaterocolpites castelaini* from the Early Albian-Late Cenomanian in Libya and from Albian-Cenomanian in Tanzania (Srivastava and Msaky, 1999).

In Brazil, *E. castelaini* was reported from the Albian-Cenomanian (Herngreen, 1975, 1981; de Lima, 1978), Middle Albian-Cenomanian (Regali et al., 1974), Late Albian-Cenomanian (Dino et al., 1999), Albian-Turonian (Daemon, 1975) and in the Albian (Lima, 1975; de Lima and Boltenhagen, 1981). *E. castelaini* was documented in Senegal from the Late Albian-Cenomanian (Salard-Cheboldaeff, 1991). In Egypt *E. castelaini* was reported in the Cenomanian (Ibrahim, 1996), Early Cenomanian (Mahmoud et al., 1999), Middle Albian-Early Cenomanian (Aboul Ela and Mahrous,1992), Late Albian-Early Cenomanian (El-Beialy, 1994; Schrank, 2001; Deaf et al., 2014). *E. castelaini* in Sudan was documented from the Aptian-Cenomanian (Kaska, 1989) and Late Albian-Early Cenomanian (Schrank, 1994; Schrank, 2001).

Schrank (1990) recovered *E. castelaini* together with *Elaterosporites klaszii* from Late Albian-Early Cenomanian strata from northern Sudan. Atta-Peters and Salami (2006) also reported

Elaterocolpites castelaini, *Elaterosporites klaszii* and *E. protensus* and suggested a Middle Albian-Cenomanian age in Ghana.

Sofrepites legouxae was first recognized in Lynx-1X, Dzata-1 and Dzata-2A wells at depths 4540 m, 3810 m and 3850 m respectively and made its last appearance at 4515 – 4520 m, 3650 m and 3354 m respectively. *S. legouxae* is an index species in this interval which is documented to range from the Late Albian-Early Cenomanian in Brazil (Herngreen 1973; Herngreen and Jimenez, 1990) and in Senegal (Jardiné and Magloire 1965; Jardiné 1967). *S. legouxae* was documented from the Late Albian-Turonian in Venezuela (Helenes and Somoza, 1999).

In Brazil *S. legouxae* was reported in the Late Albian-Cenomanian (Herngreen, 1973 and 1974; Dino et al., 1999), Early Albian-Late Cenomanian (Herngreen, 1975), Albian-Cenomanian (de Lima and Boltengagen, 1981; Herngreen and Chlonova, 1981; Kherngrin and Chlonova, 1983; Batten, 1996), and Late Albian-Early Cenomanian (Herngreen, 1981). Herngreen et al., (1996) later documented *S. legouxae* to be confined to the Late Albian-Early Cenomanian of the Albian-Cenomanian Elaterate Province. *S. legouxae* was reported in Egypt from the Early Cenomanian (Ibrahim, 1996), Late Albian-Early Cenomanian (Aboul Ela and Mahrous, 1992; Deaf et al., 2014), Albian-Early Cenomanian (Sultan, 1987) and in Nigeria from the Late Albian-Middle Cenomanian (Lawal, 1982).

Based on the FAD of *Elaterocolpites castelaini* and LAD of *Sofrepites legouxae*, subzone 2 ranges from the Late Albian-Early Cenomanian for Lynx-1X, Dzata-1 and Dzata-2A wells from 4580 m - (4515 – 4520 m), 3930 m – 3650 m and 3830 m-3354 m respectively.

Age of subzone 2: Late Albian-Early Cenomanian

Subzone 3: *Elateroplicites africaensis* Interval Zone

Definition of subzone: LAD of *Elateroplicites africaensis* and *Elaterocolpites castelaini*.

Discussions and age assessment of subzone:

Elateroplicites africaensis and *Elaterocolpites castelaini* observed in subzone 3 had its last appearance at depths 3895 – 3900 m, 3050 m and 3294 m for Lynx-1X, Dzata-1 and Dzata-2A respectively. *E. africaensis* was reported in Brazil from Albian-Cenomanian (Herngreen, 1973, 1974 and 1975; Herngreen and Chlonova, 1981; Kherngrin and Chlonova, 1983), Late Albian-Cenomanian (Herngreen, 1981), Late Albian-Turonian (Regali et al., 1974 and 1985), Albian-Turonian (de Lima et al., 1981) and Early Cenomanian (Carvalho and Pedrao, 1998). *E. africaensis* was also documented from the Late Albian-Early Cenomanian in Sudan (Schrank, 1990 and 2001) and in Egypt from Late Albian-Early Cenomanian (Schrank, 2001) and Early-Middle Cenomanian (Schrank and Ibrahim, 1995). The *E. africaensis* was reported from Albian-Cenomanian in Gabon, Congo, Angola and Cameroon (Salard-Cheboldaeff, 1991). According to Herngreen et al. (1996) *Elateroplicites* is restricted to the Middle Albian-Cenomanian.

The LAD of *Elateroplicites africaensis* and *Elaterocolpites castelaini* were used to define the top of the Middle Cenomanian which range from (4515 m – 4520 m) - (3895 – 3900 m) for Lynx-1X, 3650 m – 3050 m for Dzata-1 well and from 3312 m – 3294 m for Dzata-2A well.

Age of subzone 3: Early-Middle Cenomanian

Subzone 4: *Galeocornea causea* Interval Zone

Definition of subzone: LAD of *Galeocornea causea* and *Afropollis kahramanensis*.

Discussions and age assessment of subzone:

Galeocornea causea and *Afropollis kahramanensis* occurred together with other forms of *Elaterosporites* documented in this subzone had its LAD at 3710 m – 3720 m, 2930 m and 2922 m for Lynx-1X, Dzata-1 and Dzata-2A respectively. *G. causea* was recovered from Late Albian-Cenomanian of Senegal and Gabon (Jardiné and Magloire, 1965; Jardiné, 1967) and also in Brazil from the Albian-Cenomanian (Herngreen, 1973, 1975). Brenner (1968) reported *G. causea* from Albian-Cenomanian in Peru and the same species was recorded in Egypt from the Late Albian-Early Cenomanian (Mahmoud, 1998; Shrank & Ibrahim, 1995; Zobaa et al., 2013) and in the Middle Albian (Deaf et al., 2014).

Afropollis kahramanensis was documented in Egypt from Early Cenomanian-Middle Cenomanian (Schrank et al., 1995), Late Cenomanian (Ibrahim et al., 1996; Mahmoud et al., 2000), Late Albian/Early Cenomanian-Late Cenomanian (El Beialy, 1994), Late Albian-Early Cenomanian (El Beialy, 1994), Late Cenomanian (Ibrahim, 1996), Cenomanian (Mahmoud, 1998), Early Cenomanian (Mahmoud and Moawad, 1999), Early-Middle Cenomanian (Ibrahim, 2002), Late Cenomanian (Mahmoud and Moawad (2002), Late Albian-Late Albian/Early Cenomanian (El Beialy et al., 2008) and Late Albian-Cenomanian (Deaf et al., 2014).

The elater-bearing pollen and *Classopollis* spp. which disappeared at the end of the Late Cenomanian occurred in subzone 3 represented in Lynx-1X, Dzata-1 and Dzata-2A wells in depth intervals from (3895 – 3900 m) - (3710 – 3720 m), 3050 m – 2930 m and 3294 m – 2922 m respectively. A Late Cenomanian age is suggested for this subzone.

Age of subzone 4: Late Cenomanian

Other taxa restricted to this palynozone includes *Ephedripites brasiliensis*, *Ephedripites irregularis* and *Ephedripites barghoonii* which were documented together with the elater-bearing pollen reported above and disappeared at the end of the elaterates occurrence.

E. brasiliensis was reported in the Late Albian from Senegal and Ivory Coast (Jardinè and Magloire, 1965). *E. brasiliensis* was also recorded from Late Albian-Early Cenomanian in Ghana (Atta-Peters and Salami, 2006) and in Brazil, from the Late Albian-Early Cenomanian (Herngreen, 1973) and Albian-Cenomanian (de Lima, 1978).

Ephedripites irregularis was recovered in Brazil from Early-Middle Albian Herngreen (1973), Albian-Cenomanian (Herngreen, 1975), Aptian-Albian (de Lima, 1978), Albian-Cenomanian (Herngreen and Chlonova, 1981) and Albian-Early Turonian (Kherngrin and Chlonova, 1983). In Egypt *E. irregularis* was documented in the Albian (Sultan, 1978), Early Aptian (Sultan, 1986), Late Aptian-Early Albian (El-Beialy et al. 1990), Late Albian-Early Cenomanian (Aboul Ela and Mahrous, 1992), Late Albian-Cenomanian (Schrank et al., 1995) and in the Cenomanian (Ibrahim, 1996). *E. irregularis* was also recorded from Early Albian-Middle Albian in South America (Herngreen, 1981) and in the Tano Basin of Ghana from the Early-Middle Albian (Atta-Peters and Salami 2006).

Ephedripites barghoonii was documented from the Late Albian-Early Cenomanian of Senegal and from Albian to Cenomanian sediments from Ivory Coast (Jardinè and Magloire, 1965). *E. barghoonii* was recorded from the Early Albian-Cenomanian (Herngreen, 1973) and Early Albian-Late Cenomanian (Herngreen, 1974, 1975) in Brazil. *E. barghoonii* was recovered from the Tano Basin in Ghana and suggested to be Early Albian-Early Cenomanian in age (Atta-Peter and Salami, 2006). *E. barghoonii* was also documented from the Early Albian-Coniacian in Angola (Morgan, 1978), Aptian-Middle Albian in Venezuela (Sinanoglu, 1983) and Albian-Cenomanian in Tanzania (Srivastava and Msaky, 1999).

Classopollis brasiliensis and *Classopollis classoides* observed in this palynozone was recognized throughout most of the analyzed sample intervals. They appeared last at depths 3710 – 3720 m, 2930 m and 2922 m for Lynx-1X, Dzata-1 and Dzata-2A wells respectively. *Classopollis brasiliensis* was reported from the Middle to Late Cenomanian (Ibrahim, 2002; El Beialy et al., 2010; Tahoun and Deaf, 2016) and in the Cenomanian (Schrank et al., 1995; Ibrahim, 1996; Mahmoud et al., 2000) in Egypt. *C. brasiliensis* was documented from Middle-Late Cenomanian strata in Libya (Thusu and Van der Eem, 1985), Early Albian-Late Cenomanian in Brazil (Herngreen, 1975), Cenomanian in Brazil and Israel (Herngreen, 1975; de Lima et al., 1981). In Nigeria, *C. brasiliensis* was recorded from Middle-Late Cenomanian (Lawal and Moullade, 1986), Late Albian-Middle Cenomanian (Lawal, 1982) and Late Albian-Early Cenomanian (Ojoh, 1990). *C. brasiliensis* was also reported in the Atlantic Ocean (East) from the Cote D'Ivoire-Ghana transform margin, Sites 959, 960, 961, 962 (Masure et al., 1998).

Atta-Peters et al. (2015) assigned an Albian-Cenomanian for the interval 6900 ft – 8550 ft of ST-7H based on the existence and persistent elater bearing pollen (e.g. *Elaterosporites* spp., *Elaterocolpites* spp., *Galeocornea* spp. and *Ephedripites* spp.) which were consistent with this palynozone. The elater-bearing pollen in this palynozone have a restricted stratigraphic distribution from the Early Albian-Late Cenomanian. They appeared in the Early Albian and disappeared at the top of the Late Cenomanian (Herngreen and Duenas Jimenez, 1990; Herngreen et al., 1996).

Based on stratigraphic significant confined to palynozone I, an Albian-Cenomanian age is deduced for the analyzed samples.

4.2.2 Palynozone II (PZ-II): *Cretaceaeiporites polygonalis-C. scabratus-Dinogymnium accuminatum* Assemblage Zone

PZ-II was recognized in two of the wells, Lynx-1X well at sample intervals from 3320 m - (3690 – 3700 m) and Dzata-2A well at sample intervals from 2802 m – 2901 m (Figs. 4.1-4.3). This zone recorded less palynomorph recovery as compared to the rest of the palynozones and dominated by terrestrially palynomorphs, hence dinoflagellates where convenient would be used as an index species to support the age assignment.

Definition of Zone: PZ-II in Lynx-1X and Dzata-2A wells was characterized by the FAD of *Cretaceaeiporites polygonalis Cretaceaeiporites* cf. *scabratus and Dinogymnium accuminatum*.

Associated taxa: *Araucariacites australis, Cyathidites australis, Verrucosisporites*, *Psilastephanocolpites*, *Retitricolpites*, *Retimonocolpites* spp., *Inaperturatepollenites, D. accuminatum*, *Cyclonephelium brevispinatum, Spiniferites ramosus, Oligosphaeridium complex* and *Odontochitina porifera.*

Remarks: PZ-II is constituted by mainly terrestrial palynomorphs which are dominated by gymnosperm pollen with few pteridophyte spores and angiosperm pollen grains and low to none dinoflagellates. The palynological assemblages in Lynx-1X and Dzata-2A wells within PZ-II are low in diversity and generally fairly preserved.

Discussions and age assessment:

Turonian-Santonian sporomorphs like *Droseridites senonicus, Hexaporotricolpites emelianovi Cretaceaeiporites* spp. and dinoflagellate cysts (*Dinogymnium acuminatum*, *Odontochitina* *porifera*, etc.) were missing in Dzata-1 well. *Droseridites senonicus* was documented as a Turonian-Early Senonian (Santonian) marker species (Apaalse and Atta-Peters, 2013; Lawal and Moullade, 1986; Schrank and Ibrahim, 1995). This therefore made possible the inference of limitations or sediments erosion suggesting an unconformity between Late Cenomanian and Early Campanian of Dzata-1 well from intervals of 2910 m – 3050 m.

Cretaceaeiporites polygonalis and *Cretaceaeiporites scabratus* observed in PZ-II first appeared at depth 3670 – 3680 m and 3690 – 3700 m for Lynx-1X well, 2901 m and 2820 m for Dzata-2A well respectively. Their LAD were restricted to this palynozone at 3580 m and 2820 m for Lynx-1X and Dzata-2A respectively. *C. polygonalis* was documented in Gabon from the Albian-Early Turonian (Boltenhagen, 1975) and from the Albian-Turonian (Boltenhagen, 1980). *C. polygonalis* was recorded in Nigeria (Odebode et al., 1984) and in Cameroon, Congo and Angola (Salard-Cheboldaeff, 1991). *C. polygonalis* was documented from the Turonian-Coniacian in Angola (Morgan, 1978), Early Senonian in Nigeria (Jan du Chêne 1979) and the Late Albian-Turonian in Sudan (Schrank, 1994). *C. polygonalis* was observed in Brazil in the Coniacian (de Lima et al., 1989).

Cretaceaeiporites scabratus was reported from the Cenomanian-Early Senonian in Brazil (Herngreen, 1974; Herngreen, 1975) and in Gabon (Boltenhagen, 1975). *C. scabratus* was observed from the Turonian-Coniacian in Angola (Morgan, 1978), Early Senonian in Nigeria (Jan du Chêne, 1979), Coniacian and Late Coniacian in Nigeria (Odebode et al., 1986; Odebode, 1987). *C. scabratus* was recorded in the Senonian in Namibia (Benson, 1990), Late Albian-Turonian in Senegal and Ivory Coast (Salard-Cheboldaeff, 1991), in Sudan (Schrank, 1994), Early Turonian in Egypt (Ibrahim, 1996) and from the Late Albian-Santonian of northern Africa (Mahmoud and Mahmoud, 2007).

Odontochitina porifera in this palynozone was first recognized at depth 3320 m for Lynx-1X well, 2890 m for Dzata-1 well and 2781 m for Dzata-2A well. *O. porifera* was documented in the Senonian (Cookson, 1956), Late Turonian-Maastrichtian (Cookson, 1960) and Turonian-Senonian (Vozzhennikova, 1965) in Australia. *O. porifera* was recorded from Coniacian-Early Santonian in the Atlantic Coast Offshore (Bujak et al., 1978), Late Senonian in Guinea (Masure, 1979), Turonian-Santonian in Canada (Barss et al., 1979) and Turonian-Campanian in the North Sea (Davey et al., 1977).

O. porifera was reported from Coniacian-Santonian in the Northern Hemisphere (Williams et al., 1993), in Egypt (Abdel-Kireem et al., 1996) and from Turonian-Santonian in Algeria (Foucher et al., 1994). *O. porifera* was also observed from the Turonian-Maastrichtian in Brazil (Arai, 1994), Coniacian-Maastrichtian in Egypt (Schrank et al., 1995) and from the late Turonian-Santonian in the Atlantic Ocean (East) (Oboh-Ikuenobe et al., 1998). *O. porifera* was later documented from the late Santonian-early Campanian in England (Prince et al., 1999) and from the Santonian-Late Maastrichtian in the Northern Hemisphere (Williams et al., 2004).

In this study, the FAD of *Dinogymnium acuminatum* was observed at depth 3500 m, 2910 m and 2841 m for Lynx-1X, Dzata-1 and Dzata-2A wells respectively. *D. acuminatum* was recorded in the Senonian (Baltes, 1973) and from Turonian-Middle Santonian (Antonescu, 1973) in Romania. *D. acuminatum* was reported from the Santonian-Maastrichtian in Canada (Jenkins et al., 1974; Williams et al., 1974), the Campanian in Ghana (Davey, 1975). *D. acuminatum* was documented from the Turonian-Coniacian in Angola (Morgan, 1978) and in Nigeria from the Albian-Turonian (Odebode et al., 1984), Santonian-Maastrichtian (Oloto 1989; Oloto et al., 2013) and in the Maastrichtian (Williams et al., 2017). *D. acuminatum* was reported in the Early Senonian in Libya (El-Mehdawi, 1991) and in the Early Santonian in France (Begouen, 1993). *D. acuminatum* was recorded from the Early Santonian-Maastrichtian in Egypt (El-Beialy, 1994), Late Turonian-Early Maastrichtian in the Atlantic Ocean (East) (Oboh-Ikuenobe et al., 1998), Turonian-Coniacian in England (Pearce et al., 2003) and from the Coniacian-Late Maastrichtian in the Northern Hemisphere (Williams et al., 2004).

The absence of elater-bearing pollen and *Classopollis* spp. at the beginning of this palynozone at 3680 – 3690 m for Lynx-1X well and at 2901 m for Dzata-2A well marked the Cenomanian/Turonian boundary (Herngreen et al., 1996; Herngreen, 1998) which further supports the ?Turonian-Santonian of PZ-II.

Age of palynozone II: ?Turonian-Santonian

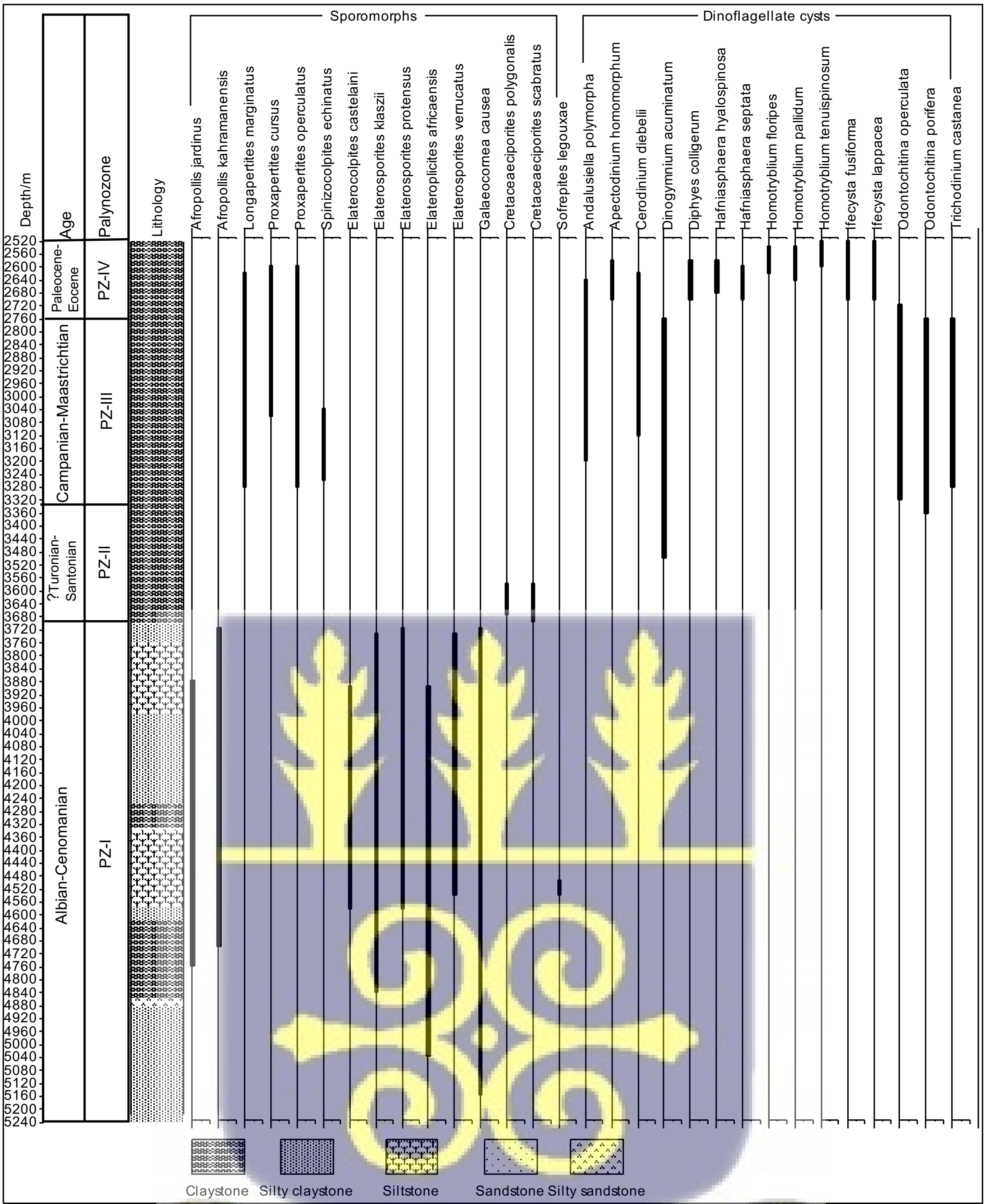

Figure 4.1: Age, palynozone, lithological column and stratigraphical significant taxa from Lynx-1X well.

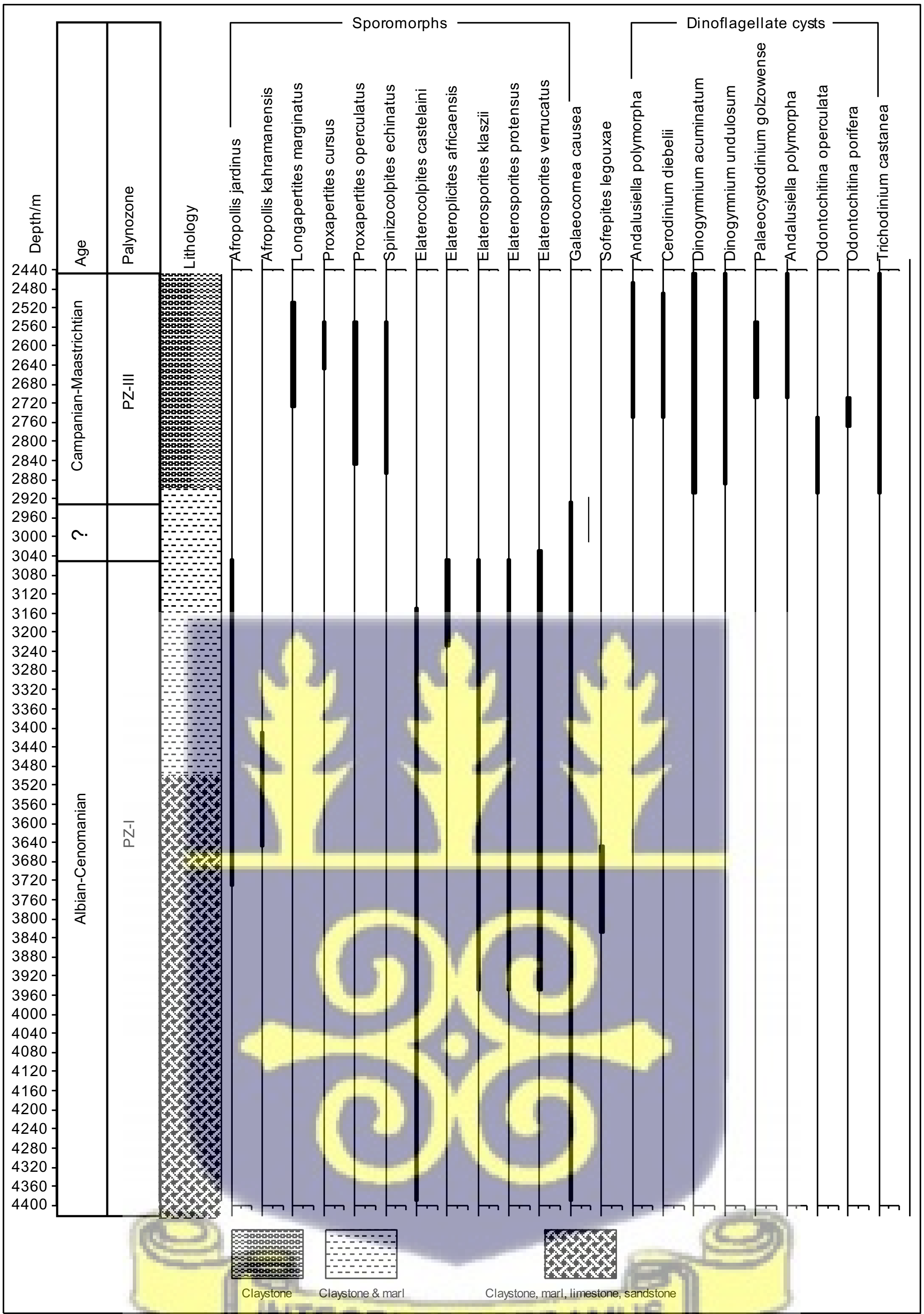

Figure 4.2: Age, palynozone, lithological column and stratigraphical significant taxa from Dzata-1 well.

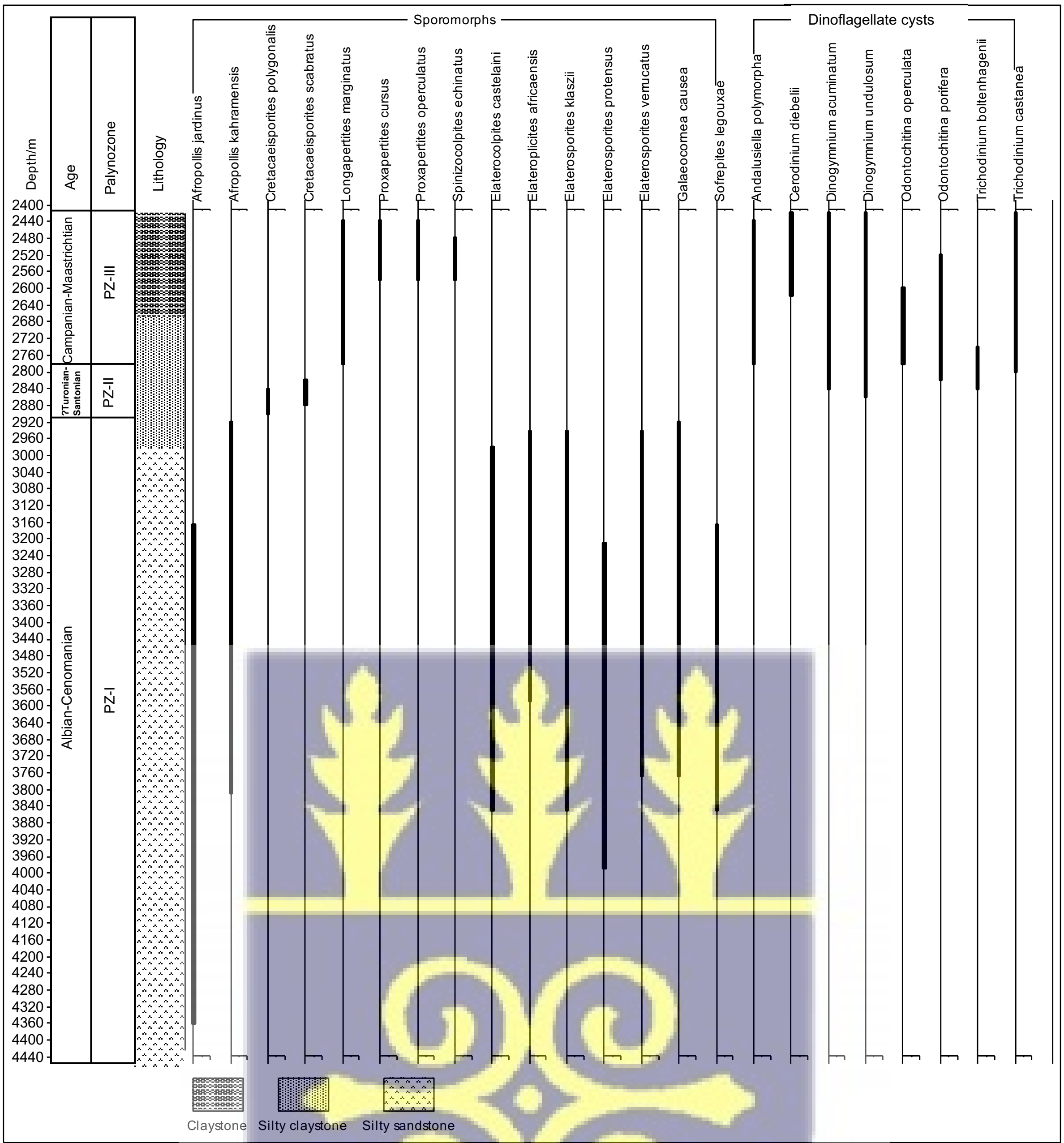

Figure 4.3: Age, palynozone, lithological column and stratigraphical significant taxa from Dzata-2A well.

4.2.3 Palynozone III (PZ-III): *Trichodinium castanea-Cerodinium diebelli-Dinogymnium acuminatum* Assemblage Zone

PZ-III occurs in all the studied wells and occurred at different depth intervals for each well. It occurred within the depth intervals (2760 – 3300 m) for Lynx-1X well, (2450 – 2910 m) for Dzata-1 and Dzata-2A (2420 – 2781 m) (Figs. 4.1-4.3).

Definition of palynozone: FAD of *Trichodinium castanea*, *Cerodinium diebeli* and LAD of *Dinogymnium acuminatum*.

Associated taxa: *Cerodinium boloniense*, *C. obliquipes*, *Coronifera oceania*, *Andalusiella* spp., *Cyclonephelium vannophorum*, *C. distinctum*, *Circulodinium distinctum*, *Odontochitina* spp., *Palaeocystodinium australinium*, *Florentina* spp., *Areoligera* spp., *Dinogymnium* spp., *Glaphyrocysta divaricata*, *Glaphyrocysta ordinata*, *Adnatosphaeridium multispinosum*, *Cordosphaeridium inodes*, *Oligosphaeridium poculum*, *O. Complex*, *Achomosphaera* spp., *Spiniferites* spp. and *Xenascus ceratoides*. Sporomorphs includes *Longapertites proxapertitoides*, *L. marginatus*, *Proxapertites operculatus*, *Proxapertites psilatus*, *Spinizocolpites echinatus*, *Deltoidspora minor*, *Dictyophyllidites harrisii*, *Foveotriletes margaritae*, *Retimonocolpites* spp., *Monosulcites* spp., *Tricolpites confessus*, *Echitriporites trianguliformis* and *Cingulatisporites ornatus*.

Remarks:

A significant change in the composition of the palynological association was recorded in all the three wells studied. The marine palynomorph (%) of total palynomorphs ranges from (61-93%) in Lynx-1X well, (64-92%) in Dzata-1 well and (67-93%) in Dzata-2A well (Figs. 4.4, 4.5 and 4.6). Quantitative distribution of terrestrial palynomorphs (pollen and spores) were represented between (7-39%) of total palynomorph in Lynx-1X well, (8-36%) in Dzata-1 well and (7-33%) in Dzata-2A well. The very rich palynofloras were dominated by marine derived forms with good to very good preservation. The gonyaulacoids recovered in this zone are dominated by chorate cysts (*Spiniferites*, *Cordosphaeridium*, *Areoligera*, *Adnatosphaeridium*). The peridinoids observed in this zone of the three wells were dominated by the genera *Andalusiella*, *Cerodinium* and *Palaeocystodinium.* Palynozone III is subdivided into two subzones 1 and 2 which are detailed below;

Subzone 1: *Trichodinium castanea* Interval Zone

Definition of subzone: The base of this subzone is defined by FAD of *Trichodinium castanea* and the top by the FAD *Cerodinium diebelli*. Other important taxa in this subzone includes *Andalusiella polymorpha*, *Palaeocystodinium australinium* and *Palaeocystodinium golzowense*.

Discussions and age assessment of subzone:

This subzone is characterized by the FAD of *Trichodinium castanea* and occurred at level 3320 m for Lynx-1X well, 2910 m for Dzata-1 well and 2781 m for Dzata-2A well. *T. castanea* was reported in Egypt in the Campanian (Schrank, 1984, 1987 and 1988; Schrank and Perch-Neilsen 1985), Cenomanian-Maastrichtian (Schrank and Ibrahim, 1995) and the Late Campanian-Maastrichtian (El-Beialy, 1995). *T. castanea* was documented in the Campanian of Cote d'Ivoire (Digbehi et al., 1996; Tea-Yassia et al., 1999). In Canada, *T. castanea* was reported in the Campanian (Williams et al., 1974; Fensome et al., 2008), Turonian-Early Campanian (Williams, 1975) and from the Kerguelen Plateau in the Campanian (Mao and Mohr, 1992). *T. castanea* was recorded from the Campanian-Maastrichtian in Nigeria (Beilstein, 1994), Campanian in Brazil (Arai, 1994) and from the Early-Late Maastrichtian in the Northern and Southern Hemisphere (Williams et al., 2004). *T. castanea* was documented in the Early Maastrichtian (Wilson, 1974; May 1980; Costa and Davey, 1992; Slimani, 1995, 2000; Williams et al., 1993; Roncaglia and Corradini, 1997; Gradstein et al., 2005).

The FAD of *Cerodinium diebelli* which was observed in Lynx-1X, Dzata-1 and Dzata-2A wells marked the beginning of the Late Campanian in this subzone. It occurred at level 3120 m for Lynx-1X well, 2750 m for Dzata-1 and 2620 m for Dzata-2A well. *C. diebelli* has been recorded in the Late Campanian-Maastrichtian of the James Ross Island area and Antarctic Peninsula (Riding, 1992), Campanian-Maastrichtian in New Jersey (Lentin et al., 1987). *C. diebelli* was also documented from the Campanian-Maastrichtian in France (Begouen, 1993), Early Maastrichtian in Nigeria (Beilstein, 1994), Late Campanian-Paleocene in England (Stover et al., 1996), Late Campanian-Early Maastrichtian in Netherlands (Herngreen et al., 1996).

C. diebelli was reported from the Early-Middle Maastrichtian in Israel (Hoek et al., 1996), in Italy (Roncaglia and Corradini, 1997) and from the CIG transform margin (Masure et al., 1998). *C. diebelli* was documented in the Late Campanian of the British Isles (Costa and Davey, 1999), in the Maastrichtian of Maud Rise and Georgia Basin, Southern Ocean (Mohr and Mao, 1997) and in the Late Maastrichtian in Tunisia (Vellekoop et al., 2015).

Various authors have documented the association of the taxa (*Cerodinium*, *Phelodium*, *Andalusiella* and *Senegalinium*) observed in PZ-III from the Campanian-Maastrichtian (Schrank, 1987, 1994; Salami, 1986, 1988; Schrank and Ibrahim, 1995; Atta-Peters and Salami, 2004).

Andalusiella polymorpha recovered in this subzone first occurred at sample depth 3200 m for Lynx-1X well, 2750 m for Dzata-1 well and 2781 m for Dzata-2A well. Eshet et al. (1992) documented *A. polymorpha* in the Maastrichtian age from Israel. *A. polymorpha* was reported in the Campanian from Venezuela and Mauritania (Lentin and 1980), Late Campanian-Early Maastrichtian in Morocco (Rauschen et al., 1982) and in Egypt (Schrank et al., 1985). *A. polymorpha* was recovered from the Campanian-Maastrichtian in Namibia (Benson, 1990) and in Nigeria (Beilstein, 1994). *A. polymorpha* was documented from the Late Campanian-Maastrichtian in Egypt (El-Beialy, 1995) and in the Early Campanian (Williams et al., 1993).

In this subzone, *Palaeocystodinium australinium* together with *Palaeocystodinium golzowense* was first recognized at depth 3180 m, 2890 m and 2781 m for Lynx-1X, Dzata-1 and Dzata-2A respectively. *P. australinium* was documented from the Maastrichtian-Paleocene from Colorado Basin in Argentina (Gamerro and Archangelsky, 1981), in New Jersey from the Campanian-Maastrichtian (May, 1980) and from Late Maastrichtian-Danian in New Jersey (Landman et al., 2004). In Canada, *P. australinium* was recorded from Maastrichtian-Paleocene (Williams and Bujak 1977; Barss et al., 1979).

P. australinium was reported from Late Maastrichtian (Rauscher et al., 1982) in Morocco from Late Maastrichtian-Early Danian (Brinkhuis and Zachariasse, 1988) in Tunisia. In Nigeria, *P. australinium* was observed in the Early Maastrichtian (Oloto, 1989), Maastrichtian-Eocene (Salami, 1983) and from the Campanian-Early Maastrichtian (Edet, 1992). In Egypt, *P. australinium* was reported in the Maastrichtian (Schrank, 1984; Schrank et al., 1985) and from Late Campanian-Maastrichtian (El-Beialy, 1995). *P. australinium* was recorded from the Late Campanian-Late Maastrichtian in Venezuela (Yepes, 2001).

Palaeocystodinuim golzowense recorded has its LAD in this palynozone for Dzata-1 well at 2450 m and Dzata-2A well at 2420 m while extending into younger sediments in Lynx-1X well at 2700 m. *P. golzowense* was documented from Late Paleocene-Early Eocene in Spain (Caro et al., 1975), Campanian-Paleocene in Gabon (Boltenhagen, 1977 and 1980) and Late Campanian-Early Maastrichtian in Israel (Hock et al., 1996). *P. golzowense* was observed from the Late Campanian-Late Maastrichtian in Venezuela (Yepes, 2001) and in the Early Maastrichtian in Italy (Roncaglia, 2002). *Palaeocystodinuim golzowense* was reported in the Maastrichtian in Egypt (El Beialy, 1995) and in Ghana (Atta-Peters and Salami, 2004). Kurita and Mclntyre (1995) observed *P. golzowense* from Canada in the Paleocene and from the Selandian-Ypresian in Russia (Iakovleva et al., 2000).

Subzone 1 of palynozone III is restricted to the Early-Late Campanian from 3320 m – 3120 m in Lynx-1X well, 2910 m – 2750 m in Dzata-1 well and 2781 m – 2620 m in Dzata-2A well.

Age of subzone: Early-Late Campanian

Subzone 2: *Dinogymnium acuminatum* Interval Zone

Definition of subzone: The base of this subzone is defined by the LAD of *Odontochitina operculata* and the top by the LAD of *Dinogymnium* spp.

Discussion and age assessment:

Odontochitina operculata in this subzone last appeared at depths, 3100 m for Lynx-1X well, 2750 m for Dzata-1 well and 2781 m for Dzata-2A well. The FAD of *O. operculata* was recognized in palynozone II at level 3320 m for Lynx-1X well, 2890 m for Dzata-1 well and 2781 m for Dzata-2A well.

In Egypt, *O. operculata* was recorded from pre-Maastrichtian strata (Urban et al.,1976; Schrank, 1987 and El Beialy, 1993), Late Campanian-Middle Maastrichtian (Schrank and Perch-Neilsen, 1985), Late Campanian (Schrank, 1988), Late Campanian-Early Maastrichtian (Ganz et al., 1990), in the Campanian (Schrank, 1991), Late Cenomanian-Maastrichtian (Schrank and Ibrahim, 1995) and from the Late Campanian-Maastrichtian (El Beialy, 1995). *O. operculata* was reported in the Early Maastrichtian of the Tano Basin, Ghana (Atta-Peters and Salami, 2004), Late Campanian-Early Maastrichtian in Israel (Hock et al., 1996) and in the Late Campanian in the Netherlands (Herngreen et al., 1996). Wilson (1978) recorded *Odontochitina operculata* in the Maastrichtian and in the Campanian (Ioannides and McIntyre, 1980) from Canada. In Morocco, *O. operculata* was documented from the Late Campanian-Early Maastrichtian (Rauscher and Doubinger, 1982). *O. operculata* occurred worldwide in the Late Campanian and crosses the Campanian-Maastrichtian boundary with the LO in the early part of the Early Maastrichtian (Wilson, 1974; May, 1980; Costa and Davey, 1992; Slimani, 1995, 2001; Williams et al., 2004; Slimani et al., 2016; Guédé et al., 2019).

The LAD of *Dinogymnium undulosum* and *Dinogymnium acuminatum* were recognized in this palynozone at depths 2760 m for Lynx-1X well, 2450 m for Dzata-1 well and 2420 m for Dzata-2A well. *D. undulosum* among other *Dinogymnium* species was documented in Canada from the Campanian-Maastrichtian (Williams et al., 1974), Late Campanian-Maastrichtian in Morocco (Rauscher et al., 1982), Early Maastrichtian in Nigeria (Edet and Nyang, 1994) and from the Late Campanian-Early Maastrichtian in the Netherlands (Herngreen et al., 1996). *D. undulosum* was recorded from the Santonian-Maastrichtian of America and Europe (Schrank, 1987). *D. undulosum* was reported from the Cenomanian-late Maastrichtian (Masure et al., 1998) and Cenomanian-Maastrichtian (Boltenhagen, 1977 and 1980).

Dinogymnium was recorded in the Early Maastrichtian (Brinkhuis and Zachariasse, 1988; Oboh-Ikuenobe et al., 1998; Slimani et al., 2010; 2016; M'Hamdi et al., 2015; Sanchez-Pellicer et al., 2017). Oboh-Ikuenobe et al. (1998) averred that the last fossil record of *Dinogymnium* worldwide were found in the Late Maastrichtian rocks, before the Maastrichtian/Danian boundary. *Dinogymnium* spp. were documented to have their LO in the Maastrichtian (Stover et al., 1996; Costa and Davey1999; Atta-Peters and Salami, 2004) and aided in identifying the Cretaceous-Paleogene (K-Pg) boundary (Williams et al., 1993, 2004).

Other important taxa recorded in this subzone includes *Glaphyrocysta divaricata, Cordosphaeridium inodes* and *Adnatosphaeridium multispinosum*. *G. divaricata* was recognized together with *Cordosphaeridium inodes* in this palynozone at depths 2860 m for Lynx-1X well, 2670 m for Dzata-1 well and 2580 m for Dzata-2A well. Oboh-Ikuenobe et al. (1998) opined that *Glaphyrocysta divaricata* and *Cordosphaeridium inodes* recorded had their FAD in the Late Maastrichtian in the Cote d'Ivoire Ghana transform margin. Masure et al. (1998) further reported *Glaphyrocysta divaricata* from the Late Campanian-Early Paleocene of the CIG transform margin and documented an Early Paleocene age for *Cordosphaeridium inodes*.

Adnatosphaeridium multispinosum was first observed at the end of this palynozone together with the LAD of *Dinogymnium* spp. *A. multispinosum* was recorded at depths, 2760 m for Lynx-1X well, 2450 m for Dzata-1 well and 2420 m for Dzata-2A well. *A. multispinosum* was reported in the Middle Maastrichtian-Paleocene from Ghana (Atta-Peters and Salami, 2004) and in the Maastrichtian age sediments from the IS-3AX well, Tano Basin (Atta-Peters and Salami, 2006). *A. multispinosum* was also documented from Nigeria in the Paleocene (Masure et al., 1998) and from the Late Paleocene-Eocene (Jan du Chene et al., 1978; Jan du Chene and Adediran, 1984). Edwards (1980) documented *A. multispinosum* from the Late Paleocene-Early Eocene in Alabama and Georgia, from Late Thanetian-Ypresian in the Netherlands (Herngreen, 1984) and from Venezuela in the Middle Eocene (Helenes et al., 1998).

Based on the discussion above, subzone 2 of PZ-III is restricted to the Early-Late Maastrichtian between depth intervals 3100 m and 2760 m in Lynx-1X, 2730 m and 2450 m in Dzata-1 and 2620 m and 2420 m in Dzata-2A.

Age of subzone: Early-Late Maastrichtian

Recovered dinoflagellates with associated sporomorphs stratigraphic ranges indicates overlap which suggest PZ-III is representative of Campanian-Maastrichtian age.

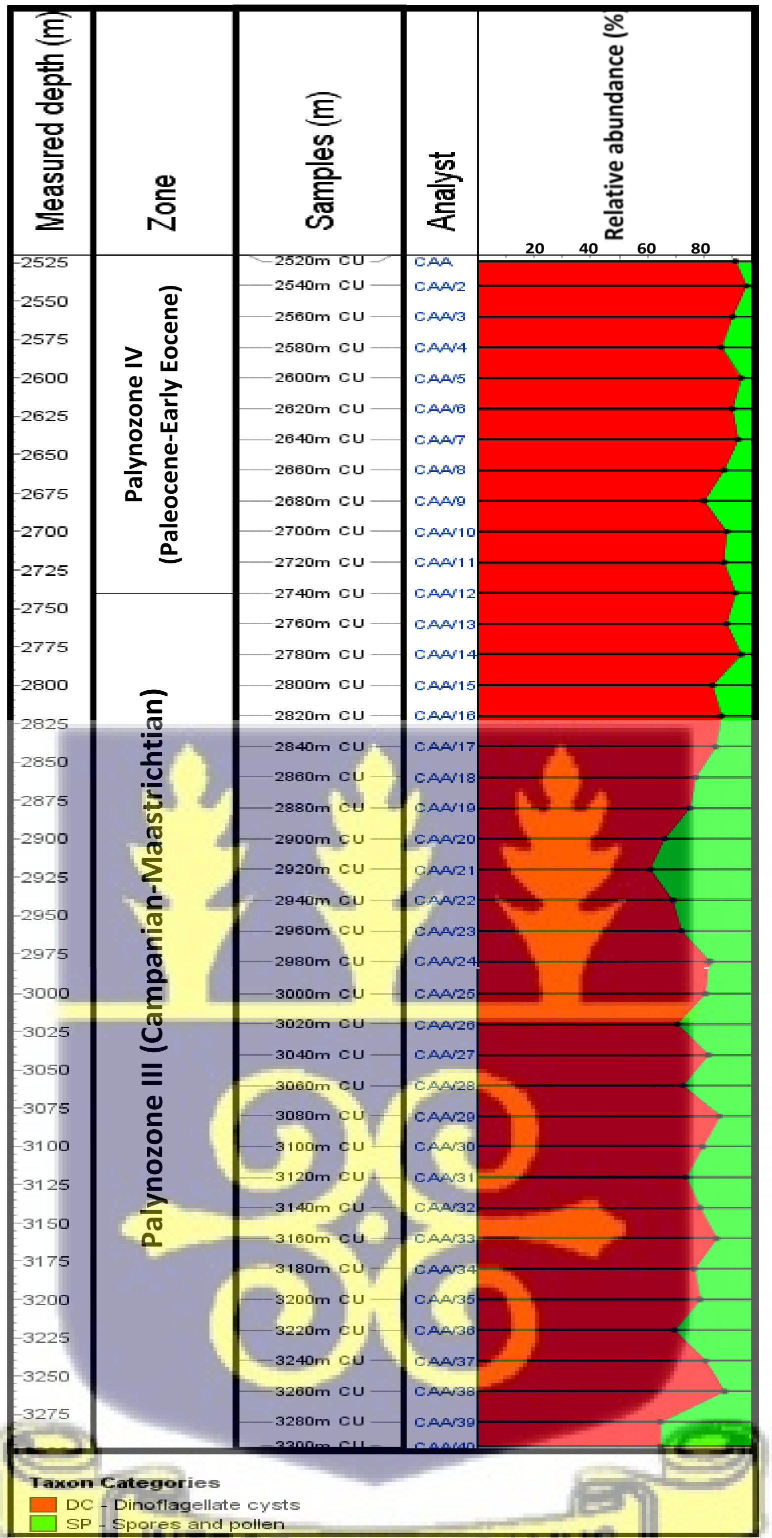

Fig. 4.4: Relative percentage composition distribution chart of dinocysts (marine palynomorphs) with spores and pollen (terrestrial palynomorphs) in Palynozone III and IV from Lynx-1X well.

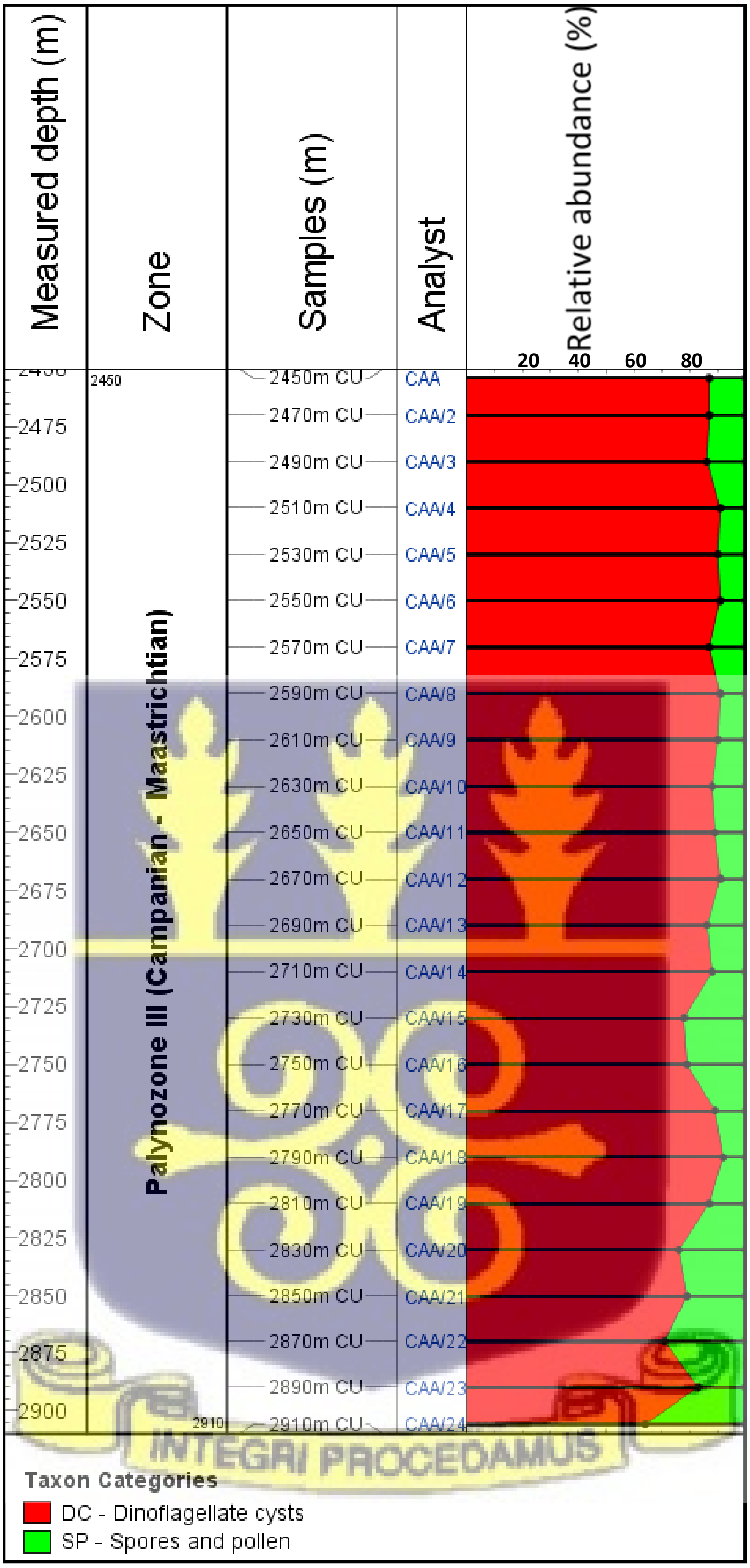

Fig. 4.5: Relative percentage composition distribution chart of dinocysts (marine palynomorphs) with spores and pollen (terrestrial palynomorphs) in Palynozone III from Dzata-1 well.

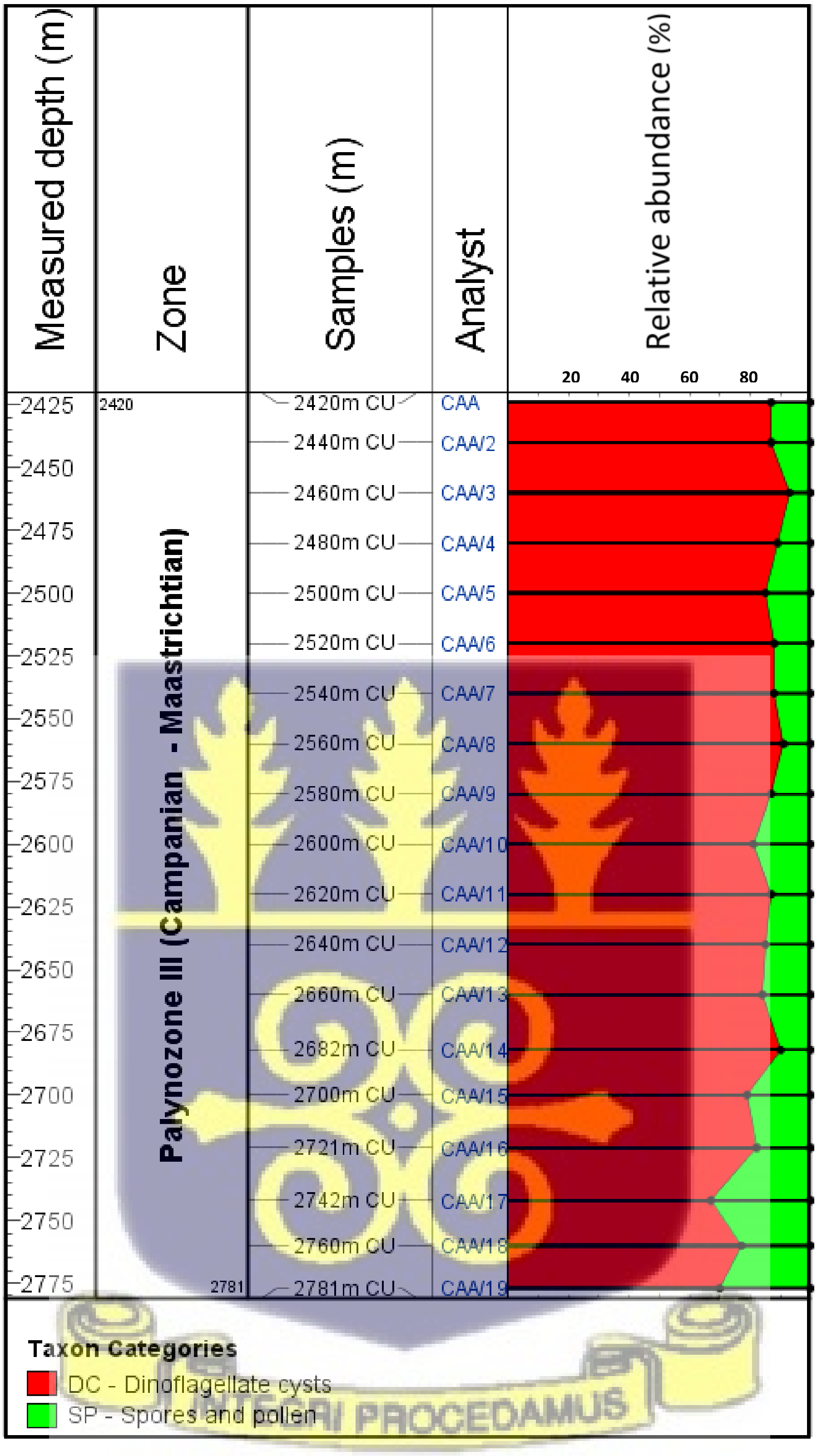

Fig. 4.6: Relative percentage composition distribution chart of dinocysts (marine palynomorphs) with spores and pollen (terrestrial palynomorphs) in Palynozone III from Dzata-2A well.

4.2.4 Palynozone IV (PZ-IV): *Cerodinium diebelli-Apectodinium homomorphum-Homotryblium tenuispinosum* Assemblage Zone

This zone was recognized only in Lynx-1X well and restricted to the sample depth intervals (2520 – 2740 m) (Figs. 4.4). Palynomorph preservation was good to very good and recovery was generally very good. Terrestrial palynomorphs (sporomorphs) were common in almost all the studied samples in this zone (5-20% of total palynomorphs). Dinoflagellate cysts (80-95%) dominated the total palynomorphs within the palynozone (Fig. 4.4, 4.5 and 4.6). Generally terrestrial palynomorphs decreased up the well within this zone.

Definition of Zone: FAD of *Apectodinium homomorphum*, *Diphyes colligerum* and LAD of *Cerodinium diebelli* and *Andalusiella polymorpha*.

Associated Taxa: *Andalusiella polymorpha, Spiniferites fluens, Spiniferites membranaceus, Spiniferites hyalospinosus, Hafniasphaera septata, Hafniasphaera hyalospinosa, Cordosphaeridium fibrospinosum, C. delimurum, Fibrocysta lappacea, Areoligera retiintexta, Adnatosphaeridium multispinosum, Hystrichokolpoma granulatum, H. proprium, Turbiosphaera galeata, Phelodinium magnificum, Coronifera oceania, Operculodinium centrocarpum, Lingulodinium machaerophorum, L. hemicystum, L. echinatum, Oligosphaeridium poculum, Senoniasphaera inornata, Alterbidinium, Oligosphaeridium complex, Cribroperidinium, Polysphaeridium subtile, Homotryblium floripes, Homotryblium tenuispinosum, Ifecysta fusiforma, Diphyes bifidium, Damassadinium heterospinosum, D. californicum, Leptodinium subtile, Lejeunecysta hyaline, Areosphaeridium diktyoplokum, Florentinia mantellii, Surculodinium longifurcatum, Selenopemphix nephroides* and *Achomosphaera* spp. Sporomorphs recovered includes *Cyathidites, Gleichniidites, Araucariacites australis, Proxapertites cursus* and *Longapertites marginatus*.

Remarks: Overall, the interval was characterized by rich palynological assemblages. Palynozone IV is subdivided into three subzones 1-3 which are detailed below;

Subzone 1: *Andalusiella polymorpha* Interval Zone

Definition of subzone: The top of this subzone is defined by the LAD of *Andalusiella polymorpha* and *Cerodinium diebelli*. Other useful taxa include *Diphyes colligerum* and *Damassadinium californicum*. It ranges from 2740 m – 2620 m.

Discussion and age assessment:

Although some taxa of this zone recovered straddle the Campanian-Maastrichtian/Paleocene, the absence of *Dinogymnium* spp. was an indication of an age younger than the Maastrichtian as *Dinogymnium* became extinct at the end of Maastrichtian (Oboh-Ikuenobe et al., 1998; Atta-Peters and Salami, 2004).

The LAD of *Cerodinium diebelli* at level 2620 m and *Andalusiella polymorpha* at 2640 m was used to define the Danian-Selandian boundary in this subzone. They range from 2760 m - 2620 m in Lynx-1X well. The LAD of *Cerodinium diebelli* is a good marker for the Danian-Selandian boundary (Powell, 1992; Oboh-Ikuenobe et al., 1998; Masure et al., 1998; Williams et al., 2004; Fensome et al., 2008; Awad and Oboh-Ikuenobe, 2016; Guede et al., 2019). The LAD of *Andalusiella* spp. (e.g. *Andalusiella polymorpha*) is also known to be in the Danian and observed in strata from the middle and low latitudes of the northern Hemisphere (Williams et al., 1993; Masure et al., 1998; Oboh-Ikuenobe et al, 1998; Slimani et al., 2016).

Damassadinium californicum and *Damassadinium heterospinosum* first appeared in this palynozone at level 2720 m. *D. californicum* was documented in the Danian from California (Fensome et al., 1993), Danian-Thanetian in the Atlantic Ocean (East) (Masure et al., 1998; Moullade et al., 1998) and in Early Paleocene in Mexico (Helenes, 1998). *D. californicum* was reported from the Late Paleocene in South Carolina (Gohn et al., 2000). *Damassadinium californicum* was observed from Late Maastrichtian-Danian in Venezuela (Pocknall et al., 2001), Late Maastrichtian-Late Selandian in the Southern and Northern Hemisphere (Williams et al., 2004) and Danian in New Jersey (Landman et al., 2004).

Diphyes colligerum was first recognized at depth 2720 m and persisted throughout the entire study samples and last occurred at 2580 m. *D. colligerum* has been reported from the Late Paleocene-Eocene in Australia (Verdier, 1970) and the Late Paleocene-Late Eocene in Canada (Eastern Offshore) (Williams, 1975). *D. colligerum* was reported from the Late Paleocene-Middle Eocene in the Atlantic Ocean (Brown and Downie, 1984), Paleocene-Eocene in England (Jolley and Spinner 1989). *D. colligerum* was recorded in the Eocene in Egypt (El-Beialy et al., 1990). This subzone ranges from 2740 m - 2620 m.

Age: Danian

Subzone 2: *Homotryblium tenuispinosum* Interval Zone

Definition of subzone: The top of this subzone is defined by the FAD of *Homotryblium tenuispinosum* at 2580 m. Other useful taxa include *Apectodinium homomorphum* and *Ifecysta* spp. (*Ifecysta fusiforma, Ifecysta pachyderma*).

Discussion and age assessment:

In this subzone, the FAD of *Apectodinium* spp. is not close to the Selandian-Thanetian boundary but within the Danian.

Homotryblium tenuispinosum, *H. pallidum* and *H. floripes* were observed in subzone 2 in PZ-IV. FAD of *H. tenuispinosum* occurred at level 2580 m while *H. pallidum* and *H. floripes* occurred earlier at level 2600 m persisted throughout the studied intervals. *H. tenuispinosum* was reported from the Paleocene-Eocene in England (Downie et al., 1971). *Homotryblium tenuispinosum* was reported from the Paleocene-Eocene (Caro, 1973). *H. tenuispinosum* was documented in Virginia from the Late Paleocene-Early Eocene (Edwards, 1996) and in Maryland (Guex et al., 1996). *H. tenuispinosum* was recorded in the Late Eocene from Egypt (El-Beialy, 1988) and from the Late Paleocene-Early Eocene in Austria (Egger et al., 2003). *H. tenuispinosum* was documented in the Thanetian in the Dahomey Basin of southwestern Nigeria (Bankole et al., 2007), in Douala Basin, Cameroun (Mbesse et al., 2012) and in Morocco (Slimani et al., 2016).

Homotryblium pallidum was documented from the Paleocene-Eocene in England (Downie et al., 1971), in Spain (Caro, 1973) and from the Ypresian-Lutetian in the Netherlands (De Coninck, 1977). *Homotryblium* sp. similar to *H. pallidum* in this zone was reported from the late Paleocene-Early Eocene in Maryland and Virginia (Guex and Edwards, 1996). *Homotryblium* spp. were recorded in the Thanetian in Kazakhstan and southern Tethys (Iakovleva et al., 2001; Crouch et al., 2003) and Thanetian from southwestern Nigeria (Bankole et al., 2007) and in Cameroun (Mbesse et al., 2012).

Ifecysta pachyderma and *Ifecysta fusiforma* were first recognized together at level 2660 m in this palynozone. In Nigeria, *Ifecysta pachyderma* and *Ifecysta* were reported from the Late Paleocene-Early Eocene (Jan du Chêne et al., 1984), *Ifecysta* from the Late Paleocene-Early Eocene (Fensome et al., 1995) and *Ifecysta fusiforma* documented from the Paleocene-? Earliest Eocene (Antolinez-Delgado and Oboh-Ikuenobe, 2007). The relative high occurrence of *Ifecysta* spp. (*Ifecysta fusiforma, Ifecysta pachyderma* and *Ifecysta* cf. *lappacea*) through this subzone supports age assignment for Late Paleocene which was reported in other studies in West Africa (Antolinez, 2006; Bankole et al., 2007; Mbesse et al., 2012; Awad and Oboh-

Ikuenobe, 2016). Subzone 2 of palynozone range from 2620 m – 2580 m based on the FAD of *Homotryblium tenuispinosum*.

Age: Selandian (Middle Paleocene)-early Thanetian (Late Paleocene)

Subzone 3: *Apectodinium homomorphum* Interval Zone

Definition of subzone: The base of the zone is defined by the LAD of *Apectodinium homomorphum*. This zone is characterized by highest relative abundances of the following taxa: *Apectodinium* spp., *Adnatosphaeridium multispinosum*, *Cordosphaeridium* spp., *Homotryblium tenuispinosum*, *Hystrichokolpoma granulatum*, *Hafniasphaera* spp. and *Polysphaeridium* spp.

Discussion and age assessment:

Apectodinium homomorphum was first recognized at depth 2700 m in PZ-IV and had its LAD in this subzone at level 2580m. *A. homomorphum* was reported in the early Eocene in Canada (Barss et al., 1979) and from Thanetian-Ypresian in Morocco (Prevot et al., 1979). *A. homomorphum* was documented from Late Paleocene-Early Eocene in Maryland (Edwards, 1996) and in Argentina (Olivero et al., 2001). *A. homomorphum* was reported in Nigeria in the Late Paleocene-Early Eocene (Jan du Chêne et al., 1978) and in the Early Eocene (Oloto, 1992). *A. homomorphum* was recorded from the Late Thanetian-Early Ypresian in Netherlands (Herngreen, 1984) and in Morocco (Soncini, 1992). *A. homomorphum* was also recovered in the Early Eocene from Egypt (El-Beialy et al., 1990), and from early Eocene-Middle Eocene in Alaska (Frederiksen et al., 2002).

Apectodinium was documented in the Selandian in Tunisia (Brinkhuis, 1994), in the Late Paleocene from Morocco (Slimani et al., 2016) and from the Côte d'Ivoire-Ghana Transform Margin (Awad and Oboh-Ikuenobe, 2016).

The highest relative abundances of *Apectodinium* spp. recorded in this subzone may be related to the latest Thanetian and earliest Ypresian, within the Paleocene-Eocene thermal maximum (PETM) interval which marks the Paleocene-Eocene transition (Powell, 1992; Bujak and Mudge, 1994; Crouch et al., 2000; Heilmann-Clausen and Egger, 2000; Crouch and Brinkhuis, 2005; Mbesse et al., 2012; Slimani et al., 2016; Awad and Oboh-Ikuenobe, 2016; Oboh-Ikuenobe et al., 2017; Guédé et al., 2019).

The FAD of *Hafniasphaera septata* and *Hafniasphaera hyalospinosa* were recognized at level 2680 m in this palynozone and increase in abundance in this subzone. *H. septata* was reported in the Late Paleocene from Australia (Hansen, 1977; Stover et al., 1987) and Early Eocene in Nigeria (Oloto, 1992). *H. septata* was recorded from the Late Paleocene-Early Eocene in Denmark (Hansen, 1979) and West Germany (Costa et al., 1988; Dill et al., 1996). *H. septata* was documented in the Paleocene from Georgia (Edwards, 2001).

Hystrichokolpoma granulatum first occurred in this palynozone at depth 2680 m. *H. granulatum* was documented from the Early Eocene-Middle Eocene (Eaton, 1976) and in the Ypresian in England (Islam, 1983). *H. granulatum* was reported from Ypresian-Lutetian in the Netherlands (De Coninick, 1977) and in the Early Paleocene in Israel (Eshet et al., 1992). In India, *H. granulatum* was recorded from Late Paleocene-Eocene (Khanna, 1979) and in the Middle Eocene (Mehrotra et al., 2002). *H. granulatum* was reported in Canada in the Middle Eocene (Head et al., 1989).

Cordosphaeridium fibrospinosum was first recognized in this palynozone at level 2700 m. with a high occurrence in this subzone. *C. fibrospinosum* was observed in England in the Ypresian (Downie et al., 1971) and from Ypresian-Lutetian (Powell, 1992). *C. fibrospinosum* was documented from the Paleocene-Late Eocene in W. Germany (Gocht, 1969), Middle Paleocene-Early Ypresian in Spain (Caro, 1973), Maastrichtian-Paleocene in Maryland

(Benson, 1976), Early Paleocene-Early Eocene in Canada (Brideaux et al., 1976) and in the Early Paleocene in Israel (Eshet et al., 1992).

Ifecysta spp., *Operculodinium*, *Glaphyrocysta* spp., *Apectodinium* spp., *Polysphaeridium* spp and *Spiniferites* recorded in this palynozone were recorded from the Late Paleocene-Early Eocene in northern Niger Delta (Anambra) Basin, Nigeria (Oboh-Ikuenobe et al. (2017). This subzone is recognized in sample intervals from 2580 m – 2520 m.

Age: Thanetian (Latest Paleocene)-Ypresian (Early Eocene)

The stratigraphic significant taxa across the entire palynozone (PZ-IV) suggests a Paleocene-Early Eocene age.

4.3 PALEOECOLOGY AND PALEOPROVINCES

4.3.1 Palaeoecological and paleoclimatic implications from sporomorphs

The palaeoenvironment was determined based on significant palynomorphs taxa with respect to their ecological inclinations and on the overall extents of palynomorph groups. The Albian-Cenomanian section of the studied wells (Lynx-1X, Dzata-1 and Dzata-2A) yielded abundant well preserved sporomorphs (pteridophytes, gymnosperms and angiosperms) few marine palynomorphs (dinocysts). Sporomorphs are continental in origin with their distribution in marine environments being dependent on wind direction, current patterns in basin and water dispersion. Degree of preservation, level of pollen production and nature of the depositional environment are other factors that determine their distribution in marine environments.

Dominant *Classopollis* spp. recovered in this study supports a deposition in a coastal region (Herngreen, 1973; Herngreen et al., 1982). The Cheirolepidiaceae which are the producers of *Classopollis* and ephedroids are xerophytic which are semiarid or arid elements (Jardiné et al., 1974). The sporomorphs dominates (99% of palynomorphs) the marine dinoflagellates (1%). This suggests the Albian-Cenomanian sediments of this study were deposited in a semiarid to arid coastal or near shore environment.

The fern spores were recorded in low amounts in the nearshore Albian-Cenomanian and ?Turonian-Santonian (Palynozone I and II) sediments of the study. These fern spores (e.g. *Deltoidspora*, *Cyathidites*, *Cicatricosisporites*) have been reported to prefer humid conditions and abundance of pteridophytic fern spores suggests a vegetation that grew on moist biotopes or wetlands (Playford, 1971; Schrank, 1987; Schrank and Mahmoud, 1998; Mahmoud and Moawad, 2002; El Beialy et al., 2011). Infrequent to common occurrences of *Inaperturopollenites* and *Araucariacites* documented in palynozone I and II were related with conifer forests and infers deposition in dry hinterlands (Mahmoud and Moawad, 2002; El Beialy et al., 2010).

The Campanian-Early Tertiary (Paleocene-Eocene) sediments (Palynozone III and IV) recovered abundant and diverse marine dinoflagellates which dominates over the sporomorphs (spore and pollen). Most of these sporomorphs were documented from the Late Cretaceous-Early Tertiary sediments from the ASA region (Schrank, 1987; El Beialy, 1995; Herngreen et al, (1996). The sporomorphs representatives are dominated by *Spinizonocolpites*, *Proxapertites*, *Longapertites* and *Foveotriletes* with some triporate (*Proteacidites*, *Echitriporites*).

Longapertites, *Proxapertites* and *Spinizonocolpites* are characteristic elements of the palmae (Muller, 1968; Schrank, 1987; El Beialy, 1995). The term palmae connotes a hot tropical to sub-tropical climate (El Beialy, 1995). According to Germeraad et al. (1968), these taxa are thought to belong to the genus Nypa which flourish in mangrove environments alongside coastal areas of the humid tropics (Schrank, 1998; Herngreen, 1998; El Beialy, 1995).

In the Campanian-Maastrichtian, other plants groups such as the green algae (*Pediastrum*) and *Botryococcus* were common but increased in abundance in the Paleocene-Eocene. *Pediastrum* have been found in high abundances in low salinity lakes and transported by fluvial systems into nearshore shelfal situations (Singh et al., 1981; Hutton, 1988). *Botryococcus* has been reported from ancient lacustrine, fluvial, lagoonal, and deltaic/nearshore marine sediments (Piasecki, 1986; Riding et al., 1991; Williams, 1992; Deaf, 2009). Fresh to brackish water conditions can be inferred from the presence of *Botryococcus*.

Based on dominant sporomorphs (*Longapertites*, *Proxapertites*) discussed above, the Campanian-Maastrichtian sediments are suggested to be deposited in a mangrove (brackish) water environments and from brackish to fresh water environment for the Paleocene-Eocene sediments in a hot tropical climate.

4.3.1.1 Paleofloral Provinces

Herngreen et al. (1996) established three palynofloral areas within the Cretaceous. These regions appear to be identified with the contemporary latitudinal climatic zones where the tropical or close central Africa-South America (ASA) region occupies. The three provinces are:

- The Pre-Albian Early Cretaceous *Dicheiropollis etruscus/Afropollis Province*.
- The Albian to Cenomanian Elaterate Province.
- The Senonian Palmae Province

The terrestrial microfloras affirms which of the provinces the deposition of the palynozones occurred.

4.3.1.1.1 *The Pre-Albian Early Cretaceous Dicheiropollis etruscus/Afropollis Province.*

The characteristics of this province are;

- The predominance of *Classopollis* and good representation of other gymnospermous pollen, especially Araucariacean and the ephedroid plexus which generally alternate in abundance in the Northern South American and African (except southern) sporomorph associations.
- Less common Bisaccate pollen and portrayed by small species with low numbers of spores.
- The occurrence of stratigraphically relevant taxa, in a stratigraphic order *Dicheiropollis etruscus*, *Tucanopollis crisopolensis*, *Afropollis* spp.

4.3.1.1.2 Albian-Cenomanian Elaterate Province

This palynofloristic area was named Northern Gondwana territory by Brenner (1976) and *Galeocornea* paleophytogeoprovince by Srivastava (1978). It was later renamed as the *Elaterosporites* phytogeoprovince by Srivastava (1981). Herngreen and Jimenez (1990) and Dino et al. (1999) studied a new data and averred that the distribution of these elaterates transcends the Africa and South America (ASA) continents as far back as China and Papua-New Guinea.

The characteristics of this paleophytogeoprovince are;

- Presence of high frequencies elater-bearing taxa, including the genera *Elaterocolpites*, *Elateroplicites*, *Elateropollenites*, *Elaterosporites*, *Galeocornea*, *Senegalosporites* and *Sofrepites*.
- Scarcity of fern spores. A large portion of the spores have a place with the psilatrilete group, *Cicatricosisporites* or *Crybelosporites pannuceus*. Numerous other cosmopolitan taxa happen unpredictably and occasionally.
- Absence of bi-and trisaccate gymnospermous pollen. *Classopollis* might be very common.
- High rates and a noteworthy morphological diversification of angiospermous pollen grains. Common *Afropollis*, *Cretacaeiporites*, *Hexaporotricolpites* and *Triorites* (which showed up in the Late Cenomanian) occurred with psilate just as reticulate tricol(por)ate species. Angiospermous pollen represented up to 70% in the low paleolatitude areas by the Late Albian time.
- Common ephedroid pollen, for example, *Ephedripites*, *Equisetosporites*, *Gnetaceaepollenites* and *Steevesipollenites*. This richly diverse and numerous polyplicate group with straight or twisted ridges are characteristic of the Elaterates Province.

Palynozone I and II as discussed earlier was deposited in the Albian to Cenomanian Elaterate Province as the sporomorph assemblage conform to the above attributes of Elaterate Province (Herngreen et al., 1996).

4.3.1.1.3 The Senonian Palmae Province

Herngreen (1980) established the Late Cretaceous Palmae Province of Africa and South America which was later redefined in greater detail limiting it to the Senonian by Herngreen and Chlonova (1981). The term Palmae Province refers to a hot tropical to sub-tropical climate and the assemblages are suggestive of a warm and humid climate (Herngreen, 1998). The palynozone IV (Paleocene-Eocene) of present study recorded taxa that fit the Senonian Palmae Province.

This province is constituted by surge in numbers (10-50%) of monocolpate Palmae types of the Psila-/retimonocolpites plexus. Taxa of the province include the genus of *Buttinia*, *Echitriporites* and the monocolpates *Longapertites*, *Mauritiidites*, *Spinizonocolpites* and *Proxapertites* which are considered to inhabit mangrove environment of the humid tropics.

The Campanian-Maastrichtian and Paleocene-Eocene (palynozone III and IV) of the study fits into the Senonian Palmae Province.

4.3.2 Paleoecological and paleoclimatic implications from dinoflagellates

Palynozone III and IV are primarily dominated by dinoflagellate cysts in all the studied wells (Lynx-1X, Dzata-1 and Dzata-2A). The gonyaulacoids (53-82% of dinocysts) dominated over the peridinoids (18-47% of dinocysts) in intervals from 3000 – 3300 m in Lynx-1X, gonyaulacoids (50-100%) and peridinoids (0-50%) from 2420 – 2781 m in Dzata-2A, gonyaulacoids (81-100%) and peridinoids (0-19%) from 2450 – 2910 m in Dzata-1 (Fig. 4.7, 4.8 and 4.9).

The Albian-Cenomanian (Palynozone I) and ?Turonian-Santonian (Palynozone II) of studied wells are dominated by pollen grains with few dinoflagellates such as *Oligosphaeridium complex*, *Subtilisphaera*, *Cyclonephelium*, *Spiniferites ramosus*, *Odontochitina porifera*. Sporomorphs dominated by sphaeroidal pollens supports the deposition in a nearshore/shallow marine environment for this assemblage.

According to Davies et al. (1982), there are four categories by which dinoflagellates can be utilized for the recognition of paleoenvironments which includes;

- The absolute abundance of dinoflagellates.
- The relative abundance of dinoflagellates to other palynomorph types.
- Dinoflagellate species variety and dominance.
- The dinoflagellate assemblage composition.

In this study, the gonyaulacoids taxa in the Campanian-Maastrichtian (PZ-III) are mostly genus of *Adnatosphaeridium, Cordosphaeridium*, *Glaphyrocysta*, *Areoligera* and *Spiniferites* whilst the peridinoid taxa consists of *Andalusiella*, *Palaeocystodinium*, *Cerodinium* and *Phelodinium*. The Paleocene-Eocene (PZ-IV) gonyaulacoids are dominated by *Spiniferites* association which include *Polysphaeridium*, *Homotryblium*, *Operculodinium, Diphyes* in addition to those genera observed in the Campanian-Maastrichtian. *Apectodinium* was observed in PZ-IV together with the peridinoid taxa in the Campanian-Maastrichtian.

Downie et al. (1971) recognized four dinoflagellate cysts-acritarch associations in the Early Eocene rocks of southern England and were named after the genus of the dominant species. These associations are:

- *Spiniferites* (as *Hystrichosphaera*) Association, which is dominated by species of the genera *Achomosphaera*, *Hystrichosphaeridium*, *Cordosphaeridium* and *Spiniferites*.
- *Areoligera* Association, dominated by the genera *Areoligera* and *Glaphyrocysta*.
- *Micrhyridium* Association, dominated by the genera of acritarch *Micrhyridium* and *Comasphaeridium*.
- *Wetzeliella Association,* dominated by the genera *Wetzeliella* and *Deflandrea*.

They opined that *Spiniferites* and *Areoligera* Associations are indicative of open marine environment; *Wetzeliella* Association indicates lagoonal, estuarine and brackish water environments; *Micrhyridium* Association suggesting inner neritic depositional environment. Majority of the samples in palynozone III (Campanian-Maastrichtian) are dominated by *Spiniferites* Association with few being dominated by *Areoligera* Association while palynozone IV (Paleocene-Eocene) had abundance of both *Spiniferites* Association and *Areoligera* Association.

Islam (1984) widened the concepts of Downie et al. (1971) and identified several groups such as the *Spiniferites* assemblage (*Achomosphaera*, *Hystrichosphaeridium*, *Cordosphaeridium*) which is typical of open marine environmental conditions; *Adnatosphaeridium, Glaphyrocysta* and *Areoligera* group which are typical of high energy open marine environments; Wetzelielloideae assemblage (*Apectodinium*, *Charlesdowniea*, *Dracodinium* and *Wetzeliella*) which are normally found in lagoonal, estuarine or brackish environments. The *Wetzeliella* Association in the present study consists of peridinoids such as *Andalusiella*, *Palaeocystodinium*, *Cerodinium*, *Phelodinium* and *Apectodinium* for palynozone IV.

In the Campanian-Maastrichtian (Palynozone III) of Lynx-1X well, the gonyaulacoids dominates over the peridinoids from intervals 3140 m – 3300 m which suggests deposition in an outer neritic environment while the intervals 2820 – 3120 m had relatively equal abundance of gonyaulacoids and peridinoids suggesting deposition in an inner-middle neritic depositional environmental conditions (Fig.4.7). The Paleocene-Eocene (Palynozone IV) of Lynx-1X well intervals (2700 – 2740 m) recorded relatively equal abundance of *Wetzeliella* Association and *Spiniferites* Association which was replaced by dominant *Spiniferites* Association from 2680 - 2520 m (Fig. 4.10). In palynozone III, open marine gonyaulacoids (*Spiniferites* Association) dominated the entire samples of Dzata-1 and Dzata-2A wells which suggests a deposition in an open marine (outer neritic) depositional environment (Fig. 4.8 & 4.9).

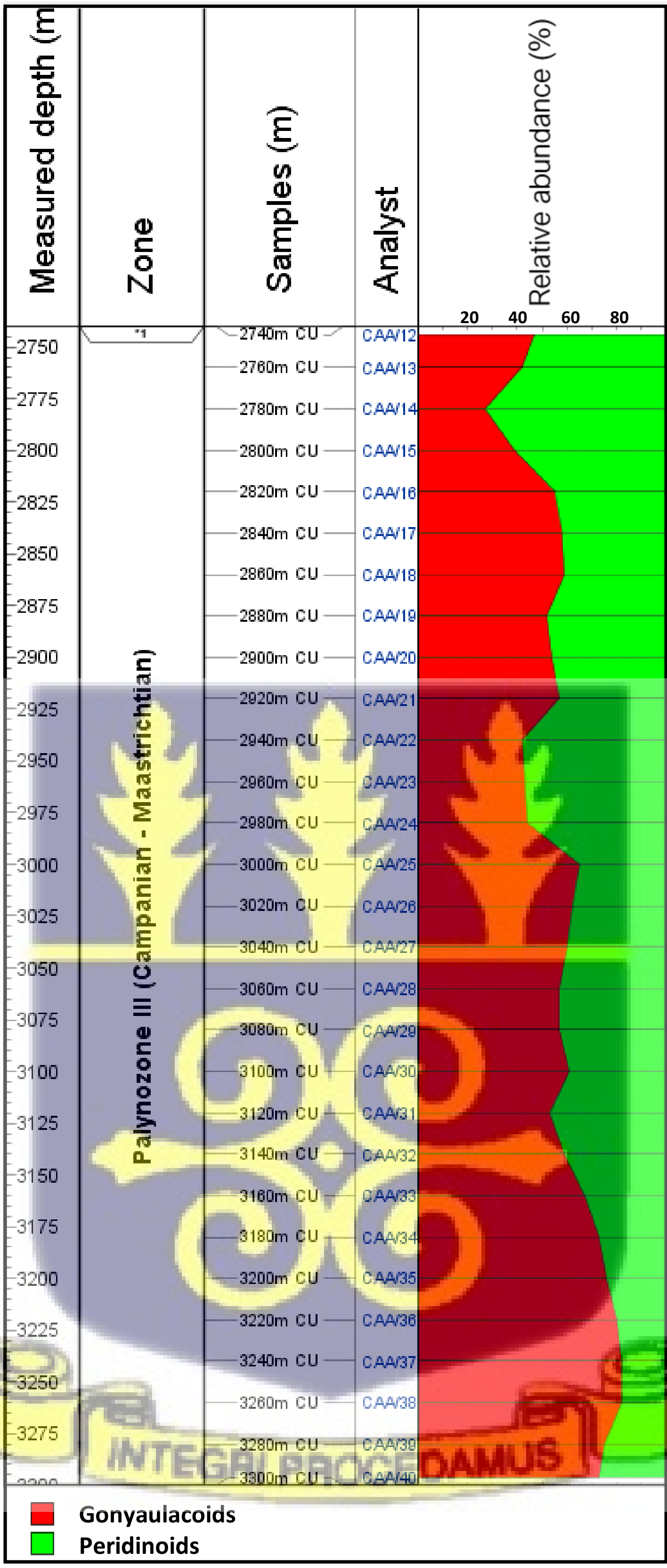

Figure 4.7: Relative percentage composition of Gonyaulacoids and Peridinoids abundance in Palynozone III of Lynx-1X well.

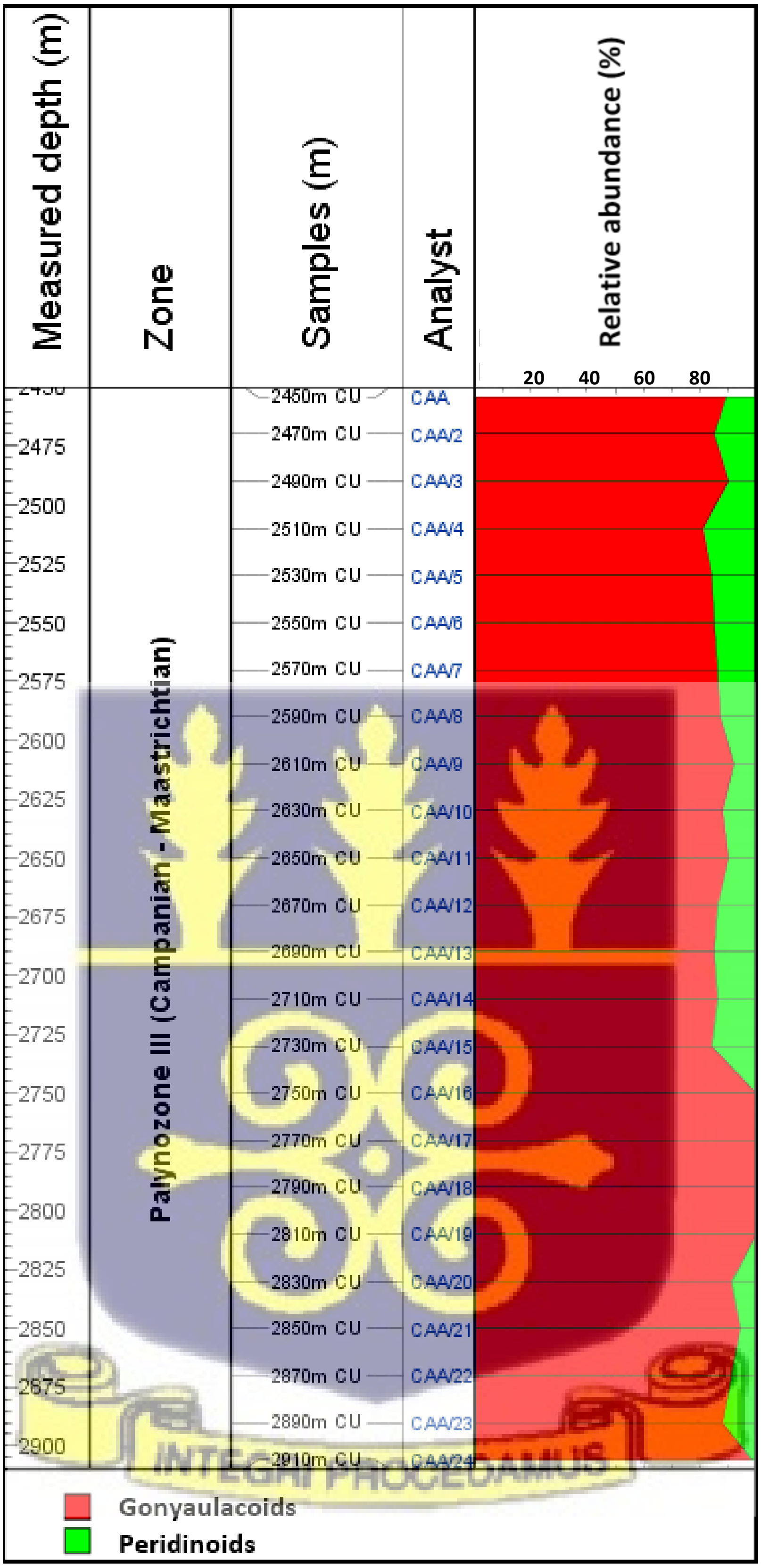

Figure 4.8: Relative percentage composition of Gonyaulacoids and Peridinoids abundance in Palynozone III of Dzata-1 well.

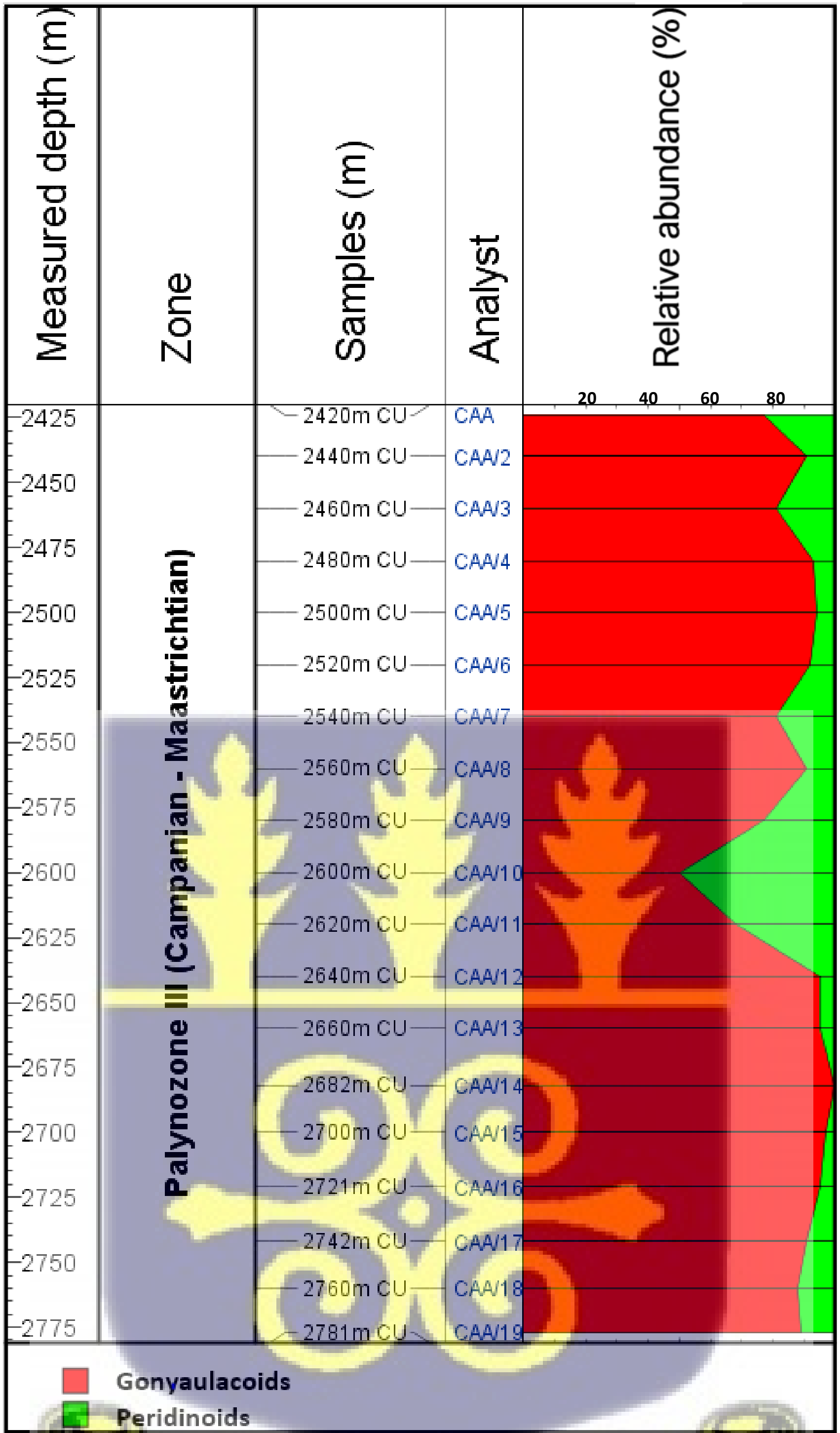

Figure 4.9: Relative percentage composition of Gonyaulacoids and Peridinoids abundance in Palynozone III of Dzata-2A well.

Apectodinium in PZ-IV was persistent throughout the studied intervals with relatively high numbers which indicates a warmer paleoenvironments. According to Powell et al. (1996) and Mudge & Bujak (1996), abundance of *Apectodinium* was identified with the Paleocene/Eocene

Thermal Maximum (PETM) in higher amounts which could be utilized to recognize the Thanetian within PZ-IV. Various palynological study of the mid and high latitude localities reported an *Apectodinium* acme (40% expansion in the dinoflagellate cyst assemblage during the PETM) and related this increment to worldwide climatic warming (Iakovleva et al., 2001; Crouch et al., 2003, 2014; Sluijs and Brinkhuis, 2009). This supports the interpretation of a warmer paleoenvironments for PZ-IV.

Palynozone IV of present study was therefore deposited in a middle-outer neritic depositional environment based on recovered dinoflagellate cysts.

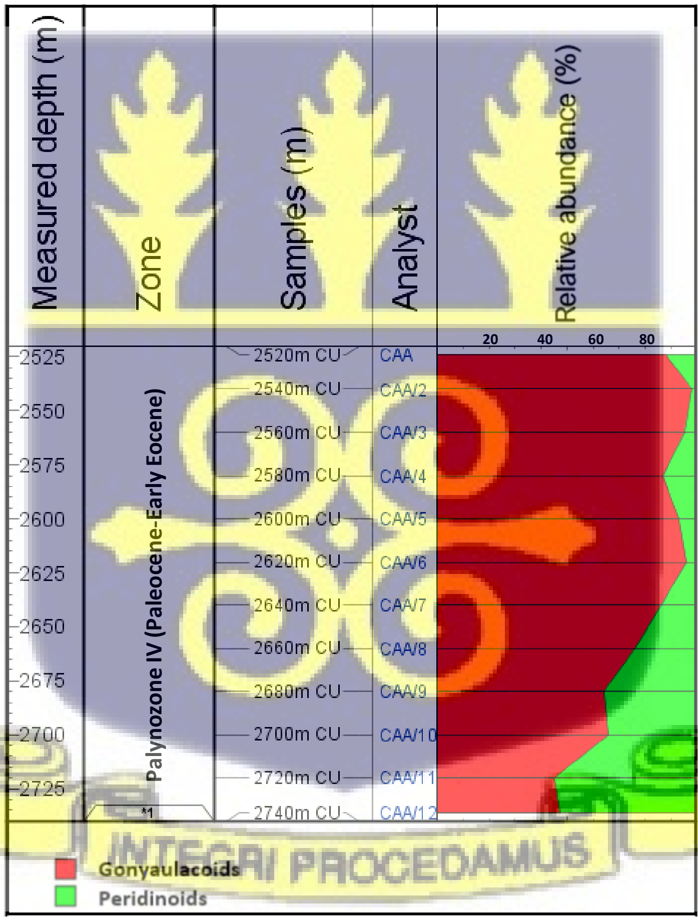

Figure 4.10: Relative percentage composition of Gonyaulacoids and Peridinoids abundance in Palynozone IV of Lynx-1X well.

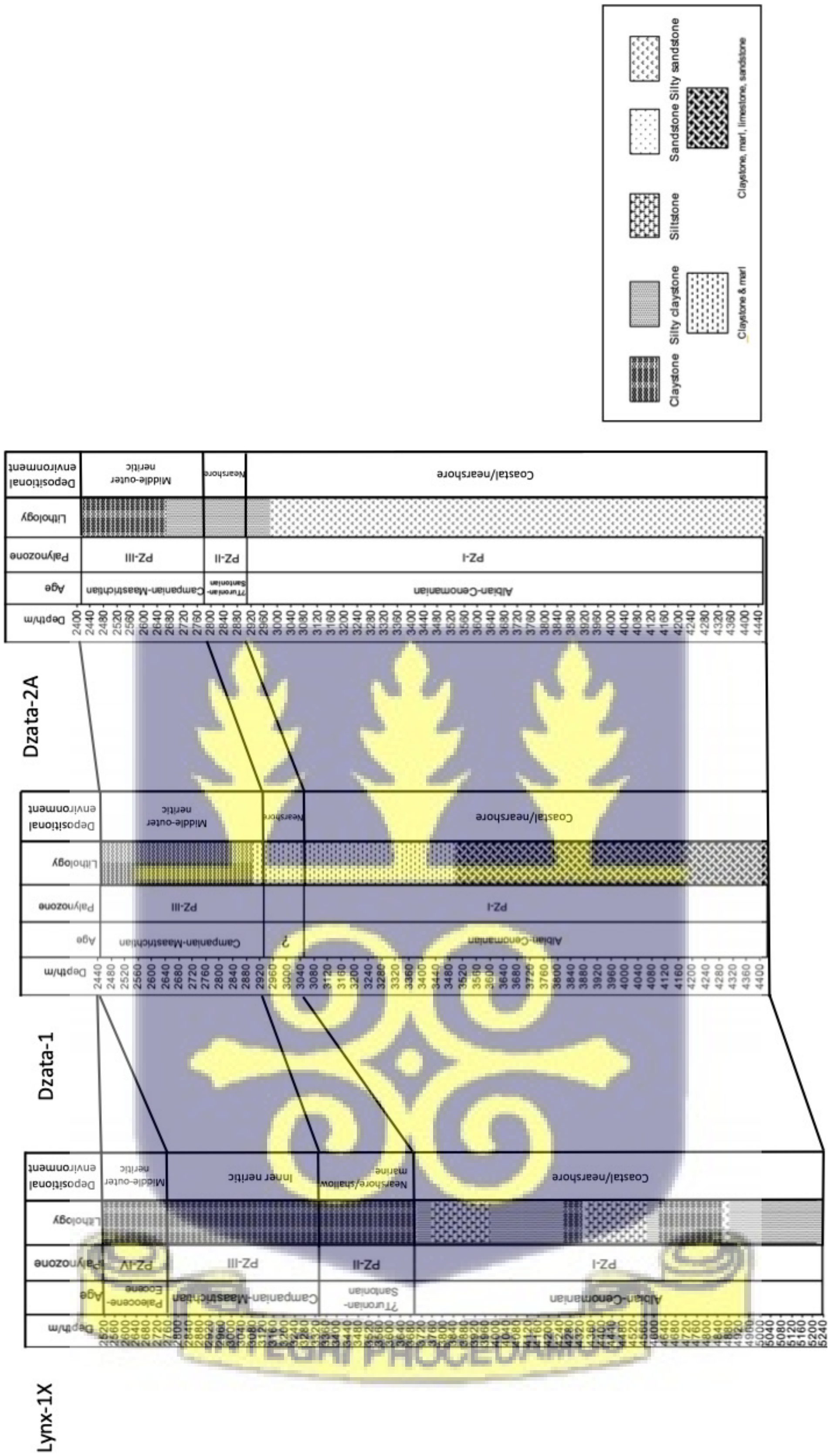

Figure 4.11: Correlation of lithology, palynozones and depositional environments of Lynx-1X, Dzata-1 and Dzata-2A.

4.3.2.2 Dinoflagellates Provincialism

Lentin and Williams (1980) investigated the distribution pattern of Late Cretaceous peridiniacean dinoflagellates cyst from North America, South America and Africa and established three provincial suites. They opined that these suites show regional differentiation rather than local paleoecological control. These suites are;

- The Malloy or Tropical-Subtropical suite, constituted by the genera *Andalusiella*, *Cerodinium*, *Phelodinium* and *Senegalinium*.
- The Williams or Warm Temperate suite, with deflandreoid dinoflagellates mainly represented by the genera *Alterbidium*, *Spinidinium*, *Chatangiella* (small to medium sizes) and *Isabelidium*.
- The McIntyre or boreal-arctic suite, characterized by *Laciniadinium* and *Chatangiella* (larger taxa).

The dinocyst collections recovered in palynozone III and IV demonstrated abundance of the "Malloy suite" taxa, including species of the genera *Andalusiella*, *Cerodinium*, *Senegalinium* and *Phelodinium*. Based on recovered peridiniacean dinoflagellates cyst in this study, the Late Cretaceous (PZ-III)-Early Tertiary (PZ-IV) fits a Tropical to Subtropical or Malloy suite of Lentin and Williams (1980).

The equivalent of Malloy suite was also recognized in the Campanian to Danian sediments from the peri-Mediterranean basin (Brinkhuis and Zachariasse, 1988; Slimani et al., 2016; M'Hamdi et al., 2014), in Cote d'Ivoire and Ghana (Oboh-Ikuenobe et al., 1998; Masure et al., 1998; Sanchez-Pellicer et al., 2017; Guede et al., 2019), in Senegal (Jan du Chene, 1988), in Ghana (Atta-Peters and Salami, 2004), Colombia and Venezuela (Yepes, 2001) and southeastern USA (Firth, 1993; Srivastava, 1995).

EXPLANATION OF PLATE 1

1: *Senoniasphaera inornata* (Drugg, 1970) Stover and Evitt, 1978; Lynx-1X, 2680 m, T46.

2: *Lingulodinium echinatum*, (Menéndez, 1965) Guerstein et al., 2008. Emend. Guerstein et al., 2008; Lynx-1X, 2520 m, W62.

3, 5: *Florentina* spp. ; Lynx-1X, 2520 m, T40.

4,6: *Diphyes colligerum* (Deflandre and Cookson, 1955) Cookson, 1965, emend. Cookson, 1965, emend. Goodman and Witmer, 1985; Lynx-1X, 2520 m, V58.

4: Lynx-1X, 2680 m, O58.

5: Lynx-1X, 2700 m, C48.

7: *Diphyes bifidium* (Antolinez-Delgado and Oboh-Ikuenobe 2007); Lynx-1X, 2520 m, O63.

8: Lynx-1X, 2520 m, K46.

9: *Polysphaeridium zoharyi*, (Rossignol, 1962) Bujak et al., 1980; Lynx-1X, 2580 m, M63.

10: *Polysphaeridium subtile*, Davey and Williams, 1966. emend. Bujak et al., 1980; Lynx-1X, 2520 m, C48.

11: *Operculodinium centrocarpum* (Deflandre and Cookson, 1955) Wall, 1967; Lynx-1X, 2520 m, J71.

12: Lynx-1X, 2520 m, J58.

PLATE 1

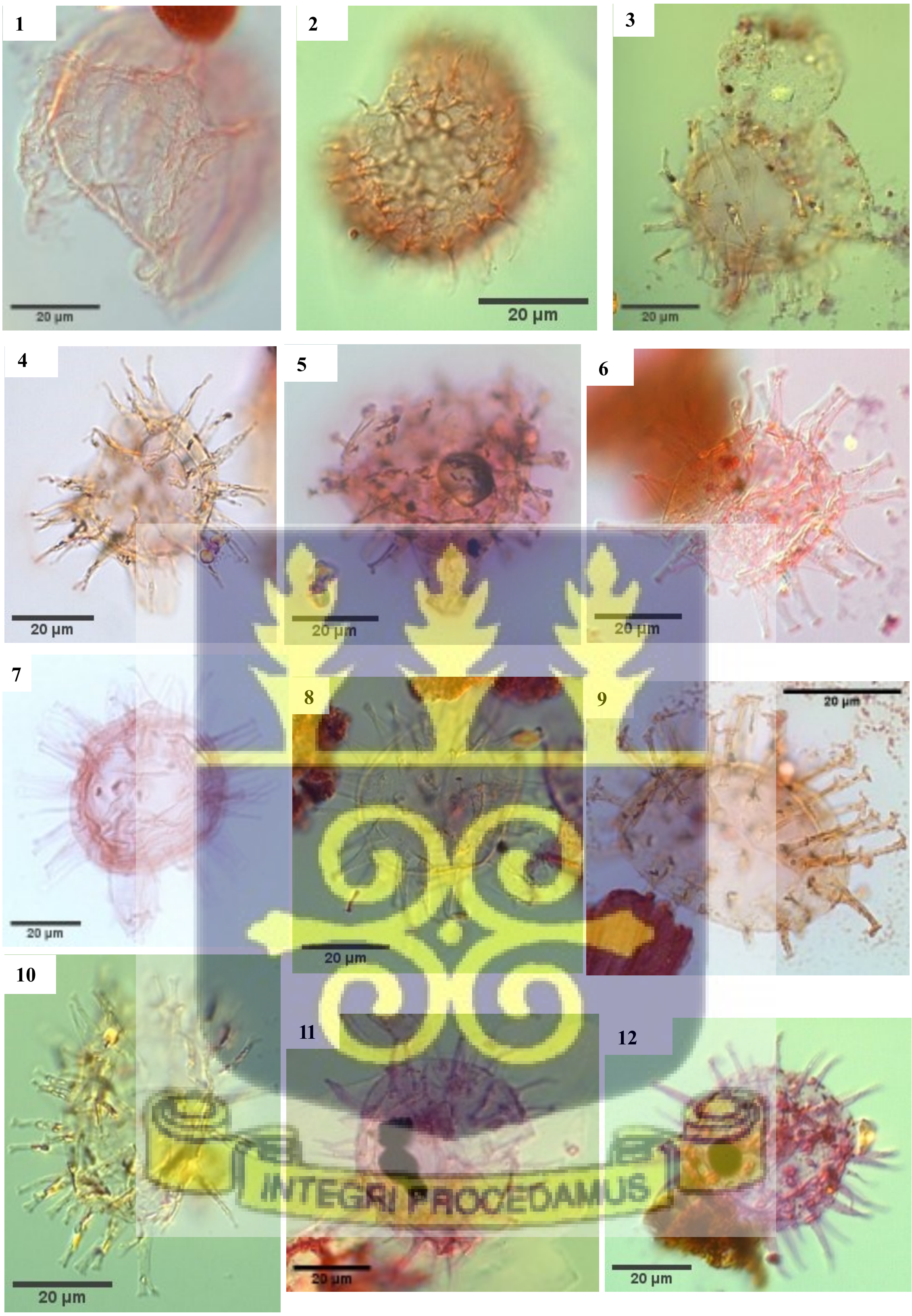
1
20 µm
2
20 µm
3
20 µm
4
20 µm
5
20 µm
6
20 µm
7
20 µm
8
20 µm
9
20 µm
10
20 µm
11
20 µm
12
20 µm

EXPLANATION OF PLATE 2

1: *Eocladopyxis* cf. *peniculata,* Morgenroth, 1966; emend. McLean, 1976; Lynx-1X, 2580 m, C62.

2: *Selenopemphix nephroides*, Benedek, 1972 Benedek, 1972. emend. Bujak et al., 1980; Benedek and Sarjeant, 1981; Head (1993); Lynx-1X, 2520 m, S62.

3, 4: *Operculodinium centrocarpum,* (Deflandre and Cookson, 1955) Wall, 1967; Lynx-1X 2520 m, W42.

4: Lynx-1X, 2520 m, P60.

5: *Apectodinium homomorphum*, (Deflandre and Cookson, 1955) Lentin and Williams, 1977; Lynx-1X, 2580 m, V56.

6: *Apectodinium* sp.; Lynx-1X, 2600 m, Y50.

7: *Homotryblium pallidum*, Davey and Williams, 1966; Bujak et al., 1980; Lynx-1X, 2540 m, W52.

8: *Homotryblium floripes*, (Deflandre and Cookson, 1955) Stover, 1975; Lynx-1X, 2600 m, O71.

9: *Homotryblium* cf. *tenuispinosum*, Davey and Williams, 1966; Lynx-1X, 2600 m, K69.

10, 11, 12: *Hafniasphaera septata* (Cookson and Eisenack, 1967) Hansen, 1977: Lynx-1X, 2540 m, Z62.

11: Lynx-1X, 2540 m, Y72.

12: Lynx-1X, 2540 m, W49.

PLATE 2

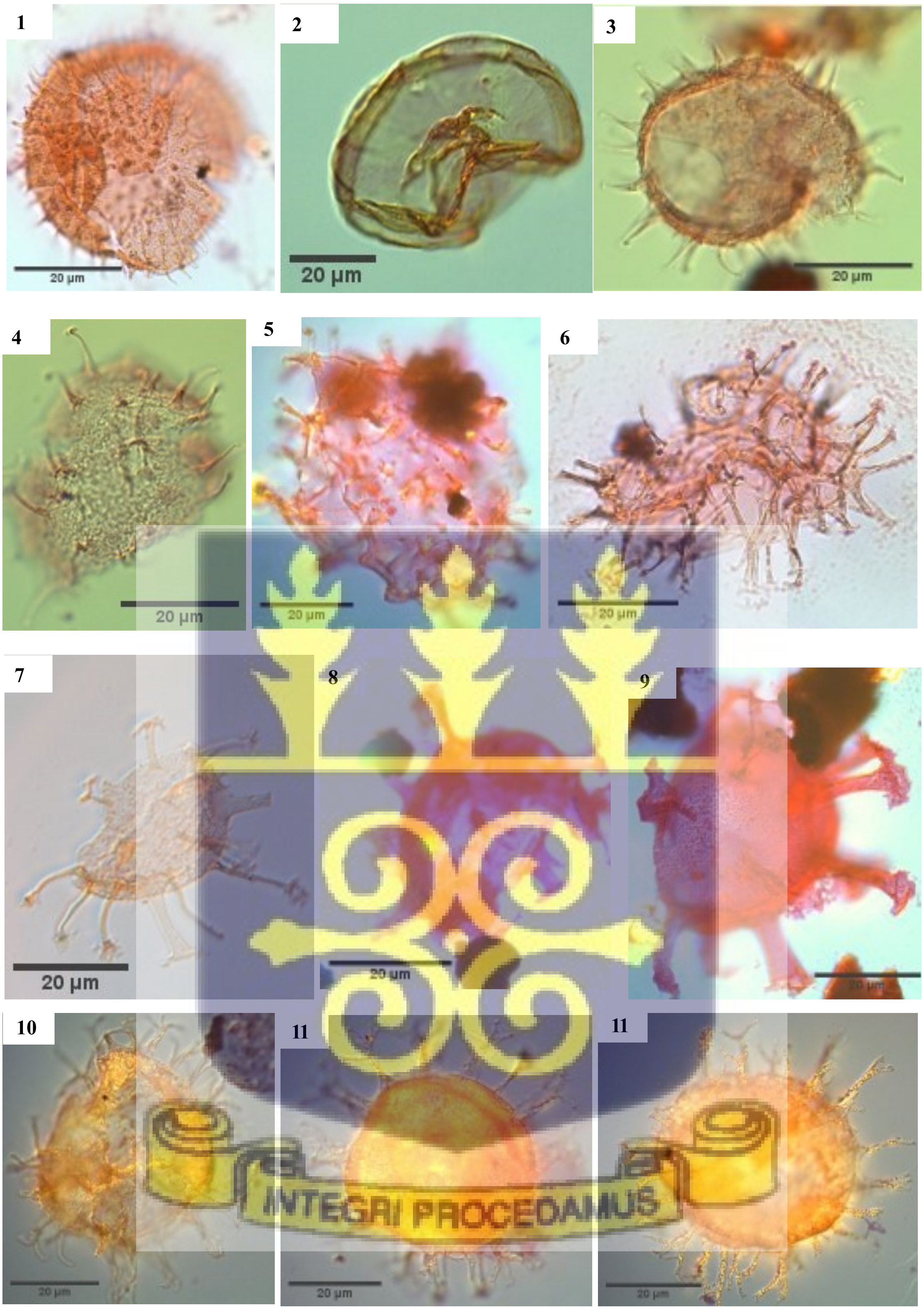
1
20 µm
2
20 µm
3
20 µm
4
20 µm
5
20 µm
6
20 µm
7
20 µm
8
20 µm
9
10
11
20 µm
11
20 µm

EXPLANATION OF PLATE 3

1: Cf. *Ifecysta lappacea* Lynx-1X 2660 m, Q61.

2,3: *Turbiosphaera galeata*, Eaton, 1976; Lynx-1X, 2560 m and 2540 m, V61 & W46.

4: *Hystrichostrogylon*; Lynx-1X, 2540 m, T40.

5: *Hystrichokolpoma proprium* (Marheinecke, 1992) Fauconnier and Masure, 2004; Lynx-1X, 2720 m, Q46.

6: *Hystrichokolpoma granulatum*, Eaton, 1976; Lynx-1X, 2540 m, W42.

7: *Damassadinium* sp. Lynx-1X, 2560 m, S54.

8: *Damassadinium heterospinosum* (Matsuoka, 1983) Fensome et al., 1993; lynx-1X, 2560 m, W58.

9: *Damassadinium californicum*, (Drugg, 1967) Fensome et al., 1993; Lynx-1X, 2560 m, M61.

10, 11: *Ifecysta* cf. *fusiforma*, Antolinez-Delgado and Oboh-Ikuenobe, 2007; Lynx-1X, 2660 m, H56.

12: *Areosphaeridium diktyoplokum*, (Klumpp, 1953) emend. Eaton, 1971; emend. Stover and Williams, 1995; Lynx-1X. 2620 m, Y47.

PLATE 3

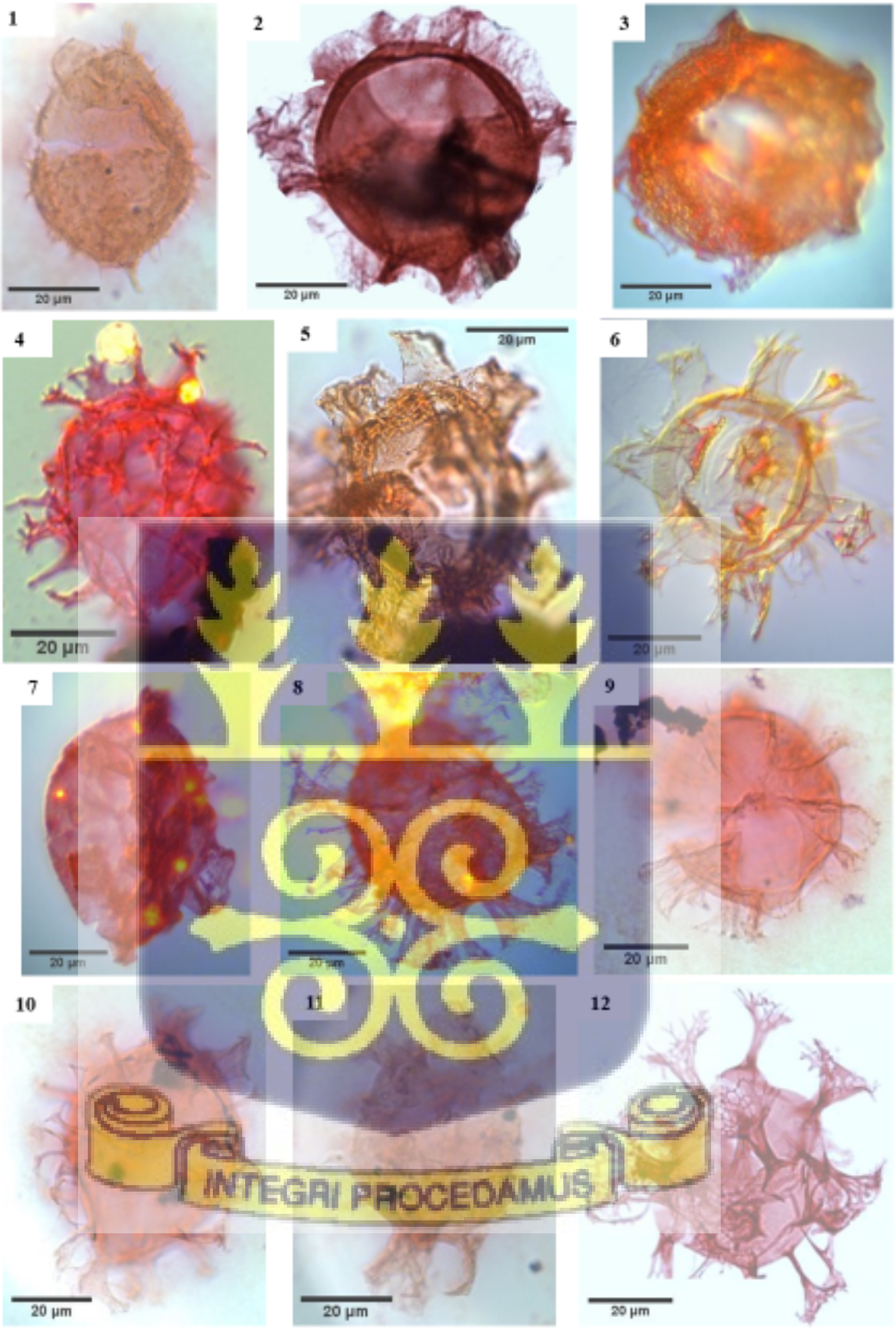
1
20 µm
2
20 µm
3
20 µm
4
20 µm
5
20 µm
6
7
8
9
20 µm
10
20 µm
11
20 µm
12
20 µm

EXPLANATION OF PLATE 4

1: *Leptodinium* sp. cf. *subtile* Klement 1960; Lynx-1X, 2600 m, U62.

2: *Leptodinium subtile*, Klement 1960; Lynx-1X, 2600 m, S50.

3: *Diphyes colligerum*; Lynx-1X, 2620 m, Q53.

4: *Fibrocysta lappacea* (Drugg, 1970) Stover and Evitt, 1978; Lynx-1X, 2700 m, S57.

5: *Diphyes bifidum,* Antolinez-Delgado and Oboh-Ikuenobe, 2007; Lynx-1X, 2660 m, T20.

6: *Florentina* cf. *mantellii*; Dzata-2A, 2600 m, S6.

7: *Florentinia mantellii* (Davey & Williams 1966) Davey and Verdier 1973; Dzata-2A, 2580 m, T56.

8: *Florentinia cooksoniae,* (Singh, 1971) Duxbury, 1980. emend. Duxbury, 1980; Dzata-1, 3150 m, V48.

9: *Florentinia laciniata*; Dzata-2A, 2600 m.

10: *Florentinia* sp.1; Dzata-1, 2850 m.

11: *Exochosphaeridium* sp.; Lynx-1X, 2700 m, C49.

12: *Xenascus ceratioides*, (Deflandre, 1937) Lentin and Williams, 1973; Lynx-1X 2860 m, K54.

PLATE 4

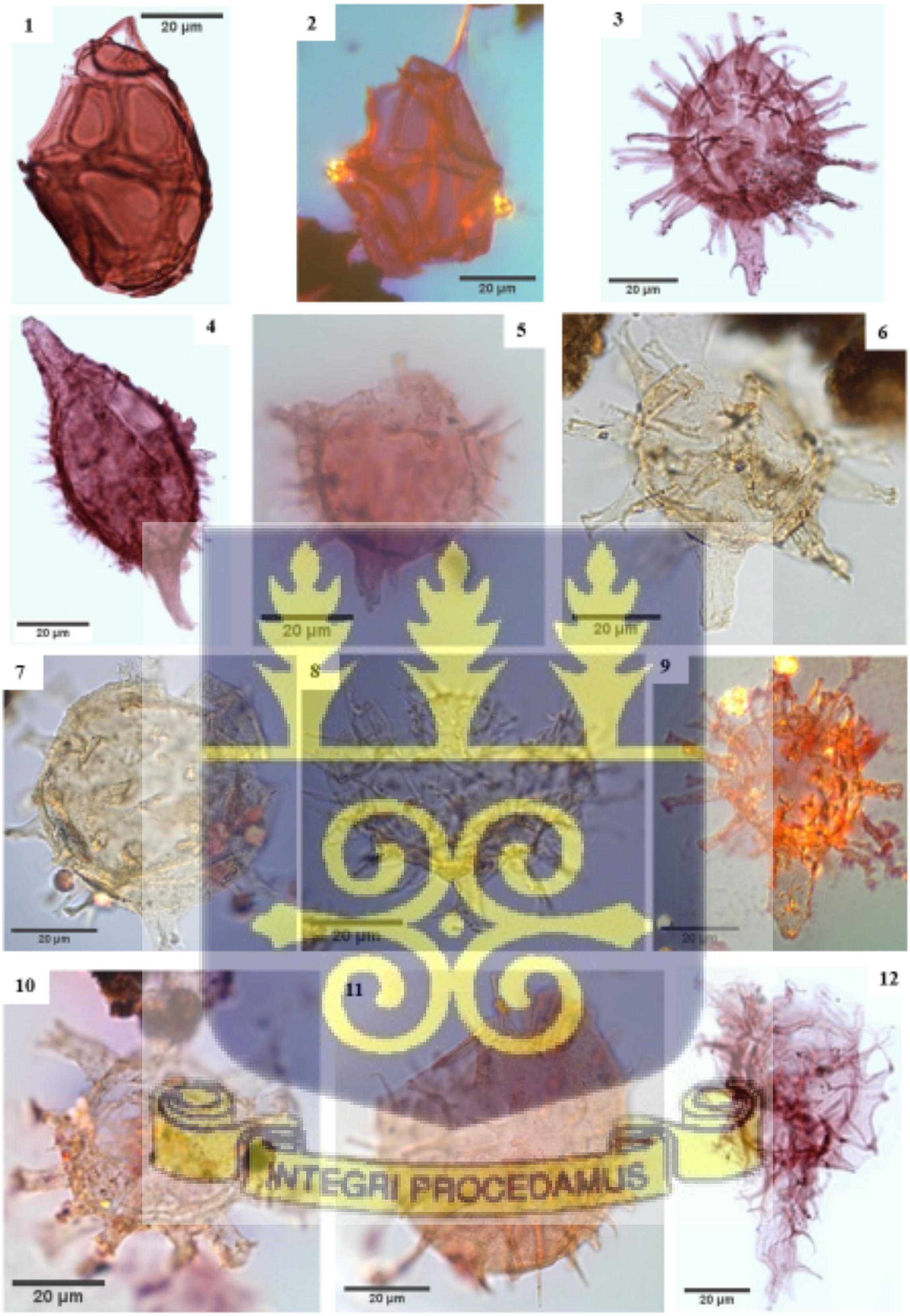
1
20 µm
2
20 µm
3
20 µm
4
20 µm
5
20 µm
6
20 µm
7
20 µm
8
20 µm
9
20 µm
10
20 µm
11
20 µm
12
20 µm

EXPLANATION OF PLATE 5

1: *Exochosphaeridium*? arnace; Lynx-1X, 3180 m, S43.

2: *Leberidocysta* sp.; Lynx-1X, 2860 m, U62.

3: *Senoniasphaera inornata*, (Drugg, 1970) Stover and Evitt, 1978; Lynx-1X, 2720 m, Q46.

4, 5, 6: *Glaphyrocysta* spp.; Lynx-X, 2660 m; M38.

5: Lynx-1X, 2640 m, Y49, S47.

7: *Glaphyrocysta semitecta* (Bujak et al., 1980) Lentin and Williams, 1981; Lynx-1X, 2640 m, S39.

8: *Glaphyrocysta ordinata* (Williams and Downie, 1966) Stover and Evitt, 1978; Lynx-1X, 2640 m, X58.

9: *Glaphyrocysta retiintexta* (Cookson, 1965) Stover and Evitt, 1978; Lynx-1X, 2640 m, J59.

10: *Areoligera* sp.1; Lynx-1X, 2640 m, W64.

11: *Areoligera* sp.2; Lynx-X, 2640 m, W64, D41.

12: *Adnatosphaeridium multispinosum*, Williams and Downie 1966; Lynx-1X, 2560 m, R44.

PLATE 5

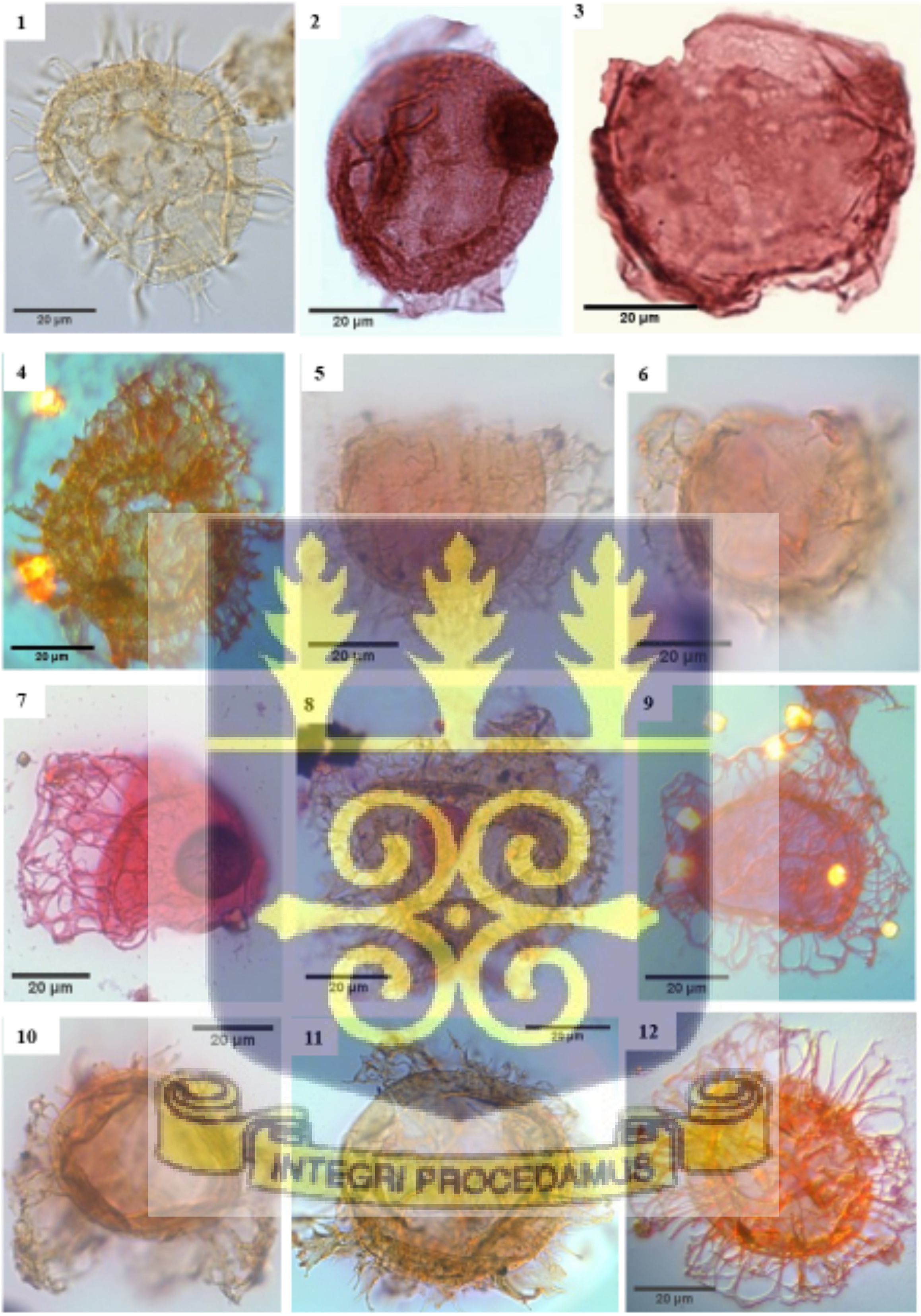

EXPLANATION OF PLATE 6

1,2, 3, 4: *Adnatosphaeridium multispinosum,* Williams and Downie 1966; Lynx-1X, 2560 m, (C52 & V45).

3,4: Lynx-1X, 2540 m, (Y60 & S50).

5,6: *Cordosphaeridium inodes* (Klumpp) Eisenack 1963; Lynx-1X, 2540 m, (R43 and G48).

7: *Surculodinium longifurcatum*; Lynx-1X, 2680 m, T59.

8: *Cordosphaeridium fibrospinosum*, Davey and Williams, 1966; Lynx-1X, 2640 m, W67.

9: *Achomosphaera* cf. *verdieri*; Lynx-1X, 2640 m, V53.

10: *Odontochitina porifera,* Cookson, 1956; Lynx-1X, 3360 m, X49.

11: *Oligosphaeridium* cf. *poculum*; Dzata-1, 3030 m, D45.

12: *Spiniferites sabulus*, Lynx-1X, 2760 m, Q46.

PLATE 6

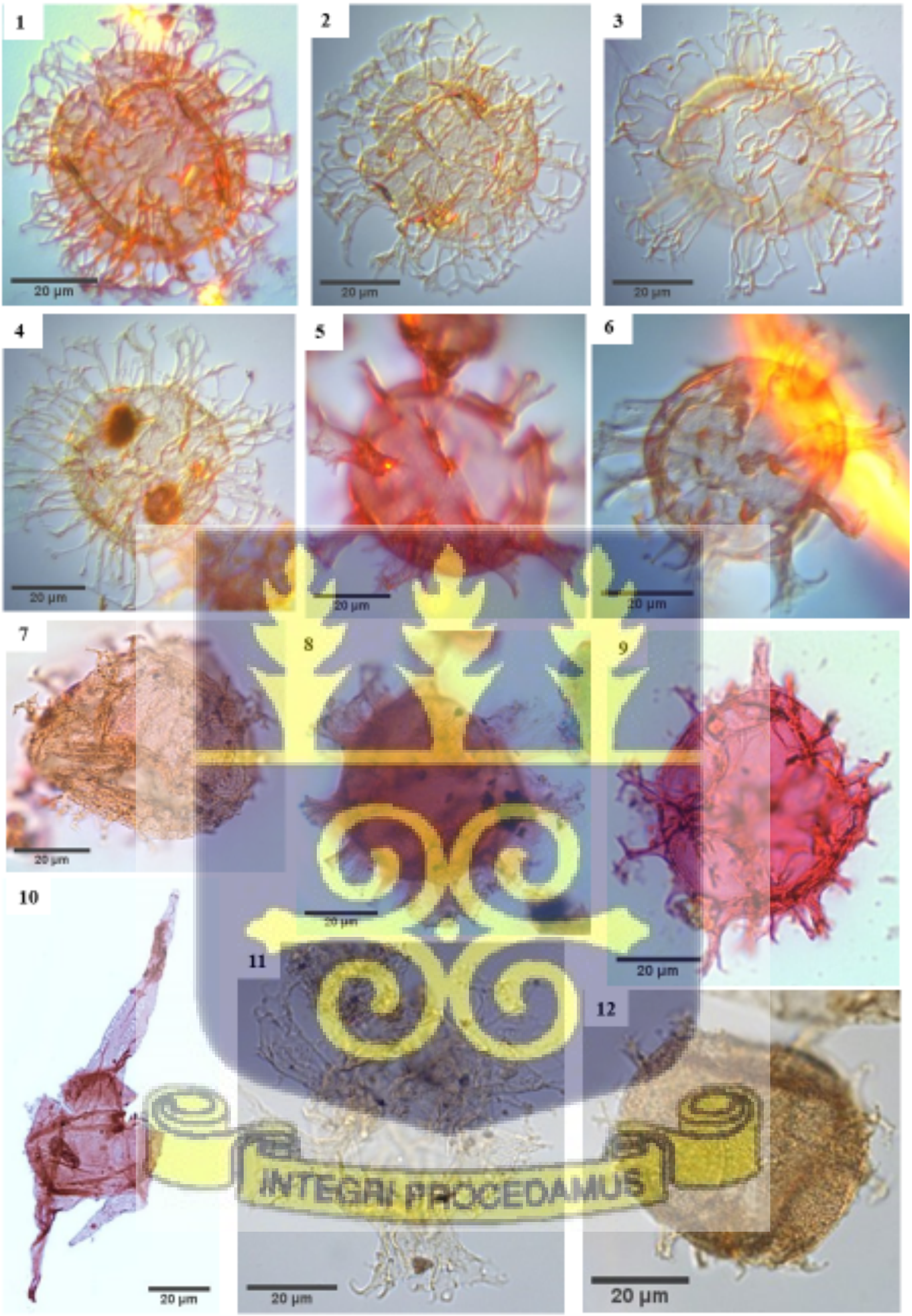
1
20 µm
2
20 µm
3
20 µm
4
20 µm
5
20 µm
6
20 µm
7
20 µm
8
20 µm
9
20 µm
10
20 µm
11
20 µm
12
20 µm

EXPLANATION OF PLATE 7

1,2,3: *Oligosphaeridium complex* (White, 1842) Davey and Williams, 1966; Lynx-1X, 3220 m, (L55 and K46).

1: Dzata-2A, 3063 m, P54.

4,5: *Spiniferites ramosus*; Lynx-1X, 2540 m, (H43 and D49).

6, 7, 8: *Achomosphaera* spp.1; Lynx-1x, 2540 m, W45.

7: Lynx-1X, 2520 m, Y52.

8: Lynx-1X, 2520 m, Q61.

9, 10, 11: *Spiniferites* spp.; Lynx-1X, 2520 m, P69.

10: Lynx-1X, 2520 m, G60.

11: Lynx-1X, 2540m, V50.

PLATE 7

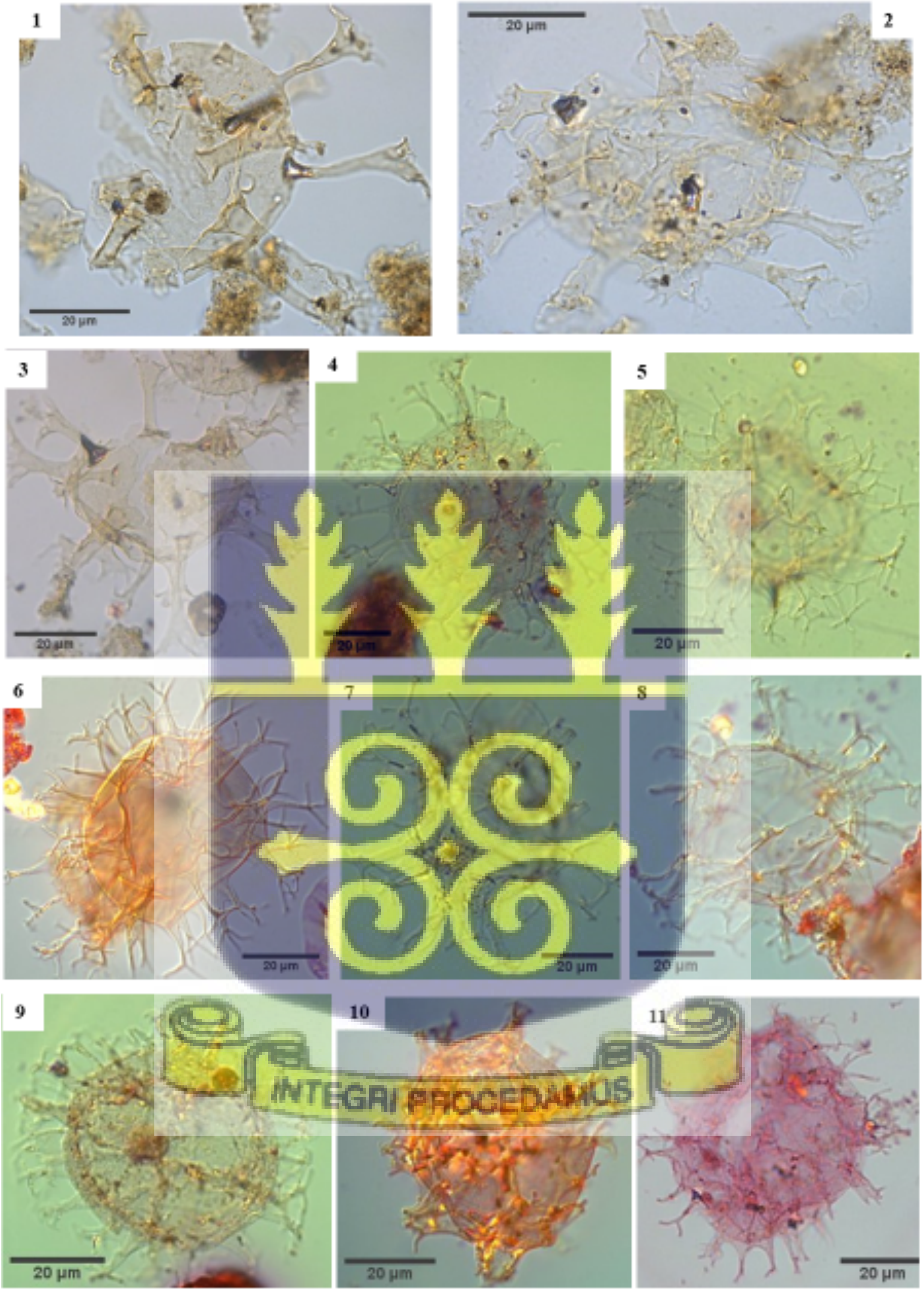

PLATE 8

1: *Spiniferites fluens* (Hansen, 1977) Stover and Williams, 1987; Lynx-1X, 2540 m, R46.

2: *Spiniferites fluens* (Hansen, 1977) Stover and Williams, 1987; Lynx-1X, 2560 m, J64.

3: *Spiniferites hyalospinosus* (Hansen, 1977) Stover and Williams, 1987; Lynx-1X, 2540 m, R47.

4: *Spiniferites bulloideus* (Deflandre and Cookson, 1955) Sarjeant, 1970; Lynx-1X, 2540 m, K46.

5, 6: *Spiniferites* cf. *mirabilis* (Rossignol, 1964) Sarjeant, 1970; Lynx-1X, 2540 m, V68.

7: *Spiniferites membranaceus* (Rossignol, 1964) Sarjeant, 1970; Lynx-1X, 2640 m, O45.

8: Lynx-1X, 2660 m, G52.

9: *Spiniferites* cf. *membranaceus* (Rossignol, 1964) Sarjeant, 1970; Lynx-1X, 2640 m, H50.

10: *Spiniferites ellipsoideus*, Matsuoka, 1983; Lynx-1X, 2640 m, J39.

11: *Spiniferites katatonos* Corradini, 1973; Lynx-1X, 2540 m, P52.

12: *Trichodinium castanea* (Deflandre, 1935) Clarke and Verdier, 1967; Lynx-1X, 2980 m, O64.

PLATE 8

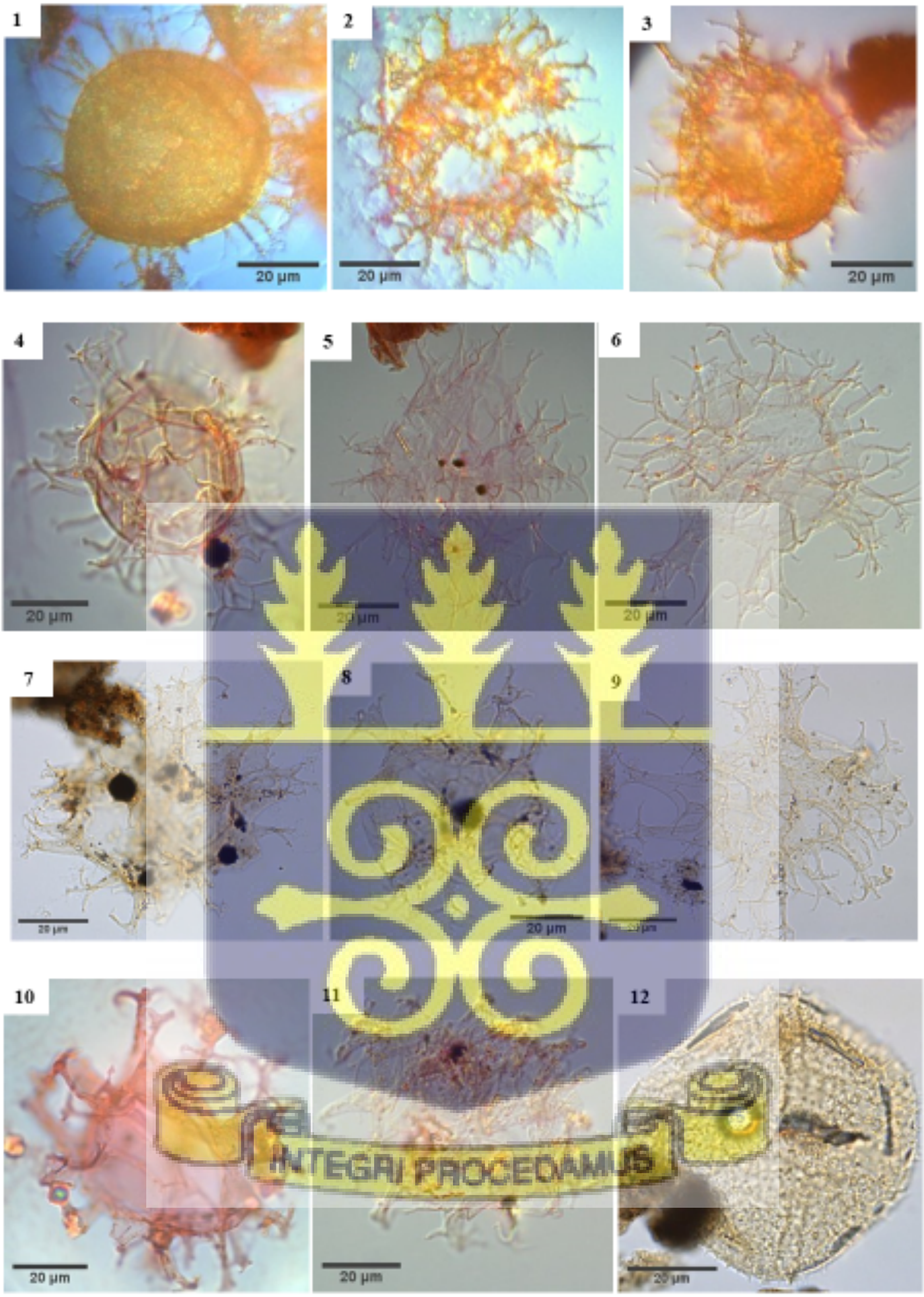

EXPLANATION OF PLATE 9

1: *Trichodinium boltenhagenii* (Fauconnier and Masure, 2004). emend. Fauconnier and Masure, 2004; Dzata-2A, 2742 m, D52.

2: *Trichodinium* cf. *boltenhagenii* (Fauconnier and Masure, 2004). emend. Fauconnier and Masure, 2004; Dzata-2A, 2742 m. O53.

3: *Cyclonephelium brevispinatum* (Millioud, 1969) Below, 1981; Lynx-1X, 2980 m, P46.

4: *Cyclonephelium brevispinatum* (Millioud, 1969) Below, 1981; Lynx-1X, 2980 m, T41.

5: *Cyclonephelium vannophorum* Davey 1969; Lynx-1X, 2940 m, U43.

6: *Cyclonephelium distinctum* Deflandre and Cookson, 1955; Dzata-1, 2850 m, M52.

7: *Circulodinium distinctum* (Deflandre and Cookson, 1955) Jansonius, 1986; Dzata-1, 2850 m, J40.

8: *Impletosphaeridium* sp.1; Lynx-1X, 3200 m, G58.

9: *Isabelidium* sp. Dzata-1, 2850 m, S63.

10: *Isabelidium* sp.; Dzata-2A, 3710 m, M48.

11: *Subtilisphaera perlucida* (Alberti 1959) Jain and Millepied, 1973; Dzata-2A, 4050 m, F61.

12: *Andalusiella gabonensis* (Stover and Evitt, 1978) Wrenn and Hart, 1988; Lynx-1X, 2760 m, V45.

PLATE 9

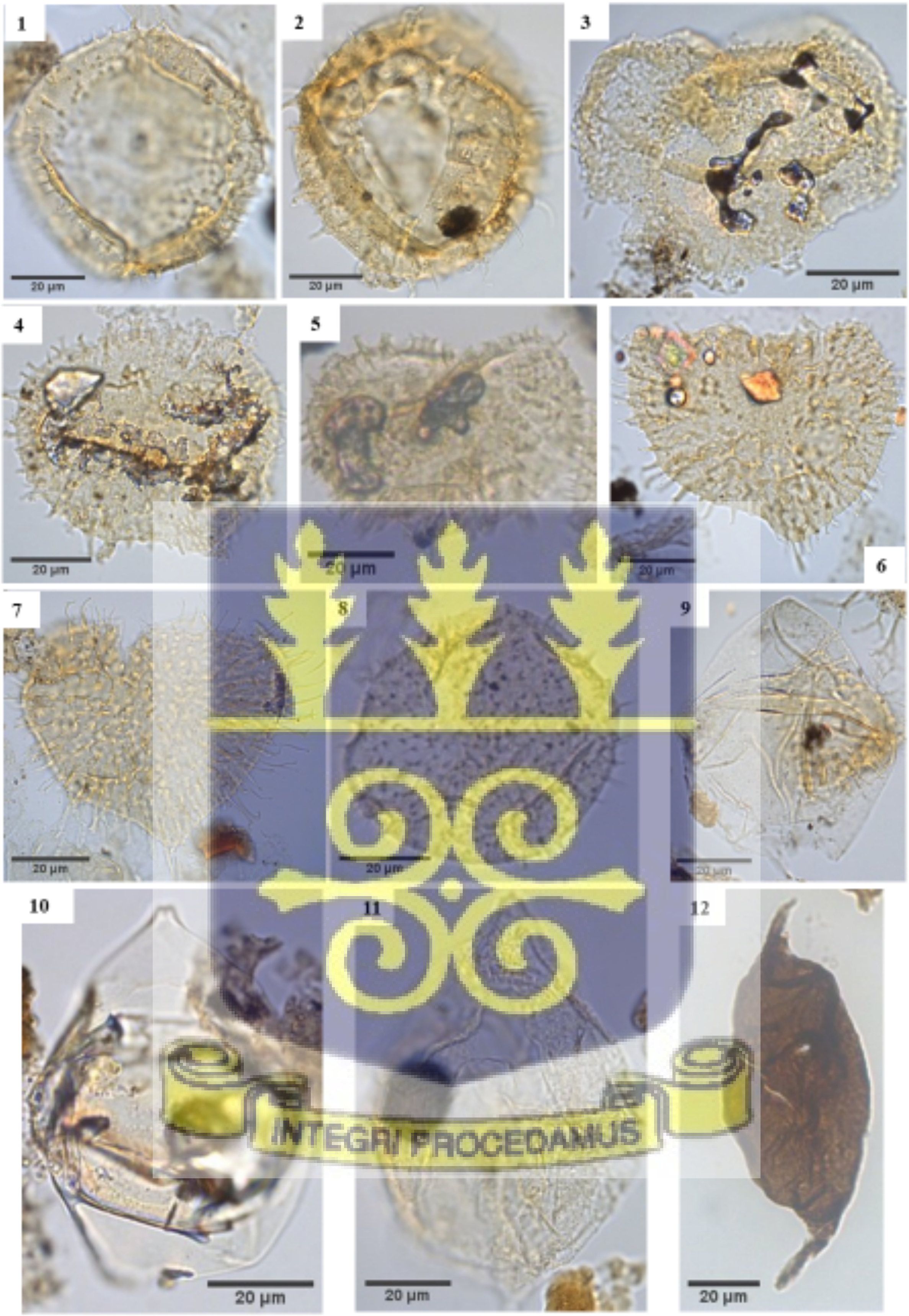

EXPLANATION OF PLATE 10

1: *Andalusiella polymorpha*; Lynx-1X, 3280 m, H70.

2: *Andalusiella* sp.; Lynx-1X, 2800 m, V46.

3: *Cerodinium boloniense*, (Riegel, 1974) Lentin and Williams, 1989; Dzata-1, 2630 m, T65.

4: *Phelodinium* cf. *kozlowskii*; Dzata-2A, 2600 m, R49.

5, 6: *Cerodinium obliquipes* (Deflandre and Cookson, 1955) Lentin and Williams, 1987; Dzata-1, 2850 m, W50.

6: Dzata-1, 2830 m, S61.

7: *Senoniasphaera* cf. *lordii* (Cookson and Eisenack, 1968) Lentin and Williams, 1976; Lynx-1X, 3040 m, F60.

8: *Apteodinium* cf. *apiatum* McIntyre and Brideaux, 1980; Lynx-1X, 2580 m, W58.

9: *Palaeocystodinium* sp.1; Lynx-1X, 2720 m.

10: *Palaeocystodinium golzowense* Alberti, 1961; Dzata-2A, 2580 m, N62.

11: *Palaeocystodinium* cf. lidiae (Górka, 1963) Davey, 1969; Lynx-1X, 2720 m, H48.

12: *Palaeocystodinium australinium* (Cookson) Lentin and Williams 1976; Lynx-1X, 2720 m, C50.

PLATE 10

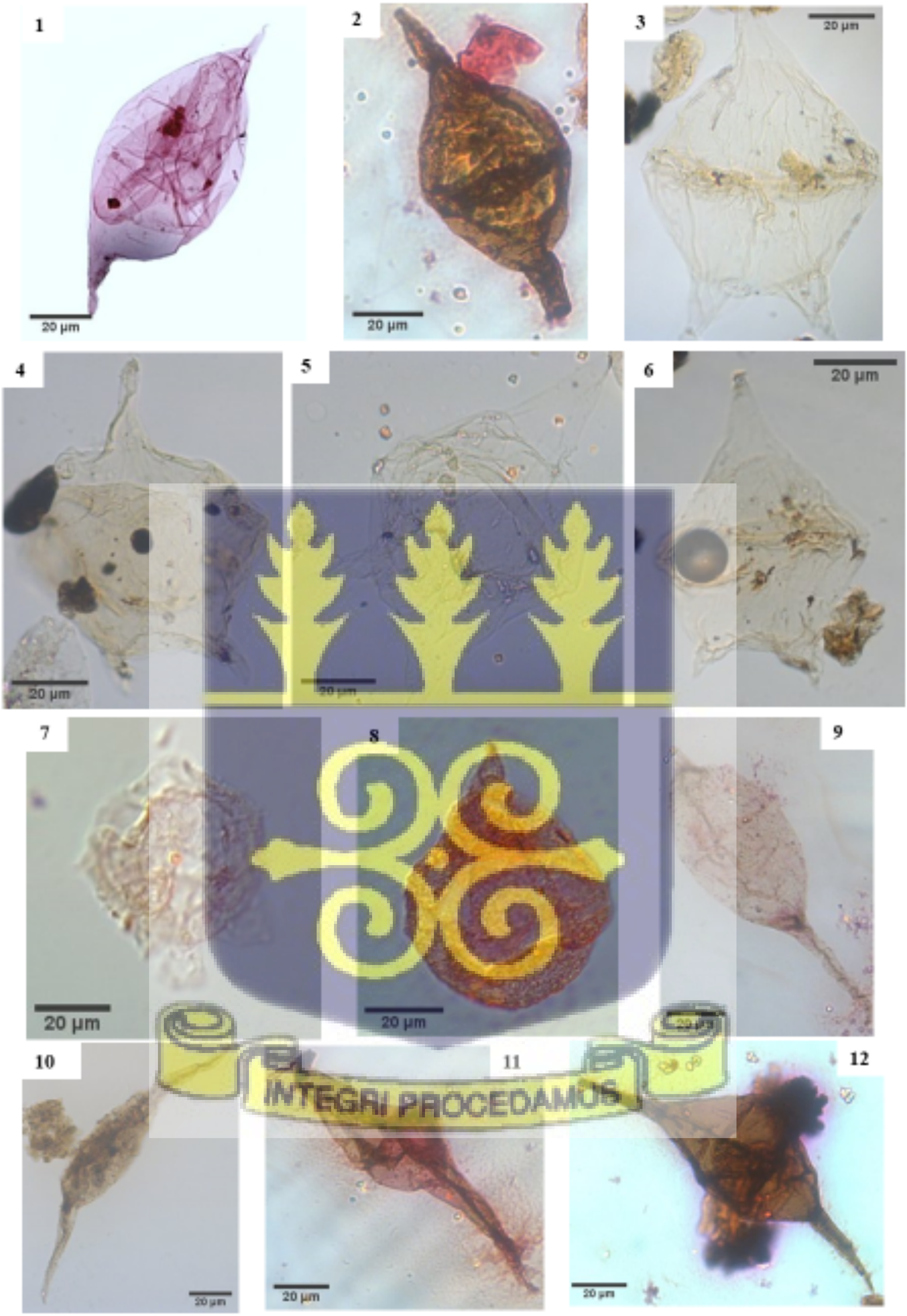
1
20 µm
2
20 µm
3
20 µm
4
20 µm
5
6
20 µm
7
20 µm
8
20 µm
9
10
20 µm
11
20 µm
12
20 µm

EXPLANATION OF PLATE 11

1: *Cerodinium diebelii* (Alberti, 1959) Lentin and Williams, 1987; Lynx-1X, 2760 m, C61.

2: *Palaeocystodinium golzowense* Alberti, 1961; Lynx-1X, 2680 m, H41.

3: *Palaeocystodinium* cf. *rafii* Antolinez-Delgado and Oboh-Ikuenobe, 2007; Dzata-1, 2590 m, K61.

4: *Odontochitina porifera*, Cookson, 1956; Dzata-1, 2610 m, G42.

5: *Odontochitina operculata* (Wetzel, 1933) Deflandre and Cookson, 1955; Dzata-1; 2650 m, Q64.

6: *Dinogymnium albertii*, Lynx-1X, 2980 m, D58.

7, 8: *Dinogymnium acuminatum*; Lynx-1X, 3180 m, G42.

8: *Dinogymnium acuminatum*; Dzata-2A, 2700 m, H54.

9: *Dinogymnium longicorne*; lynx-1X, 3180 m, M46.

10: *Dinogymnium denticulatum*, Evitt, Clarke et Verdier 1973; Dzata-2A, 2720 m, N58.

11: *Dinogymnium* cf. *westralium* (Cookson and Eisenack) Evitt et al., 1967; Dzata-1, 2870 m, P54.

12: *Dinogymnium* cf. *undulosum*, Cookson and Eisenack, 1970; Dzata-1, 2890 m, H38.

13; *Dinogymnium acuminatum*; Dzata-1, 2850 m, W62.

PLATE 11

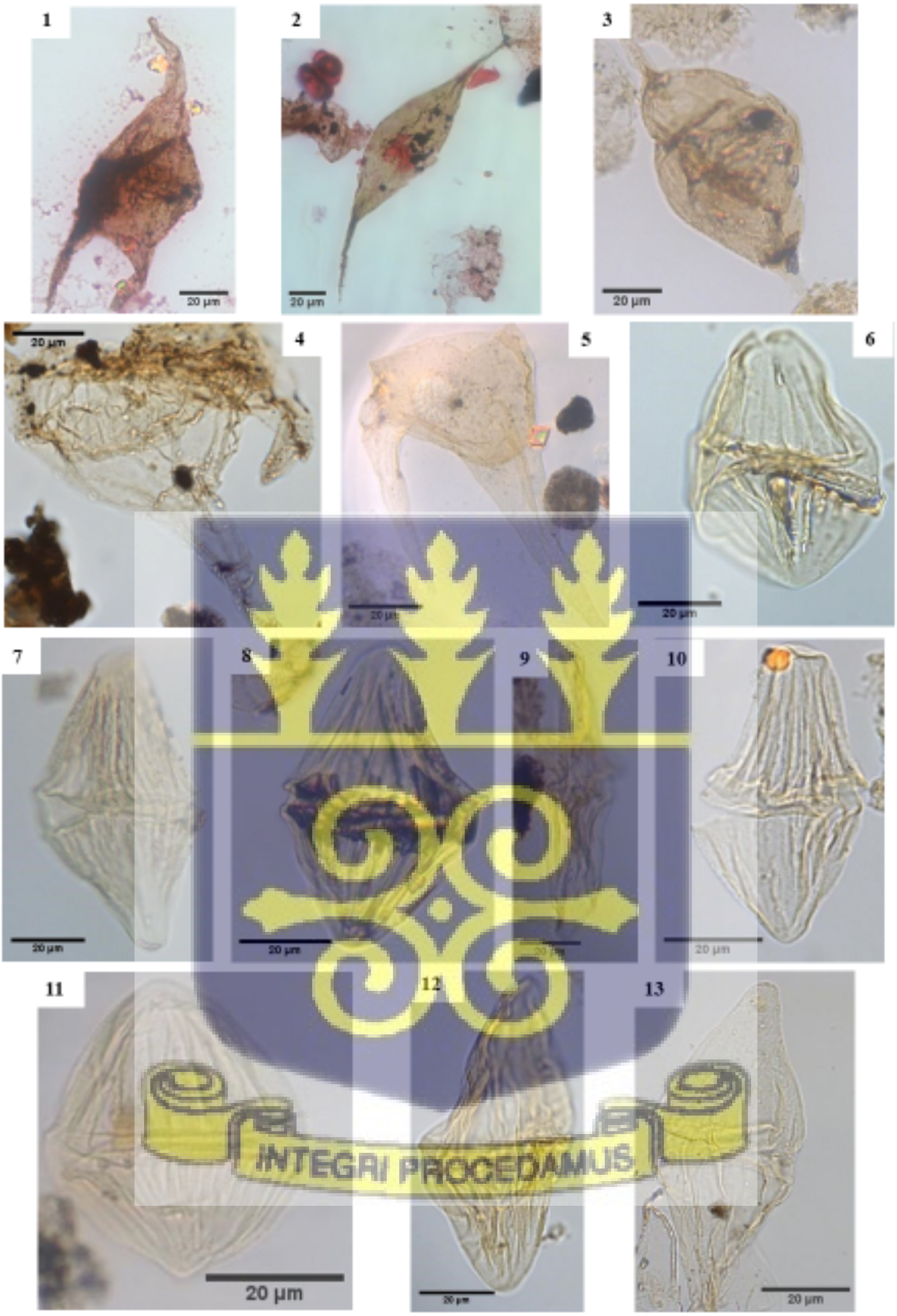

EXPLANATION OF PLATE 12

1: *Dinogymnium denticulatum*, Evitt, Clarke et Verdier 1973; Lynx-1X, 3160 m, L44.

2: *Dinogymnium acuminatum*; Lynx-1X, 3000 m, D50.

3: *Dinogymnium* sp.1; Dzata-1, 2830 m, L52.

4: Dinogymnium sp.2; Dzata-1, 2900 m, K62.

PLATE 12

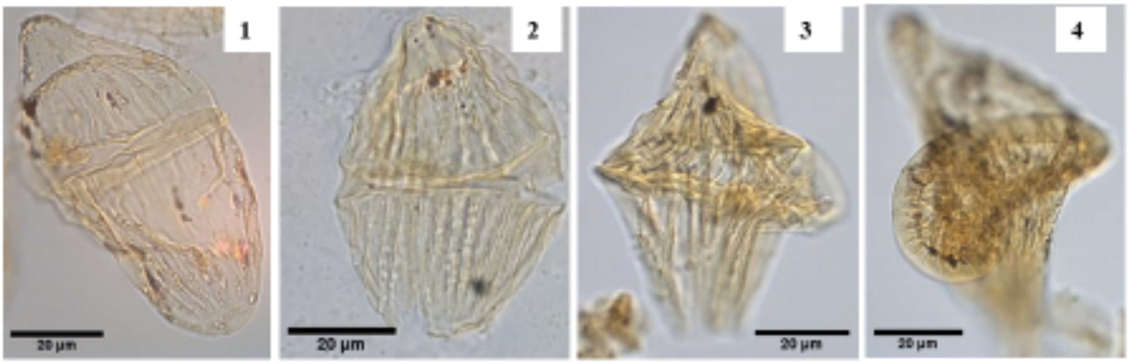

EXPLANATION OF PLATE 13

1: *Deltoidspora minor* (Couper) Pocock 1970; Lynx-1X, 3000 m, M54.

2: *Triplanosporites* cf. *giganteus*; Lynx-1X, 3000 m, X62.

3: *Dictyophyllidites harrisii Couper*, 1958; Dzata-1, 2830n, W43.

4: *Foveotriletes margaritae* (Van der Hammen) Germeraad, Hopping and Muller 1968; Lynx-1X, 2860 m, N44.

5:? *Araucariacites*; Lynx-1X, 2520 m, P48.

6: *Retimonocolpites* sp.; Dzata-1, 2850 m, Q60.

7: *Monosulcites* sp.; Lynx-1X, 2760 m, N52.

8: *Monosulcites* sp.; Lynx-1X, 2760 m, K65.

9: *Tricolpites confessus*, Stover and Partridge 1973; Dzata-2A, 2742 m, S42.

10: *Proteacidites* sp.; Dzata-1, 2850 m, U55.

11: *Echitiporites trianguliformis*; Dzata-1, 2850 m, V40.

12: *Triporate* sp.; Lynx-1X, 3000 m, X67.

13: *Uvaesporites* sp., Dzata-1, 2630 m, U45.

14: *Proxapertites operculata*; Lynx-1X, 2560 m, W50.

15: *Proxapertites* sp; Lynx-1X, 3000 m, R55.

16, 17: *Proxapertites* cursus Van Hoeken-Klinkenberg, 1966; Dzata-1, 2810 m, P55.

17: Dzata-1, 2850 m, H44.

18: *Longapertites* sp.1; Lynx-1X, 3000 m, M46; x630.

19, 20, 21: *Longapertites marginatus*, van Hoeken-Klinkenberg, 1964; Lynx-1X, 2760 m, T40.

20: Lynx-1X, 2760 m, N60.

21: Lynx-1X, 3040 m, S64.

22:? *Zlivisporis* sp.; Lynx-1X; 2980 m, L52.

23: *Inaperturopollenites* sp.; Dzata-2A, 3450 m, N50.

24: *Cicatricosisporites brevilaesuratus* Couper, 1958; Dzata-2A, 3450 m, E46.

25: *Classopollis* cf. b*rasiliensis* Herngreen, 1975; Lynx-1X, (3690 – 3700 m), V50.

26, 27, 28: *Classopollis* spp.; Dzata-1; 3470 m, V60.

PLATE 13

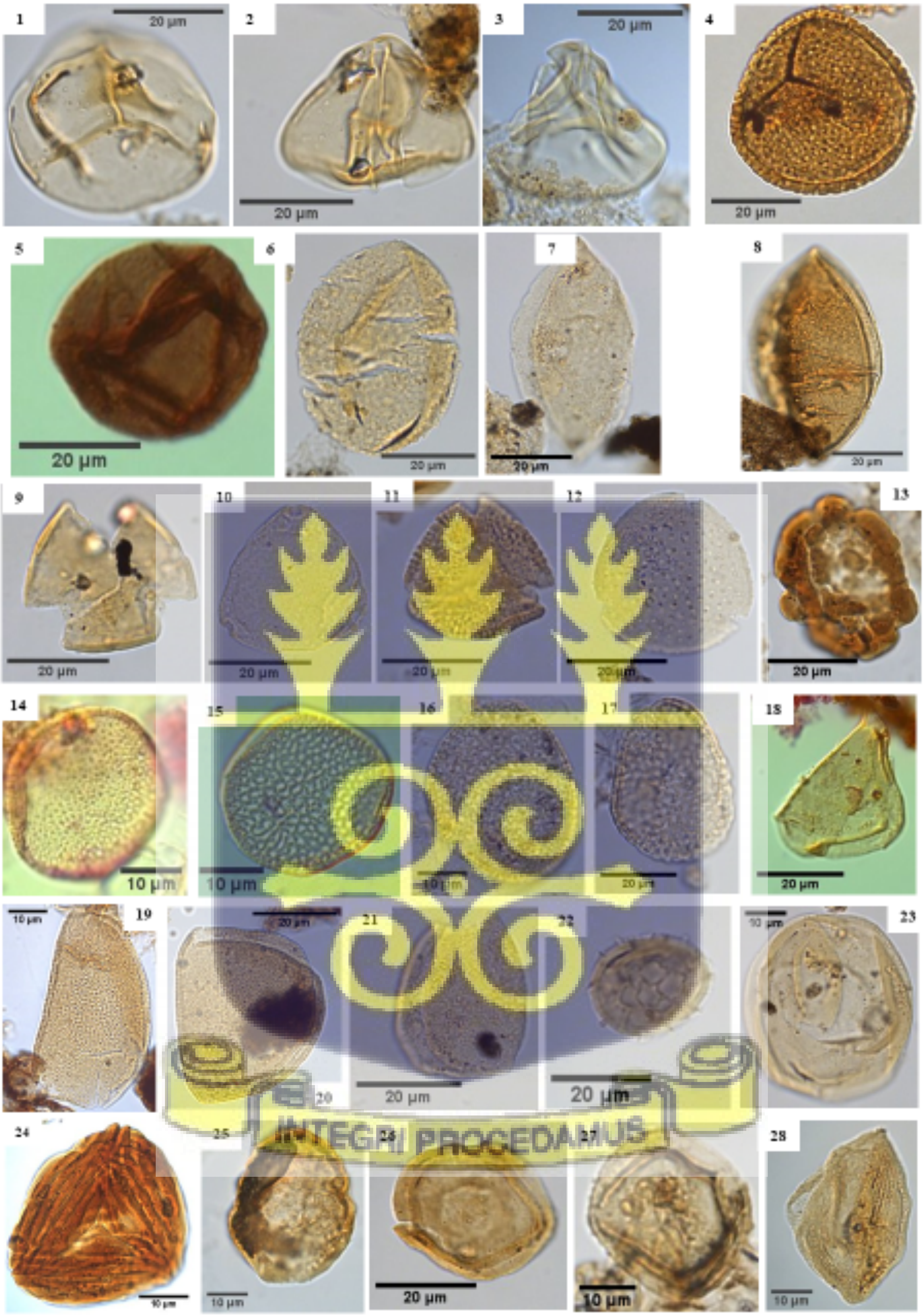

EXPLANATION OF PLATE 14

1, 2: *Classopollis classoides*, Pflug, 1953; Dzata-1, 3410 m, P49.

3: Tetrad of *Classopollis torosus*, Burger 1965; Dzata-1, 3410 m, G48.

4: *Classopollis martinotti*; Dzata-1, 3070 m, F70.

5: *Cretacaeisporites* cf. *polygonalis* (Jardiné et Magloire) Herngreen, 1973; Dzata-2A, 2841 m, C42.

6: *Ephedripites barghoornii* (Pocock, 1964); Dzata-2A, 3450 m, Q50.

7, 8: *Ephedripites jansonii*; Dzata-2A, 3294 m, L63 and U48.

9, 10, 11, 12, 13: *Ephedripites* spp.; Dzata-1, 3090 m, G40.

10: Lynx-1X, (3710 – 3720 m), C54.

11, 12, 13: Dzata-1, 3410 m; X64.

14, 15: *Galaeocornea causea* Stover, 1963; Dzata-2A, 2943 m, M47.

16: *Afropollis jardinus* Doyle et al., 1982; Dzata-1, 3470 m, Y60.

17, 18: *Afropollis kahramanensis* Ibrahim & Schrank, 1995; Dzata-1, 3470 m, Y67.

18: Dzata-1, 3470 m, L63.

19: *Elaterosporites klaszii* (Jardiné and Magloire) Jardiné, 1967; Dzata-2A, 2943 m, N50.

20: *Elaterosporites verrucatus* (Jardiné´ and Magloire) (Jardiné´, 1967); Dzata-2A, 2943 m, V41.

21: *Elateroplicites africaensis*, Herngreen 1973; Dzata-2A, 3294 m, T68.

PLATE 14

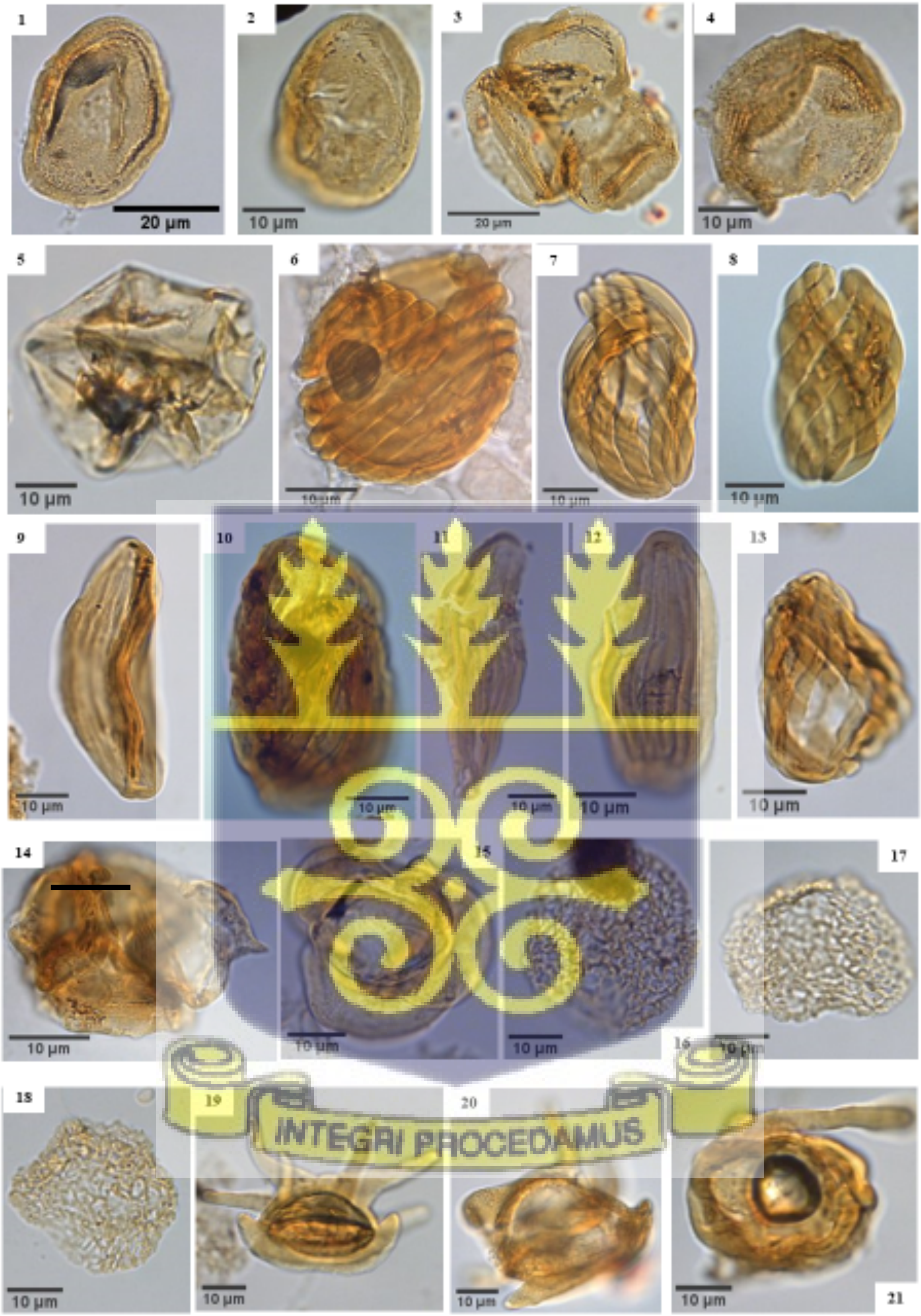
1
20 µm
2
10 µm
3
20 µm
4
10 µm
5
10 µm
6
7
8
9
10 µm
10
11
12
10 µm
13
10 µm
14
10 µm
15
10 µm
16
17
18
10 µm
19
10 µm
20
10 µm
10 µm
21

EXPLANATION OF PLATE 15

1: *Elateroplicites africaensis*, Herngreen 1973; Dzata-2A, 3294 m, U52.

2: *Sofrepites* sp.; Dzata-2A, 3333 m, P70.

3: *Sofrepites legouxae* (Jardiné, 1967); Dzata-2A, 3412 m, V46.

4, 5, 6, 7 : *Elaterocolpites castelaini*, Jardine´ et Magloire, 1965; Dzata-1, 3950 m, R40, U56.

6, 7: Dzata-2A, 3730 m, W48.

8: *Araucariacites australis* (Cookson, 1947, ex. Couper, 1953); Dzata-2A, 3210 m, T44.

PLATE 15

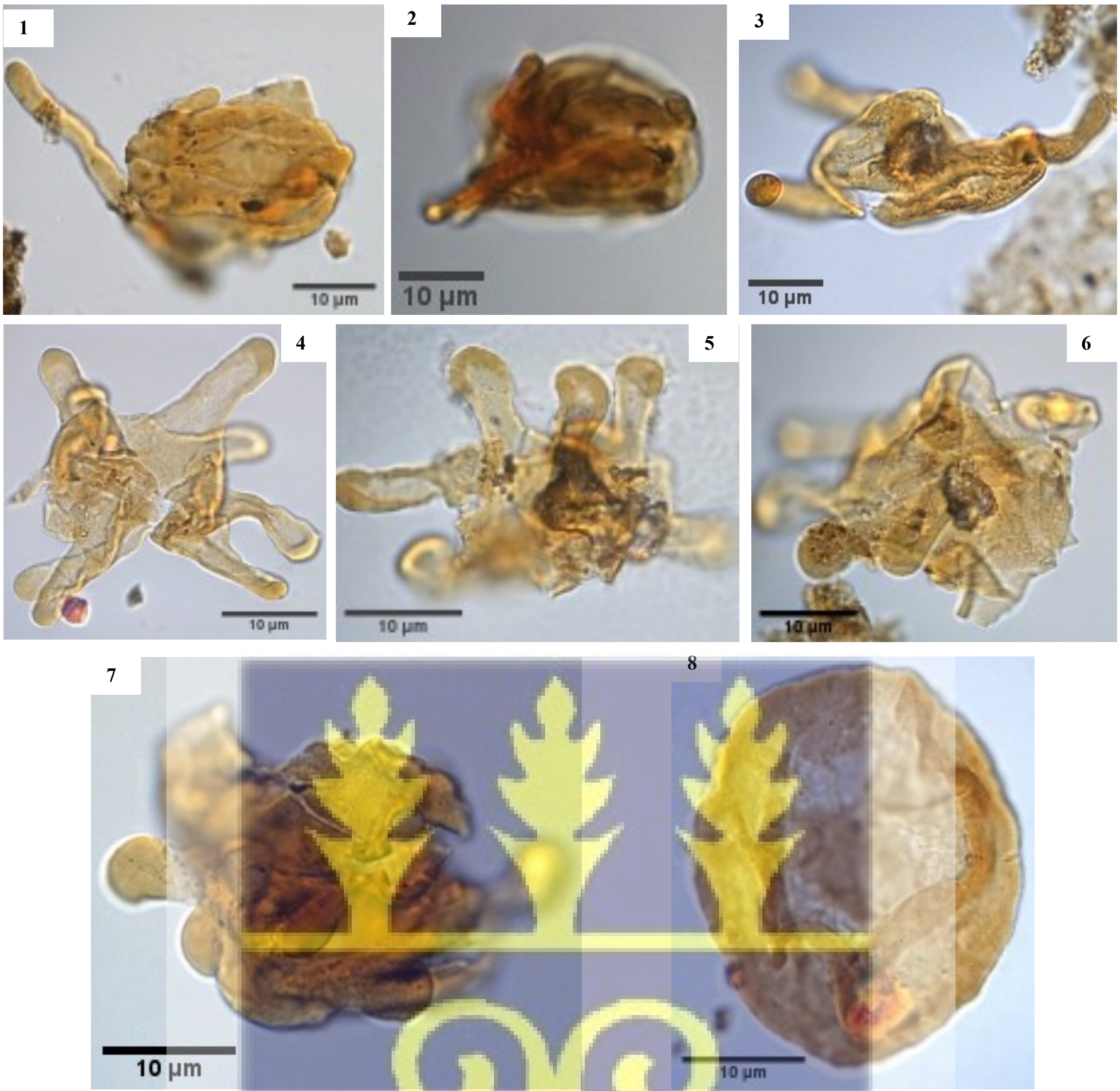

CHAPTER FIVE

PALYNOFACIES ANALYSIS AND PALAEOENVIRONMENTAL INTERPRETATIONS

5.1 INTRODUCTION

Muller (1959) established that, the distribution patterns of palynomorphs and other particulate organic matter (POM) can be used for facies recognition and palaeogeographic reconstruction. The term palynofacies was introduced by Combaz (1964) to describe the quantitative and qualitative palynological investigation of the total particulate organic matter assemblage. He further explained the term to encompass the total complement of acid-resistant organic matter recovered from a sediment or sedimentary rock by palynological processing techniques, using hydrochloric acid and hydrofluoric acid, as observed under a microscope.

Different definitions for palynofacies have been assigned by different authors. Hughes and Moody-Stuart (1967) described the term palynological facies in a similar manner as "palynofacies" of Combaz (1964) to include all organic elements. Batten (1973) in his definition applied the term palynofacies to refer to the general aspect of kerogen preparation. Quadros (1975) used words Organopalynology and Organopalynofacies for the study of organic matter in sedimentary rocks. Batten (1982a, 1982b) used this concept for the determination of thermal maturity and source potential investigations in addition to palaeoenvironmental and biostratigraphic studies.

According to Boulter and Riddick (1986), palynofacies analysis is the study of particulate organic matter assemblages concerned with changes in the relative abundance of various types of organic debris such as palynomorphs, zooclasts, phytoclasts and amorphous organic matter (AOM). Traverse (1988) characterized palynofacies as "the collection of palynomorphs taxa in a portion of a sediment, representing local environmental conditions and not typical of the regional palynoflora". Powell et al. (1990) redefined the term as "a distinctive assemblage of HCl and HF insoluble particulate organic matter (palynoclasts) whose components mirror a particular sedimentary environment".

Tyson (1993) published a spearheading contribution in the area of palynofacies analysis and averred that the compositional changes in palynofacies are helpful in palaeoenvironmental interpretations of sedimentary rocks as such changes are the result of the interaction of several parameters (for example terrestrial versus marine palynomorph influx, source and rate of sediment influx, water salinity, depth and oxygen concentrations, etc.) within a given depositional environment. Traverse (1994) disclosed that since 1960 the term palynofacies was used to refer to a more or less local concentration of particular palynomorphs, showing a sort of biofacies. Traverse (1994) pointed out that the application of the word has since been geologically oriented, and palynofacies is used essentially to indicate information about the enclosing rock, particularly its environment of deposition which should be called palynolithofacies.

Tyson (1995) introduced the modern concept of palynofacies and defined it as ''a body of sediment containing a distinctive assemblage of palynological organic matter thought to reflect a specific set of environmental conditions or to be associated with a characteristic range of hydrocarbon-generating potential" which is dependent on the total assemblage of particulate organic matter. Based on this definition, Tyson (1995) referred to palynofacies as an incredible analytical tool which when utilized alongside geological and geophysical information could be utilized in various investigations of geology (stratigraphy, sedimentology and palaeoenvironmental investigations), palaeontology (biostratigraphic studies), petroleum exploration, environment studies etc.

Mendonça Filho (1999) referred the term palynofacies to the investigation of the particulate organic matter present in sediments and sedimentary rocks utilizing the organic matter isolation strategies for sample preparation (kerogen concentration) and applying microscopy techniques as principal tool for acquiring data and statistical methods for its interpretation. According to Mendonça Filho et al. (2012), palynofacies analysis comprises the integrated investigation of all aspects of the kerogen assemblage which incorporates the identification of the individual particulate components, evaluation of their absolute and relative distribution and preservation states.

The palaeoenvironmental interpretations introduced for each palynofacies type is dependent on the quantitative analysis of selected palynomorph constituents and total POM, which are known to have a palaeoenvironmental implications. These incorporate terrestrially derived palynomorphs, for example, miospores (e.g. pteridophyte spores, gymnosperm pollen, angiosperm pollen etc.), and aquatic phytoplankton (for example dinoflagellate cysts). Furthermore, there might be terrestrially derived phytoclasts, which can be represented by black wood (inertinite/charcoal), brown wood (e.g. tracheids), plant cuticle and membranous tissues. Minor constituents present include microforaminiferal test linings and freshwater green algae. Some sporomorphs are markers of distinct ecological parameters and along these lines permit not just a potent distinguishing proof of palaeoclimatic conditions but additionally grant reconstruction of the vegetation developing on the source regions.

5.1.1 Classification of Palynofacies Constituents

Various classifications have been proposed by many palynologists for palynofacies constituents (e.g. Batten, 1973; Bujak et al., 1977; Masran and Pocock, 1981; Boulter and Riddick, 1986; Hart, 1986; Tyson, 1993 and 1995; Batten, 1996; Mendonça Filho, 1999;

Mendonça Filho et al., 2010, 2012) based on degradational state and biological derivatives (i.e., plant fragments, phytoplankton, etc.). Notwithstanding, the different classification schemes are as yet not standardized after numerous studies considering degradational state and natural subordinates (i.e., plant sections, phytoplankton).

Staplin (1969) classified two main groups of sedimentary organic matter i.e. 'Primary materials' and 'Modified materials'. The primary materials consist of cuticles, sporomorphs, lignified wood fragments, charcoal, resins, freshwater plankton and marine organisms. Modified materials on the other hand comprises of unorganized amorphous sapropelic material further divided into Sapropel A and sapropel B.

Bujak et al. (1977) characterized the four principal kinds of organic particles which are; (1) amorphogen (amorphous: structureless organic matter), (2) phryogen (non-woody plant material, including palynomorphs), (3) hylogen (from woody material) and (4) melanogen (opaque organic matter). Amorphogen and phryogen are more likely to give liquid hydrocarbons in time although hylogen and melanogen are most drastically averse to be produce gas.

Hart (1986) categorized organic particles into phytoclasts (includes miospores, megaspores, wood and cuticle fragments; protistoclasts which includes algae, dinocysts, acritarchs and microforaminiferal linings; zooclasts (i.e. arthropod, graptolite, and chitinozoans debris) and receptoclasts (inorganic or organic particles that are areas of precipitation or localization of organic chemical). Pocock et al. (1988) divided organic matter into the following classes: Terrestrial sourced materials (Structured and Biodegraded), Fusinites and Inertinites, Fungi (Sclerotinite), Resins (Resinite), Amorphous and Structured aqueous materials. They discussed Amorphous and Structured aqueous materials with reference to their environmental view point and as a source material for the production of fossil hydrocarbons. Another scheme utilized to categorize the sedimentary organic matter (SOM) was proposed by (Steffen and Gorin 1993; Pittet and Gorin 1997; Bombardiere and Gorin 1998) and summarized in table 5.1.

Tyson (1993, 1995) identified three main groups of morphologic components of organic matter (palynofacies) assemblage namely; palynomorphs (organic walled constituents that remain after maceration using HCl and HF acids), phytoclasts (tissues fragments derived from higher plants or fungi) and amorphous organic matter-AOM (structureless material derived from non-fossilizing algae, phytoplankton or bacterially derived AOM, higher plants resins).

Table 5.1: Classification of the sedimentary organic matter (after Steffen and Gorin 1993; Pittet and Gorin 1997; Bombardiere and Gorin 1998).

Origin	Group		Constituent	
Continental (Allocthonous)	Phytoclasts		Opaque to semi opaque	Equidimensional Blade shaped
			Translucent	
	Miospores	Pollen	Bisaccate Non saccate	
		Spores		
Marine (Autochthonous)	Amorphous Organic matter		Non-fluorescent Fluorescent	
	Microplankton		Dinoflagellate cysts Acritarchs Algae Microforaminiferal linings test (MFLT)	

Batten (1996) classified palynological matter into Palynomorphs, Structured Organic Matter and Unstructured Organic Matter and stated the constituents of the classification as mentioned below;

(a): Palynomorphs (spores and pollen grains; fungal sclerotia, spores, fruiting bodies and other reproductive parts; dinoflagellate cysts; Acritarchs; Prasinophyceae algae; Chlorococcalean algae; zygnemataceae and other green alga; cyanobacteria; foraminiferal linings; chitinozoans; scolecodonts; miscellaneous).

(b): Structured Organic Matter (STOM) incorporates: I. Phytoclasts (Wood (black and brown); Charcoal and other black phytoclasts; Cuticles; Bark and cork; Other (non-cuticular) tissues; Tubes, filaments and hairs; Fungal hyphae), II. Zooclasts.

(c): Unstructured Organic Matter (USTOM) which includes: (Amorphous organic matter; AOM of terrestrial derivation; AOM of aquatic region; gelified matter; resin and amber; solid bitumen).

(d): Reworked organic matter.

Oboh-Ikuenobe et al. (1997) also proposed a classification technique in which twelve types of organic matter were identified and summarized in table 5.2.

Tyson (1995) opined that, the main objectives of palynofacies investigations are to assess the origin of the organic matter (regarding its botanical precursors), relative percentages and preservation of the various constituents, generation of hydrocarbons, fluctuating degree of thermal alteration (maturity) of the organic matter, nature of the deposition palaeoenvironment (terrestrial inputs), reducing versus oxidizing conditions and differentiation of fresh water, brackish or marine environments in terms of palaeosalinity.

Nonetheless, the scheme adapted in the study follows the classification scheme of Tyson (1993, 1995) which gives detail palynological classification of individual palynofacies constituents which is dependent on an unadulterated palynological terminology for palaeoenvironmental investigations utilizing transmitted light microscopy. Constituents of kerogen mainly recognized in the study are based on the classification schemes proposed by Tyson (1993, 1995) which identified three main groups within the kerogen assemblage. These are; Amorphous organic matter (AOM), Phytoclasts (translucent and opaques) and Palynomorphs. According to Tyson's (1995) classification of palynofacies constituents, palynological organic matter components can either be structureless or structured palynological organic matter.

Table 5.2: Organic Matter Classification in sediments (after Oboh Ikuenobe et al. 1997).

Palynodebris	Characteristics	Size (μm)
Amorphous organic matter	Structureless, irregularly shaped, yellowish-amber to brown masses: usually gel-like	Variable
Marine palynomorphs	Dinoflagellates, acritarchs and chitinous inner linings of foraminiferal tests	30-90
Algae	Aquatic algal remains mainly *Pediastrum*	20-70
Resins	Unstructured amber-colored exudates, mainly from stem tissues	Variable
Black debris	Opaque particles with sharp angular outlines: lath-shaped, or in some cases more equidimensional	20->200
Yellow-brown frag-ments	Structureless particles of yellow to light brown color: attributable to highly degraded herbaceous material (leaf mesophyll?)	5-80
Black-brown frag-ments	Unstructured dark brown to nearly black particles: attributable to highly degraded woody material	Variable
Cuticle fragments	Platy epidermal-patterned fragments of waxy cuticle coating leaves, stems and roots: pale yellow to light brown in color	30->200
Plant tissues	All other herbaceous material including parenchyma	Variable
Wood	Light to dark brown particles with sharp angular edges and/or discernible cellular structure: mainly lath-shaped	30->200
Sporomorphs	Land plant spores and pollen dispersed by water into continental and marine environments	10-80
Fungi	Fungal remains such as spores, hyphae and mycelia	5->100

5.1.2 Structureless organic matter

Structureless organic matter includes materials such as amorphous organic matter (AOM), resin, and humic gel.

The Amorphous Organic matter (AOM) refers to structureless dispersed particulate organic matter (kerogen) whether of marine or non-marine origin. According to Tyson (1995), structureless organic matter is an organic matter that lacks a definite internal structure when observed utilizing light microscopy, lacks a distinct and recognizable outline, and which does not infer its biological affinity. It is basically produced by biodegradation of algal phytoplankton blooms, gotten from zooplankton faecal pellets, or got from biodegradation of cyanobacteria and thiobacteria (Tyson, 1995; Mendonça Filho et al. (2010, 2012). According to Lewan (1986), carbon isotope evidence showed that all the typical AOM in ancient marine basinal fine-grained sediments were ultimately derived from phytoplankton or bacteria. Tyson (1995) further stated that, in mass terms, nearly all fossilized marine organic matter is represented by AOM. The principal control on the appearance of AOM is its preservation state so during degradation it turns out to be progressively more dull (greyish in colour), less cohesive and less resistant to palynological oxidation treatment and heterogenous when viewed under fluorescence (Tyson, 1989).

AOM concentrations has also been utilized to demonstrate oxygenation (reducing or oxidizing) conditions of bottom water in ancient sedimentary depositional environments. The high relative or absolute abundances of AOM was usually associated with sediments beneath upwelling water masses and taken to indicate bottom water of low (dysoxic) oxygen concentrations (Davey and Rogers, 1975; Tissot and Pelet, 1981; Summerhayes, 1983). AOM has been found to decline in shallow shelf sediments and increase in a basinward direction, in darker-coloured, organic-rich facies with dysoxic-anoxic conditions (e.g. Dow and Pearson, 1975; Bujak et al., 1977). According to Masran and Pocock (1981), the typical oil-prone AOM preserved under reducing conditions is colourless to neutral grey and referred to it as 'grey amorphous'. This was differentiated from 'yellow-amber amorphous' attributed to amorphous material derived from dominantly terrestrially derived materials.

According to Langenheim (1969) and Larsson (1978) resins are the products of higher plants mainly trees, which occupy tropical to subtropical lowland forests and typically gets preserved in waterlogged environments such as ombrogenous mires. Their shape and colour varies from yellow, orange, red rounded globules with angular, conchoidal or irregular surface fractures

(Larsson, 1978). Resin is a highly resistant and known in ancient sediments as amber and is mainly produced by coniferous gymnosperms and to a small degree by dicotyledonous angiosperm trees (e.g. Tyson, 1995). Masran and Pocock (1991) suggested the high frequency of resins to be generally accumulated along prodeltaic-deltaic setting. They may also show up more common in non-marine settings (Oboh, 1992). Globules of the resins often come across in organic residues turn out as transparent bodies displaying conchoidal fractures. They are good source of liquid hydrocarbons (Pocock et al., 1988).

The biodegradation of the root and bark tissues of land plants produces humic gels, where these tissues were initially released from the plant roots and bark by destructive oxidation. Humic gels are considered as inconsequential contributors to AOM in ancient marine sediments (Tyson, 1995).

Table 5.3 and 5.4 shows the classification system of the individual palynological components based on Tyson (1995), which demonstrate the proper use of the classification for the examination of kerogen under transmitted white light.

Table 5.3: Phytoclast and Amorphous Groups (After Tyson, 1995).

Group	Subgroup
Phytoclast	Opaque phytoclast (black wood) Translucent phytoclast (brown wood)
Amorphous Organic matter	'AOM' Phytoplankton or bacterially-derived amorphous organic matter (traditionally referred to as 'AOM') Resin Derived mostly from higher plants Amorphous products Products of the diagenesis of macrophyte tissues

5.1.3 Structured organic matter (Table 5.3 and 5.4)

Structured organic matter is made of discrete and recognizable individuals or colonial entities (i.e. palynomorphs) and plant or animal fragments (i.e. phytoclasts, zooclasts) that show their biological affinities Tyson (1995). Palynomorphs can for the most part be assigned botanical or zoological affinities, whereas phytoclast particles with coherent, angular to irregular outlines that may show some internal structures can be attributed at least to a type of larger plant (i.e. phytoclasts) or animal (i.e. zooclasts) debris.

5.1.3.1 Phytoclasts (Translucent and Opaques (black debris)):

Bostick (1971) introduced the term 'phytoclast' to portray all particles with size clay or fine-sand derived from higher plants or fungi. They are parts of tissues got from higher plants or fungi and its autofluorescence relies upon derived tissue. Phytoclasts can be translucent (nonopaque) or opaque (black) and non-biostructured, biostructured, structured or 'pseudoamorphous' (Mendonça Filho et al.,2012).

Translucent phytoclasts (non-opaque phytoclasts): Wood tracheids are one of the most widely recognized members of the biostructured translucent phytoclasts. The bulk of dispersed wood phytoclasts gets preserved in sediments in changing conditions of preservation with their cellular structures decaying after burial (Oboh-Ikuenobe et al., 1999). Their high relative and absolute abundances in antique marine sediments are known to show strong terrestrial influx, with deposition in nearshore proximal settings (for example fluvio-deltaic systems) that were near the parent land plants (Müller, 1959; Pocklington and Leonard, 1979). Hydrodynamic equivalence of woody phytoclasts controls their distribution in sediments, as woody phytoclasts are made of relatively large and dense particles, their high concentrations have usually been found to correlate to coarse silts and very fine sands (Habib, 1983; Firth, 1993; Tyson, 1993).

Cuticles which are part of the translucent phytoclasts depicts the outermost waxy covering of the single layer of epidermal cells of leaves, stems of most plants (Batten, 1996). Preservation of cuticles occurs in fluvio-deltaic, lacustrine and low energy environments (Tyson, 1987, 1995) and their abundances in the sediments reduces away from the delta distributaries (Gastaldo and Huc, 1992). Cuticles have been generally documented in high percentages from low energy, onshore fluvio-deltaic and lacustrine palaeoenvironments (e.g. Batten, 1973; Nagy et al., 1984; Smyth et al., 1992). Cuticle debris is most buoyant variety of organic matter of the structured terrestrial organic matter and results from the settling of the flotation and suspension loads under low energy conditions (Fisher, 1980).

Opaque phytoclast (Black debris): Black (opaque) wood concentrations in antique sediments have additionally been discovered to be of extraordinary palaeoenvironmental significance, and they have been found to reflect deposition polarity (onshore-offshore location), distance of sediment transport, and oxygenation level of host sediments (Deaf, 2009). The process of decay and the accompanying loss of weight are most fast when wood is exposed to the atmosphere. The opaque phytoclast is normally expressed to be a result of terrestrial post-depositional alteration, depicting variations in the water column permitting exposure to sub-aerial oxidation and oxidation during transport (Tyson, 1993, 1995; Mendonça Filho et al.,2012). According to Batten (1996) wood gets degraded to 'black debris' by exposure to oxygenated conditions by microbial and fungal action. Black wood fragments in high percentages have been archived from ancient high energy, proximal, coarse grained sediments of fluvial and delta-top systems (Fisher, 1980; Nagy et al., 1984; Smyth et al., 1992). The particle size of black wood has been documented to generally reduce in offshore direction (e.g. Habib, 1982; Gorin and Monteil, 1990). Black wood offshore particle size reduction was attributed to the fragmentation of large black wood particles during the long-distance transport with associated reduction in concentration of black wood (Tyson, 1995).

Membranes: Mendonça Filho et al. (2012) intimated that, membranes are pale grey particles, thin, commonly transparent, with form of sheets and clear outlines, showing no visible cellular structures and depicts the cutine layer of the epidermis of leaves or branches from higher plants which can be strongly or weakly fluorescent. Membranous tissues are type of structured plant debris that are retrieved from the collenchyma and parenchyma of the non-epidermal, non-lignified tissues. These tissues are sensitive structures and are made of promptly degradable cellulosic material (Tyson, 1995). According to Tyson (1995) concentrations of the tissues are high in non-marine and proximal deltaic facies and tend to be rare in offshore direction. In prevailing oxic conditions they tend to degenerate three times quicker than more durable lignified woods (e.g. Stout et al., 1981).

5.1.3.2 Palynomorphs

The palynomorphs refers to all discrete acid resistant, organic walled microfossils. The term palynomorph was proposed by Tchudy (1961) to allude to all discrete HCl and HF-resistant, organic-walled (unicellular, multicellular, or colonial) microfossil that might be present in palynological preparations. They are discrete, coherent, individual or colonial entities and categorize into terrestrial (sporomorphs) and aquatic (marine and fresh water) subgroups (Tyson, 1995) (Table 5.3).

5.1.3.2.1. Marine palynomorphs: This includes dinoflagellate cysts, acritarchs and prasinophytes.

Dinoflagellate cysts are organic-walled, fossilized bodies that are produced by unicellular algae during the non-motile resting (sexual) phase of their life cycle and are made of generally resistant 'dinosporin' and are archived in the geologic record from the late Triassic to the present (Evitt, 1985). They are totally marine organisms and significant primary producers

(Traverse, 2007). The cysts get fossilized and can be perceived by the plated surface, apical, and antapical horn and processes. According to Tyson (1993) the high concentrations of the dinoflagellate cysts occur in temperate to tropical shelf territories away from active fluvial-deltaic sources and in zones of the improved primary productivity. The proportion of dinocysts to sporomorphs (the marine influx index or marine: continental ratio) shows transgressive-regressive trends in ancient sediments (Habib, 1979; Lister and Batten, 1988; Prauss, 1989). High assorted variety and low dominance of dinoflagellate cysts happen in distal offshore marine shelf settings (Lister and Batten, 1988; Habib et al., 1992) and low assorted variety, high predominance assemblages demonstrate nearshore settings. High dinoflagellate cysts diversity likewise demonstrates high stands of global sea-level changes (Bujak and Williams, 1979; Goodman, 1987; Prasad et al., 2013). Lower numbers and/diversity have also been attributed with some dysoxic-anoxic palynofacies (Tyson, 1989; Batten and Marshall 1991; Batten, 1996).

Acritarchs are hollow, organic-walled, eukaryotic unicellular of unknown biological affinities, which go from the mid-Precambrian to pre-Quaternary (Armstrong and Brasier, 2005) and are geographically widespread (Tyson, 1995). Their high relative abundances demonstrate shallow marginal marine settings of mainly brackish water in the in the Mesozoic ((Davey, 1970; Downie et al., 1971; Burger, 1980; Prauss, 1989; Deaf, 2009).

Prasinophyte algae on the other hand are a group of non-cellulosic, green, flagellate algae, which have a geographical range from the Ordovician to Recent (Armstrong and Brasier, 2005). The presence of fossilized structures (phycomata) of prasinophyte algae have been discovered to be related with shelfal and oceanic settings with organic-rich sediments deposited in dysoxic-anoxic conditions (Tyson, 1984, 1989). Fossil prasinophyceae are rarely related with fresh water, unlike some modern taxa (Tappan, 1980). Their presence in the basin margin successions is primarily taken to suggest marine or brackish-marine conditions, or short-lived marine incursions (Guy-Ohlson and Norling, 1988; Lister and Batten, 1988; Batten, 1996).

5.1.3.2.2. Freshwater microplankton

Freshwater and marine algae parts can both be found in palaeopalynological slides with assortment in shapes and sizes relying upon genus and species. They retain their colonial structure, have a lustrous colour and show up clearly under UV fluorescent light (Tyson, 1995; Traverse, 2007). Fresh water forms include chlorococcalean algae, for example, *Pediastrum* and *Botryococcus* alga. The presence of fossil colonies of *Botryococccus* alga occur with amorphous organic matter and proposes accumulation in dysoxic-anoxic conditions (Batten, 1996). The presence of *Botryococcus* and/or *Pediastrum* in the sedimentary record is associated with the formation of high-quality oil source rocks (Cane, 1976; Hutton, 1988). Fresh to brackish water conditions can be surmised from the presence of *Botryococcus*, as it has been recorded from antiquated lacustrine, fluvial, lagoonal, and deltaic/nearshore marine sediments (Piasecki, 1986; Riding et al., 1991; Williams, 1992). *Pediastrum* has additionally been found with high abundances in low salinity lakes and furthermore transported by fluvial systems into nearshore shelfal situations (Singh et al., 1981; Hutton, 1988). Other chlorococcalean algae include *Scenedesmus* and *Tetraedron.*

5.1.3.2.3. Zoomorph

It is constituted by animal-derived palynomorphs including foraminiferal linings, chitinozoa and scolecodonts. It is recognizable as fragment zoomorph palynomorphs (Tyson, 1989 and 1995; Mendonça Filho et al., 2012).

Microforaminiferal linings, a term formulated by Wilson and Hoffmeister (1952) applies to the acid resistant foraminiferal remains (less than 150 µm in size), found in the palynological preparations. The natural dissolution or breakage of calcareous microforaminiferal tests brings about liberation of their organic linings (Golubic and Schneider, 1979; Mc Neil, 1997) which keep up pretty much internal test morphology of the original foraminifers (Concheyro et al., 2014). The relative abundances of microforaminiferal test linings can be used to indicate depositional settings under normal marine conditions (Lister and Batten, 1988; Stancliffe, 1989). Batten (1982) showed that recurrence of microforaminiferal linings increments in marine facies are related with rich amorphous organic matter. The linings are generally recorded with dinoflagellate cysts in the sediments deposited along the coasts (Warrington, 1982; Davies, 1985; Kumaran and Rajshekhar, 1992; Singh et al., 2013). They have been effective occupants of each aquatic environment from deep oceans to brackish water lagoons, estuaries and scarcely in freshwater streams, lakes (Gandhi and Solai, 2010).

Scolecodonts are elements of the jaw of benthic polychaete annelid forms which range from Ordovician to recent and they occur in marine settings (Tyson, 1995).

Chitinozoa are an extinct group marine organic-walled, flask or bottle-shaped microfossils (50 μm to 2 mm in size) that occur in rocks of Ordovician to Devonian age. Chitinozoa have proved to be very useful in biostratigraphic dating of those Paleozoic fine-grained metasediments in which all the organic matter is opaque. They also have potential as thermal maturity indices; because with the progressive thermal alteration the test changes from translucent and amber colored to brown and finally black (opaque) (Tyson, 1995; Mendonça Filho et al., 2012).

5.1.3.2.4. Sporomorph (Terrestrial Palynomorphs):

Spores and pollen-grains are the terrestrial constituent of the palynomorphs and are the result of the life-cycle of embryophytic plants (Traverse, 2007) which forms important components of the palynofacies. The embryophytes are plants that produce true embryos, the spore producing bryophytes and pteridophyte (fern type) and the pollen grains producing gymnosperms (e.g. conifers) and angiosperms (Traverse, 2007; Tyson, 1995; Mendonça Filho et al., 2012).

Spores and pollen grains after their production gets dispersed by insects, wind and water. Their exines gets deposited in shallow water estuarine, lagoonal and lacustrine sediments and are useful in the interpretation of depositional environments and the reconstruction of the vegetational histories (Pocock et al., 1988). Their concentration is restricted to the vicinity of the active fluvio-deltaic sources (Mudie, 1982). The hydrodynamic equivalence of spores has been discovered to be constrained by spore sizes, where high proportions of ornamented, thick-walled, more dense spores have been found to concentrate in proximal high energy nearshore settings and reduce from the source land in contrast with smooth, thin-walled, less dense spores (e.g. Lund and Pedersen, 1985; Mutterlose and Harding, 1987; Tyson, 1989; Dybkjaer, 1991; Deaf, 2009).

Pteridophyte spores are generally known to flourish in warm humid low lands (for example riversides and coastal areas: Pelzer et al., 1992; Abbink et al., 2004) and subsequently high abundances of pteridophyte spores (e.g. *Deltoidspora*, *Concavissimisporites*, and *Impardecispora*) have been recommended as a proxy for humid conditions (e.g. Abbink et al., 2004; Bornemann et al., 2005).

Pollen grain can take many forms and the sphaeroidal grains forms such as the *Araucariacites* are considered as some of the most buoyant members of the sporomorph group (Deaf, 2009). The circumpolles *Classopollis* has been archived to increase in a basinward direction with respect to their relative abundances (e.g. Hughes and Moody-Stuart, 1967; Habib, 1979), furthermore, subsequently recommended as an indicator of relative proximity to fluvio-deltaic systems (Tyson, 1984; 1993; 1995). It is known as an important proxy indicator for palaeoclimatic conditions (Deaf, 2009). As indicated by Doyle et al. (1982), lower abundances of the angiosperm pollen *Afropollis* of possible Winteraceaen affinity have been recorded from warm and dry intracontinental basins.

The presence of fungal spores can indicate a close proximity to, or redeposition from, active fluvio-deltaic source areas (especially deltaic, estuarine, or lagoonal oxic facies) and their association with high abundance of dinoflagellate cysts and foraminiferal linings are indicative of upwelling areas (Tyson, 1995; Mendonça Filho et al., 2012).

The sporomorph group absolute abundances have been found to decline exponentially in an offshore trend in ancient environments (e.g. Reyre, 1973; Habib, 1982). Furthermore, Tyson (1995) proposed that there is some relationship between high abundances of miospores regularly found in fluvio-deltaic systems with the sand and silt lithologies normally found in such systems.

5.2 PALYNOFACIES ASSOCIATIONS AND PALAEOENVIRONMENTAL INTERPRETATIONS.

According to Tyson (1995), the choice of palynofacies parameters ultimately depends upon the objectives of the investigation and the classifications of the kerogen and palynomorphs used in data collection. This study adopts the classification scheme of Tyson (1993, 1995) for palynofacies analysis.

Generally, palynofacies studies are utilized for depositional and paleoenvironmental reconstruction and kerogen analysis (Tucker, 1988; Gorin and Steffen, 1991; Tyson, 1995; Jaramillo and Oboh-Ikuenobe, 1999; Batten et al., 2005).

Table 5.4: Major subdivisions of the Palynomorph Group (After Tyson, 1995).

Natural categories	Sub-categories often used in palynofacies studies
Sporomorph subgroup	
Pteridophyte isospores	Smooth & thin-walled vs. thick and strongly
Microspores (<200μm)	ornamented spores
	Saccate spores
Pteridophyte megaspores (>200μm)	
Gymnosperm pollen and prepollent	Bissacate pollen
	Simple, small, sphaeromorph pollen
Angiosperm pollen	
Fungal spores	
Fungal sclerotia	
Phytoplankton subgroup (including meroplankton)	
Dinoflagellates cysts (dinocysts)	
Peridiniales (Taylor)	Peridinoid cysts
Gonyaulacales (Taylor)	Gonyaulacoid cysts
	Proximate and proximochorate morphotypes
	Chorate morphotypes
	Holocavate and circumcavate morphotypes
Prasinophyte phycomata	
Tasmanitids	
Crassosphaerids	
Pterospermellids	
Cymatiosphaerids ('herkomorphs')	
Acritarchs	
Acanthomorphitae	Forms with short processes
	Forms with long processes
Polygonomorphitae	
Netromorphitae	
Cyanobacteria	
Chroococcales (e.g. Gloeocapsomorpha)	
Rivulariaceae (e.g. Celyphus)	
Oscillatoriales	
Chlorococcale colonial algae	
Botryococcaceae (Botryococcus)	
Hydrodictyaceae (Pediastrum)	
Rhodophyte spores ('circular bodies')	
Zoomorph subgroup	
Foraminiferal test-linings	
Scolecodonts	
Chitinozoa	

The amorphous organic matter (AOM)-Palynomorphs-Phytoclasts (APP) ternary kerogen plot of Tyson (1995) is used to characterize kerogen assemblages to identify the environment of deposition and kerogen types (Figure 5.1 and Table 5.5).

Palynological and palynofacies data plot on the APP ternary diagram of Tyson (1993) also enabled the discrimination of the respective samples into clusters which refer to the palynofacies associations. Binary or ternary diagrams are regularly used to characterize the typical signatures of optical assemblages from the relative proportions of significant organic constituents. According to Tyson (1995) the main advantage of ternary diagrams is that they give a spatial separation that is useful for grouping samples into empirically defined associations or assemblages. As stated in Mendonça Filho et al. (2012), one of the more complete diagrams utilized in palynofacies investigation is the APP diagram because it correlates the percentage of the three main groups of kerogens identified in transmitted white light. Apart from the APP diagram, there are various diagrams used to represent palynofacies data and utilized to interpret its results which is dependent on the objectives of the study and data collected. The Microplankton-Spore-Pollen (MSP) ternary diagram was utilized by Federova (1977) and Duringer and Doubinger (1985) to indicate general depositional environments and associated regressive-transgressive trends (e.g. Traverse, 1988; Tyson, 1993, 1995).

Palynomorphs themselves have environmental significance because they occur in terrestrial and marine environments and can infer palaeoclimatic and palaeoenvironmental characteristics (e.g. Tyson 1995). Terrestrial palynomorphs (sporomorphs) are mainly used as substantial indicators of the conspicuous allochthonous fluviatile input as well as proximity to shoreline trends within the depositional palaeoenvironment (Tyson, 1995; Pittet and Gorin, 1997; Tahoun et al., 2017; Mansour et al., 2018). In this study the APP kerogen plot of Tyson (1995) is used to interpret paleoenvironmental conditions (Fig 5.1) and Table 5.5 representing palynofacies definitions on APP ternary with kerogen type and generation potential (after Tyson, 1993, 1995).

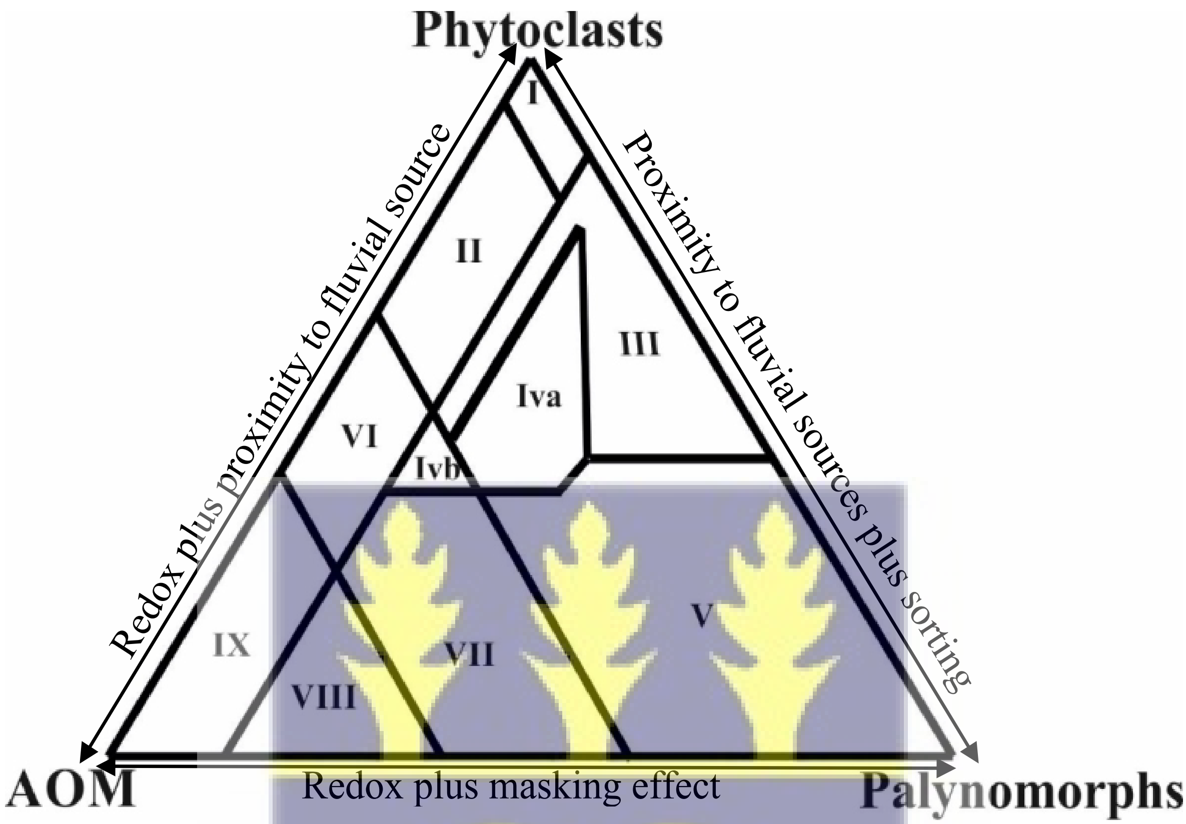

Figure 5.1: AOM-Palynomorphs-Phytoclasts (APP) ternary plot showing environment of deposition and kerogen types (after Tyson, 1993).

Table 5.5: Palynofacies defined on the triangle -APP with kerogen type and generation potential (after Tyson, 1993, 1995).

Field	Environment	Comments	Spores	Microplankton	Kerogen Type
I	Highly proximal shelf or basin	High phytoclast supply dilutes all other components	Usually high	Very low	III, gas prone
II	Marginal dysoxic-anoxic basin	AOM diluted by high phytoclast input, but AOM preservation moderate to good. Amount of marine TOC dependent on basin redox state and dilution	High	Very low	III, gas prone
III	Heterolithic oxic shelf (proximal shelf)	Generally low AOM preservation. Absolute phytoclast abundance dependent on actual proximity to fluvio-deltaic source. Oxidation and reworking common.	High	Common to abundant Dinocysts dominant	III or IV, gas prone
IV	Shelf to basin transition	Passage from shelf to basin in time (e.g. Increased subsidence, water depth) or space (e.g. Basin slope). Absolute phytoclast abundance depends on proximity to source and degree of redeposition. Amount of marine TOC depends on basin redox state. Iva dysoxic-suboxic, Ivb suboxic-anoxic.	Moderate to high	Very low-low	III or II, mainly gas prone
V	Mud-dominated oxic shelf (distal shelf)	Low to moderate AOM (usually degraded) palynomorphs abundant. Light coloured bioturbated. calcareous mudstones are typical	Usually low	Common to abundant Dinocysts dominant	III>IV, gas prone
VI	Proximal suboxic-anoxic shelf	High AOM preservation due to reducing basin conditions. Absolute phytoclast content may be moderate to high due to turbidite input and /or general proximity to source.	Variable low to moderate	Low to common. Dinocysts dominant	II, oil prone
VII	Distal dysoxic-anoxic shelf	Moderate to good AOM preservation. Low to moderate palynomorphs. Dark coloured slightly bioturbated mudstones are typical.	Low	Moderate to common. Dinocysts dominant	II, oil prone
VIII	Distal dysoxic-oxic shelf	AOM –dominated assemblages. Excellent AOM preservation. Low to moderate palynomorphs (partly due to masking). Typical of organic-rich shales deposited under stratified shelf sea conditions.	Low	Low to moderate. Dinocysts dominant, % prasinophytes increasing	II>I, oil prone
IX	Distal suboxic-anoxic shelf/ basin	AOM-dominated assemblages. Low abundance of palynomorphs partly due to masking. Frequently alginitic rich. Deep basin or stratified shelf sea deposits, especially sediments starved basins.	Low	Generally low prasinophytes often dominant	II>I, highly oil prone

5.2.1 Lynx-1X well

Seven (7) palynofacies associations (PF-1 to PF-7) have been identified in the Lynx-1X well between the interval 5300 m – 2520 m based on the quantitative analysis from microscopic observations of proportions of the particulate organic matter (POM) groups represented in Table 5.6 and Figure 5.21.

Table 5.6: Percentage composition of palynofacies associations of particulate organic matter (POM) in Lynx-1X well.

Palynofacies associations	AOM	Opaque phytoclasts	Translucent Phytoclasts	Palynomorphs
PF-1	14	81	4	1
PF-2	45	44	9	2
PF-3	71	23	5	1
PF-4	68	15	16	1
PF-5	58	10	6	26
PF-6	30	18	25	27
PF-7	28	28	5	39

5.2.1.1 Palynofacies type 1 (PF-1) (Opaque phytoclasts) dominant with moderate AOM) (Fig 5.2a).

This palynofacies associations is identified between sample depths intervals (5295 m – 5300 m) - (5035 m – 5040 m), (4715 m – 4720 m) -(4655 m – 4660 m), 4540 m - (4055 m – 4060 m) and (3975 m – 3980 m) - (3955 m – 3960 m). It is dominated by opaques (up to 81% of total POM) with AOM, translucent phytoclasts and palynomorphs (mainly sporomorphs) contributing 14%, 4% and 1% respectively (Fig. 5.b). Marine palynomorphs are absent. Common among recovered sporomorphs include *Classopollis* spp, *Ephedripites* spp. with associated taxa of *Afropollis* spp, *Elaterosporites* spp., *Retimonocolpites, Araucariacites* and *Cyathidites*.

Palaeoenvironmental interpretation: PF-1 displays dominance of opaque phytoclasts which are dark brown to black in color and composed of moderately well-preserved equant to lath-shaped fragments of different sizes. Some of the opaque particles have pitted structure showing that they are derived from tracheid tissues. The samples in PF-1 plotted in field II of Tyson's APP ternary diagram which suggests a redox condition of deposition in a marginal dysoxic-anoxic basin (Fig. 5.3). PF-1 recorded low to none occurrence of spores and might be attributed to the oxidation of some of the palynomorphs to be recovered as opaques. The very high percentage of opaque phytoclasts are the result of oxidation conditions, and either proximity to terrestrial sources or redeposition of terrestrial organic matter from fluvio-deltaic environment (Tyson 1989, 1993; Kholeif and Ibrahim, 2010; Carvalho et al., 2013). Zobaa et al. (2013) infers that, deposition of sediments might have occurred close to fluvial sources where some of the phytoclasts were oxidized to opaques during transportation. Chiaghanam et al. (2013) further suggested the dominance of opaque phytoclasts to indicate fluvio-deltaic/nearshore environment. A marginal dysoxic-anoxic basin condition in a fluvio-deltaic/nearshore environment is suggested for PF-1.

Kerogen Type: This palynofacies association is identified as kerogen type III-IV (gas prone) based on the dominance of opaque phytoclasts with low to none palynomorphs dominated by sporomorphs.

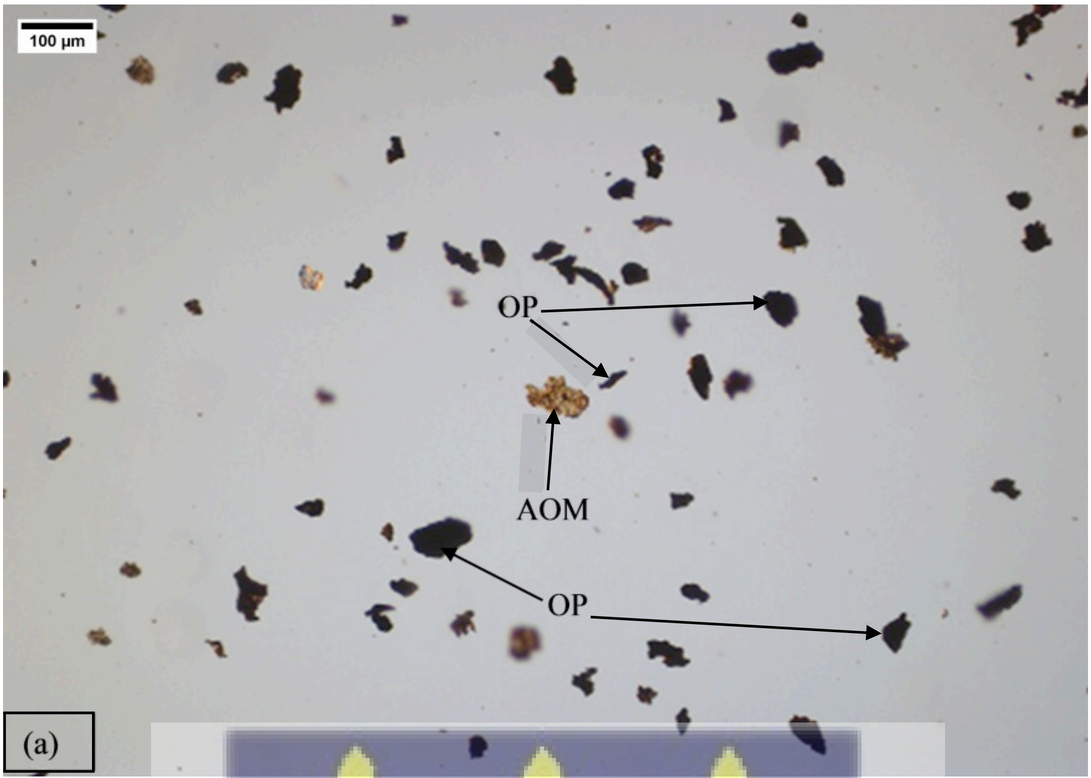

Figure 5.2: (a) Representative photograph of palynofacies association PF-1, sample depth 3600m from the Lynx-1X well. Key to labels: AOM = amorphous organic matter, OP = Opaque phytoclast. (b) Pie chart showing relative abundance (%) of the different constituents of palynofacies association PF-1 from the Lynx-1X well.

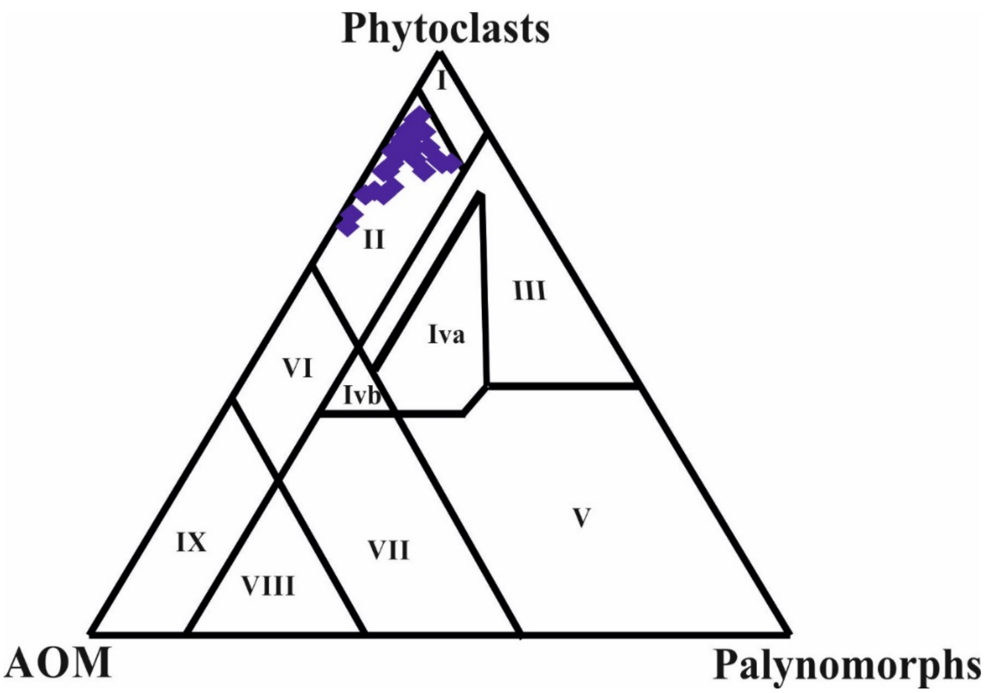

Figure 5.3: APP Ternary diagram for PF-1 samples from Lynx-1X well (after Tyson, 1993).

5.2.1.2 Palynofacies type 2 (PF-2) (Equal abundance of AOM and Opaque phytoclasts) (Fig. 5.4a).

PF-2 is recognized at sample depths between (4995 m – 5000 m) - (4735 m – 4740 m), (4635 m – 4640 m) - (4580 m) and (4035 m – 4040 m) - (3995 m – 4000 m). Opaque phytoclasts and AOM dominates the total organic matter composition of this palynofacies with relatively equal amount (up to 44% and 45% respectively) (Fig. 5.4b). Phytoclasts constitute 9% with palynomorphs (mainly sporomorphs) 2% of POM.

Palaeoenvironmental interpretation: AOM present consists mainly of moderate to good preserved pale yellow to orange particles mostly showing diffused fragments with granular forms present in small amounts. The translucent phytoclasts are brown in colour and opaque phytoclasts are equant and lath-shaped. The palynomorphs recovered are usually orange to medium brown and their relative abundance same as PF-1 and composed of terrestrial taxa (mainly pollen grains). PF-2 plots in the field VI of the APP diagram of Tyson (1995) indicating deposition in a proximal suboxic-anoxic shelf environment (Fig. 5.5). Palynomorphs recovered are wholly sporomorphs dominated by pollen grains in small amounts. The abundance of opaques and AOM with low sporomorphs dominated by the pollen group indicates deposition in a proximal marginal marine/nearshore environment which is supported by Microplankton-Spore-Pollen (MSP) ternary plot (Fig. 5.6). The discussion above suggest PF-2 is deposited under a proximal suboxic-anoxic shelf conditions in a proximal marginal marine/nearshore environment.

Kerogen Type: This palynofacies association is classified as kerogen type II/III (gas prone) based on moderately preserved pale yellow to orange AOM and the high diluting effect of the opaques.

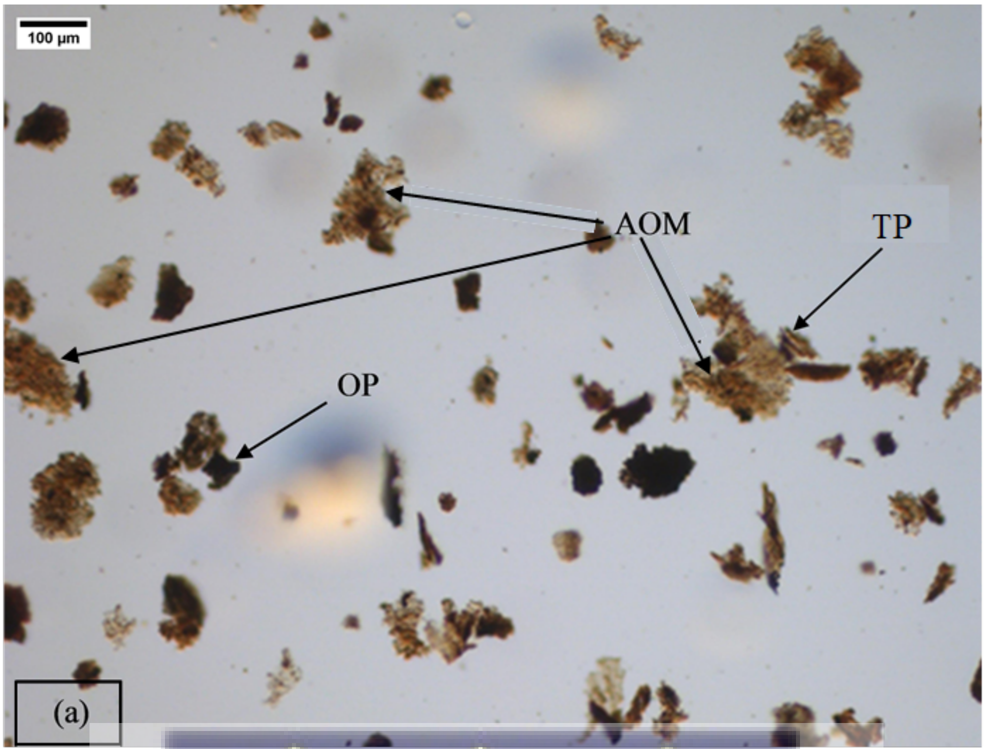

Figure 5.4: (a) Representative photograph of palynofacies association PF-2, sample depth 3600m from the Lynx-1X well. Key to labels: AOM = amorphous organic matter, OP = opaque phytoclast, TP = Translucent Phytoclast. (b) Pie chart showing relative abundance (%) of the different constituents of palynofacies association PF-2 from the Lynx-1X well.

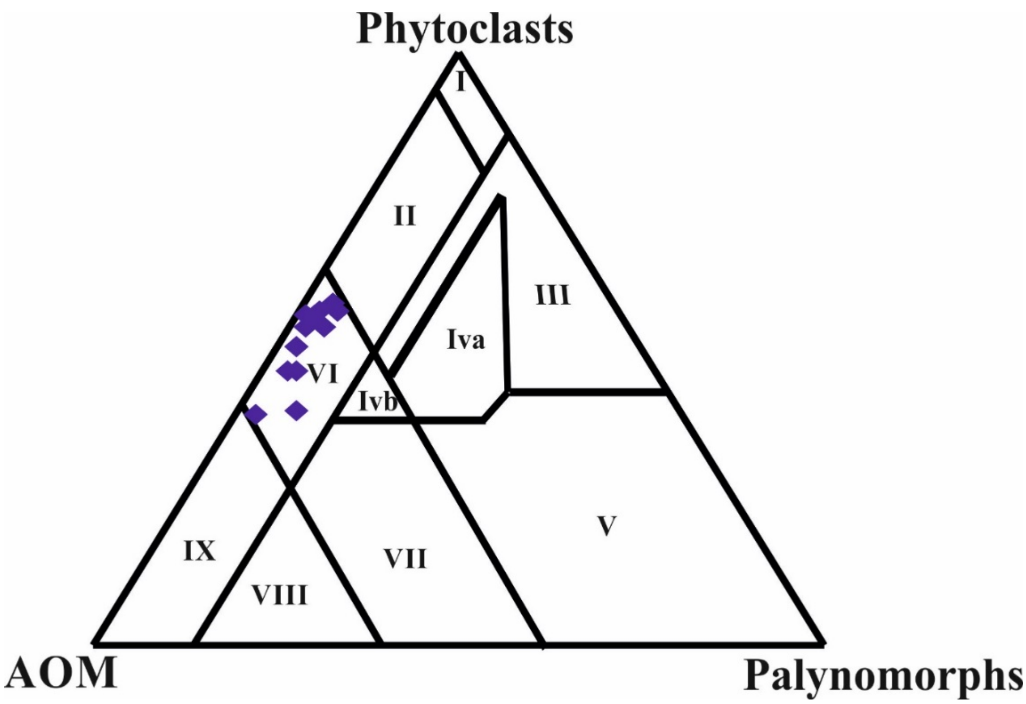

Figure 5.5: APP Ternary diagram of studied samples from the Lynx-1X well (after Tyson, 1993).

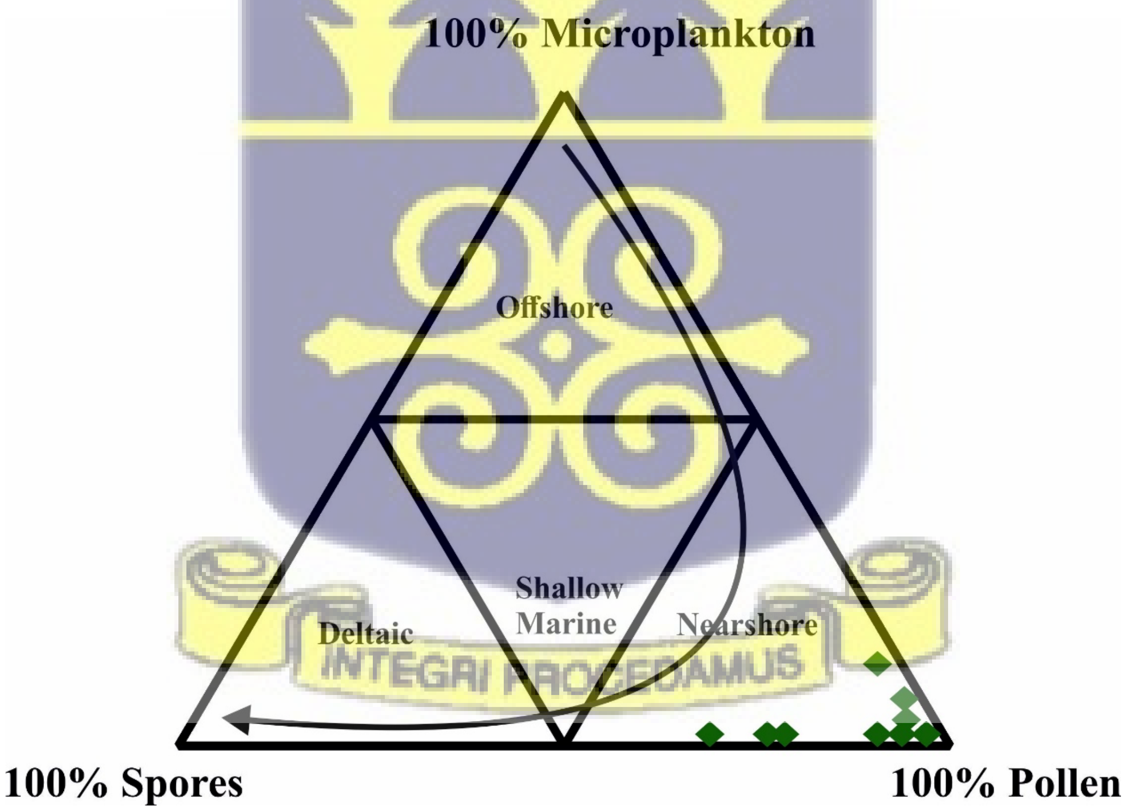

Figure 5.6: MSP Ternary plot for PF-2 samples from Lynx-1X well (After Federova, 1977; Duringer and Doubinger, 1985).

5.2.1.3 Palynofacies type 3 (PF-3) (AOM dominant with high opaques) (Fig. 5.7a)

PF-3 occurs at sample depths between (3750 m – 3760 m) - (3656 m – 3660 m) and 3520 m – 3320 m. It is characterized by high percentage of AOM (71%) and common opaque phytoclasts (23%). PF-3 has relative abundance of translucent phytoclasts (5%) and palynomorphs (1%) of total POM (Fig. 4.7b). AOM is yellowish to orange in colour and well preserved. The palynomorphs are composed of terrestrial origin and dominated by pollen grains with occasional dinocyst (Fig. 5.21).

Palaeoenvironmental interpretation: The dominance of AOM is suggested to be as a result of the combination of environments with high preservation rates and low energies in reducing basins with increased water column which result in a dysoxic-anoxic bottom conditions (Batten, 1983; Tyson, 1993, 1995; Ibrahim et al., 2002; Kholeif and Ibrahim, 2010). According to Tyson (1993) miospores being the least component of a palynofacies may suggest a shallower offshore setting as increase in miospores percentages were equated to proximity of depositional sites to active sources of terrestrial organic matter input. The plot of PF-3 samples on Tyson's APP ternary diagram were constrained in field IX (Fig. 5.8), indicating deposition in a distal suboxic-anoxic basin condition. MSP diagram supports the marginal marine to shallow marine depositional settings (Fig. 5.9) which is inferred due to the presence of some dinoflagellates and the percentage of opaques. From the discussions above, it is suggested that deposition of the samples yielding palynofacies PF-3 took place in a marginal marine to shallow marine environment under distal suboxic-anoxic conditions.

Kerogen Type: The kerogen type represented by the palynofacies association is type II>I (highly oil prone) based on the dominance of well-preserved pale yellowish to orange AOM.

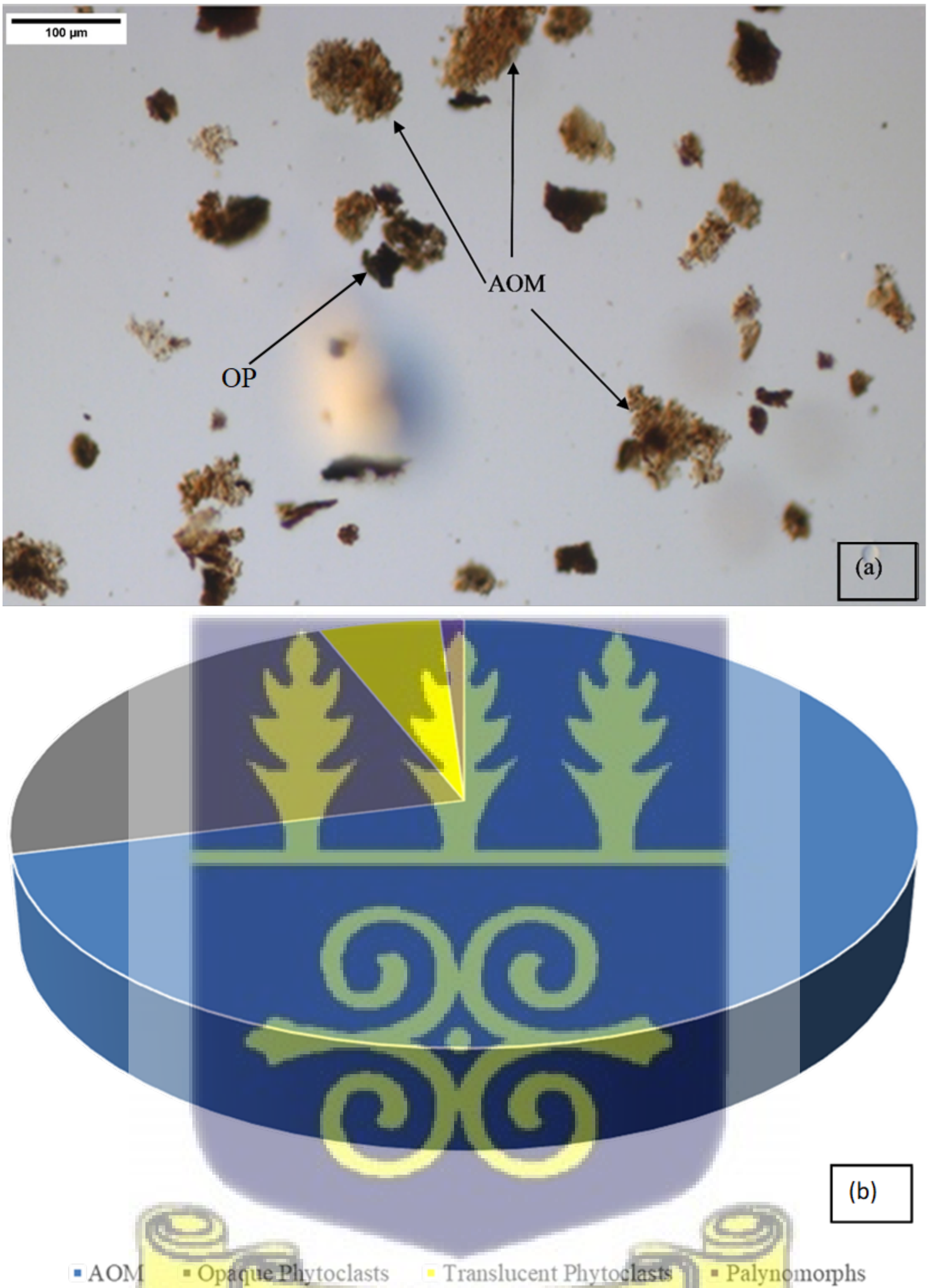

Figure 5.7: (a) Representative photograph of palynofacies association PF-3, sample depth 3660m from the Lynx-1X well. Key to labels: AOM = amorphous organic matter, OP = Opaque phytoclast. (b) Pie chart showing relative abundance (%) of the different constituents of palynofacies association PF-3 from the Lynx-1X well.

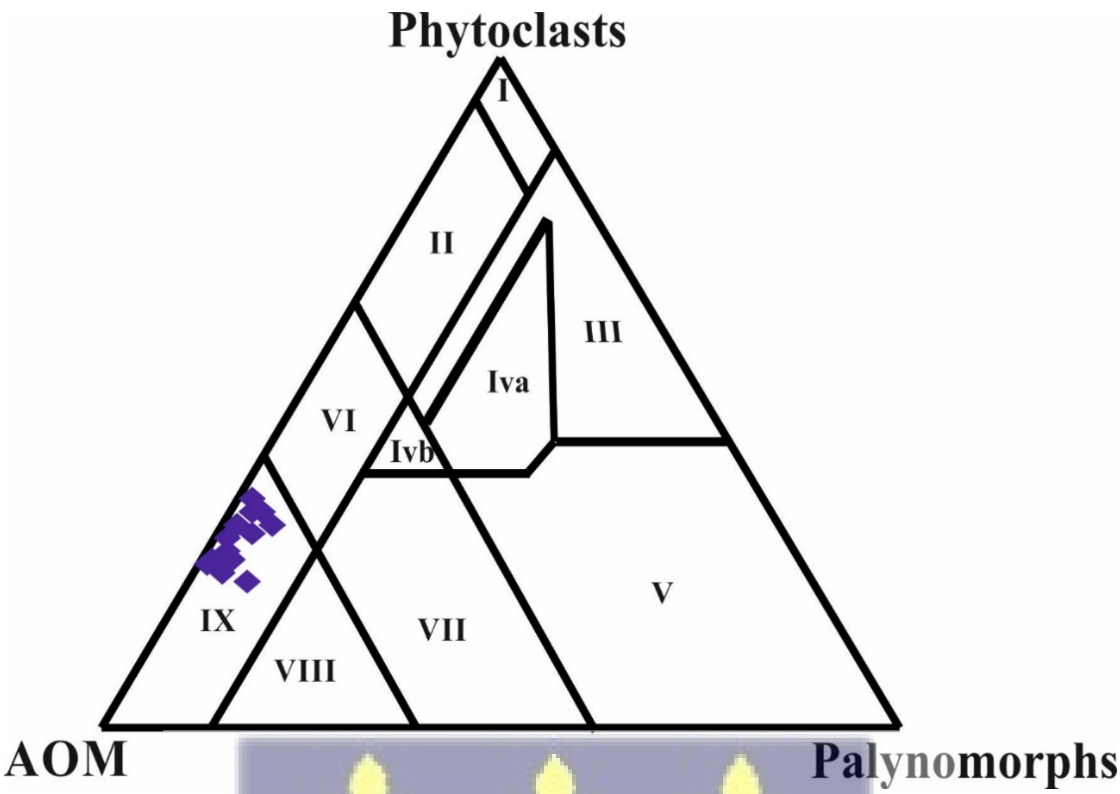

Figure 5.8: APP Ternary diagram for PF-3 samples from Lynx-1X well (after Tyson, 1993).

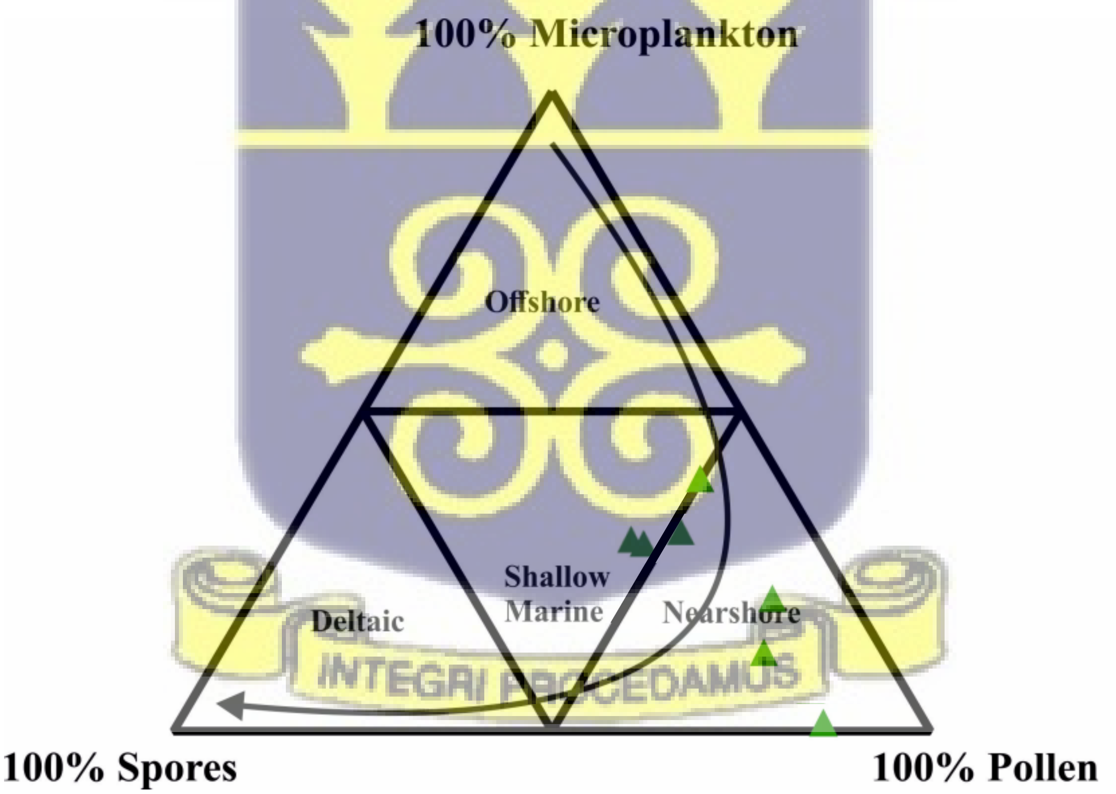

Figure 5.9. MSP Ternary plot of studied samples from the Lynx-1X well (After Federova, 1977; Duringer and Doubinger, 1985).

5.2.1.4 Palynofacies type 4 (PF-4) (AOM dominant with relatively equal abundance of opaques and phytoclasts (Fig. 5.10a)

This palynofacies type is recorded at samples depth intervals from 3640 m – 3540 m. The facies are dominated by AOM (68% of total POM) with relatively equal amounts of opaques (15%) and phytoclasts (16%) (Fig. 4.10b). AOM is mainly well-preserved pale yellow to orange particles and similar to PF-3. The translucent phytoclasts are moderate to well preserved and brown in colour with opaque phytoclasts having dark brown to black in colour. Palynomorphs (mainly of terrestrial origin) make up 1% of POM and consist mainly of pollen grains.

Palaeoenvironmental interpretation: Amorphous organic matter preservation is primarily controlled by oxygen content and there exists a relationship between its colour and depositional environment (Valdes et al., 2004). PF-4 samples were constrained in field IX of Tyson's APP ternary diagram indicating deposition in a distal suboxic-anoxic basin condition (Fig. 5.11) in a shallow marine environment due to the dominance of AOM and absolute diluting effects of phytoclasts. According to Tyson (1995), this field of AOM dominated assemblages with low occurrence of palynomorphs is partly due to masking. Based on the above discussion, PF-4 is suggested to be deposited under a distal suboxic-anoxic basin condition in a shallow marine environment.

Kerogen Type: The field is characterized as kerogen type II>I (highly oil prone) based on the dominance of AOM.

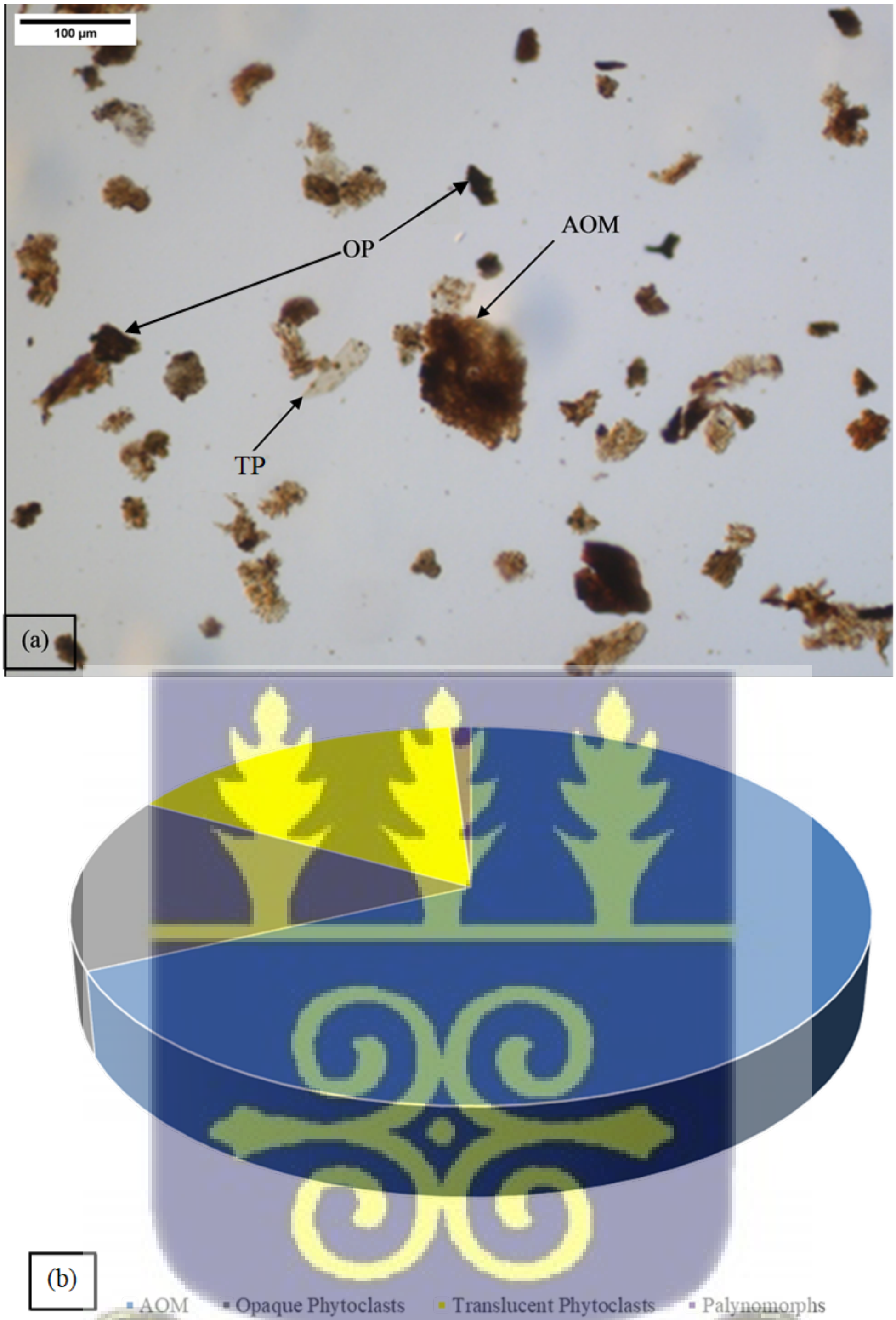

Figure 5.10: (a) Representative photograph of palynofacies association PF-4, sample depth 3600m from the Lynx-1X well. Key to labels: AOM = amorphous organic matter, OP = opaque phytoclast, TP = translucent phytoclast. (b) Pie chart showing relative abundance (%) of the different constituents of palynofacies association PF-4 from the Lynx-1X well.

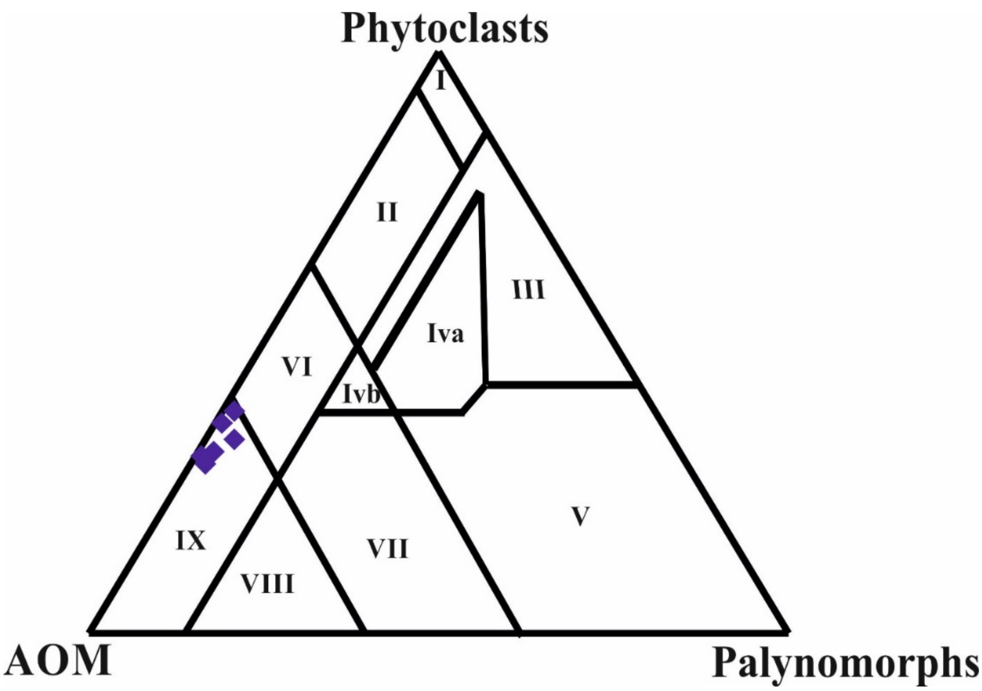

Figure 5.11. APP Ternary diagram for PF-4 samples from Lynx-1X well (after Tyson, 1993).

5.2.1.5 Palynofacies type 5 (PF-5) (AOM dominant with palynomorphs) (Fig. 5.12a)

PF-5 occurs at sample depths interval from 3300 m – 2900 m. It is dominated by moderate to good preservation of AOM (58%) and palynomorphs (26%) of total POM of which marine palynomorphs (dinocysts) constitutes 75% while the sporomorphs forms the remaining 25% of total palynomorphs. PF-5 has relative abundance of opaque phytoclasts (10%) and phytoclasts (6%) of total POM (Fig 5.12b).

Palaeoenvironmental interpretation: AOM present are mostly pale yellow to orange particles. The opaques (black debris) are dark brown to black in colour exhibiting varied sizes. The plot of samples on the APP ternary diagram are constrained in field VIII (Fig. 5.13), indicating deposition in a distal dysoxic-oxic shelf conditions. The gonyaulacoid cysts mainly of chorate forms dominate (70% of total marine palynomorphs) over the peridinoid cysts within this interval represented by the Gonyaulacoids/Peridinoids (G/P) plot (Fig. 5.20) with very high G/P ratio.

Marine components dominate over terrestrial which indicates deposition far away from the shoreline (Williams et al., 2018). The most common marine palynomorphs genera are *Spiniferites*, *Trichodinium*, *Adnatosphaeridium*, *Oligosphaeridium*, *Cordosphaeridium*, *Andalusiella*, *Palaeocystodinium* and *Cerodinium* and among the sporomorphs are *Cyathidites*, *Cicatricosisporites*, *Proxapertites* and *Longapertites*.

Work done by Davey (1970), Habib (1983), Tyson (1984), Balch et al. (1983) and De Vernal & Giroux (1991) on fossil dinoflagellate cysts and modern dinoflagellates suggested that dinoflagellate cysts tend to increase in Gonyaulacoids/Peridinoids (G/P) ratio in an oceanward direction until they reach the continental slope, after which dinoflagellate start to show a reduction in species abundances and diversity. However, the presence of *Spiniferites*, *Exochosphaeridium* and *Florentinia* in this palynofacies association is commonly related to open marine, outer shelf settings, with *Spiniferites* recorded in high numbers in these intervals (Marshall and Batten, 1988; Brinkhuis, 1994). The dominance of the chorate dinocysts over the cavate and proximate cysts recorded from all samples within this palynofacies type generally indicate development of strong marine transgression and deposition in an open marine environment (Tyson, 1993; Williams, 1992; Riding and Hubbard, 1999). The increase in frequencies of *Oligosphaeridium* and *Florentinia* in PF-5 are well documented to be representative for the open marine (middle shelf) conditions (Wall et al., 1977; Dale, 1983; Lister and Batten, 1988).

The increase in frequencies of peridinoids at levels from 3100 – 2900 m of PF-5 suggests deposition moving from deeper open marine settings (outer neritic) from 3300 – 3120 m into a shallower open marine setting (middle neritic) from 3100 – 2900 m (Fig. 5.20). Open marine gonyaulacoid cysts which dominates recovered dinoflagellate cysts from supports the offshore depositional environment of this palynofacies type (Downie et al., 1971; Islam, 1984) and supported by the MSP ternary plot (Fig. 5.14). Low concentrations of phytoclasts recovered in PF-5 supports the suggested offshore setting, where irrelatively low concentrations were equated to weak terrestrial influx and deposition in distal settings located far from land vegetation (Muller, 1959; Pocklington and Leonard, 1979; Tyson, 1993). The strong increment of palynomorphs especially the marine taxa with low occurrence of sporomorphs recorded in this palynofacies association leads to a deduction that ties in with the general suggestion of a more offshore marine setting, as sporomorphs absolute abundances recorded from sediments of ancient environments are found to decrease exponentially in an offshore trend (e.g. Reyre, 1973; Habib, 1983; Habib and Drugg, 1987; Deaf 2009). Low to zero occurrence of pteridophytes (e.g. *Cyathidites* and *Deltoidspora*) in the studied intervals suggests a deposition far from those riverside and coastal areas (Kedves, 1986; Schrank and Mahmoud, 1998) and compliment the more offshore depositional setting of PF-5.

Kerogen Type: PF-5 is classified as kerogen type II>I (oil prone) based on the dominance of AOM and marine dinocysts.

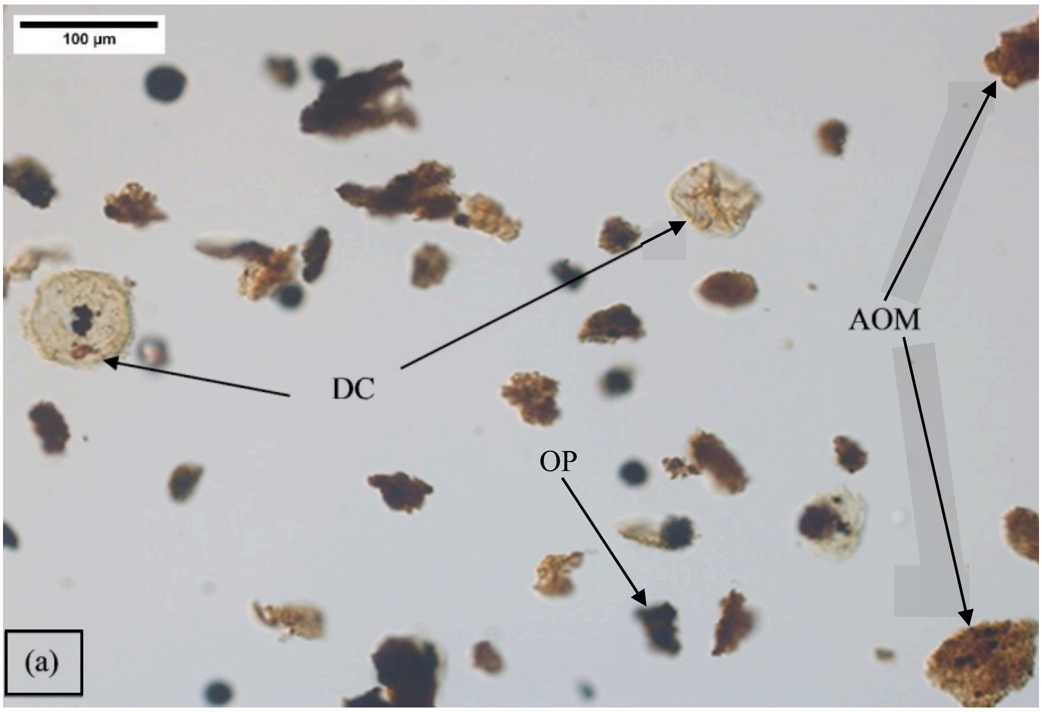

Figure 5.12: (a) Representative photograph of palynofacies association PF-5, sample depth 3060m from the Lynx-1X well. Key to labels: AOM = amorphous organic matter, DC = dinoflagellate cysts, OP= opaque phytoclast. (b) Pie chart showing relative abundance (%) of the different constituents of palynofacies association PF-5 from the Lynx-1X well.

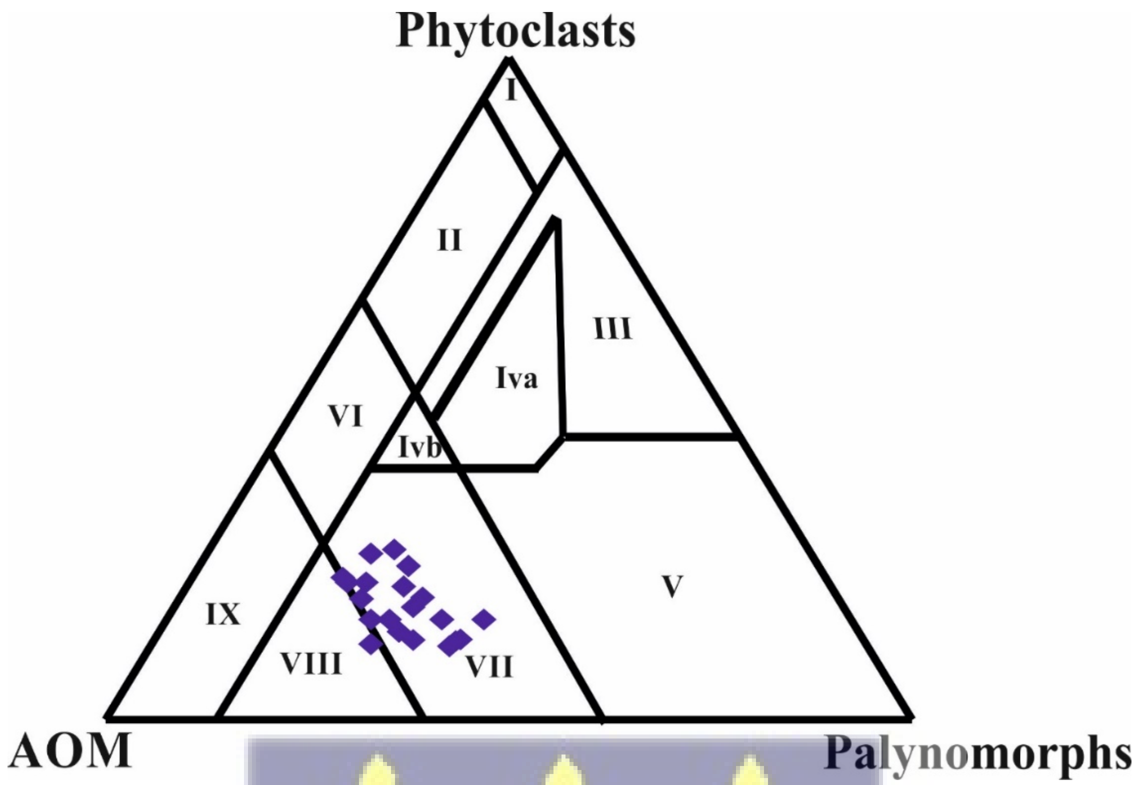

Figure 5.13: APP Ternary diagram for PF-5 from Lynx-1X well (after Tyson, 1993).

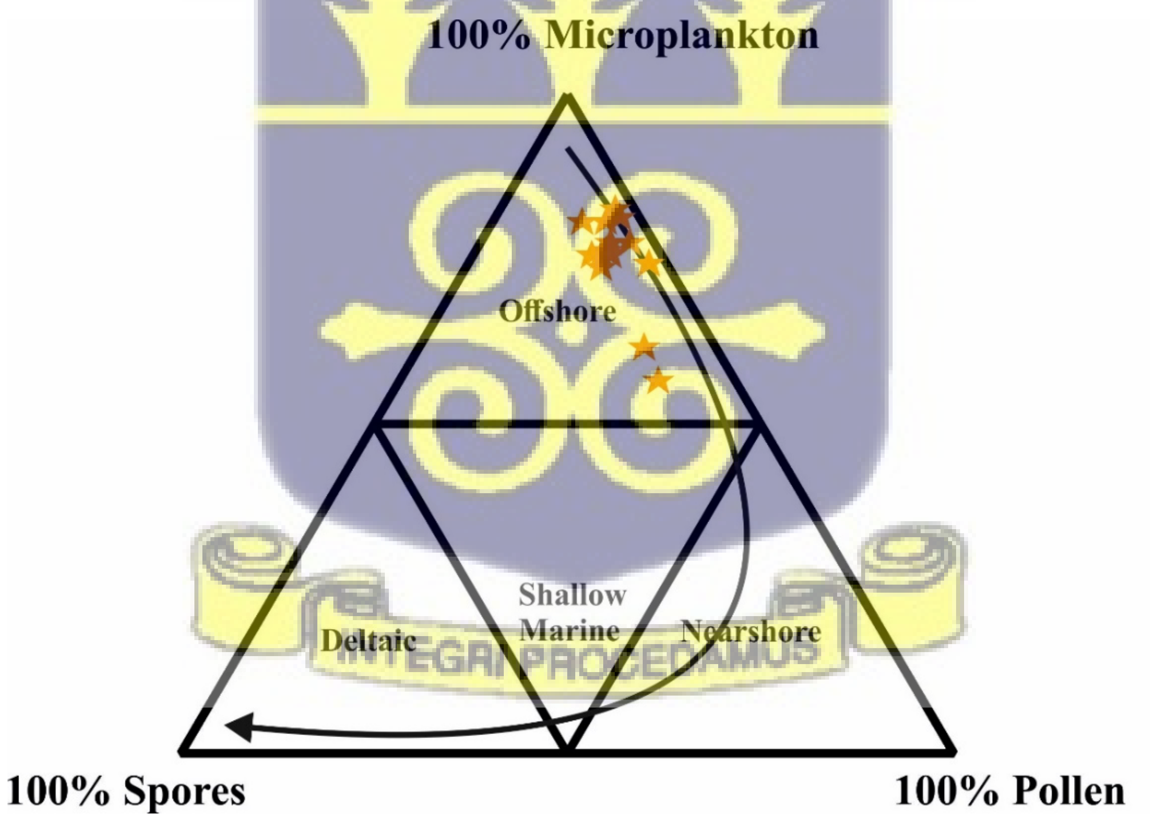

Figure 5.14: MSP Ternary plot for PF-5 samples from Lynx-1X well (After Federova, 1977; Duringer and Doubinger, 1985).

5.2.1.6 Palynofacies type 6 (PF-6) (AOM, phytoclasts and palynomorphs abundant) (Fig. 5.15a).

PF-6 is recognized in sample depths from 2880 m – 2720 m. This interval recorded 30% of AOM of the total organic matter composition with palynomorphs and phytoclasts constituting 27% and 25% respectively (Fig. 5.15b). Opaque phytoclasts contribute 18% of the total POM. Marine palynomorphs dominates the palynomorph assemblage (Fig. 5.21).

Palaeoenvironmental interpretation: AOM present consists mainly of well-preserved pale yellow to orange particles. The translucent phytoclasts consist mainly of pale brown, moderate to well preserved structured plant fragments. Dinoflagellate cysts dominates the assemblage and contributes 72% of total palynomorphs (Fig. 5.20). The peridinoid cysts dominates (67% of total dinocysts) over the gonyaulacoid cysts (33% of total dinocysts) in depth intervals (2800m-2720m) with low G/P ratio while the gonyaulacoid cysts dominates (65% of dinocysts) over the peridinoids from 2880m-2820m with high G/P ratio (Fig. 5.20). Sporomorphs contribute (av. 28%) and dominated by pollen grains similar to those in PF-5. PF-6 plots in the field Iva and IVb of the Tyson APP diagram indicating deposition in a shelf to basin transition (IVa=dysoxic; IVb= suboxic-anoxic) conditions (Fig. 5.16). The recovered marine palynomorphs species in this palynofacies type is similar to PF-5 with dominance of peridinoids genus such as *Cerodinium*, *Andalusiella*, *Dinogymnium*, *Palaeocystodinium*, etc. from interval 2800m-2720m which are typical of shallow marine environment. Dam et al. (1998) inferred the predominance of peridinoid dinocysts cited above to reflect a period of transgression and therefore an increase in sea-surface temperature. Open marine gonyaulacoids similar to those discussed in PF-5 (e.g. *Oligosphaeridium complex, Florentina mantellii, Spiniferites ramosus, Spiniferites cornutus, Spiniferites* sp., *Areoligera*) dominates the interval 2880m-2820m. The sporomorphs components is similar to those discussed in PF-5 and indicates terrestrial influence on the depositional environment. The reduction in AOM frequencies in this association compared to PF-5 and increase in relative abundance of peridinoid cysts from 2800m-2720m reflects a proximal offshore setting. PF-6 above indicate a deposition in a shelf to basin transition condition in an offshore, most likely from an inner-neritic to middle-neritic environments.

Kerogen Type: PF-6 is constituted by kerogen type III and II (oil prone) based on the abundance of AOM, palynomorphs (dominated by marine dinocysts) and phytoclast.

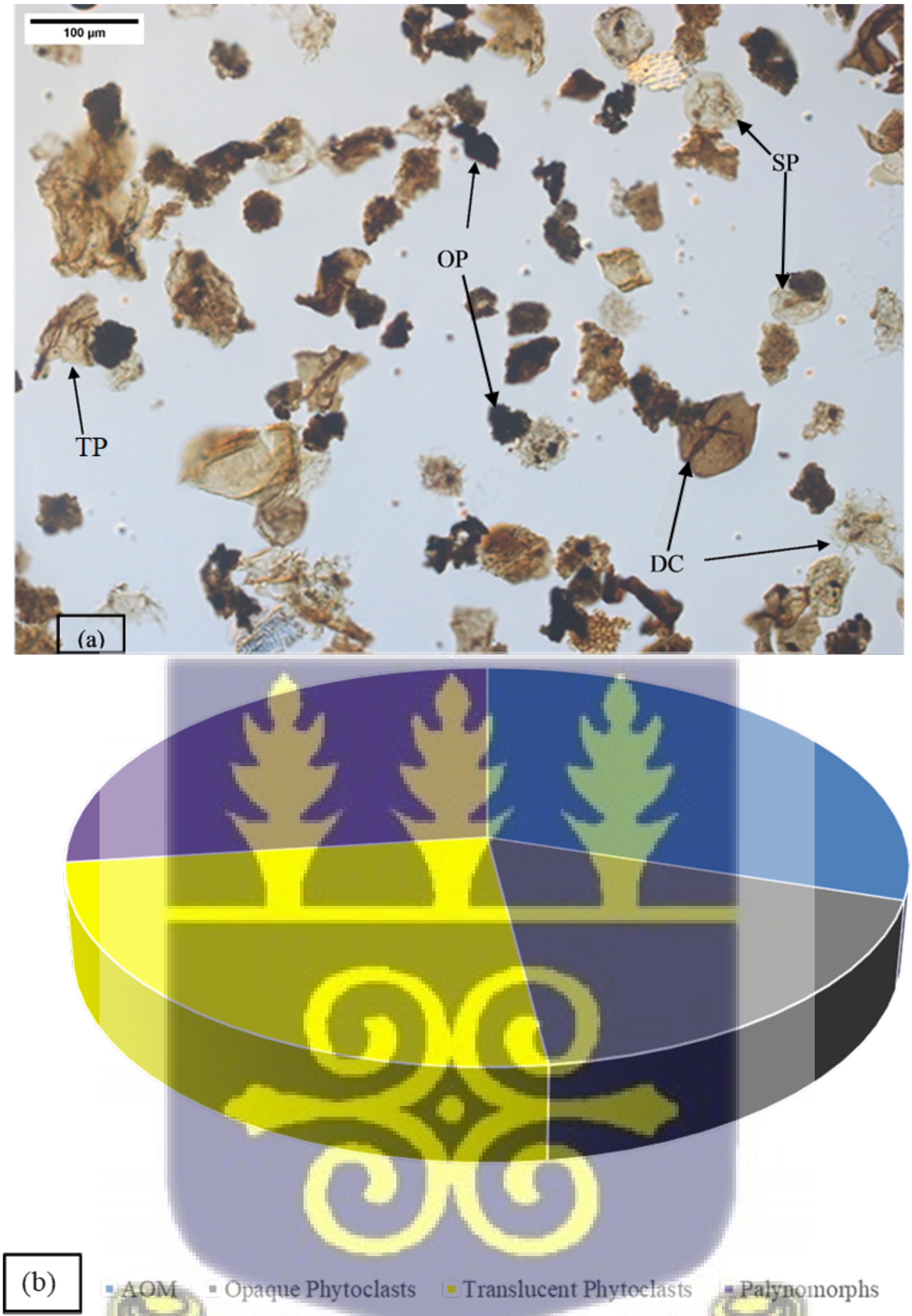

Figure 5.15: (a) Representative photograph of palynofacies association PF-6, sample depth 3060m from the Lynx-1X well. Key to labels: AOM = amorphous organic matter, SP = sporomorph, DC = dinoflagellate cysts, OP = opaque phytoclast, TP = translucent phytoclast. (b) Pie chart showing relative abundance (%) of the different constituents of palynofacies association PF-6 from the Lynx-1X well.

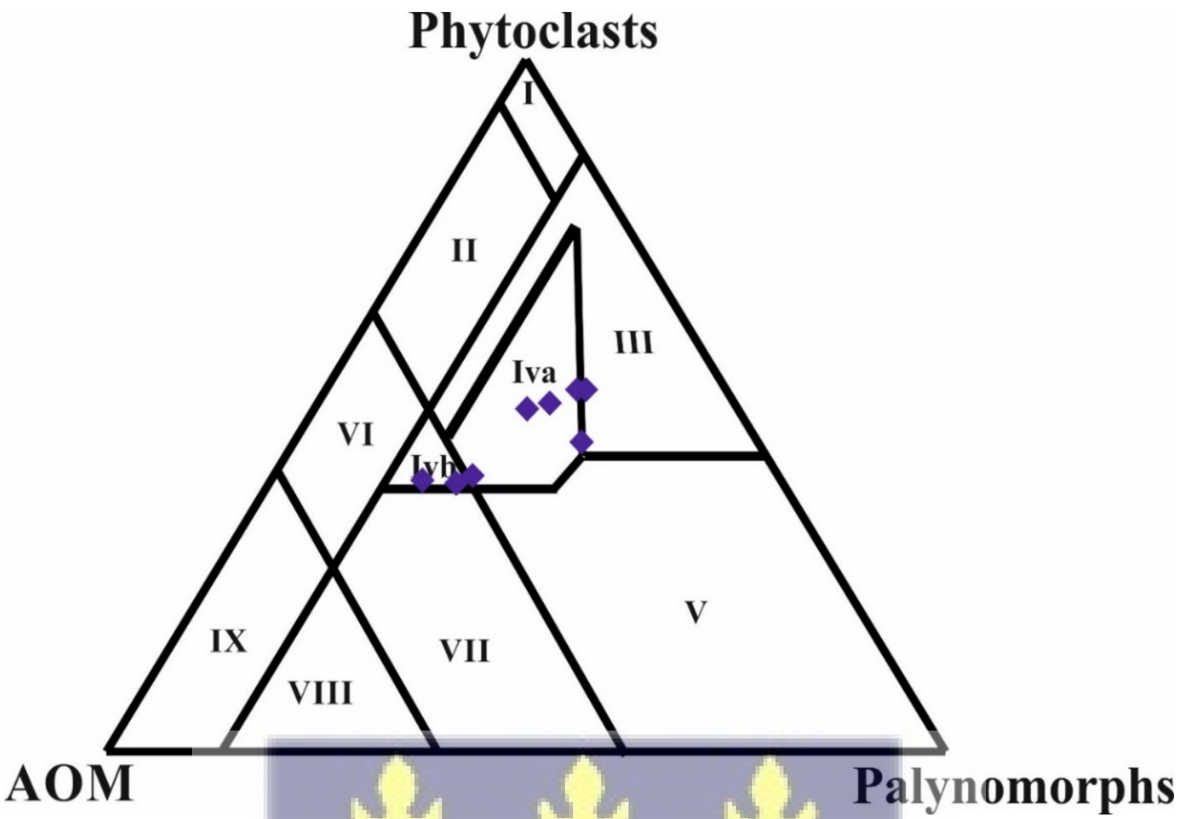

Figure 5.16: APP Ternary diagram for PF-6 samples from Lynx-1X well (After Tyson, 1993).

5.2.1.7 Palynofacies type 7 (PF-7) (Palynomorphs with equal abundance of AOM and opaques) (Fig. 5.17a).

PF-7 occurs between sample depths from 2700 m – 2520 m (Fig. 5.21). It is made up of equal relative abundance of AOM (28%) and opaque phytoclasts (28%) with abundant palynomorphs (39%) (Fig. 5.17b). Phytoclasts make up 5% of total POM. Most palynomorphs are yellowish orange to light brown in colour. The palynomorphs of marine origin (dinocysts) dominates the assemblage and contribute 80% of total palynomorphs with the sporomorphs making up 20% and dominated by pollen grains with associated pteridophyte spores. The dinocysts are dominated by gonyaulacoids which contributes 86% of the dinocysts with some common species in PF-6. Peridinoid cysts contributes the remaining 14% of dinocysts.

Palaeoenvironmental interpretation: On Tyson's APP ternary diagram PF-7 plots in field V which reflects distal mud-dominated oxic shelf conditions (Fig. 5.18). Common among the gonyaulacoid cyst genera are chorate forms (*Spiniferites*, *Operculodinium*, *Lingulodinium*, *Adnatosphaeridium*, *Damassadinium, Glaphyrocysta, Diphyes* and associated with minor amounts of *Homotryblium*, *Achomosphaera*, *Turbiosphaera, Polysphaeridium, Oligosphaeridium*, *Cordosphaeridium*, *Areoligera*, *Fibrocysta*, *Hystrichokolpoma*, *Coronifera* and *Fibrocysta*. Common among the peridinoid cyst genera are the cavate and proximate forms (*Ifecysta*, *Apectodinium, Palaeocystodinium*, *Cerodinium* and associated with minor amounts of *Andalusiella* and *Cribroperidinium*). The dominance of the gonyaulacoid cysts (Fig. 5.20) in this palynofacies association suggests an offshore environment of deposition (outer neritic) and supported by SPM plot which plotted in the offshore region of the ternary diagram (5.19). Occurrence of phytoclasts and opaques in moderate equal amounts supports the suggested offshore setting and discussed earlier in PF-6. PF-7, therefore, support an outer neritic environment under distal mud-dominated oxic shelf conditions.

Kerogen Type: PF-7 is characterized by kerogen type II/III (gas prone) based on moderate AOM and opaques phytoclasts with abundant marine palynomorphs (Tyson, 1993, 1995).

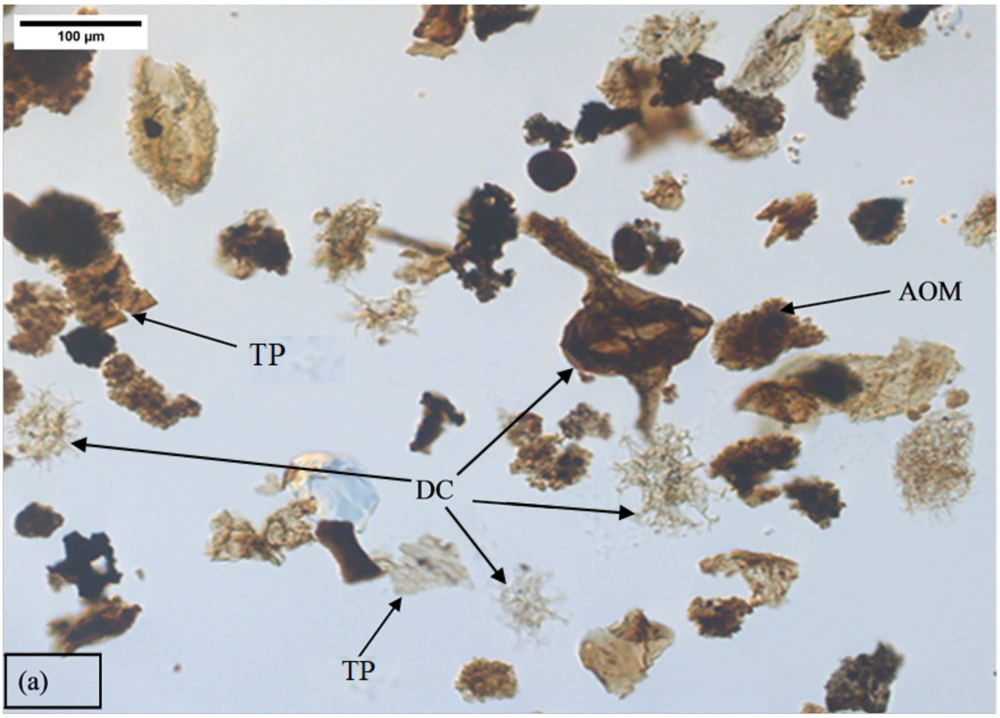

Figure 5.17: (a) Representative photograph of palynofacies association PF-7, sample depth 2560m from the Lynx-1X well. Key to labels: AOM = amorphous organic matter, SP = sporomorph, DC = dinoflagellate cysts, OP = opaque phytoclast, TP = translucent phytoclast. (b) Pie chart showing relative abundance (%) of the different constituents of palynofacies association PF-7 from the Lynx-1X well.

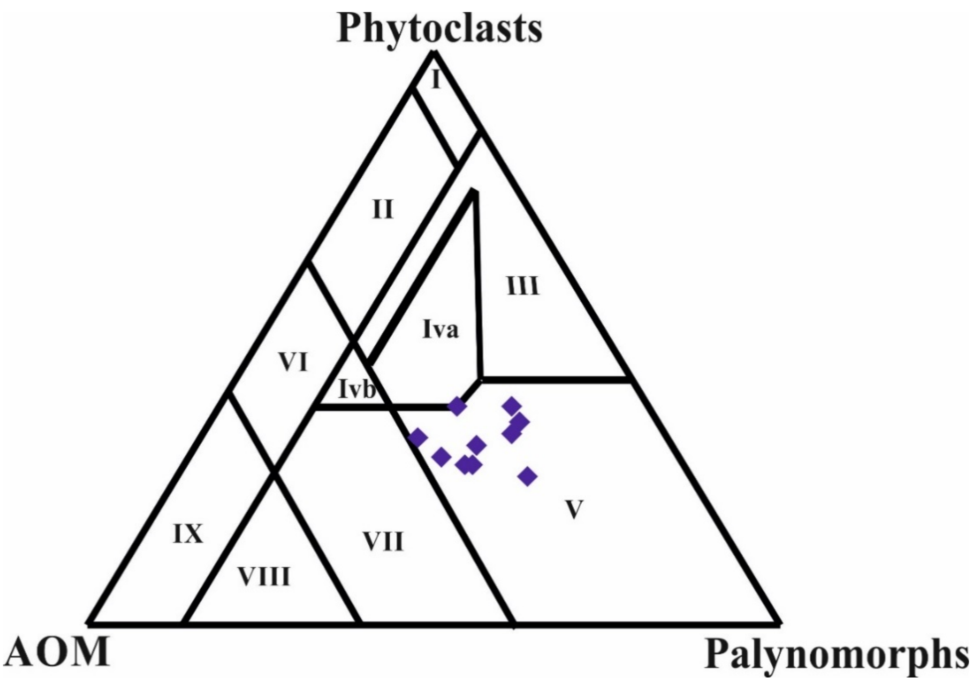

Figure 5.18: APP Ternary diagram for PF-7 samples from Lynx-1X well (after Tyson, 1993).

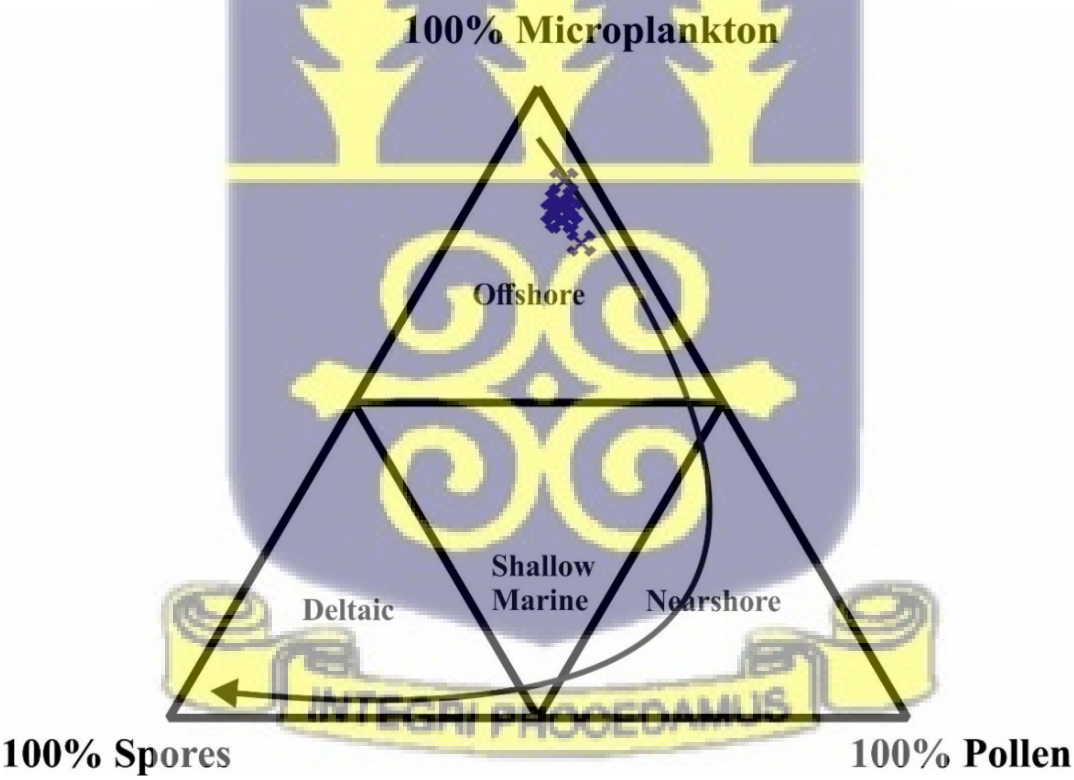

Figure 5.19: MSP Ternary plot for PF-7 samples from Lynx-1X well (After Federova, 1977; Duringer and Doubinger, 1985).

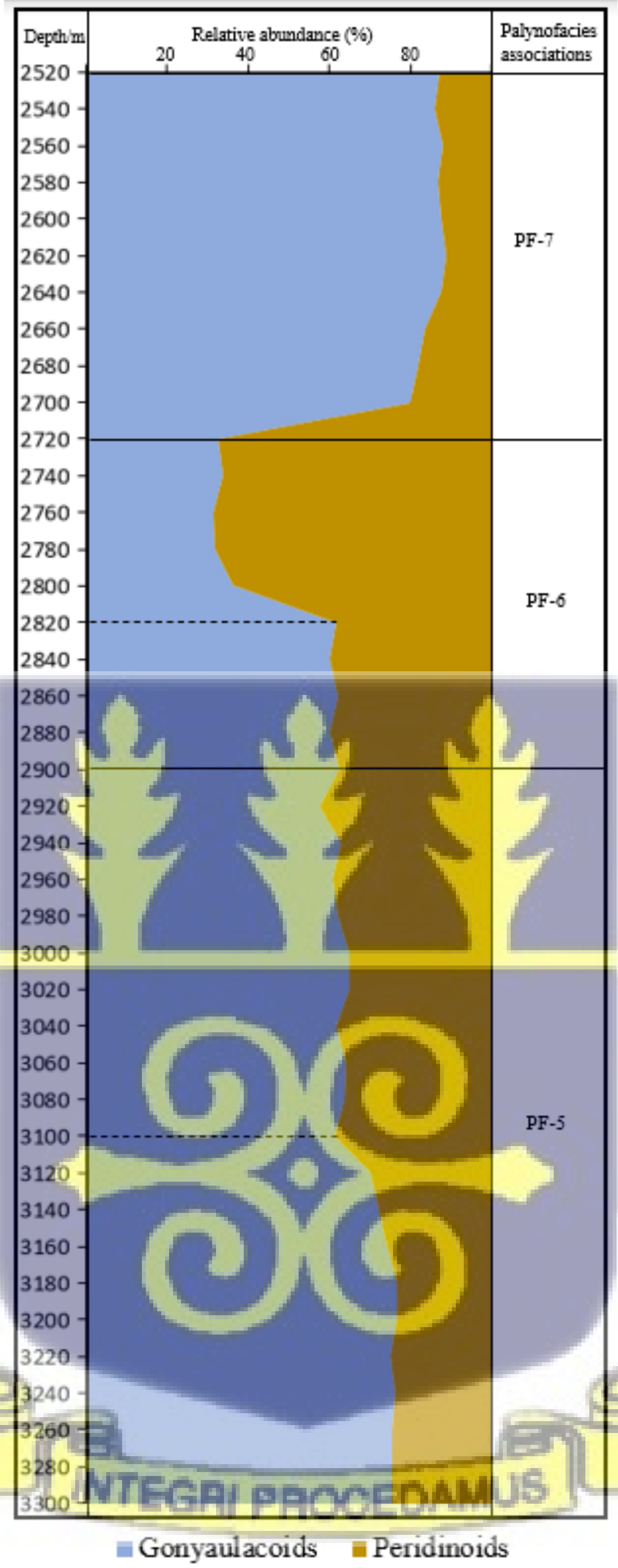

Figure 5.20: Relative percentage composition of Gonyaulacoids and Peridinoids in Lynx-1X well.

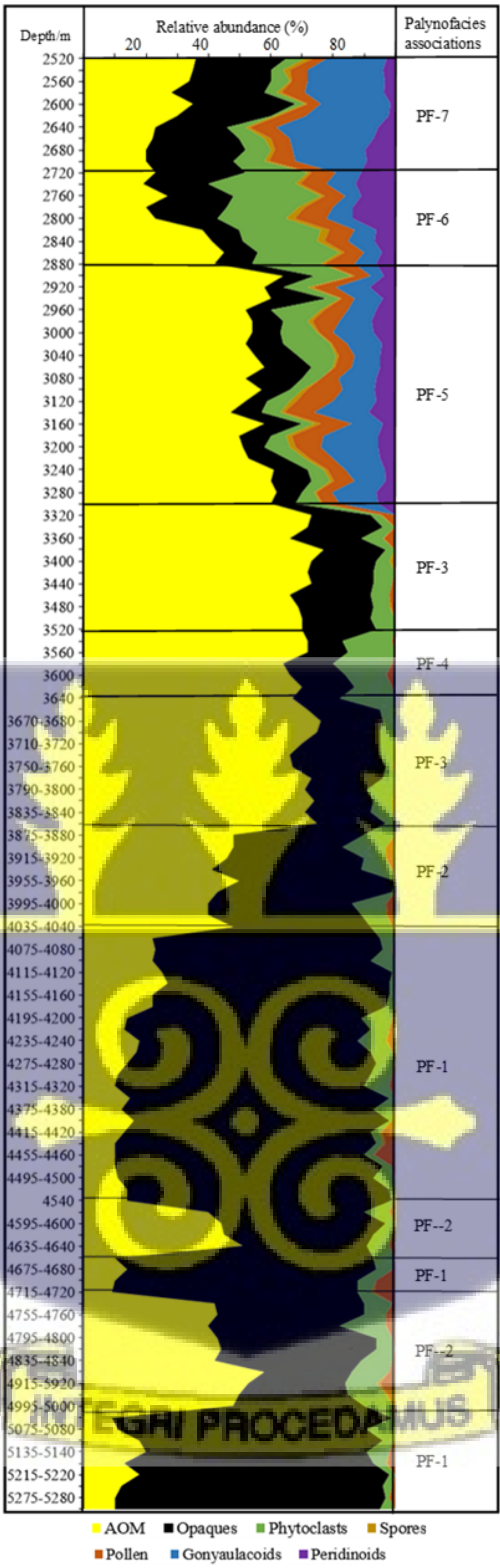

Figure 5.21: Palynofacies assemblages showing POM (%) from Lynx-1X well.

5.2.2 Dzata-1 well

Five palynofacies associations has been recognized between the interval 4390 m - 2450 m dependent on the proportions of the particulate organic matter (POM) groups. These associations are Palynofacies type 1(PT-1), Palynofacies type 2 (PT-2), Palynofacies type 3 (PT-3), Palynofacies type 4 (PT-4) and Palynofacies type 5 (PT-5) (Table 5.7, Fig. 5.38).

5.2.2.1 Palynofacies type 1 (PT-1) (AOM dominant with abundant Opaque phytoclasts) (Fig. 5.22a)

PT-1 is identified between depth interval from 4390 – 4030 m. It is dominated by AOM and abundant opaque phytoclasts making up of 52% and 33% of total POM respectively (Fig. 5.22b). Palynomorphs (mainly of terrestrial origin) 7% and translucent phytoclasts making up 8% of POM. AOM preservation is moderate and pale yellow in colour. The opaque phytoclasts are dark brown to black whilst the translucent phytoclasts are yellowish brown in colour. The palynomorphs are mainly light orange to medium brown.

Table 5.7: Percentage composition of palynofacies associations of particulate organic matter (POM) in Dzata-1 well.

Palynofacies associations	AOM	Opaque phytoclasts	Translucent Phytoclasts	Palynomorphs
PT-1	52	33	8	7
PT-2	24	28	27	21
PT-3	7	88	2	3
PT-4	72	4	6	18
PT-5	33	46	13	8

Palaeoenvironmental interpretation: PT-1 were constrained in field VI of Tyson's APP ternary diagram indicating deposition in a proximal suboxic-anoxic shelf condition (Fig. 5.23). The dominant sphaeroidal pollen grains (av. 90% of sporomorphs) (e.g. *Araucariacites, Classopollis, Inaperturopollenites*) over pteridophyte spores (*Cyathidites*, *Deltoidspora*) in PT-1 suggests a proximal offshore setting due to the absence of marine elements and abundant opaque phytoclasts. The sporomorph group is indicative of deposition in a more nearshore environment and supported by SPM plot (Fig. 5.24). Other associated pollen grains include *Afropollis* and *Ephedripites* which indicates an arid to semi-arid warm climatic conditions (e.g. Mahmoud and Moawad, 2002) and commonly inhabit in palaeotropical humid coastal plains (Schrank, 2001; El Beialy et al., 2011). Recovered foraminiferal linings at depth intervals (4370 m – 4230 m) indicates a form of marine influence on these facies. Based on the discussions, the AOM is diluted by phytoclasts input which is generally the opaque type and sporomorphs constituents in PT-1, it suggests a deposition in a nearshore environment under proximal suboxic-anoxic conditions.

Kerogen Type: PT-1 is characterized by kerogen type II and III (oil prone) based on dominant AOM and abundant opaque phytoclasts.

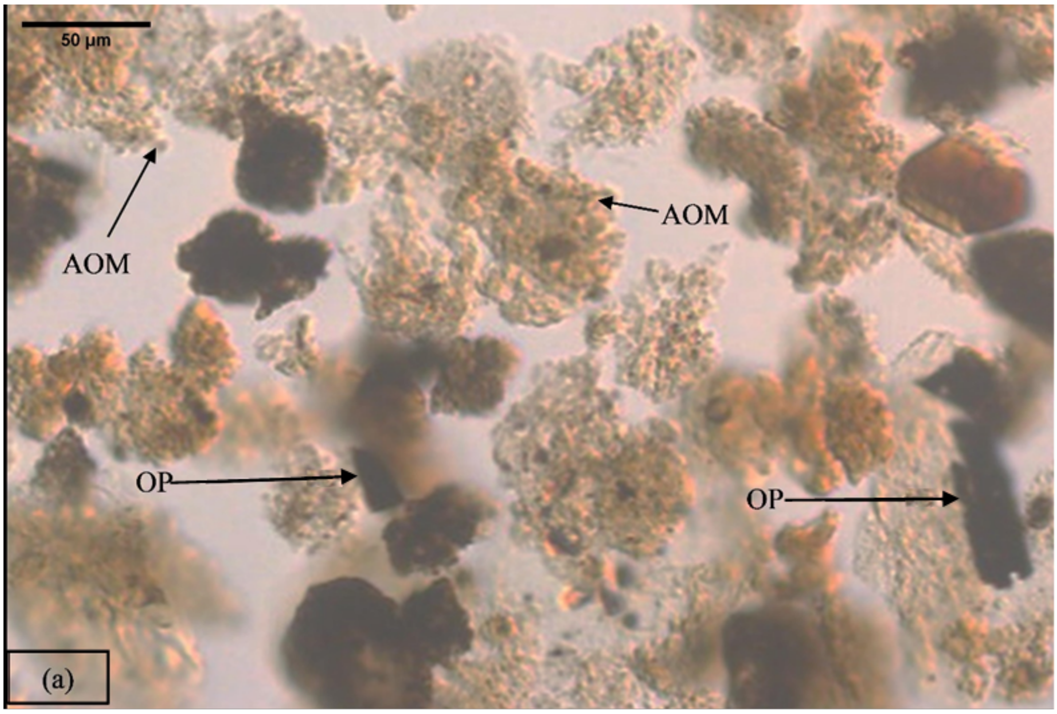

Figure 5.22: (a) Representative photograph of palynofacies association PT-1, sample depth 4370m from the Dzata-1 well. Key to labels: AOM = amorphous organic matter, OP= opaque phytoclast. (b) Pie chart showing relative abundance (%) of the different constituents of palynofacies association PT-1 from Dzata-1 well.

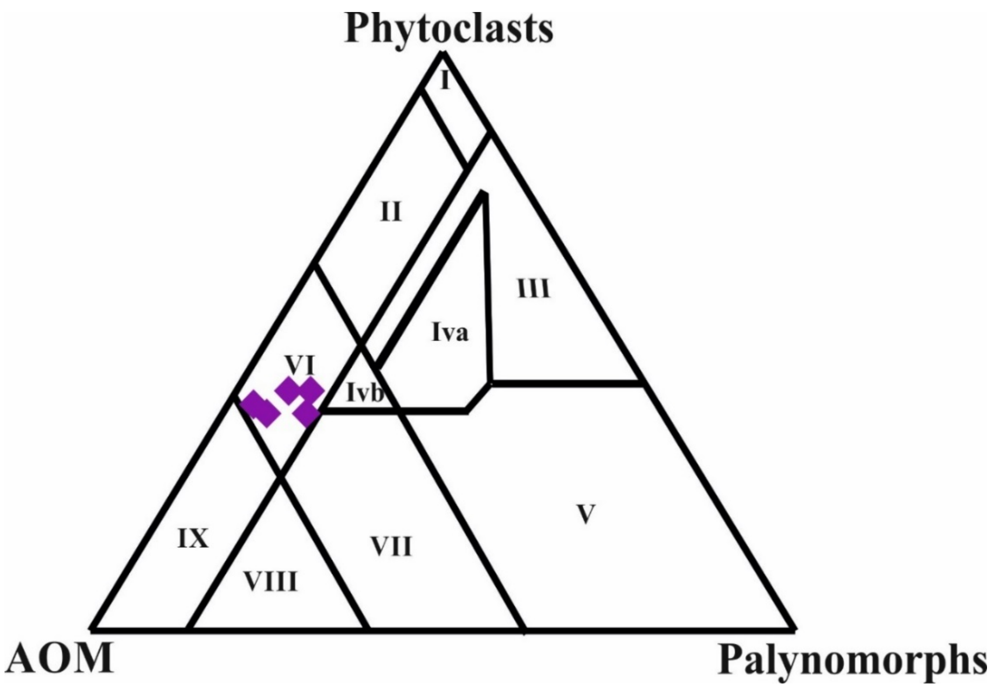

Figure 5.23: APP Ternary diagram for PT-1 samples from Dzata-1 well (after Tyson, 1993).

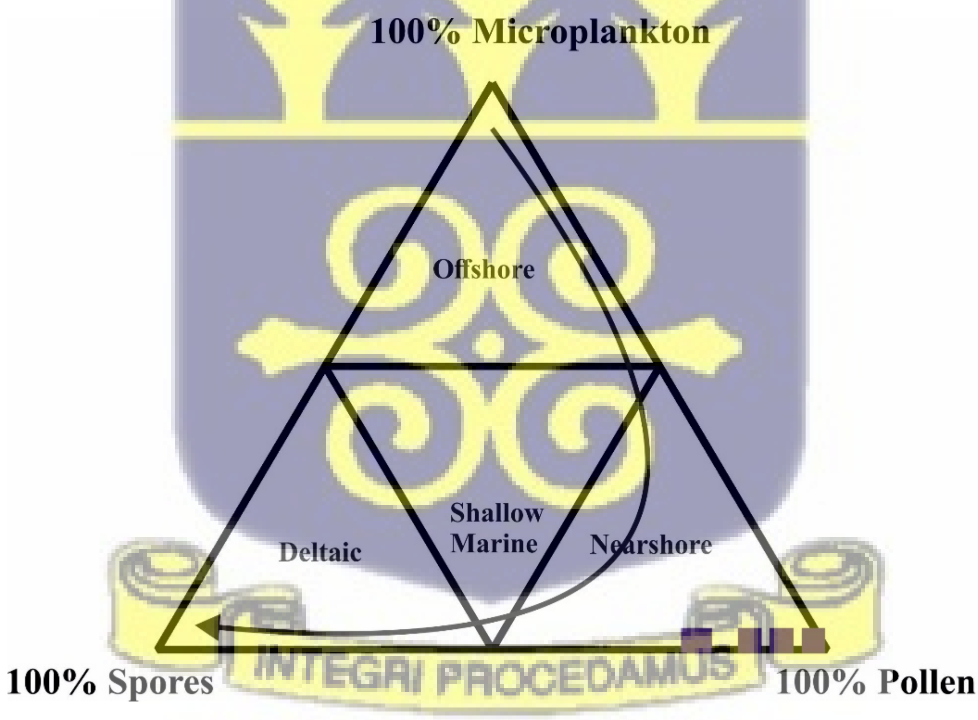

Figure 5.24: MSP Ternary plot for PT-1 samples from Dzata-1 well (After Federova, 1977; Duringer and Doubinger, 1985).

5.2.2.2 Palynofacies type 2 (PT-2) (Relatively equal abundance of opaques phytoclasts and phytoclasts (non-opaques) with AOM and palynomorphs) (Fig. 5.25a).

This palynofacies assemblage covers the depths between 4010 – 3710 m and 3630 – 3230 m. It is characterized by the relative equal abundance of opaque phytoclasts (28%) and translucent phytoclasts (27%). AOM (24%) and palynomorphs (21%) of total POM (Fig. 5.25b). Palynomorphs of terrestrial origin (mainly sphaeroidal pollen grains) dominates (98% of total palynomorphs) this palynofacies association (Fig. 5.38). Sporomorphs recovered from this palynofacies type include *Classopollis* spp, *Ephedripites* spp., *Elaterosporites* spp. with associated taxa of *Afropollis*, *Retimonocolpites, Araucariacites* and *Cyathidites*.

Palaeoenvironmental interpretation: The plot of samples on Tyson's APP ternary diagram were constrained in field Iva indicating deposition in a dysoxic-suboxic conditions (Fig. 5.26). Most pteridophytic spore associations (e.g. *Cyathidites*, *Deltoidspora*) are low to zero in count for most of the intervals. The high amount of miospores (dominated by sphaeroidal pollen grains) occurrence and high relatively equal abundance of opaques and translucent phytoclasts would support a nearshore environment and supported by SPM plot (Fig 5.27). The decrease in the amount of AOM which has been found in shallow shelf sediments (e.g. Dow and Pearson, 1975; Bujak et al., 1977) can be attributed to the dilution by phytoclasts which is influenced by run-off from and proximity to adjacent landmass thereby suggesting a shallow marine influence. Based on the discussions above, PT-2 indicates a deposition in a dysoxic-suboxic conditions in a nearshore environment.

Kerogen Type: It is constituted by kerogen type III (gas prone) based on the relative equal abundance of phytoclasts (opaques and translucent) and palynomorphs dominated by sporomorphs.

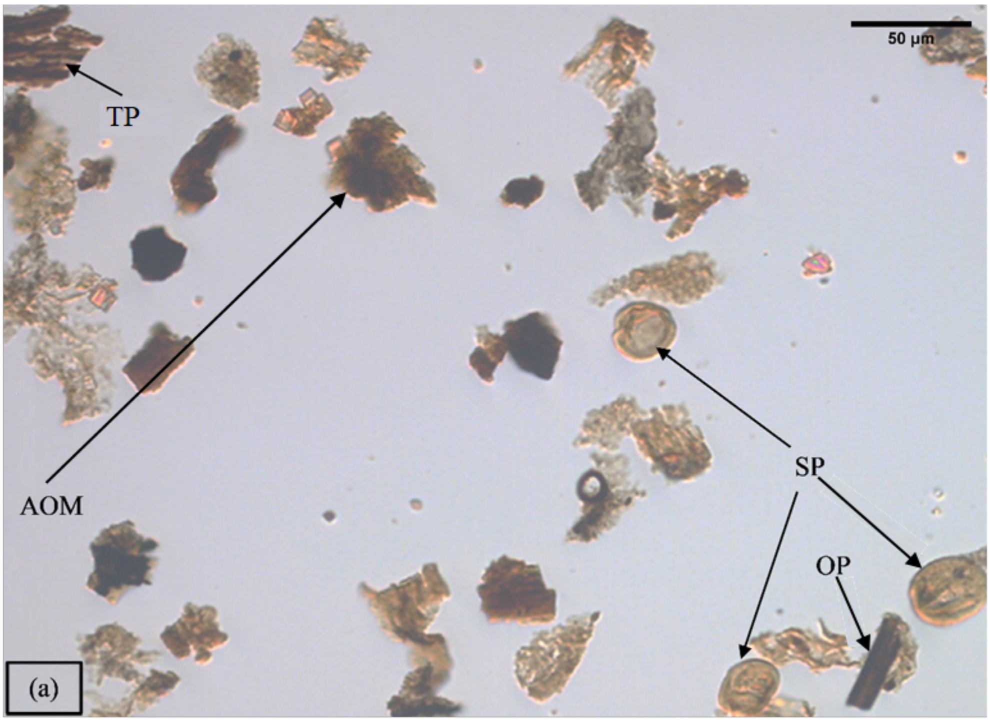

Figure 5.25: (a) Representative photograph of palynofacies association PT-2, sample depth 3610m from the Dzata-1 well. Key to labels: AOM = amorphous organic matter, SP = sporomorph, OP = opaque phytoclast, TP = translucent phytoclast. (b) Pie chart showing relative abundance (%) of the different constituents of palynofacies association PT-2 from Dzata-1 well.

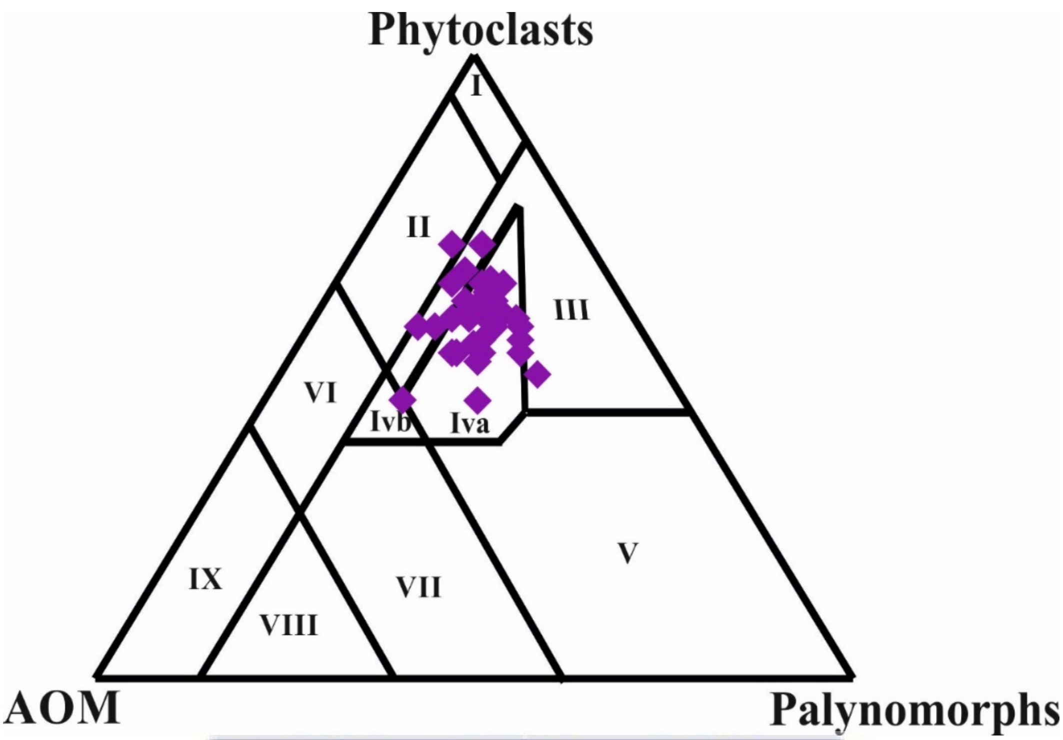

Figure 5.26: APP Ternary diagram for PT-2 samples from Dzata-1 well (after Tyson, 1993).

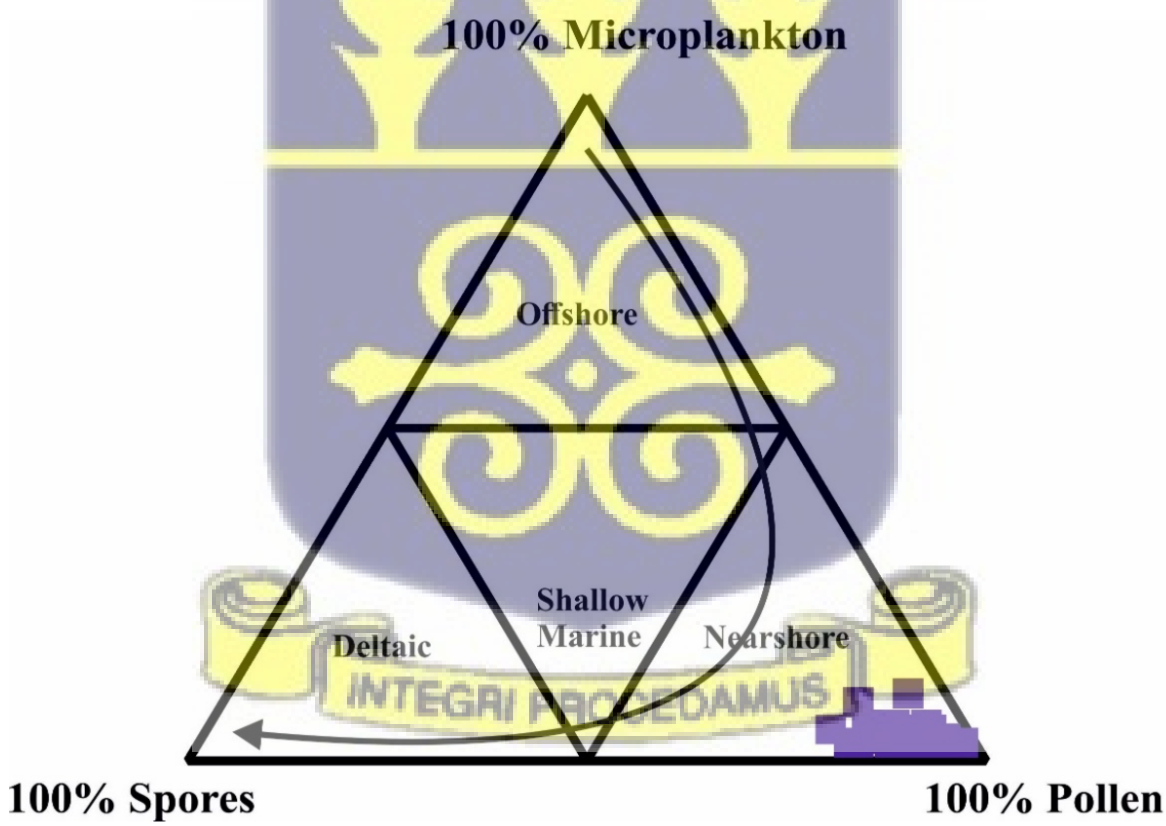

Figure 5.27: MSP Ternary plot for PT-2 samples from Dzata-1 well (After Federova, 1977; Duringer and Doubinger, 1985).

5.2.2.3 Palynofacies type 3 (PT-3) (Opaques dominant) (Fig. 5.28a).

PT-3 is located between depth interval from 3690 m – 3650 m in the Dzata-1 well. The dominant element within this palynofacies association is opaque phytoclasts (up to 88% of POM). It contains AOM, palynomorphs and translucent phytoclasts with relative abundance of 7%, 3% and 2% respectively (Fig. 5.28b). Palynomorphs recovery is dominated by (99-100%) terrestrial palynomorphs. The sporomorphs (dominated by sphaeroidal pollen grains) mainly *Classopollis* spp. with few *Ephedripites* and associated taxa of *Retimonocolpites* and *Cyathidites*.

Palaeoenvironmental interpretation: The facies of PT-3 display dominance of opaque phytoclasts which are dark brown to black in colour. AOM, translucent phytoclasts and palynomorphs are medium to dark brown in colour. PT-3 plot in field II of Tysons APP ternary diagram indicating deposition in a marginal dysoxic-anoxic basin condition (Fig. 5.29). Chiaghanam et al. (2013) suggested the dominance of opaque phytoclasts to indicate fluvio-deltaic/nearshore environment. The dominance of opaque phytoclasts within this association are as a result of oxidation conditions, and either proximity to terrestrial sources or redeposition of terrestrial organic matter from fluvio-deltaic environment (Tyson 1993; Kholeif and Ibrahim, 2010; Carvalho et al., 2013). Zobaa et al. (2013) inferred that, the deposition of sediments with dominant opaques might have occurred close to fluvial sources where some of the phytoclasts were oxidized to opaques during transportation. Dominant opaques and palynomorphs dominated by sphaeroidal pollen grains supported by SPM ternary plot suggest a nearshore environment of deposition (Fig. 5.30). Based on the discussions, PT-3 must have been deposited in a marginal dysoxic-anoxic basin condition in a fluvio-deltaic/nearshore environment.

Kerogen Type: PT-3 is identified as kerogen type III (gas prone) based on dominant opaque phytoclasts.

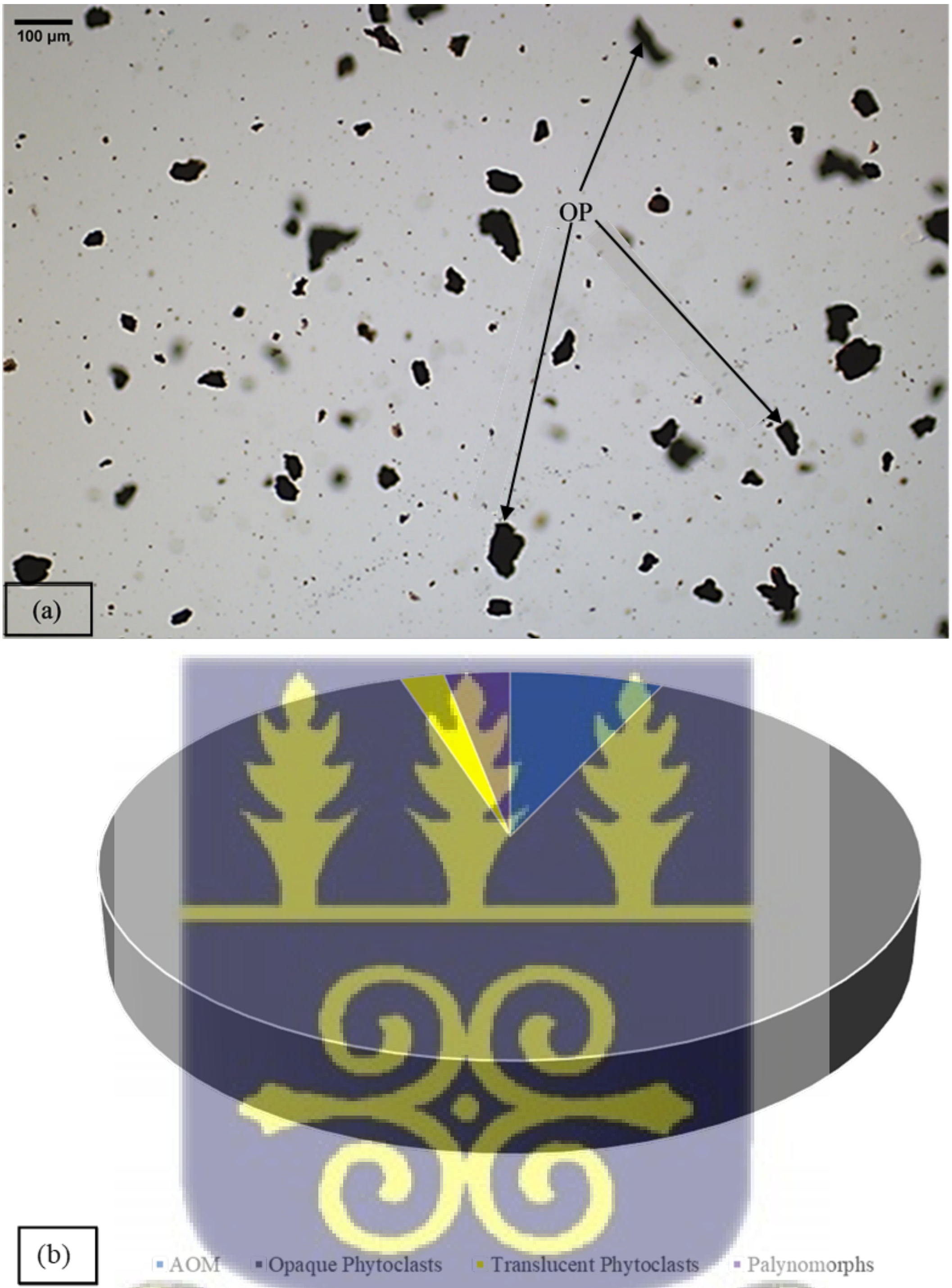

Figure 5.28: (a) Representative photograph of palynofacies association PT-3, sample depth 3670m from the Dzata-1 well. Key to label: OP = opaque phytoclast. (b) Pie chart showing relative abundance (%) of the different constituents of palynofacies association PT-3 from Dzata-1 well.

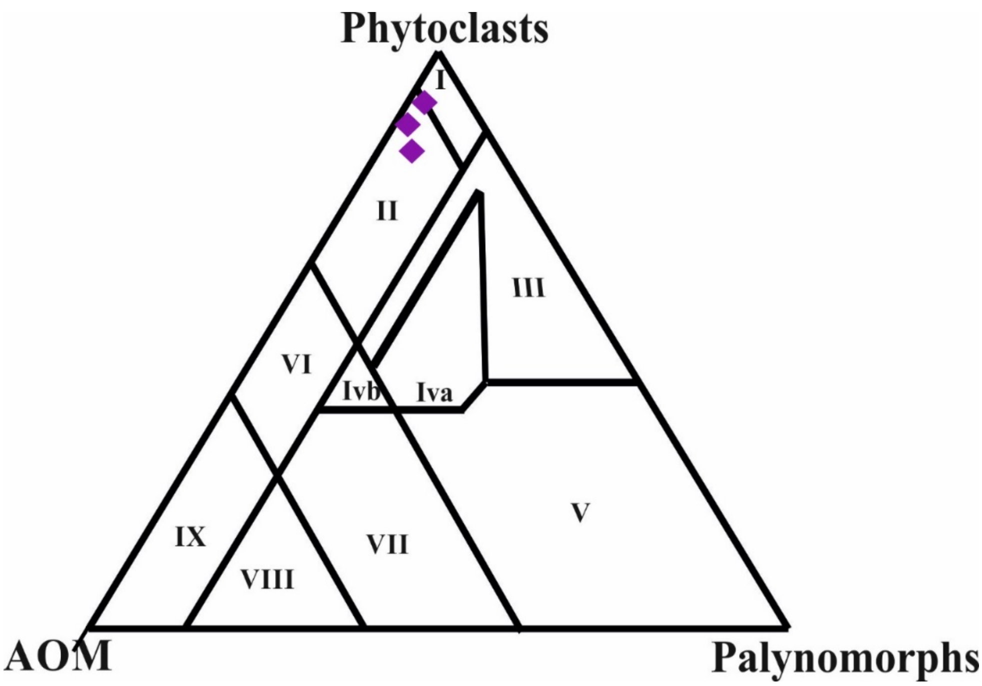

Figure 5.29: APP Ternary diagram for PT-3 samples from Dzata-1 well (after Tyson, 1993).

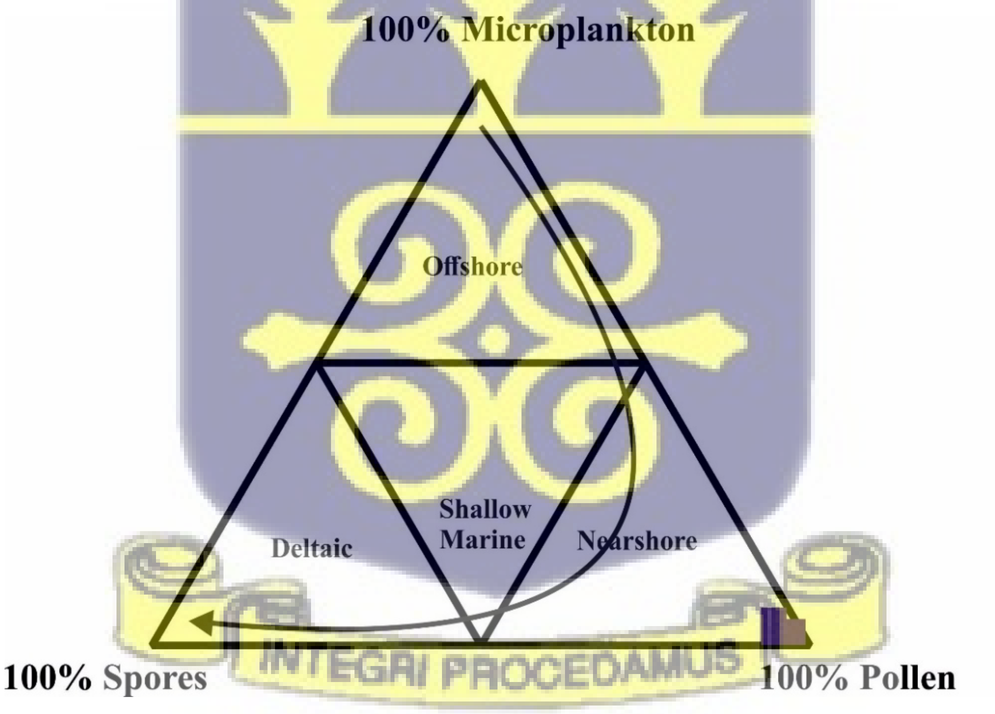

Figure 5.30: MSP Ternary plot for PT-3 samples from Dzata-1 well (After Federova, 1977; Duringer and Doubinger, 1985).

5.2.2.4 Palynofacies type 4 (PT-4) (AOM dominant with palynomorphs) (Fig. 5.31a).

This palynofacies occurs between sample depths 3210 m – 3170 m and 3010 m – 2450 m. The AOM dominates (72%) the total organic matter composition of this palynofacies (Fig. 5.31b). AOM is pale yellow to orange particles and of moderate to good in preservation state. Palynomorphs is 18% of total POM) with opaques and translucent phytoclasts forming 4% and 6% respectively of total POM.

Palaeoenvironmental interpretation: PT-4 plotted in field VIII of Tyson's APP ternary which indicate a deposition in a distal dysoxic-oxic shelf conditions (Fig. 5.32). AOM dominant with weak terrestrial influx (phytoclasts) indicates offshore settings for these facies. The sample interval 3210 m – 3170 m is primarily dominated by elements of terrestrial origin (97%) dominated by pollen grains (e.g. sphaeroidal forms) increased in offshore trends with recorded low amount of pteridophytes spores (e.g. *Cyathidites* and *Deltoidspora*). The interval 3010m-2450m is dominated by about 85% marine palynomorphs (of which 90% are chorate cysts group of gonyaulacoids). The most common gonyaulacoid cyst genera are *Spiniferites*, *Cordosphaeridium*, *Glaphyrocysta*, *Trichodinium*, *Adnatosphaeridium*, *Florentinia* and *Oligosphaeridium*. The most common peridinoid cyst genera are *Andalusiella*, *Palaeocystodinium* and *Cerodinium*. Most common among the sporomorphs are *Araucariacites*, *Cyathidites*, *Proxapertites*, *Longapertites* and associated with minor amounts *Cicatricosisporites*, *Monosulcites*, *Tricolpites*, *Deltoidspora* and *Foveotriletes*. The gonyaulacoid cysts (90% of total dinocysts) dominates over the peridinoid cysts (Fig. 5.34). Occurrence of common open marine gonyaulacoid chorate cysts such as *Oligosphaeridium complex*, *Florentina mantellii*, *Spiniferites* spp., *Cordosphaeridium multispinosum* etc. dominate dinoflagellate cysts from the interval (3010 – 2450 m) which supports the offshore depositional environment and supported by SPM diagram (Fig. 5.33). According to Muller, (1959), Pocklington and Leonard (1979), Tyson (1993), the low frequency occurrence of phytoclasts in PT-4 is equated to weak terrestrial influx and deposition in distal settings located far from land vegetation. The palynofacies association present from interval 3210 m – 3170 m suggests an inner-middle neritic environment while interval 3010 m – 2450 m is deposited in an outer neritic environment under distal dysoxic-oxic shelf conditions.

Kerogen Type: PT-4 is classified as kerogen type II>I (oil prone) based on dominant AOM with palynomorphs.

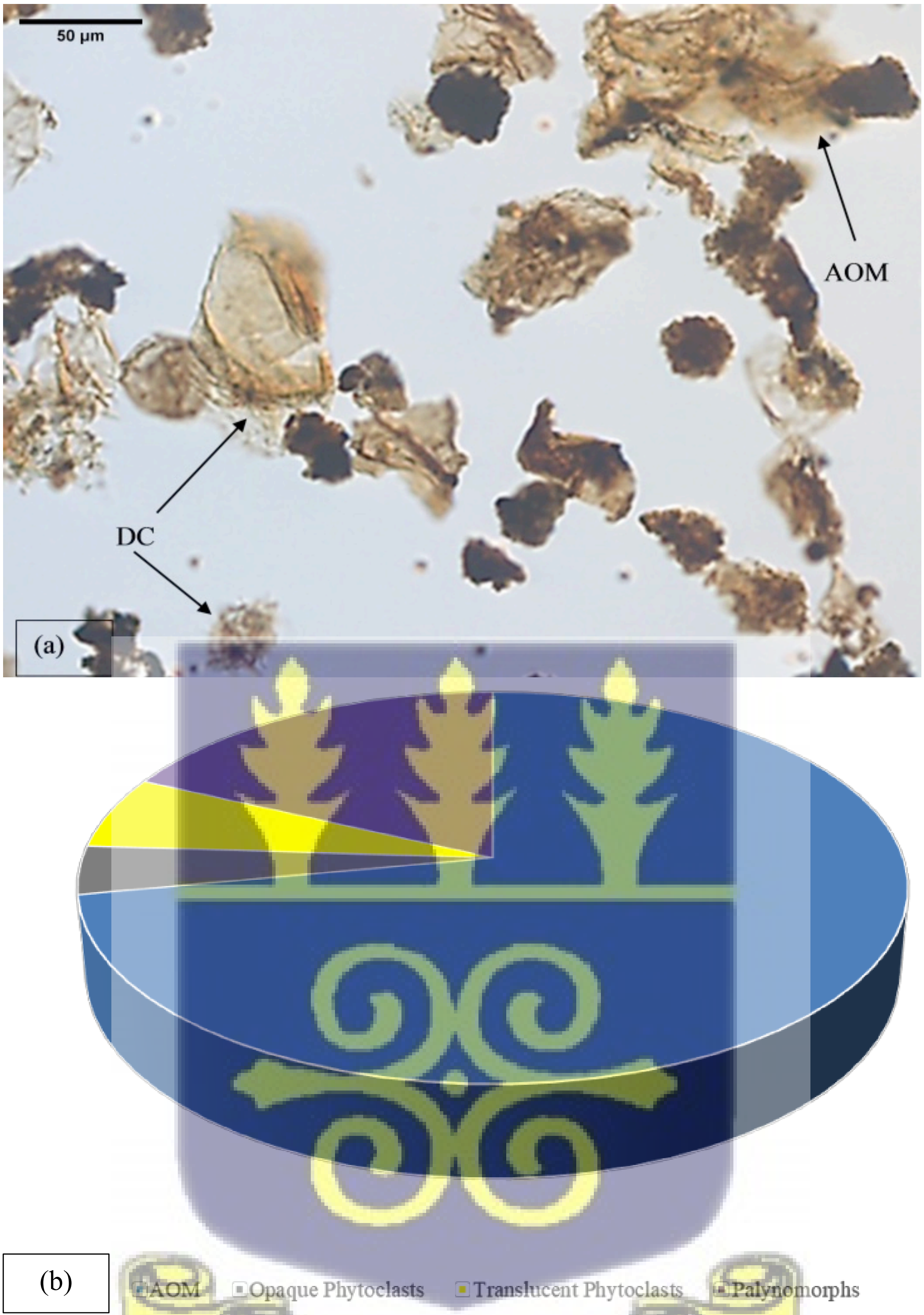

Figure 5.31: (a) Representative photograph of palynofacies association PT-4, sample depth 2910m from the Dzata-1 well. Key to labels: AOM = amorphous organic matter, DC = dinoflagellate cysts. (b) Pie chart showing relative abundance (%) of the different constituents of palynofacies association PT-4 from the Dzata-1 well.

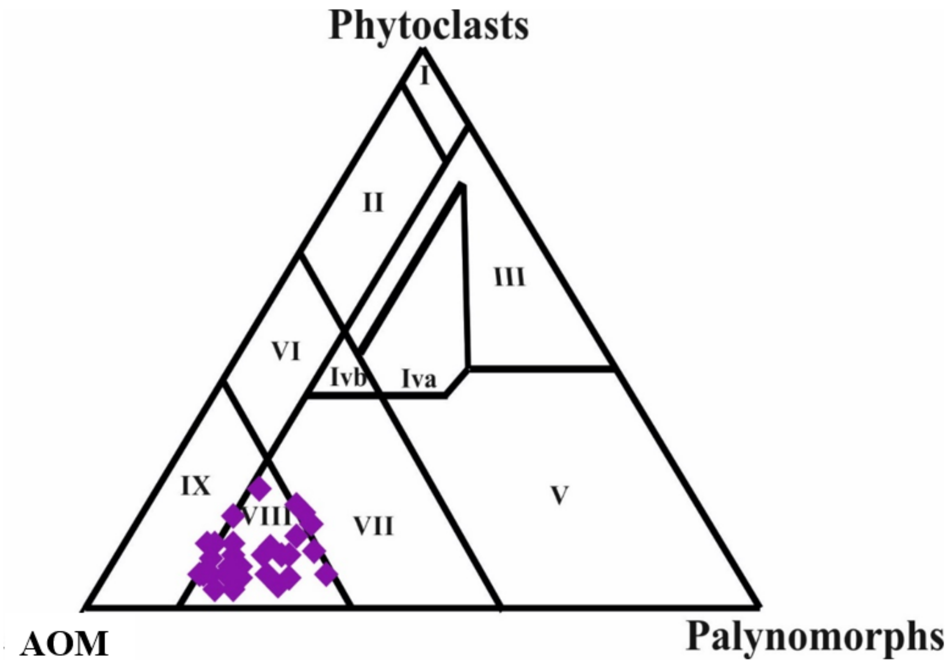

Figure 5.32: APP Ternary diagram for PT-4 samples from Dzata-1 well (after Tyson, 1993).

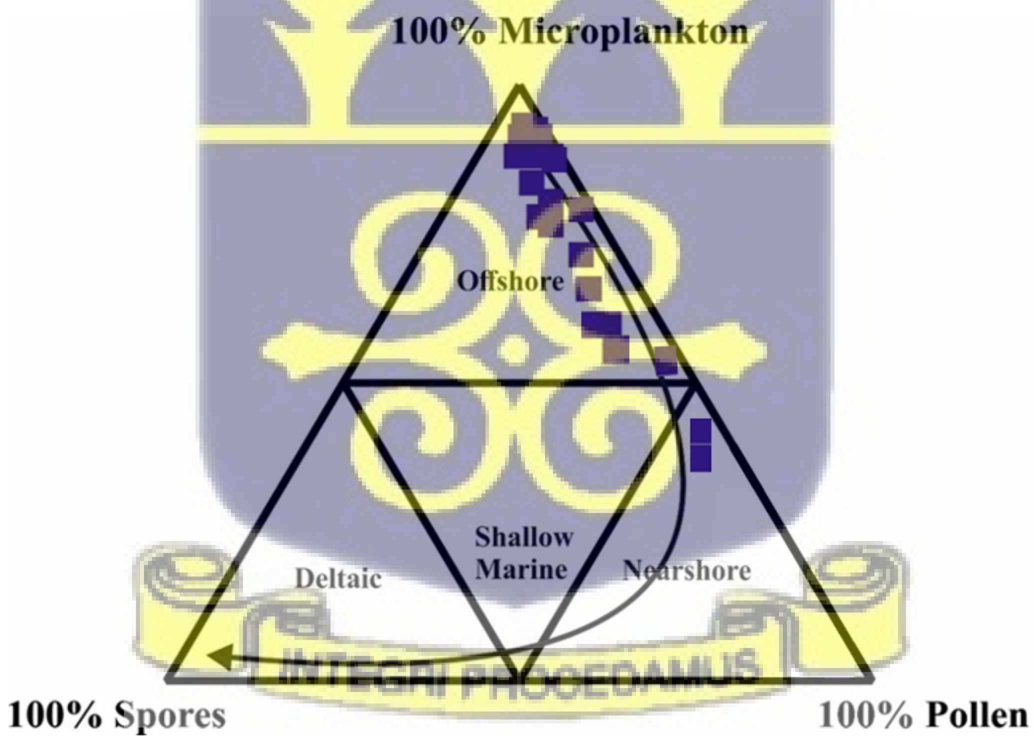

Figure 5.33: MSP Ternary plot for PT-4 samples from Dzata-1 well (After Federova, 1977; Duringer and Doubinger, 1985).

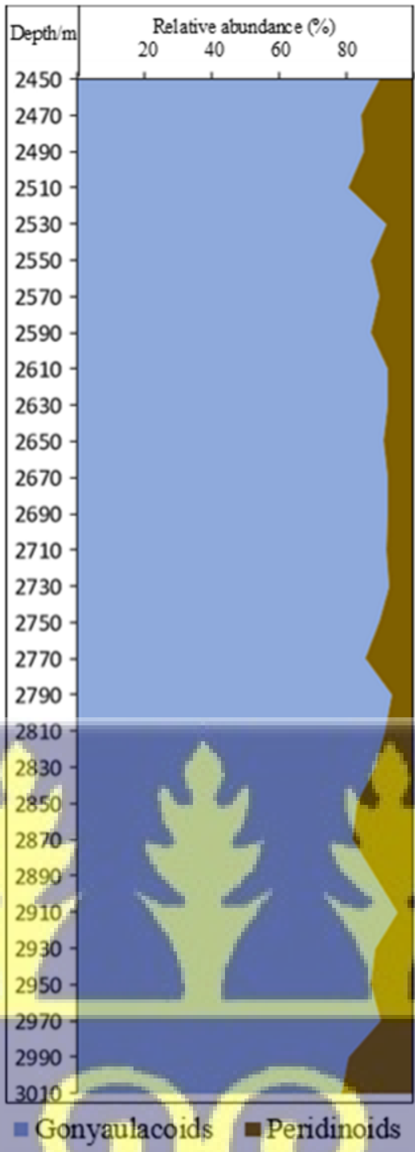

Figure 5.34: Relative percentage composition of Gonyaulacoids and Peridinoids in Dzata-1 well.

5.2.2.5 Palynofacies type 5 (PT-5) (Abundant opaque phytoclasts and AOM) (Fig. 5.35a).

This palynofacies is represented by sample depths interval from 3150 – 3030 m. The dominant element within this palynofacies association is opaque phytoclasts (46%) of total POM. AOM have relative abundance of 33%, translucent phytoclasts (13%) and palynomorphs (8%) (Fig. 5.35b). AOM present are generally moderately preserved and pale yellow to orange in colour. The opaque phytoclasts are dark-brown to black in colour and translucent phytoclasts are brown in colour.

Palaeoenvironmental interpretation: This facies indicates a deposition under a marginal dysoxic-anoxic basin conditions as inferred from the ternary diagram of Tyson (1995), which plots in the palynofacies field II (Fig. 5.36). Palynomorphs recovered from these facies are mainly sporomorphs (dominated by sphaeroidal pollen grains) (Fig. 5.38). Dominant sphaeroidal gymnosperm pollen grains over pteridophyte spores suggests deposition of sediments must have taken place in settings that were far from fluvio-deltaic sources. The abundance of opaque phytoclasts together with moderate translucent phytoclasts would rather suggest a more nearshore environment which is further supported by MSP plot (Fig. 5.37). In PT-5, the phytoclasts (opaques and translucent) and AOM components associated with the palynomorph content suggests a nearshore environment, close to the terrestrial source area under marginal dysoxic-anoxic basin conditions.

Kerogen Type: It is characterized by kerogen type III (gas prone) based on the abundant opaque phytoclasts and AOM with translucent phytoclast.

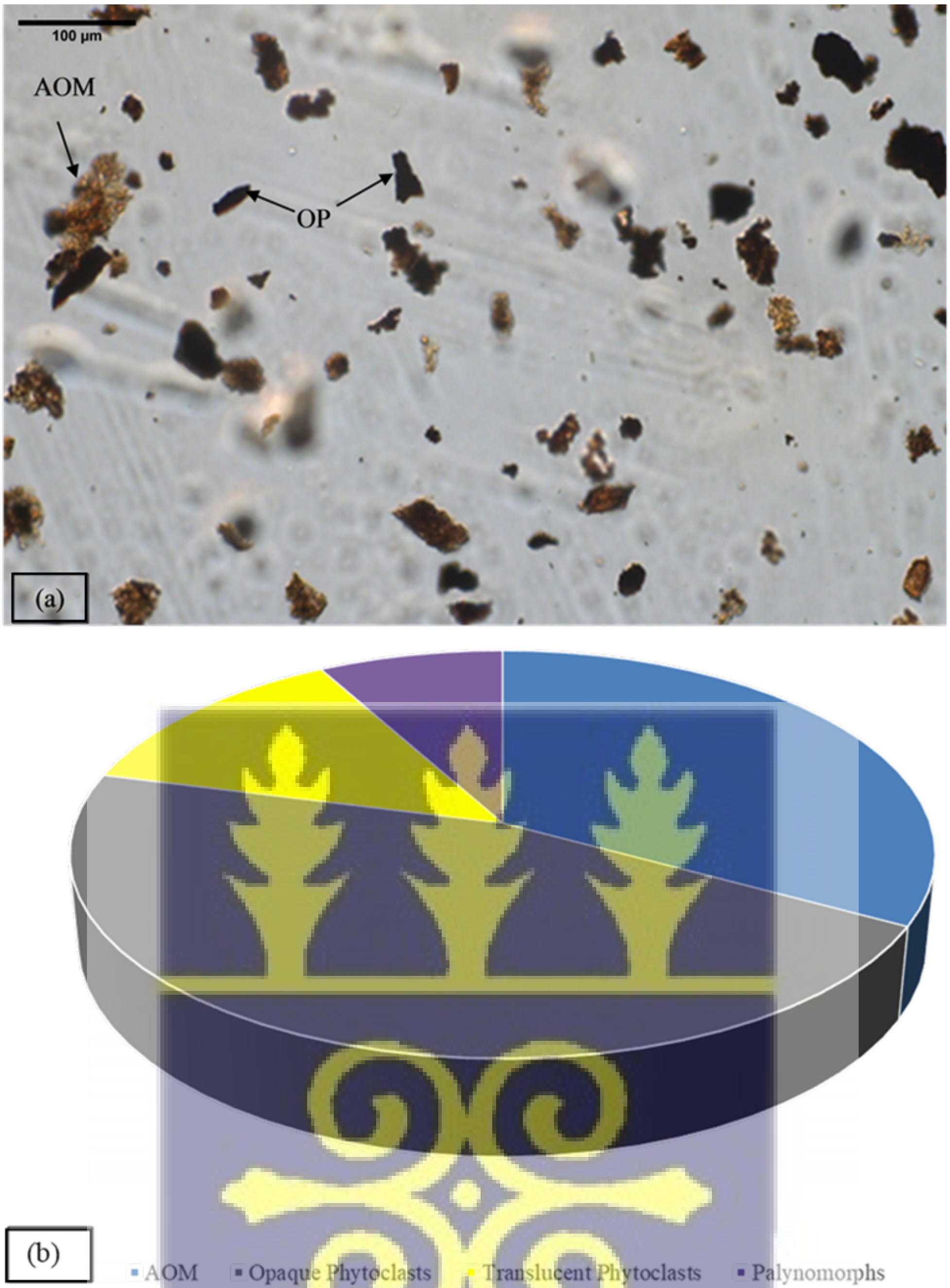

Figure 5.35: (a) Representative photograph of palynofacies association PT-5, sample depth 3110m at from the Dzata-1 well. Key to labels: AOM = amorphous organic matter, OP = opaque phytoclast. (b) Pie chart showing relative abundance (%) of the different constituents of palynofacies association PT-5 from Dzata-1 well.

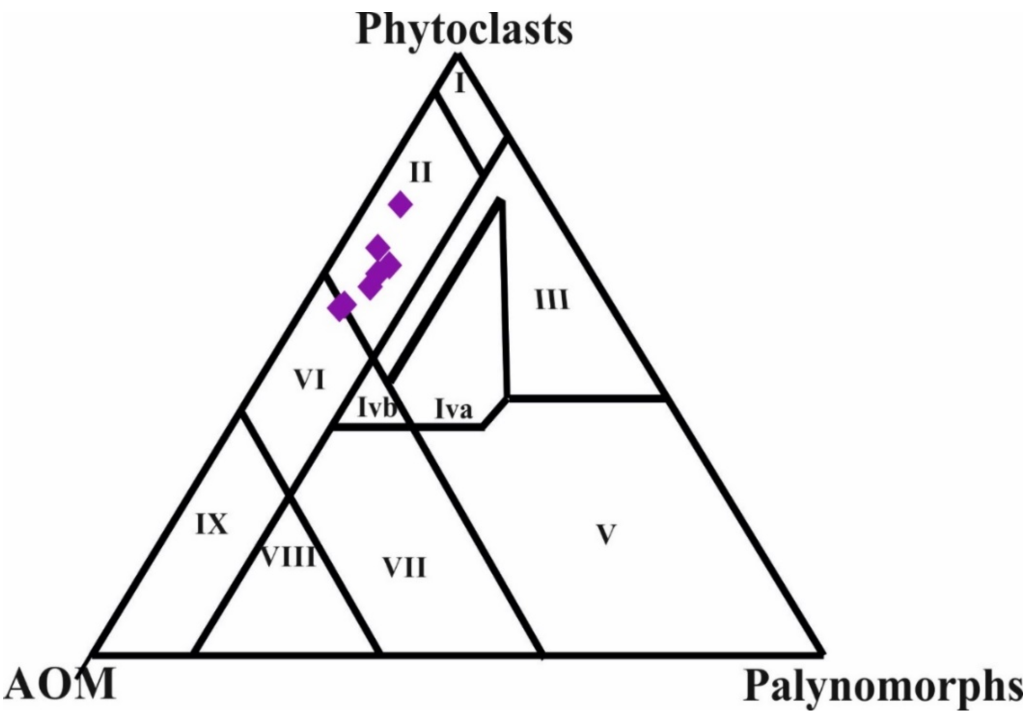

Figure 5.36: APP Ternary diagram for PT-5 samples from Dzata-1 well (after Tyson, 1993).

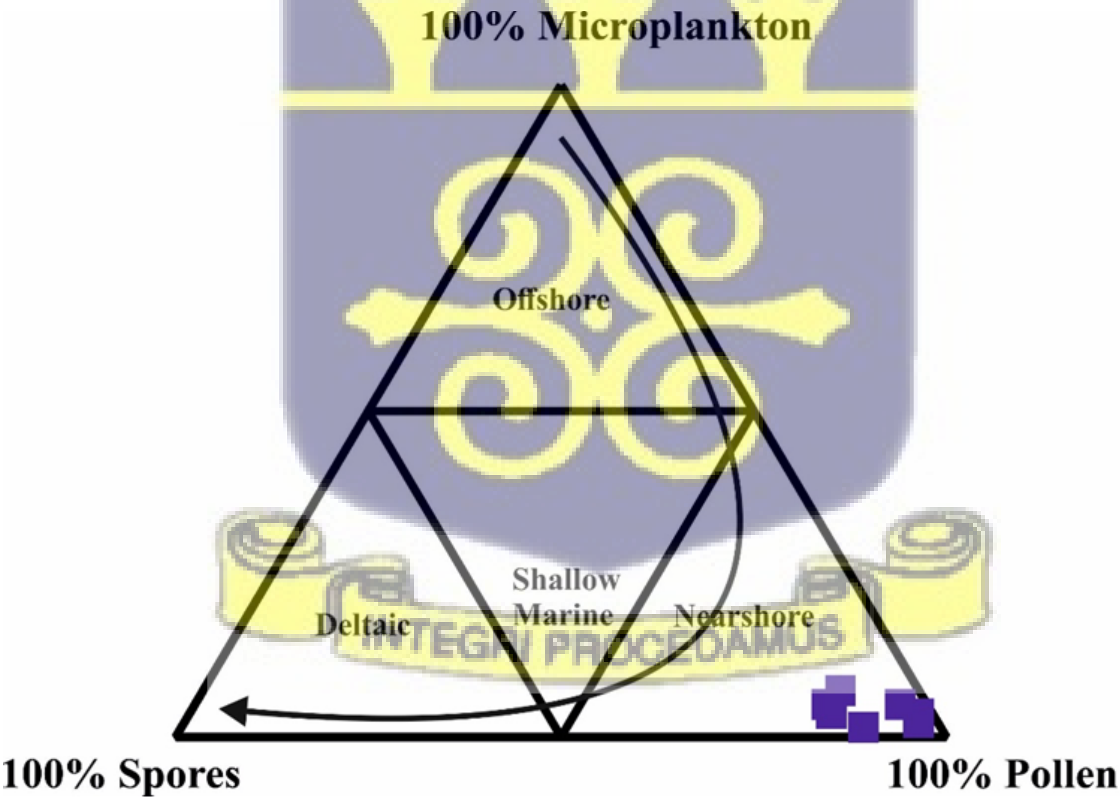

Figure 5.37: MSP Ternary plot for PT-5 samples from Dzata-1 well (After Federova, 1977; Duringer and Doubinger, 1985).

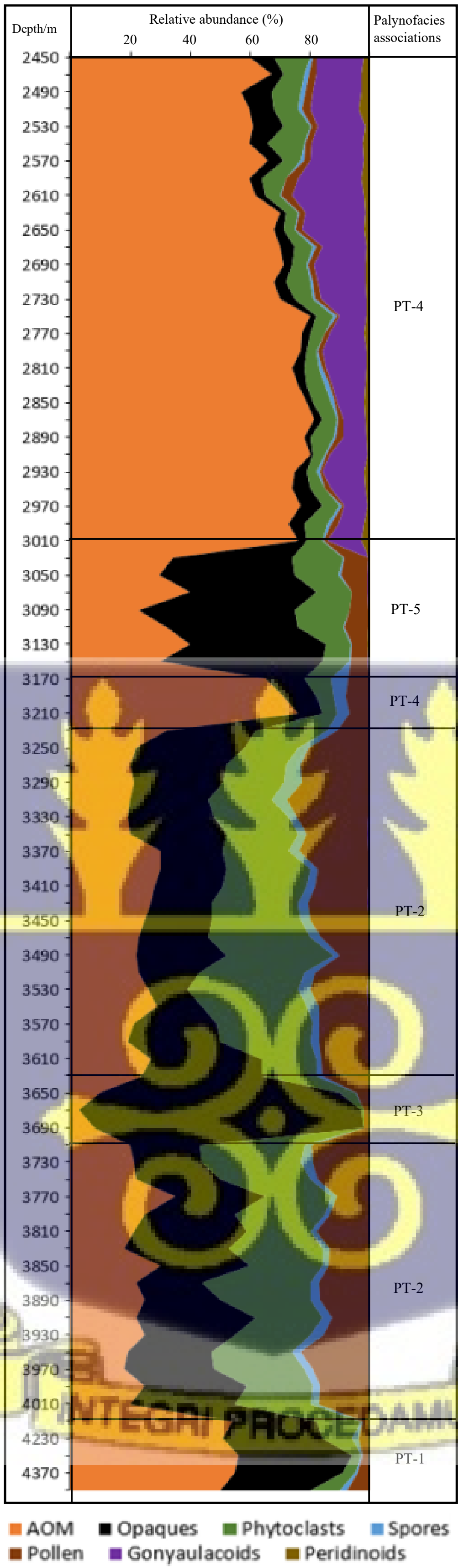

Figure 5.38: Palynofacies associations showing POM (%) from Dzata-1 well.

5.2.3 Dzata-2A

Six palynofacies associations based on the proportions of the particulate organic matter (POM), were identified between 4426 – 2420 m in the Dzata-2A well with their relative abundance in percentages tabulated in table 4.8 and displayed in Figure 5.58.

Table 5.8: Percentage composition of palynofacies associations of particulate organic matter (POM) in Dzata-2A well.

Palynofacies associations	AOM	Opaque Phytoclasts	Translucent Phytoclasts	Palynomorphs
PT-A	60	27	9	4
PT-B	33	18	24	25
PT-C	64	6	8	22
PT-D	37	32	23	8
PT-E	81	6	8	5
PT-F	57	8	17	18

5.2.3.1 Palynofacies type 1 (PT-A) (AOM dominant with abundant opaque phytoclasts) (5.39a).

PT-A occurs between sample depths 4426 – 3930 m and 3630 – 3550 m. It is characterized by dominant AOM (60%) and high opaque phytoclasts (27%) of total POM (Fig. 5.39b; Fig. 5.58). AOM preservation is good. PT-A has relative abundance of translucent phytoclasts (9%) and palynomorphs (4%) of total POM. The opaque phytoclasts are dark-brown to black in colour, equant and lath-shaped of varied sizes. Translucent phytoclasts are brown in colour and orange to medium brown in palynomorphs.

Palaeoenvironmental interpretation: The plot of samples on Tyson's APP ternary diagram were constrained in field VI (Fig. 5.40), indicating deposition in a proximal suboxic-anoxic shelf condition. The palynomorphs are of terrestrial origin dominated by gymnosperm sphaeroidal pollen grains (e.g. *Araucariacites*, *Classopollis*, *Inaperturopollenites*) over pteridophyte spores (e.g. *Deltoidspora*, *Cyathidites*, *Cicatricosisporites*). The dominance of

AOM is inferred to be as result of the combination of environments with high preservation rates and low energies in reducing basins with increased water column resulting in dysoxic or anoxic bottom condition (Batten 1983; Tyson 1993; Tyson 1995; Ibrahim et al., 2002; Kholeif and Ibrahim 2010). Sporomorphs are the least component of this facie which may suggest a shallower offshore setting as increase in sporomorphs percentages were equated to proximity of depositional sites to active sources of terrestrial organic matter input (Tyson, 1993). MSP diagram supports the nearshore to shallower offshore setting (Fig. 5.41). Based on the discussion above, Palynofacies type 1 (PT-A) indicates a deposition in a nearshore to shallow marine (inner neritic) environment under a proximal suboxic-anoxic shelf condition.

Kerogen Type: These facies are characterized by kerogen type II/III (oil prone) based on the dominant AOM with high opaques.

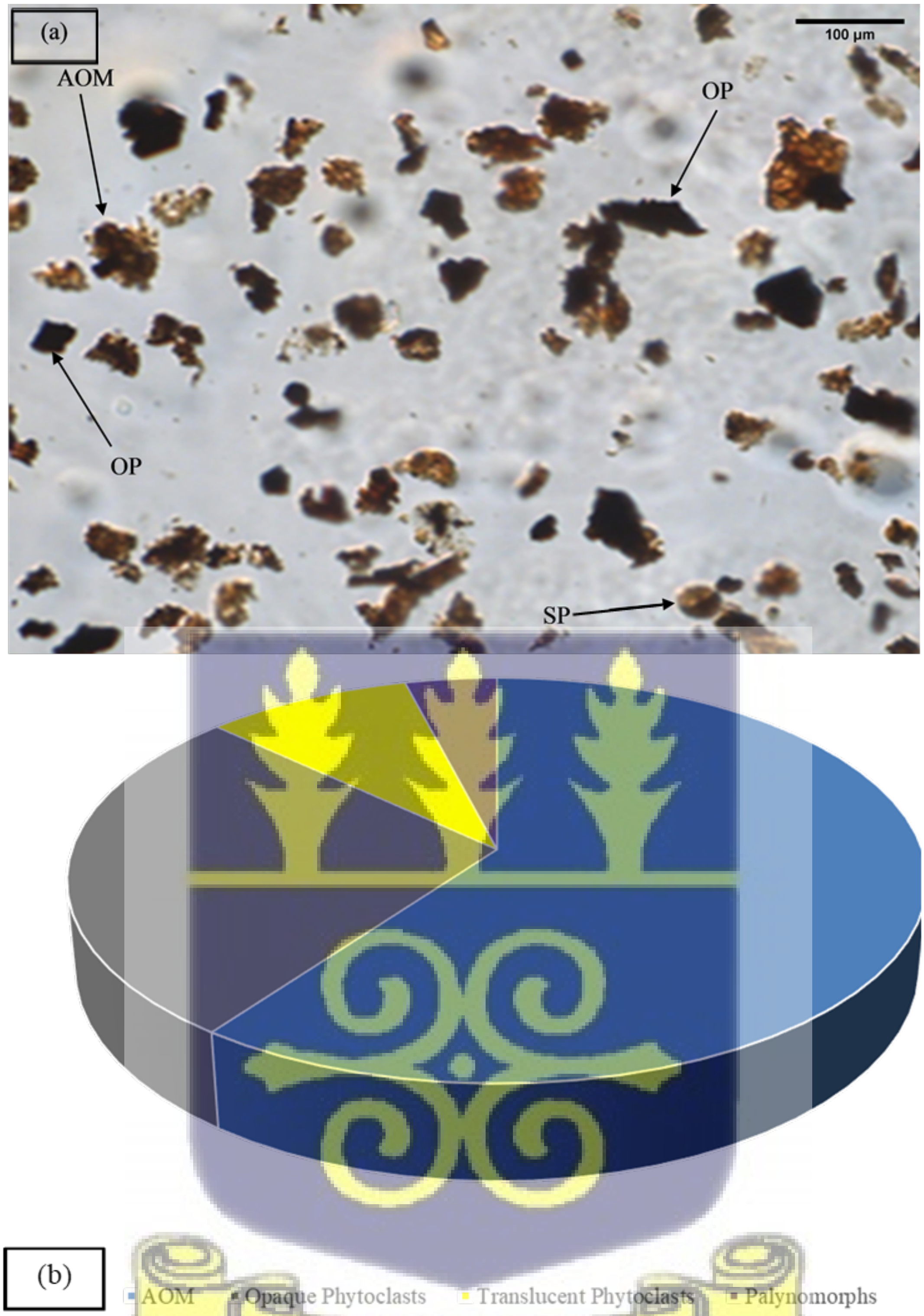

Figure 5.39: (a) Representative photograph of palynofacies association PT-A, sample depth 3990m from the Dzata-2A well. Key to labels: AOM = amorphous organic matter, SP = sporomorph, OP = opaque phytoclast. (b) Pie chart showing relative abundance (%) of the different constituents of palynofacies association PT-A from Dzata-2A well.

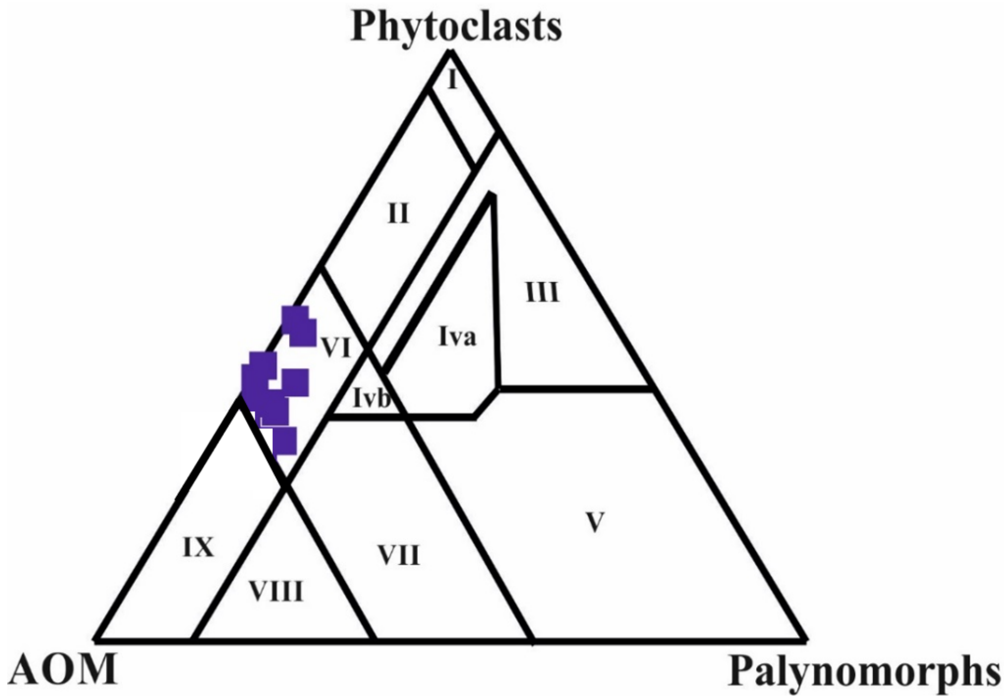

Figure 5.40: APP Ternary diagram of studied samples from the Dzata-2A well (after Tyson, 1993).

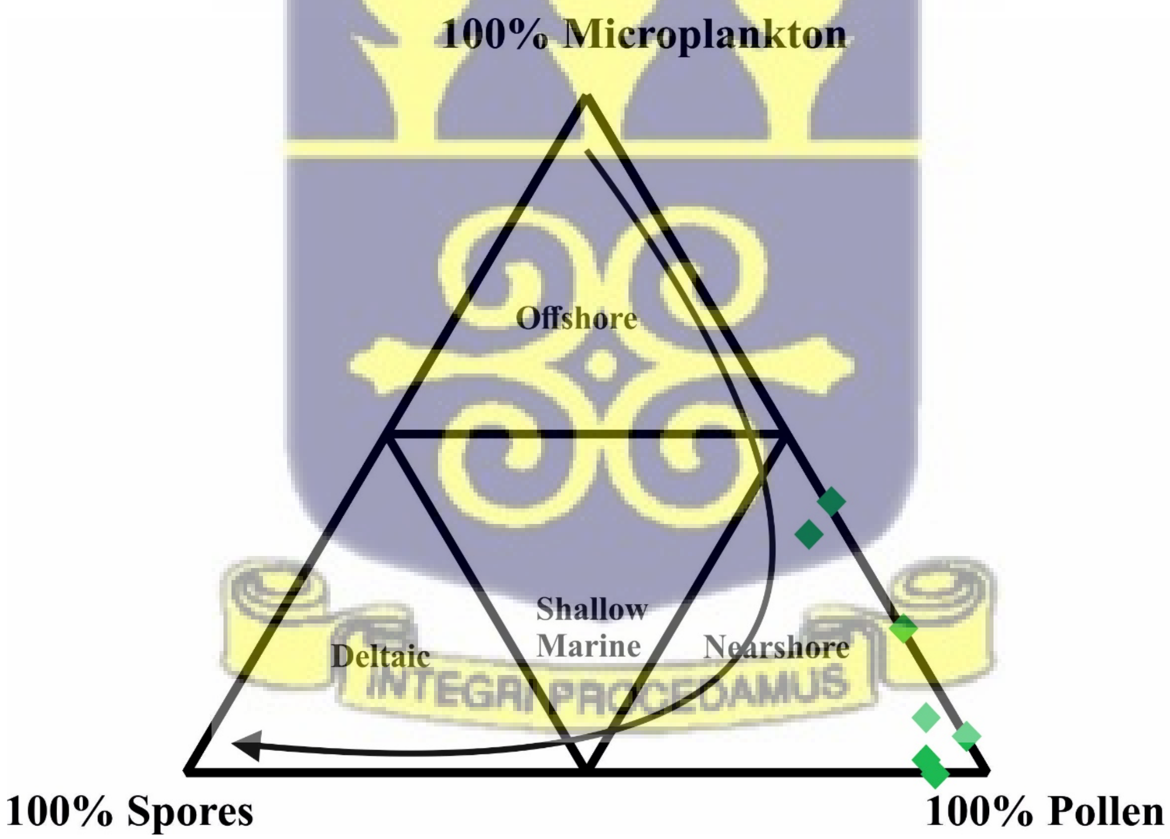

Figure 5.41: MSP Ternary plot for PT-A samples from Dzata-2A well (After Federova, 1977; Duringer and Doubinger, 1985).

5.2.3.2 Palynofacies type 2 (PT-B) (Abundant AOM with relatively equal abundance of phytoclasts and palynomorphs) (Fig. 5.42a).

PT-B is documented in sample depth intervals between 3810 – 3650 m. The elements of this palynofacies are constituted by AOM (33%), translucent phytoclasts (24%) and palynomorphs (25%) with relatively low occurrence of opaque phytoclasts (18%) of total POM (Fig. 5.42b). PT-B is primarily dominated by palynomorphs of terrestrial origin (95%) dominated by pollen grains (sphaeroidal forms) with marine dinoflagellates cysts constituting 5% and dominated by peridinoid cysts (80% of total dinocysts) (Fig. 5.58). Palynomorphs are generally orange and pale brownish in colour whilst the translucent phytoclasts mainly consist of pale brown with moderately preserved structured plant fragments.

Palaeoenvironmental interpretation: PT-B plots in field IVa of Tyson's APP ternary which indicates a deposition in a shelf to basin transition under a dysoxic-suboxic conditions (Fig. 5.43). High occurrence of xerophytes (e.g. *Classopollis* and *Ephedripites*) suggests a deposition in a semi-arid to arid climatic conditions of this facies. High percentages of the translucent phytoclasts indicates freshwater influx on this facie. Peridinoids cysts dominate over the gonyaulacoids (G/P) which indicates an inner neritic/nearshore depositional environment and supported by MSP plot (Fig. 5.44). The relative proportions of AOM, phytoclasts (opaques and translucent) and palynomorphs components in PT-B infers an inner neritic/nearshore depositional environment under dysoxic-suboxic conditions.

Kerogen Type: PT-B is characterized by kerogen type III or II (gas prone) based on the abundance of AOM, phytoclasts and palynomorphs (mainly of terrestrial origin).

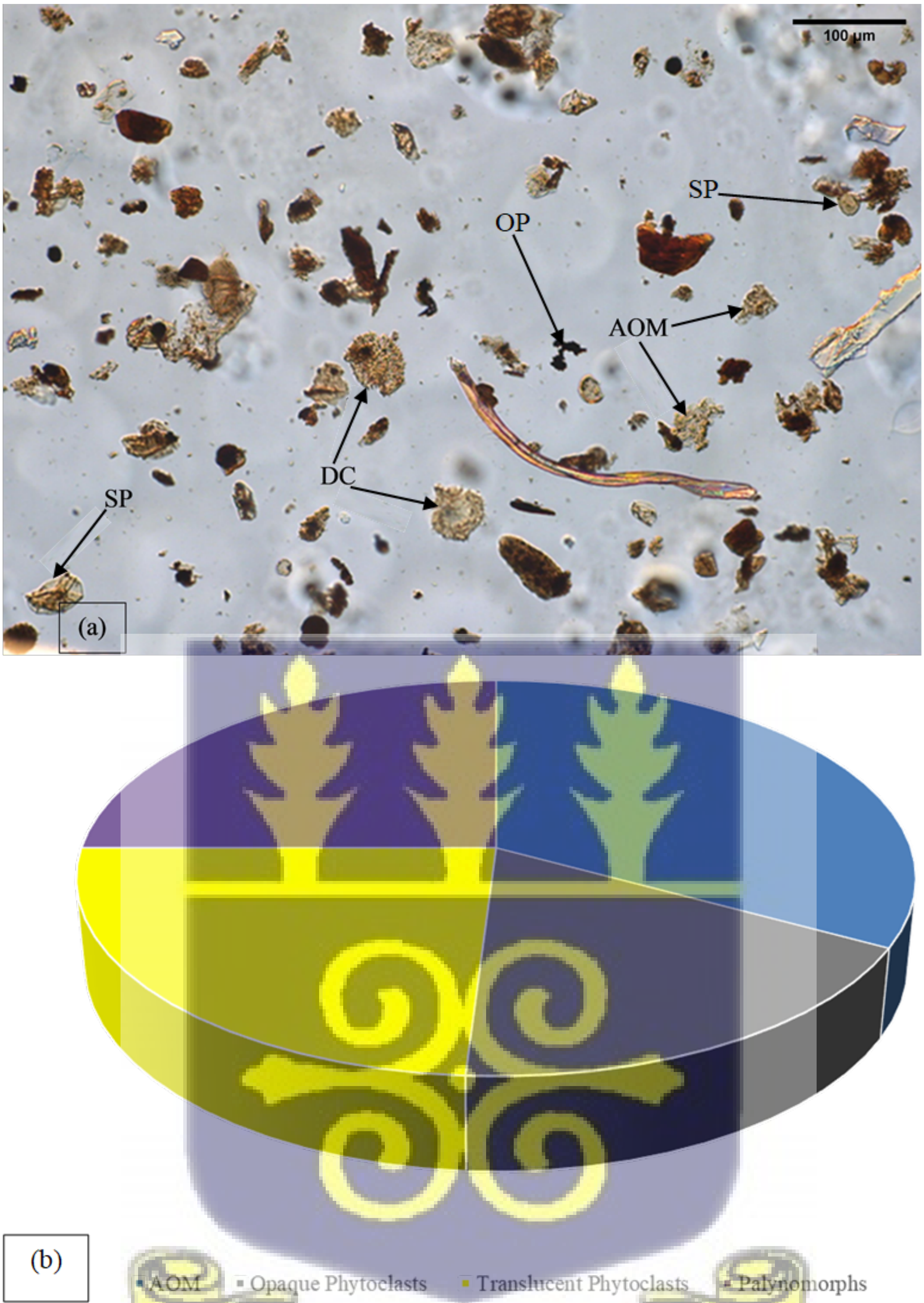

Figure 5.42: (a) Representative palynofacies association of PT-B, sample depth 3790m from the Dzata-2A well. Key to labels: AOM = amorphous organic matter, SP = sporomorph, DC = dinoflagellate cysts, OP = opaque phytoclast. (b) Pie chart showing relative abundance (%) of the different constituents of palynofacies association PT-B from Dzata-2A well.

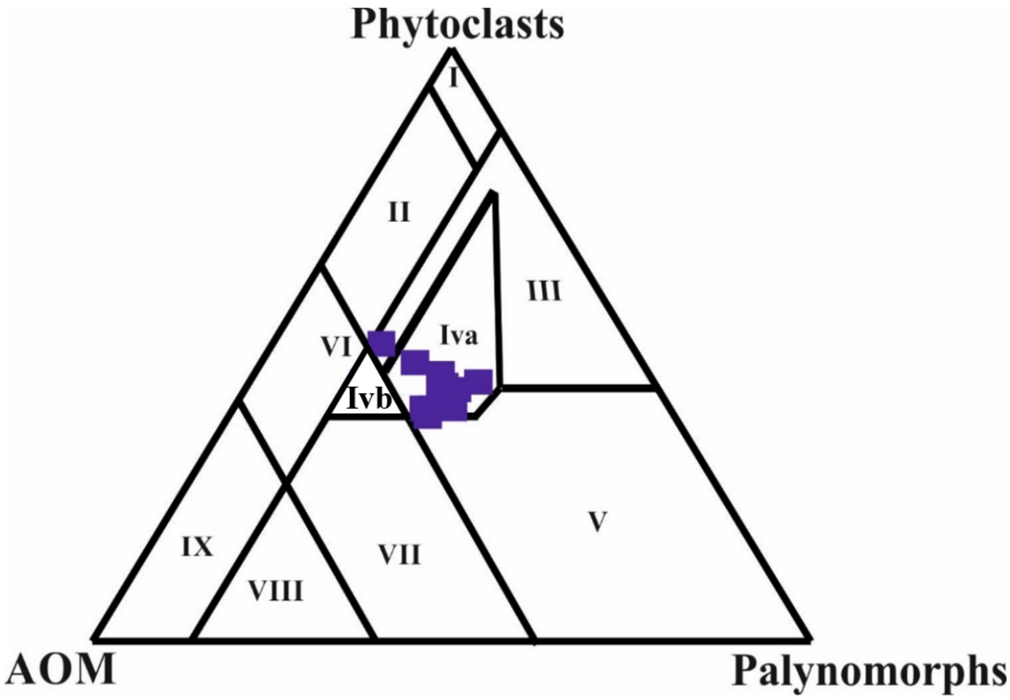

Figure 5.43: APP Ternary diagram for PT-B samples from Dzata-2A well (after Tyson, 1993).

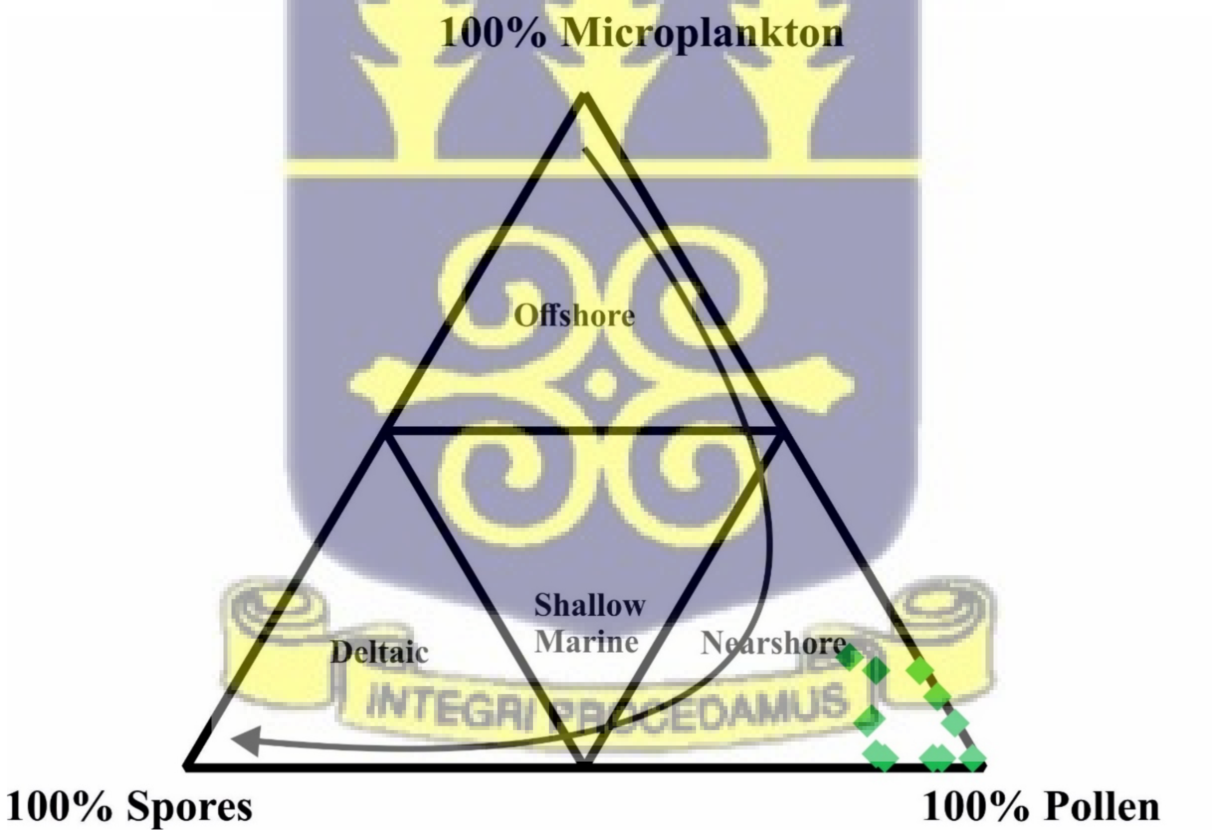

Figure 5.44: MSP Ternary plot for PT-B samples from Dzata-2A well (After Federova, 1977; Duringer and Doubinger, 1985).

5.2.3.3 Palynofacies type 3 (PT-C) (AOM dominant with high palynomorphs) (Fig. 5.45a).

PT-C is recognized between sample depths 3530 – 3396 m and 2580 – 2420 m. AOM dominates the total organic matter composition of this palynofacies by 64%. The palynomorphs group (22%) of POM dominated by sporomorphs from interval 3530 m – 3396 m and marine components from interval 2580 m – 2420 m altogether with low counts of opaques and translucent phytoclasts (6% and 8%) respectively (Fig. 5.45b; Fig 5.58).

Palaeoenvironmental interpretation: This palynofacies association (PT-C) plots in the field VIII of Tyson's APP diagram which indicates deposition in a distal dysoxic-oxic shelf (Fig. 5.46). Tyson (1995) suggested that preservation of AOM is enhanced when the site of deposition is located relatively far from high terrestrial organic matter input with prevailing reducing conditions. Palynomorphs of terrestrial origin are dominated by sphaeroidal gymnosperm pollen grains (e.g. *Classopollis*, *Araucariacites*) which constitute 97% of the palynomorphs which is recorded between sample intervals 3530 – 3396 m. The samples from intervals of the topmost section of the well (2580 – 2420 m) are dominated by marine palynomorphs (av. 85%) of total palynomorphs. The marine elements are primarily dominated by chorate gonyaulacoids (90%) over the cavate peridinoids (10%) of total marine palynomorphs (Fig. 5.57). Open marine gonyaulacoid chorate cysts such as *Oligosphaeridium complex*, *Florentina mantellii*, *Spiniferites* spp. and *Cordosphaeridium multispinosum* recovered from the interval (2580 m – 2420 m) suggests a more offshore (middle-outer neritic) depositional environment. Intervals from 3530 m – 3396 m is dominated by sporomorphs (mainly sphaeroidal gymnosperm pollen grains (97%)), few pteridophytes (e.g. *Cyathidites*, *Deltoidspora*, etc.) with associated constituents of POM which depicts a nearshore/inner neritic depositional environment. The transition of depositional environment of PT-C from nearshore/inner neritic to open marine (middle-outer neritic) is supported by MSP plot (Fig. 5.47). The low amounts of phytoclasts are equated to weak terrestrial influx and deposition in distal settings located far from land vegetation (Muller, 1959; Pocklington and Leonard, 1979; Tyson, 1993). Based on the above discussion, PT-C is deposited in a distal dysoxic-oxic shelf conditions from a nearshore/inner neritic environment between sample depth 3530-3396 m and a middle-outer neritic environment for samples between 2580-2420 m.

Kerogen Type: This field is characterized by kerogen type II>I (oil prone) based on the dominant well preserved AOM with high palynomorphs (av. dominated by marine elements).

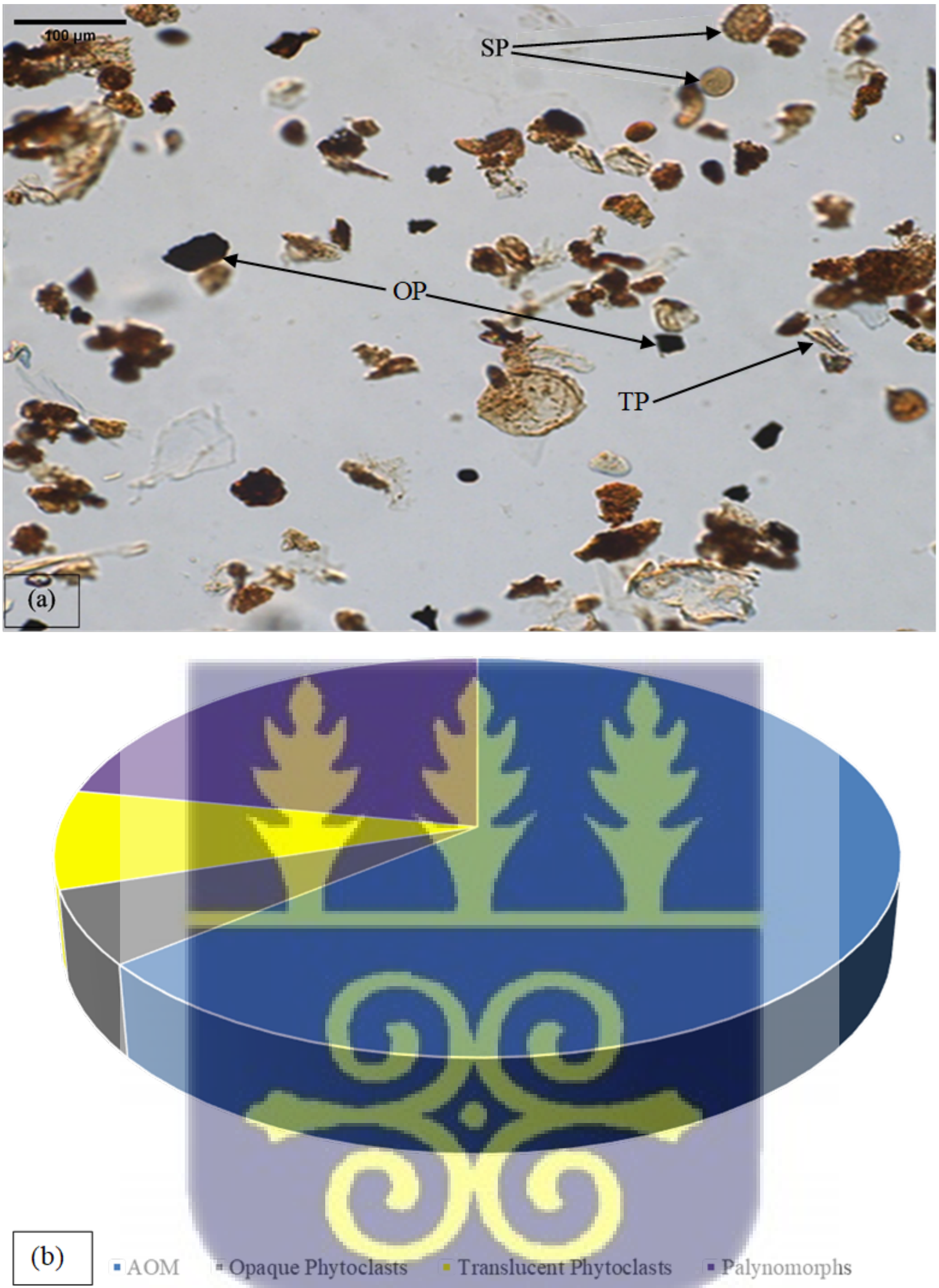

Figure 5.45: (a) Representative photograph of palynofacies association PT-C, sample depth 2580m from the Dzata-2A well. Key to label: SP = sporomorph. (b) Pie chart showing relative abundance (%) of the different constituents of palynofacies association PT-C from Dzata-2A well.

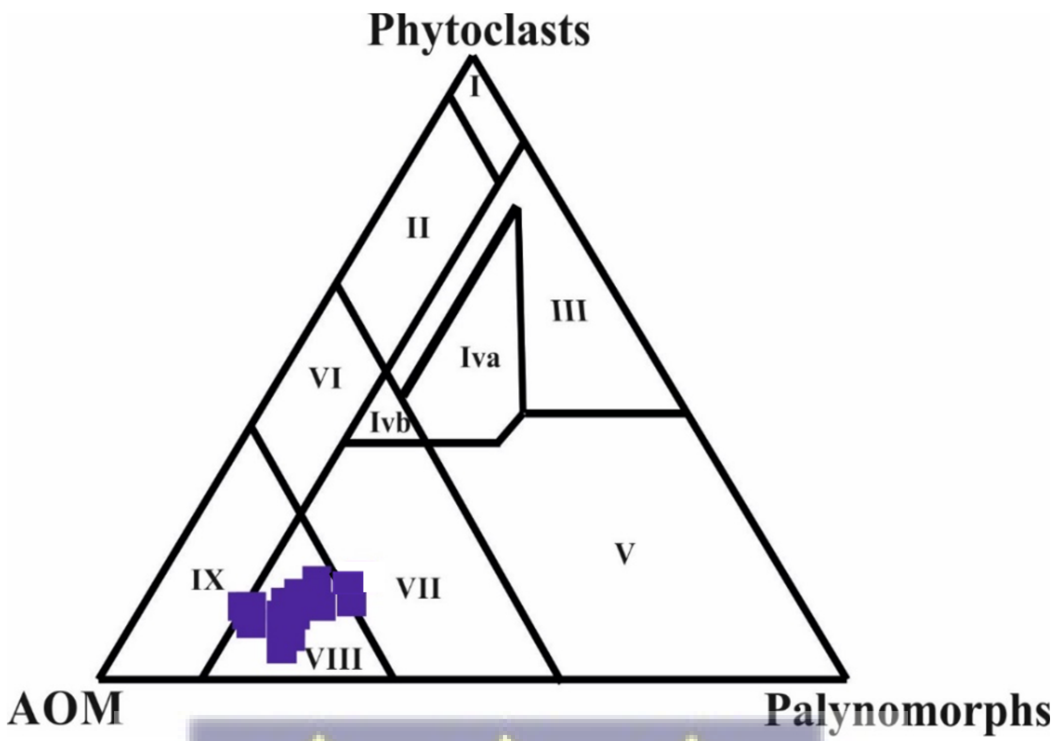

Figure 5.46. APP Ternary diagram for PT-C samples from Dzata-2A well (after Tyson, 1993).

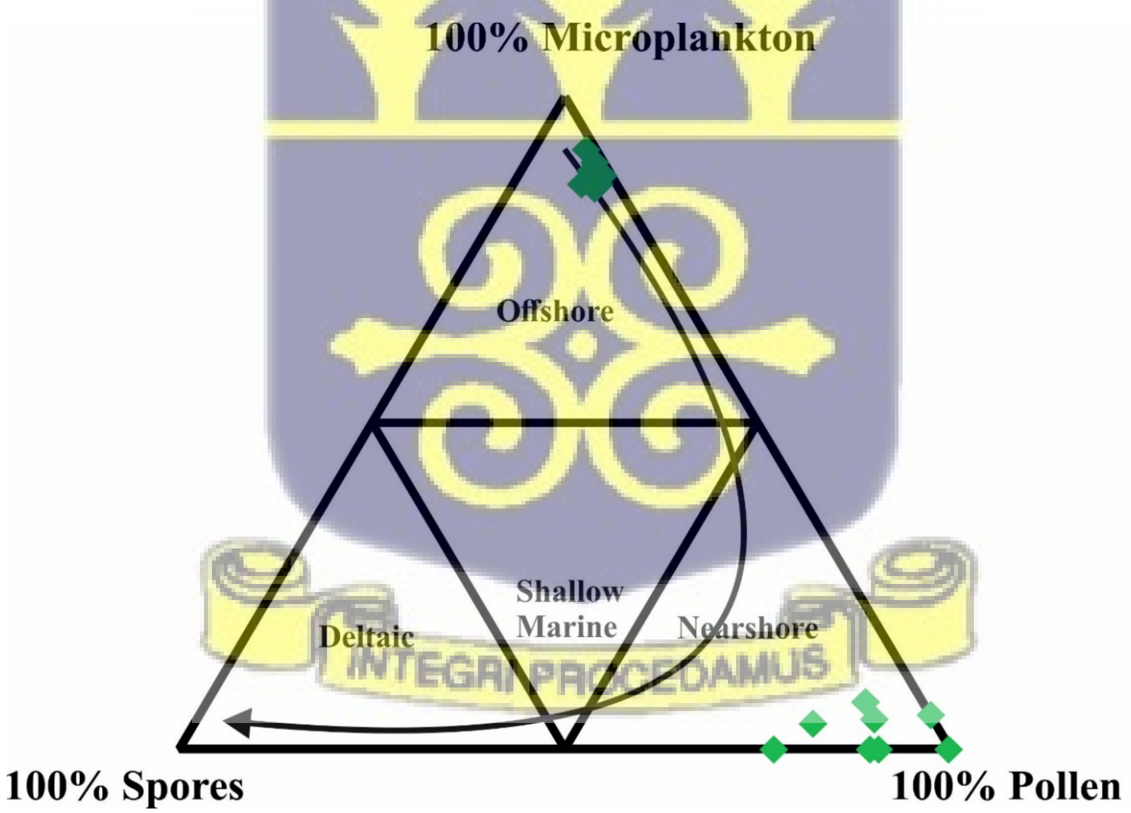

Figure 5.47: MSP Ternary plot for PT-C samples from Dzata-2A well (After Federova, 1977; Duringer and Doubinger, 1985).

5.2.3.4 Palynofacies type 4 (PT-D) (Abundance of AOM and opaque phytoclasts with high translucent phytoclasts) (Fig. 5.48a).

PT-D occurs between sample depths from 3375 m – 3168 m. It is made up of relative abundance of AOM (37%), opaques (32%), phytoclasts (23%) and palynomorphs (8%) of total POM (Fig. 5.48b). Palynomorphs of terrestrial origin (sphaeroidal pollen grains) dominates the assemblage and contributing 99% of total palynomorphs and similar to those recovered in PT-B (Fig. 5.58). Generally the palynomorphs are orange to pale brownish in colour with the translucent phytoclasts consisting mainly of pale brown. The opaque phytoclasts are dark brown to black in colour.

Palaeoenvironmental interpretation: On Tyson's APP ternary diagram, PT-D plots in field II which reflects marginal dysoxic-anoxic basin conditions (Fig. 5.49). Recovered sporomorphs in this palynofacies type include *Classopollis* spp, *Ephedripites* spp., *Elaterosporites* spp. with associated taxa of *Retimonocolpites, Araucariacites* and *Cyathidites*. Pteridophytic spore assemblages (e.g. *Cyathidites*, *Deltoidspora*) are low to none in occurrence for most of these intervals. Sporomorphs dominated by sphaeroidal pollen grains occurrence and relatively abundant phytoclasts (opaques and translucent) suggests a nearshore environment and supported by MSP plot (Fig 5.50). Based on the discussions above with POM constituents, palynofacies type 4 (PT-D) indicates a nearshore/inner neritic depositional environment under marginal dysoxic anoxic basin conditions.

Kerogen Type: PT-D is constituted by kerogen type III (gas prone) based on abundant AOM and opaque phytoclast with high translucent phytoclasts.

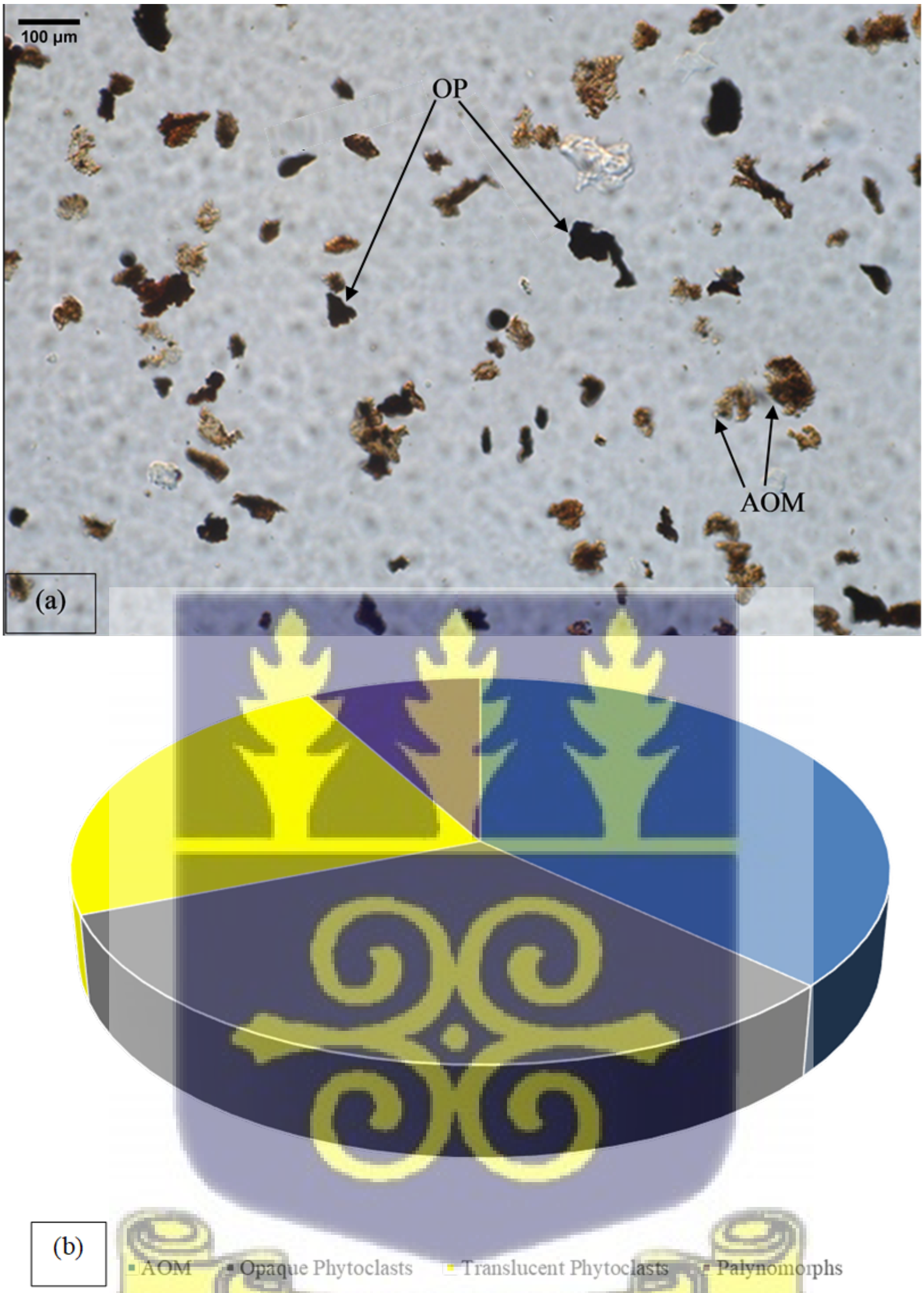

Figure 5.48: (a) Representative photograph of palynofacies association PT-D, sample depth 3312m from the Dzata-2A well. Key to labels: AOM = amorphous organic matter, OP = opaque phytoclast. (b) Pie chart showing relative abundance (%) of the different constituents of palynofacies association PT-D from Dzata-2A well.

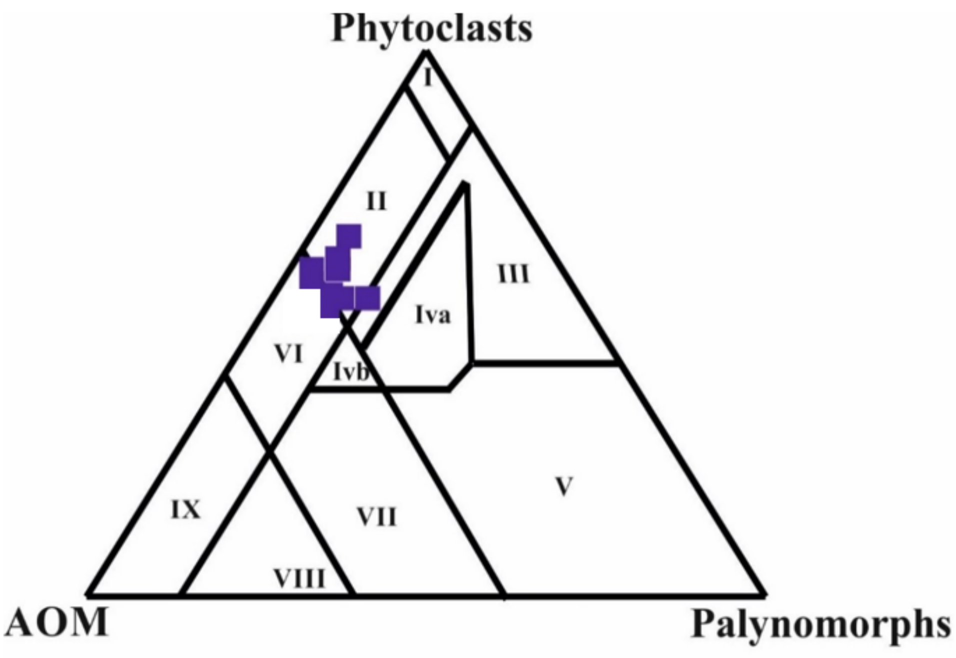

Figure 5.49. APP Ternary diagram for PT-D samples from Dzata-2A well (after Tyson, 1993).

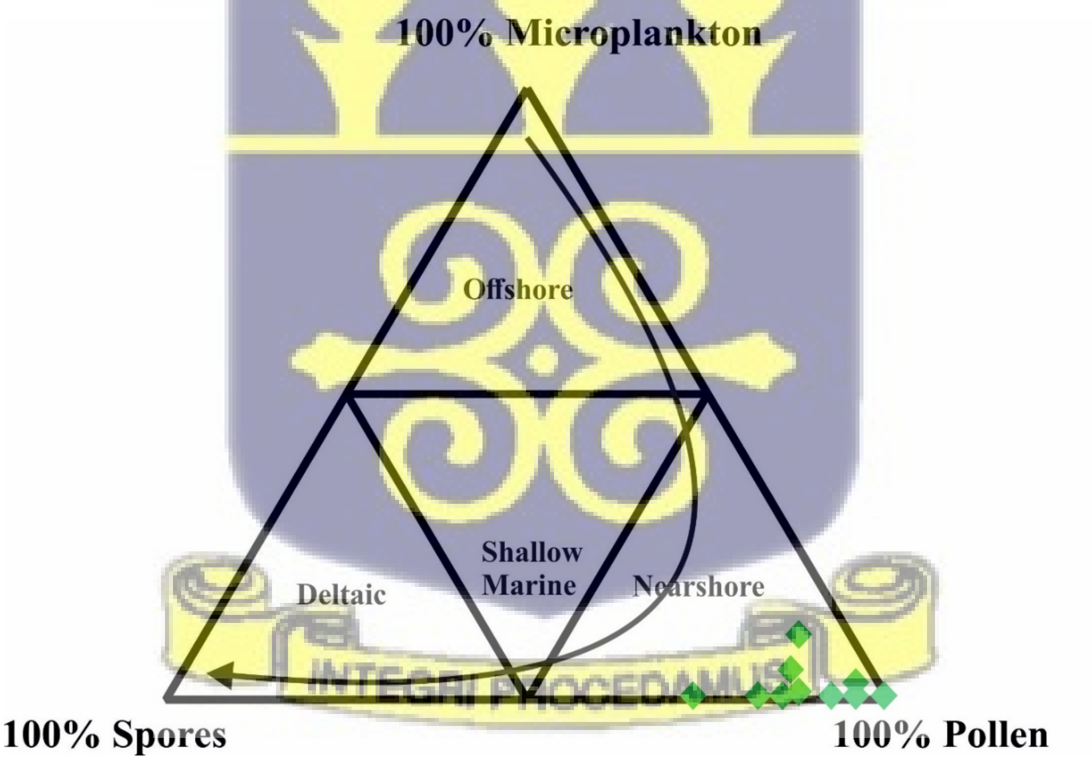

Figure 5.50: MSP Ternary plot for PT-D samples from Dzata-2A well (After Federova, 1977; Duringer and Doubinger, 1985).

5.2.3.5 Palynofacies type 5 (PT-E) (AOM dominant) (5.51a).

PT-E facies occurs between sample depths 3147 – 3105 m and 2943 – 2600 m. It is characterized by very high AOM (81%) of the total organic matter composition with very little proportions of opaques, translucent phytoclasts and palynomorphs (6%, 8% and 5%) respectively (Fig. 5.51b). AOM preservation is good and pale yellow to orange in colour. Sample intervals from 3147m-3105m is constituted by 98% sporomorphs (dominated by sphaeroidal pollen grains of total palynomorphs of POM (5%)) while sample intervals from 2943m-2600m is composed of 78% marine palynomorphs from total palynomorphs (dominated by 93% chorate gonyaulacoid cysts (Fig. 5.57) with the remaining 22% being sporomorphs (dominated by sphaeroidal pollen grains) (Fig. 5.58).

Palaeoenvironmental interpretation: PT-E plotted in field IX of Tyson's APP ternary which indicates a deposition in a distal suboxic-anoxic basin condition (Fig. 5.52). Common gonyaulacoid cysts recovered in interval 2943 m – 2600 m include the genus of *Spiniferites*, *Trichodinium* and *Oligosphaeridium* with minor occurrence of peridinoids (*Andalusiella*, *Palaeocystodinium* and *Cerodinium*). Sphaeroidal pollen grains recorded in higher amounts than pteridophyte spores from 2943 m – 2600 m. Intervals from 3147 m – 3105 m generally recorded low to none amount of pteridophytes throughout this palynofacies type with occurrence of pollen of palmae (e.g. *Proxapertites* and *Longapertites*) which flourish in mangrove environments alongside coastal areas of humid tropics (Schrank, 1998; Herngreen, 1998; El Beialy, 1995). The low occurrence of phytoclasts which supports the offshore depositional environment for PT-E (Fig. 5.53). Dominant AOM (>60%) of POM recorded indicates reducing conditions and increased water column stability (Tyson, 1995; Ibrahim et al., 2002).

Based on discussions above and constituents of POM together with associated palynomorphs, PT-E must have been deposited from inner to middle neritic environment at depths intervals

3147 m – 3105 m to middle-outer neritic environment at 2943 m – 2600 m under distal suboxic-anoxic basin condition.

Kerogen Type: characterized by kerogen type II≥I (highly oil prone) based on the dominance of well-preserved AOM.

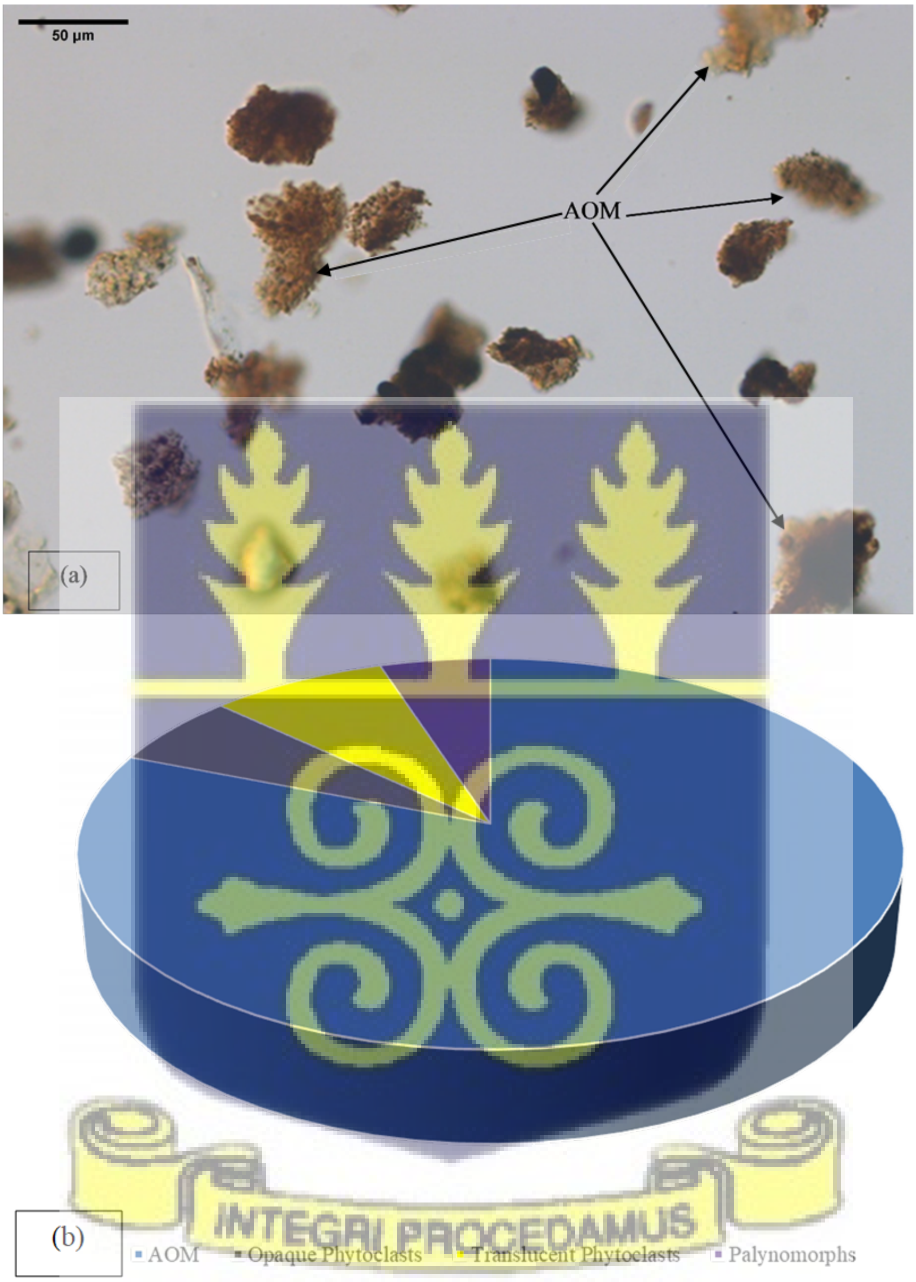

Figure 5.51: (a) Representative photograph of palynofacies association PT-E, sample depth 2880m from the Dzata-2A well. Key to label: AOM = amorphous organic matter. (b) Pie chart showing relative abundance (%) of the different constituents of palynofacies association PT-E from Dzata-2A well.

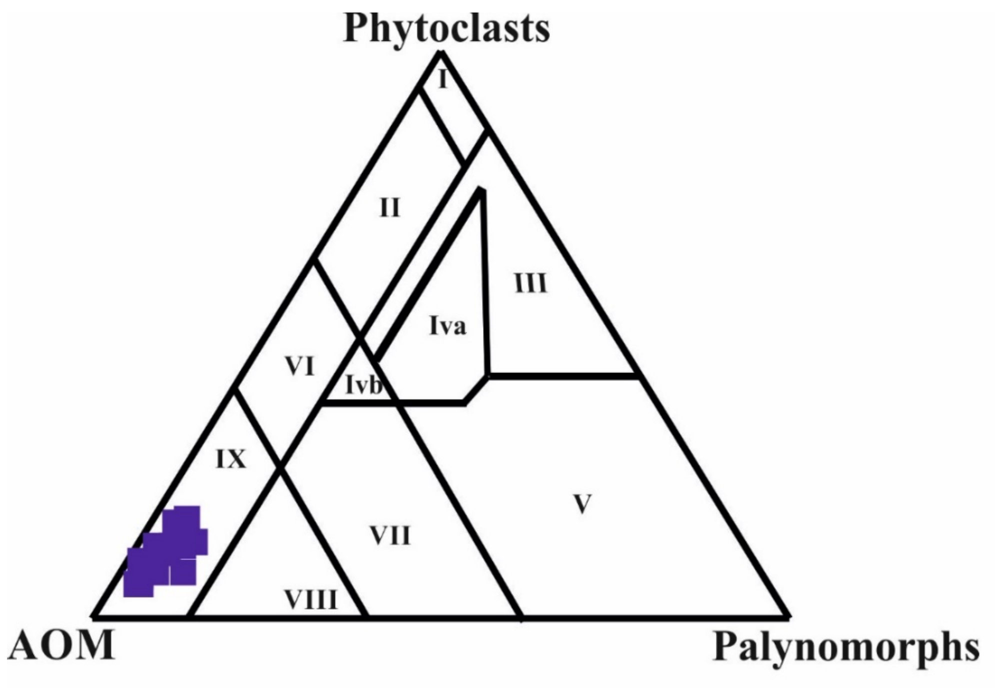

Figure 5.52: APP Ternary diagram for PT-E samples from Dzata-2A well (after Tyson, 1993).

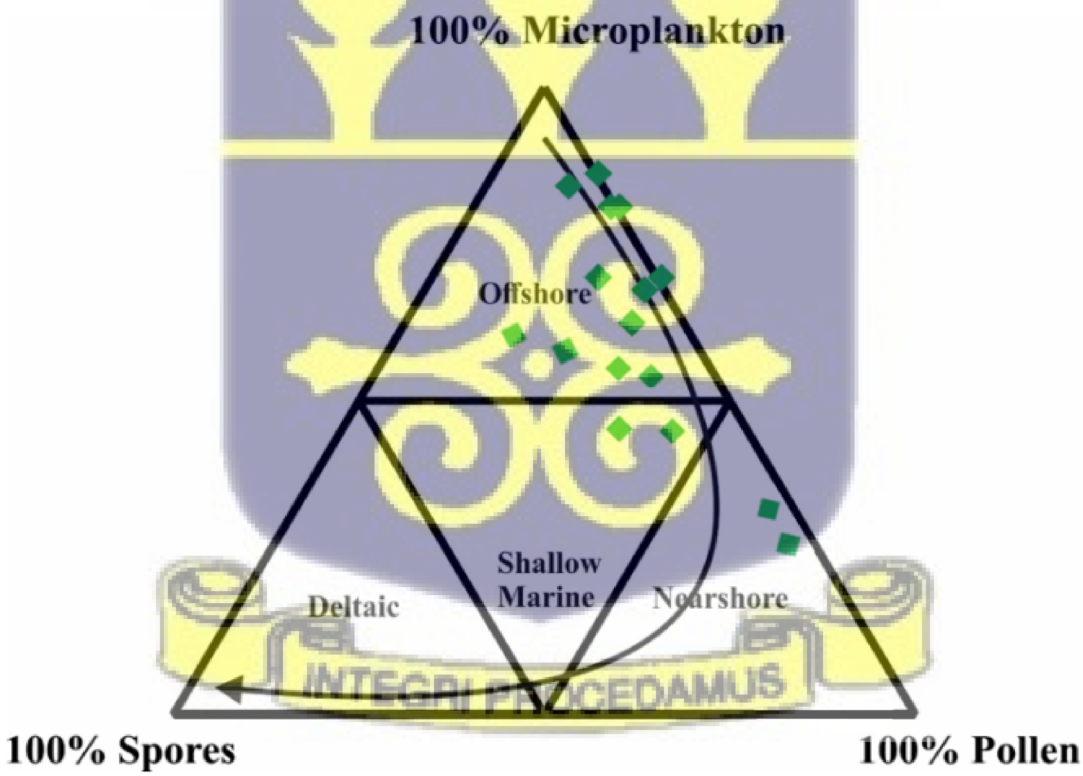

Figure 5.53: MSP Ternary plot for PT-E samples from the Dzata-2A well (After Federova, 1977; Duringer and Doubinger, 1985).

5.2.3.6 Palynofacies type 6 (PT-F) (AOM dominant with relatively equal abundance of translucent phytoclasts and palynomorphs) (Fig. 5.54a).

PT-F is recorded at sample depths between 3084 - 2964 m. AOM (57%) dominates this palynofacies with relatively equal amount of phytoclasts and palynomorphs (17% and 18%) respectively and opaque phytoclasts (8%) of POM (Fig. 5.54b). AOM recovered is pale yellowish to orange in colour with good preservation. Palynomorphs recovered are wholly of terrestrial origin (mainly sphaeroidal forms).

Palaeoenvironmental interpretation: PT-F plots in the field VII of Tyson's APP diagram indicating deposition in a distal dysoxic-anoxic shelf environment (Fig. 5.55). The sporomorphs dominated by sphaeroidal pollen grains (e.g. *Classopollis*) with minor associated pteridophytes (e.g. *Cyathidites*). According to Kholeif and Ibrahim (2010), the very low occurrence of opaque phytoclasts suggests low salinity due to close proximity to fluvio-deltaic sources. The POM and its associated palynomorphs infers a nearshore/shallow marine depositional environment supported by MSP ternary diagram (Fig. 5.56). The discussion above suggests PT-F must have been deposited in a nearshore/shallow marine environment under a distal dysoxic-anoxic shelf environment.

Kerogen Types: The samples of PT-F are characterized by kerogen type II/III (oil prone) based on the dominant AOM relatively terrestrial palynomorphs.

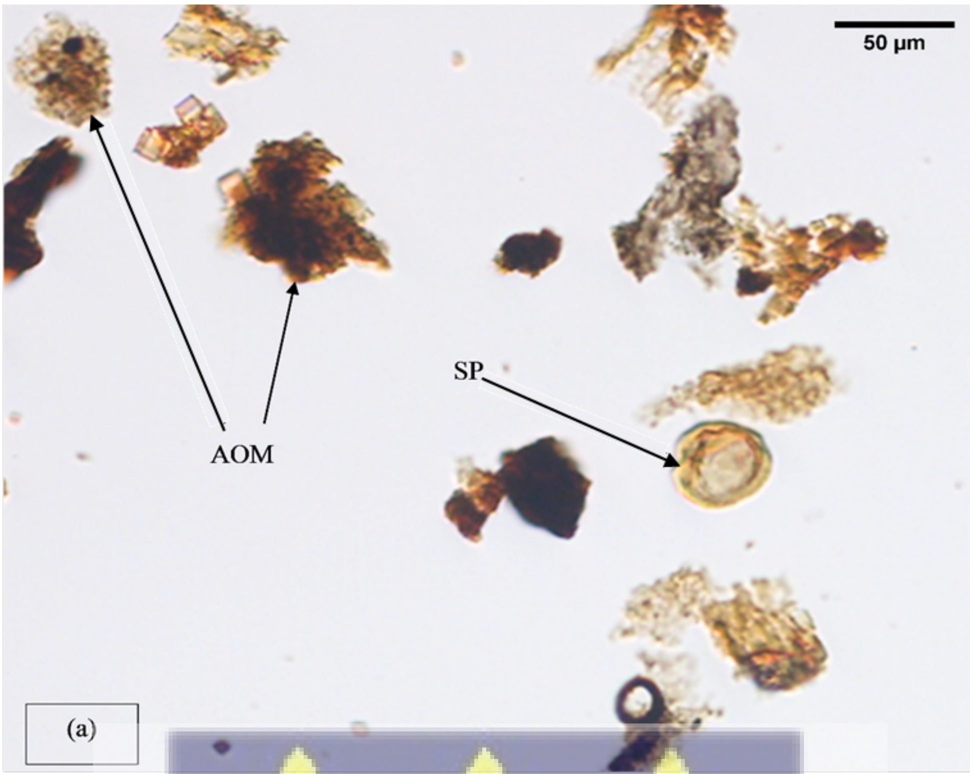

Figure 5.54: (a) Representative photograph of palynofacies association PT-F, sample depth 3042m from the Dzata-2A well. Key to labels: AOM = amorphous organic matter, SP = sporomorph (b) Pie chart showing relative abundance (%) of the different constituents of palynofacies association PT-F from Dzata-2A well.

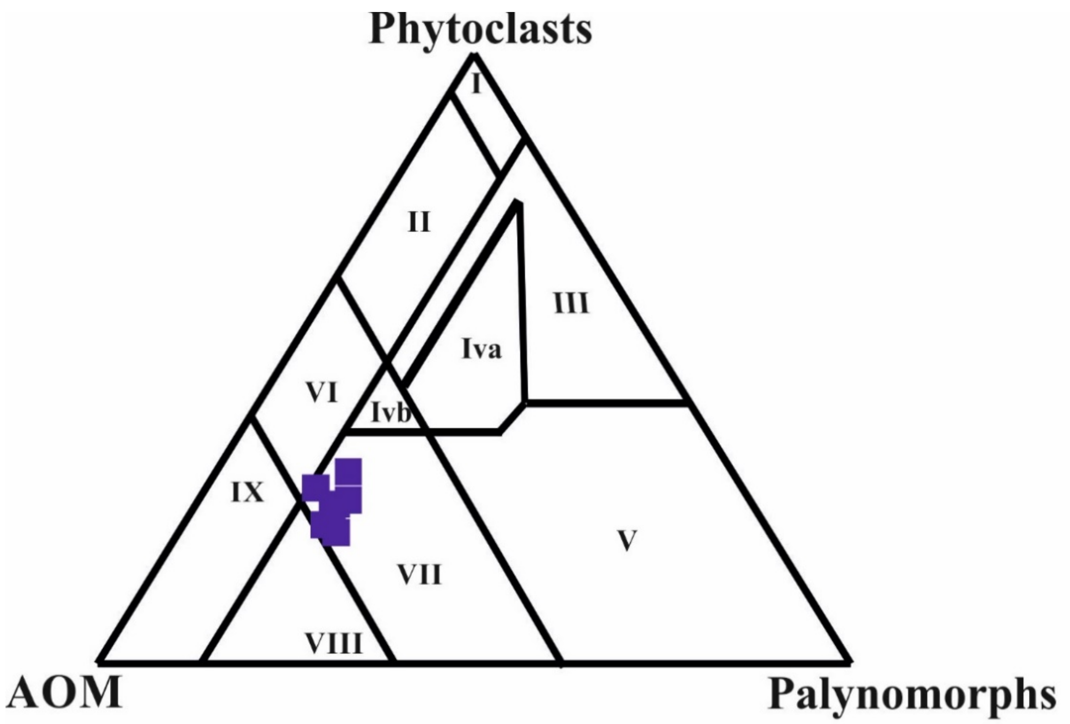

Figure 5.55. APP Ternary diagram for PT-F samples from Dzata-2A well (after Tyson, 1993).

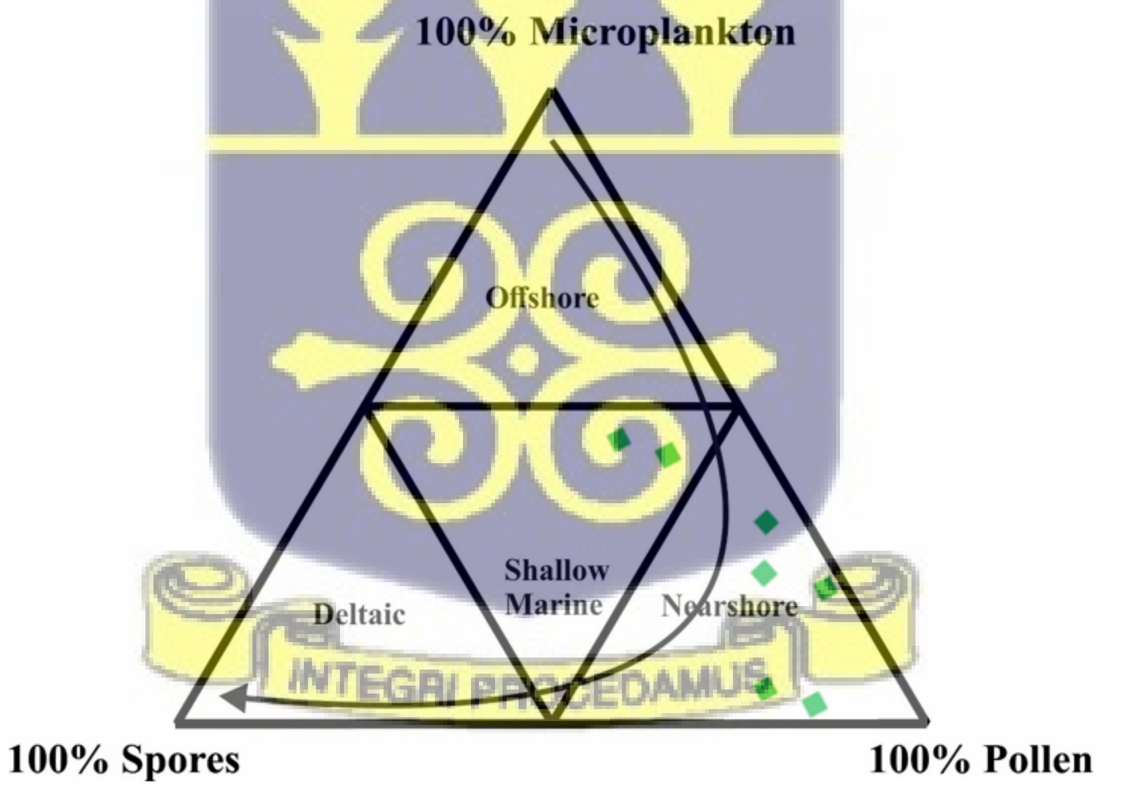

Figure 5.56: MSP Ternary plot for PT-F samples from Dzata-2A well (After Federova, 1977; Duringer and Doubinger, 1985).

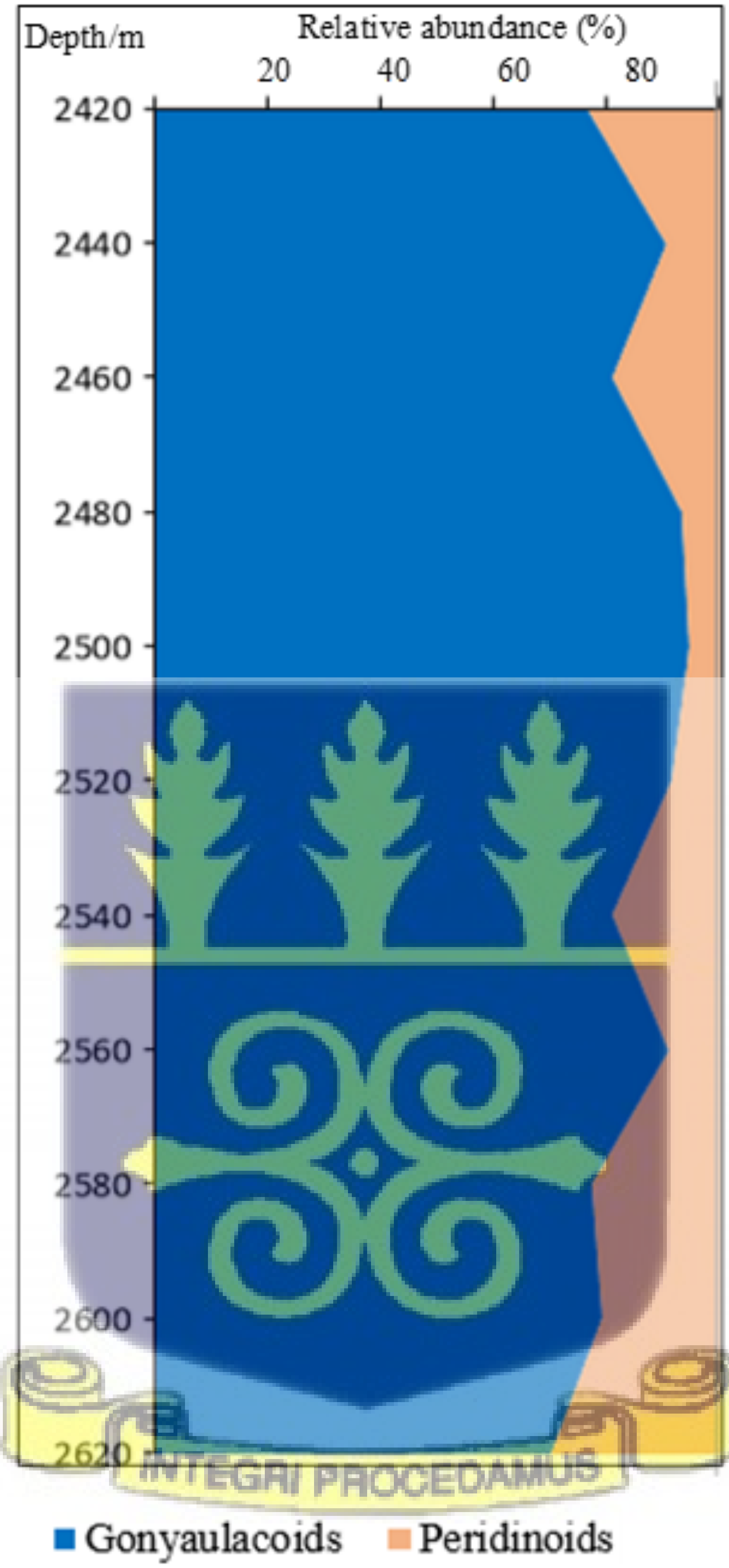

Figure 5.57: Relative percentage composition of Gonyaulacoids and Peridinoids of 5% total palynomorphs from Dzata-2A well.

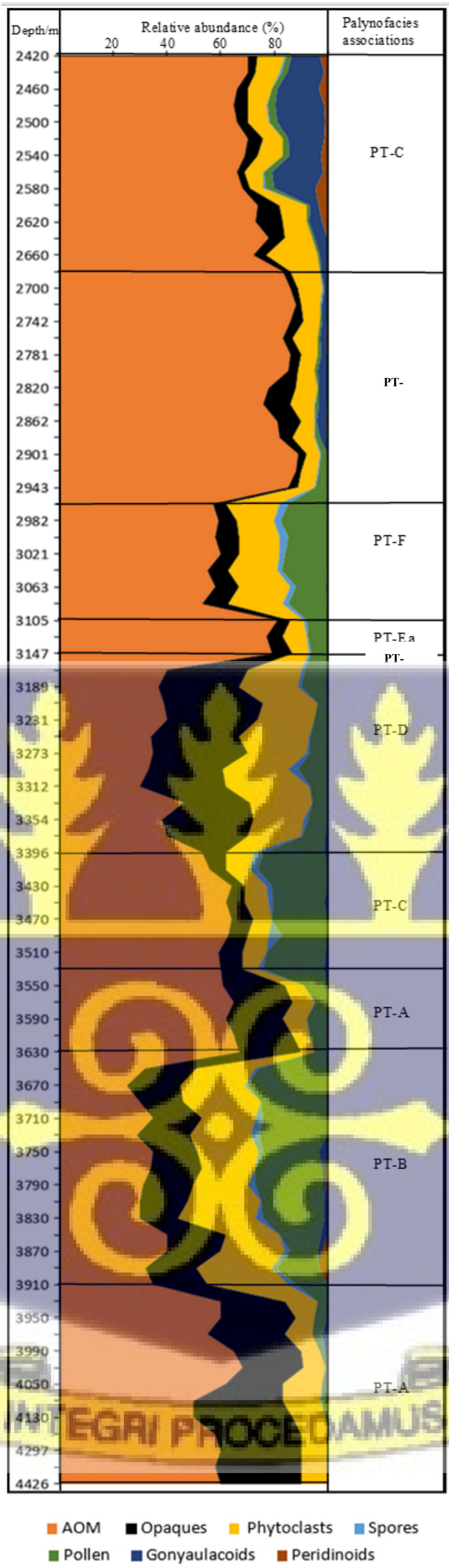

Figure 5.58: Palynofacies associations showing POM (%) from Dzata-2A well.

CHAPTER SIX

SOURCE ROCK EVALUATION

6.1 INTRODUCTION

Hunt (1995) define petroleum source rock as the fine-grained sediment with enough organic matter, which can generate and release enough hydrocarbons to form a commercial accumulation of oil or gas. He categorized source rocks according to oil generation into three classes which are; immature source rocks that have not yet generated hydrocarbons; mature source rocks that are in generation phase; post mature source rocks which are those that have already generated all crude oil type hydrocarbons. Common source rocks are normally shales and limestones, which contain significant amount of organic matter (Tissot and Welte, 1984). Tissot and Welte (1984) enumerated the key analyses that have to be carried out in a source rock evaluation for hydrocarbon potential which includes the amount (total organic carbon content), type (oil or gas prone material) and the level of thermal maturation (immature or mature) of organic mature in sediments. Pyrolysis is almost the best routine tool for determining the kerogen type and maturity (Espitalié et al., 1977)

According to Allen & Allen (1990) and Hunt (1996), hydrocarbons are generated in source rocks by the thermal alteration of organic matter with increasing depth of burial that increases temperature with time. Vitrinite reflectance (Ro) is one method of evaluating the thermal alteration of sedimentary rocks (Héroux et al., 1979) which successfully demonstrated to be a reliable indicator of organic maturation in sedimentary successions widely used in the oil industry to define potential areas of petroleum generation in a basin (Peters and Cassa 1994).

6.2 METHODOLOGY

The geochemical data of Lynx-X and Dzata-2A wells were obtained from the Core Laboratory of Ghana National Petroleum Corporation. Results were obtained for 120 and 101 samples from Lynx-1X and Dzata-2A wells respectively. The results were derived from the standard preparation and analysis for total organic carbon, Rock-Eval pyrolysis and vitrinite reflectance measurements to evaluate the hydrocarbon source potential. Samples were obtained using sampling interval of 20m. Analyses were done on the results of the pyrolysis data obtained following the guidelines in table 6.1 and discussed below. Geological information as well as the rock eval data is displayed in (Appendix 7 and 8).

Data from Rock-eval pyrolysis, total organic carbon and vitrinite reflectance measurements which were subjected to scatter plots for source rock evaluation with the view of identifying the type, richness, quality and thermal maturity of source rock samples. Scatter plots are cross plots whereby the parameters obtained from pyrolysis are plotted against each other and used in interpreting the properties and hydrocarbon potential of the area of study.

The basic parameters obtained by Rock-Eval pyrolysis are:

- S_1=the amount of free hydrocarbons (gas and oil) in the sample (in milligrams of hydrocarbon per gram of rock). S_1 normally increases with depth. Contamination of samples by drilling fluids and mud can give an abnormally high value for S_1.
- S_2=the amount of hydrocarbons generated through thermal cracking of non-volatile organic matter. S_2 is an indication of the quantity of hydrocarbons that the rock has the potential of producing should burial and maturation continue.
- S_3=the amount of CO_2 (in milligrams CO_2 per gram of rock) produced during pyrolysis of kerogen. S_3 is an indication of the amount of oxygen in the kerogen and is used to calculate the oxygen index.

- T_{max} = the temperature at which the maximum release of hydrocarbons from cracking of kerogen occurs during pyrolysis (top of S_2 peak). Tmax is an indication of the stage of maturation of the organic matter.
- TOC = total organic carbon content of samples, were determined by adding the residual organic carbon detected in pyrolysis residues to the pyrolyzed organic carbon, which in turn is measured from the hydrocarbon compounds issuing from pyrolysis.

The following parameters were calculated from Rock Eval pyrolysis data:

- Hydrogen Index (HI) = [100 x S_2]/TOC). HI is a parameter used to characterize the origin of organic matter. Marine organisms and algae, in general, are composed of lipid- and protein-rich organic matter, where the ratio of H to C is higher than in the carbohydrate-rich constituents of land plants.
- Oxygen Index (OI) = [100 x S_3]/TOC). OI is a parameter that correlates with the ratio of O to C, which is high for polysacharride-rich remains of land plants and inert organic material (Tissot and Welte, 1984).
- Production Index (PI) = S_1/ [S_1 + S_2]). PI is used to characterize the evolution level of the organic matter.
- The vitrinite reflectance (R_o) was estimated from the T_{max} values obtained from the Rock-Eval pyrolysis (Dembicki Jr., 2009) and expressed mathematically as: $R_{calculated}$ = (0.018 ⁄ T_{max}) 7.16.

Table 6.1 below serve as a guide for interpretation of the source rock potential of the study area. Cross plots of the various parameters were done using softwares such as Microsoft excel, Delta graph, Corel draw and Inkscape app.

Table 6.1. Guidelines for interpreting source rock quantity, quality and maturation, and commonly used Rock-Eval parameters.

Quantity	TOC	S_1(mg HC/g rock)	S_2(mg HC/g rock)
Poor	<0.5	<0.5	<2.5
Fair	0.5-1	0.5-1	2.5-5.0
Good	1-2	1-2	5-10
Very Good	2-4	2-4	10-20
Excellent	>4	>4	>20
Quality	**HI (mg HC/g TOC)**	**S2/S3**	**Kerogen Type**
None	<50	<1	IV
Gas	50-200	1-5	III
Gas and Oil	200-300	5-10	II/III
Oil	300-600	10-15	II
Oil	>600	>15	I
Maturation	**Ro (%)**	**Tmax (^{o}C)**	**TAI**
Immature	0.2-0.6	<435	1.5-2.6
Early Mature	0.6-0.65	435-445	2.6-2.6
Peak Mature	0.65-0.9	445-450	2.7-2.9
Late Mature	0.9-1.35	450-470	2.9-3.3
Post Mature	>1.35	>470	>3.3

SOURCE: {Epstein et al. (1977), Espitalié et al. (1984), Peters (1986), Traverse (1988), Peters and Cassa (1994), Fowler et al. (2005)}

6.3 EVALUATION OF LYNX-1X AND DZATA-2A WELLS

6.3.1 Organic Carbon richness and Hydrocarbon Potential

Batten (1996) stated that for a rock to be a hydrocarbon source, that particular rock should have had a sufficient amount of organic matter for the generation and the expulsion. Peters (1986) used the measure of pyrolysis derived S_2 of the rock samples and TOC to determine the source rock richness and hydrocarbon potentiality. The organic richness of samples containing TOC (wt%) under 0.5% are classified as poor, 0.5 to 1.0% TOC are fair, and those containing over 1.0% TOC are a good source. Samples which contain S_2 under 2.5 mg/g are poor source rocks, S_2 from 2.5 to 5 mg/g are fair source rocks, S_2 from 5-10 mg/g are good source rocks, and those with more than S_2>10 mg/g are viewed as very good source rocks (Table 6.1).

Analysed samples from Lynx-1X well have organic carbon (TOC) ranges from 0.5-6.0 wt% (Fig. 6.1, Appendix 7). Samples of the Paleocene-Eocene (2525 – 2755 m) have TOC (wt%) ranging from 0.53-1.63 wt% which reflects organic richness from fair to good source rocks and with S_2 values (0.25-3.82mg/g) indicating poor to fair source potential (Fig. 6.1). The Campanian-Maastrichtian rocks (2775-3305 m) is characterized by TOC (wt%) values from 1.19-4.15 wt% which indicates good to excellent organic source richness and characterized by S_2 values (2.54-6.58mg/g) which reflects fair to good source potential (Fig. 6.1). The Turonian-Santonian? rocks (3325-3695 m) have TOC values (1.58-3.08 wt%) which denotes good to very good source rock. The S_2 values ranges from 4.67-18.93 mg/g which indicates good to very good source potential (Fig. 7.1). Albian-Cenomanian rocks (3715 - 5297.5 m) has TOC values ranging from 0.51-6.48 wt% which reflects fair to excellent source rock with most of the measured intervals indicating fair to very good organic richness. The hydrocarbon potentiality characterized by S_2 values which ranges from 0.2-8.68 mg/g demonstrates poor to good source potential (Fig. 6.1).

Analysed samples from Dzata-2A well have organic carbon (TOC) ranging from 0.6-6.0 wt% (Appendix 8). The Campanian-Maastrichtian rocks (2418-2420 m) - (2781-2784 m) have organic carbon (TOC) values ranging from 1.67-6.1 wt% which is considered as good to excellent organic source richness. The S_2 values ranging 3.33-27.37 mg/g indicates good to excellent source potential. Measured intervals from the Turonian-Santonian? rocks ((2799-2802 m) - (2919-2922 m)) have TOC values (1.97-4.02 wt%), reflecting good to excellent source rocks with intervals having good to very good organic richness. The S_2 values recorded range from 7.94-21.28 mg/g denoting good to excellent hydrocarbon potentiality. Samples from the Albian-Cenomanian source rocks ((2940-2943 m) - (4170-4180 m)) have organic carbon (TOC) values which range from 0.51-1.86 wt% which is reflective of a fair to good organic richness. S_2 values ranges from 0.25-4.48 mg/g indicating a fair source potential.

The Rock-Eval pyrolysis for both wells indicate that 70-80% of analysed samples are good to very good potential source rock. However, greater than 50% of the samples have S_2 values less than 10mg/g which suggest a good hydrocarbon potentiality for Lynx-1X and Dzata-2A wells (Fig. 6.1). S_2 which measures the existing potential of a rock to generate hydrocarbons is considered as a more practical metric of source rock potential than the TOC since the TOC includes “dead carbon” which is unable to generate hydrocarbons (Peters and Cassa 1994; Alaug et al., 2014). Therefore, ?Turonian-Santonian age samples in the studied wells are considered as better potential source rocks than the Campanian-Maastrichtian and Albian-Cenomanian source rocks.

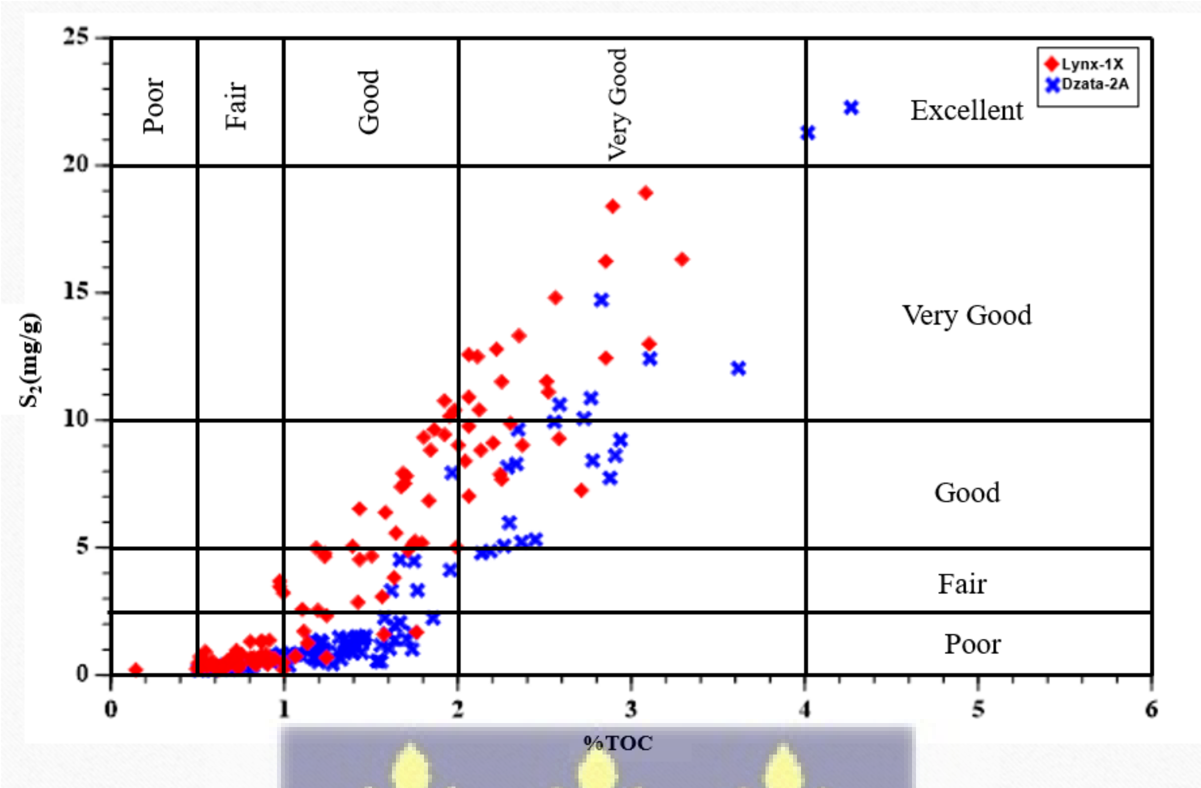

Figure 6.1: S_2 against TOC% showing the Hydrocarbon potentiality and source efficiency

The plot of S_2 against TOC% (Fig. 6.2) was also used to deduce the kerogen types of the studied samples from Lynx-X and Dzata-2A wells. The plot showed that majority of the samples plotted between Kerogen type II and III which indicate oil and gas prone hydrocarbons (Fig. 6.2). Few of the samples plotted in Type I (Oil) in Lynx-well and type IV Kerogen zone for both wells.

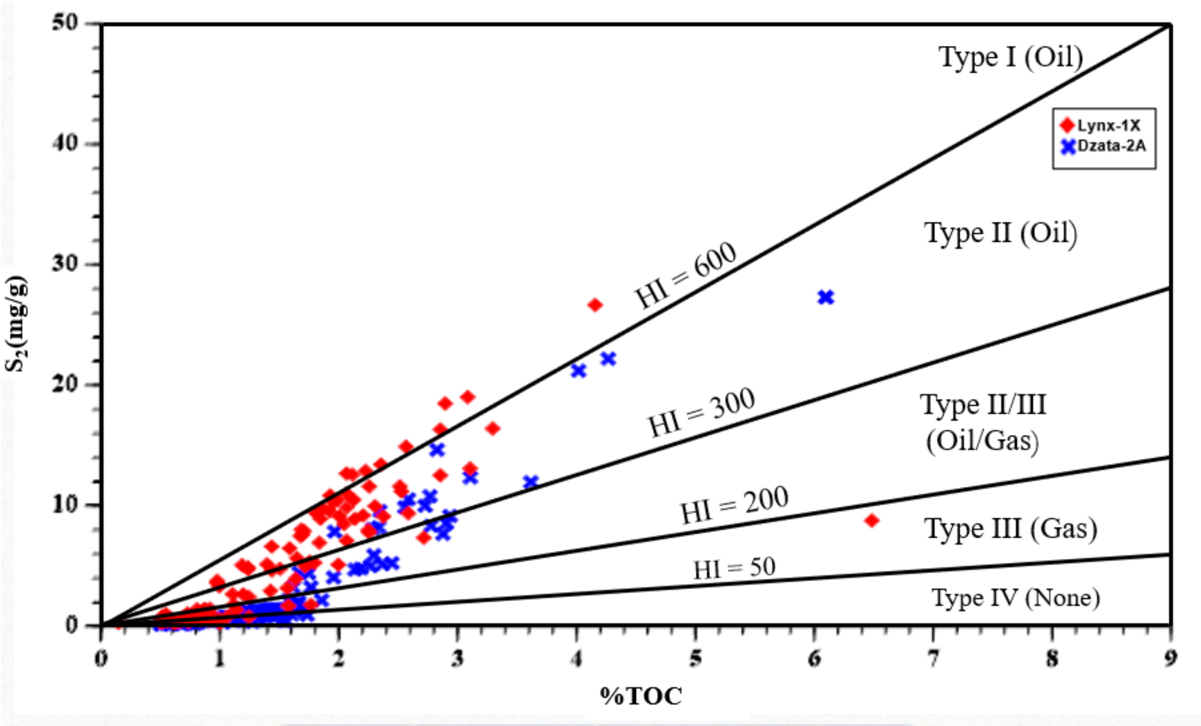

Figure 6.2: S_2 against TOC% plot showing types of kerogens

In this study, the plot of HI/TOC for Lynx-1X and Dzata-2A wells combines generation potential and kerogen types (Fig. 6.3). With respect to TOC, four samples in both wells plotted within excellent generation potential. Majority of the samples plotted within 1-4% TOC which indicates a good to very good generation potential.

According to Tissot and Welte (1984), the Genetic Potential (S_1 + S_2) of a given formation is the amount of petroleum (oil and gas) that kerogen is able to generate if it is subjected to an adequate temperature during a sufficient interval of time. It gives a qualitative estimate of hydrocarbon resource potential but cannot be used to predict the type of hydrocarbons (i.e gaseous or liquid) that will be produced during pyrolysis. Waples et al (1992) intimated that, a rock with Genetic Potential less than 2 mgHC/g rock represents a gas prone or non-generative zone. However, the values between 2-6 mgHC/g rock is representative of a moderate source rock with fair oil and gas generation potential and those with GP values higher than 6 mgHC/g rock indicates a good source rock. Rocks which have extremely high GP values of about 100-

200 mgHC/g rock would provide either an excellent source rock with enough burial depth or an oil shale when burial depth is shallow.

With reference to Waples et al (1992) stated above, analysed samples from the Paleocene-Eocene sediments in Lynx-1X well with GP values ranging from 0.35-3.96 mgHC/g rock is indicative of a gas/non-generative zone to a moderate source with fair oil and gas generation potential and supported by the very low TOC values (0.53-1.63) (Fig. 6.4). The Campanian-Maastrichtian rocks GP of Lynx-1X (2.66 - 26.78 mgHC/g rock) and Dzata-2A (3.45 - 27.66 mgHC/g rock) represents moderate source rock with fair oil and gas generation potential to a good source rock. Most of the very high TOC values ((1.19-4.15) and (1.67-6.1)) for Lynx-1X and Dzata-2A wells respectively in these sample intervals further assign a good source (Fig. 6.4). The ?Turonian-Santonian rocks of Lynx-1X with GP values (4.78 - 19.1 mgHC/g rock) and Dzata-2A (8.03-21.46) which represents moderate to good source supported by high TOC content (1.58-3.08) and (1.97-4.02)) for Lynx-1X and Dzata-2A respectively for majority of the samples ranging from good to very good organic richness and fair hydrocarbon potentiality for S_1 values (0.11-0.18 for Lynx-1X and 0.8-0.18 for Dzata-2A) (Fig. 6.4). Analysed samples from the Albian-Cenomanian rocks are characterized by the lowest GP values. For Lynx-1X well GP value ranges from 0.25-15.23 mgHC/g rock and 0.3-4.62 mgHC/g rock for Dzata-2A well which represent a moderate to good source potential (Fig. 6.4).

The hydrocarbon potential of the study succession in both wells suggests a fair to very good.

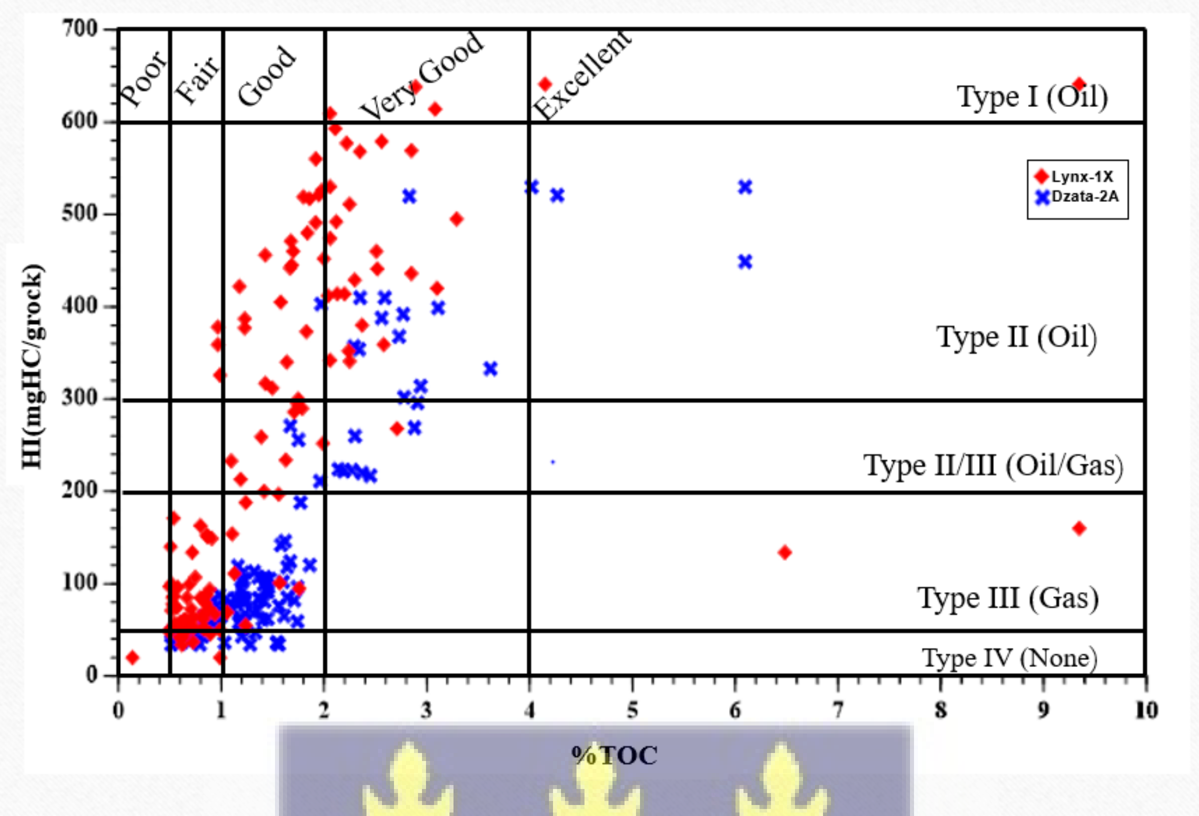

Figure 6.3: Plot of Hydrogen Index against TOC% indicating kerogen types and generation potential.

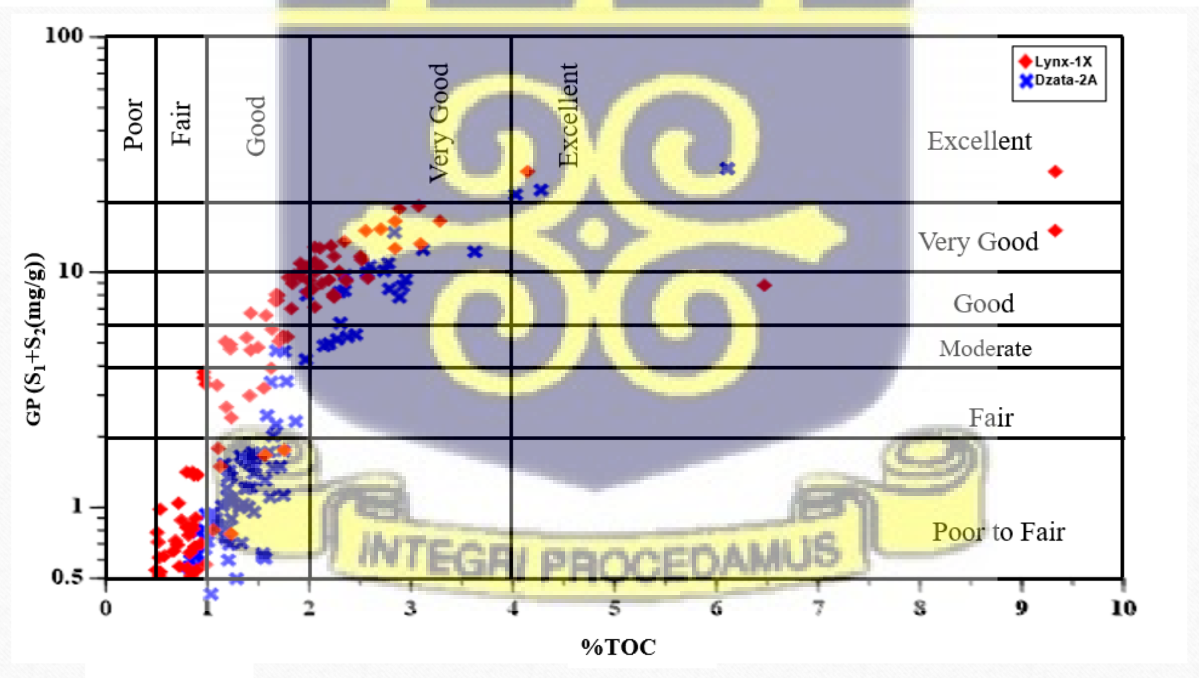

Figure 6.4: Plot of GP (S_1+S_2) against TOC% indicating hydrocarbon potentiality for the well samples.

6.3.2 Kerogen Types

Kerogen or organic matter type is important in evaluating source rock potential and essentially has a first order control on the nature of the hydrocarbons. Kerogen types are normally identified by optical and by organic geochemical methods by plotting the values of elemental analysis of C, O, H on the Van Krevelen diagram which defines the four types of kerogens (Peters and Cassa 1994; Tissot et al., 1974). Hydrogen indices values (HI) were used to differentiate between the types of organic matter (Epstein et al., 1977; Espitalié et al., 1984; Waples, 1985; Peters, 1986; Traverse, 1988; Peters and Cassa, 1994; Fowler et al., 2005).

With reference to Table 6.1, HI values lower than 50 mg/g contains kerogen type IV with no potential source; 50-200 mg/g values is a potential source for generating gas (type III kerogen); 200-300 mg/g values comprise more of type III kerogen than type II which is capable of generating mixed oil and gas but mainly gas; 300-600 mg/g values consist of type II kerogen and indicates a good source potential for generating oil with minor gas; HI values greater than 600 mg/g contains mainly kerogen Type I with excellent potential to generate oil.

Analysed samples from Lynx-1X well in this study have HI values which ranges from 42-326 mg/g and OI values from 24-99 mg/g (Appendix 7) for the Paleocene-Eocene samples which is represented by eight samples and indicates no potential (kerogen type IV) to good source potential for generating oil and gas (type II, III) but mainly gas (Fig. 6.5). In the Campanian-Maastrichtian the twenty-eight samples have HI values ranging from 197-641 mg/g and OI values from 13-35 mg/g (Appendix 7). These values reflect potential source for generating gas (type III kerogen) to excellent potential of generating oil (Kerogen type I). The majority of the samples plot in type II and III kerogen zone (Fig. 6.5). Twenty-one samples analysed from the ?Turonian-Santonian is represented by HI values (290-614 mg/g) and OI values (14-37 mg/g) where most of the samples belong to type II and III kerogen capable of generating oil and gas (Fig. 6.5). HI values range from 20-471 mg/g and OI values range from 9-88 mg/g of the

Albian-Cenomanian analysed samples (63) reveal kerogen types IV, III, II/III and II where majority of the samples plot in kerogen types II/III and III which is considered to generate oil and gas but mainly gas (Fig. 6.5).

The Dzata-2A well has HI and OI values ranging from 188-449 mg/g and 15-43 mg/g respectively for the Campanian-Maastrichtian (20 samples), reflecting types III, II/III and II kerogens (Fig. 6.5). Most of the samples contains more type III than II kerogen which is a good source for generating more gas than oil. The seven samples analysed from ?Turonian-Santonian has HI values ranging from 357-530 mg/g and OI values ranging from 14-23 mg/g which is characterized by type II kerogen and is considered a good source potential for generating oil. In the Albian-Cenomanian, 74 samples were analysed and HI values of range (34-256 mg/g) and OI values ranging from 23-118 mg/g (Appendix 8) were recorded. This indicates kerogen Types IV, III and II/III. Majority of the samples plot in kerogen type III which is a potential source capable of generating gas with few samples concentrating in kerogen type II/III which indicates potential for generating oil and gas but mainly gas (Fig. 6.5).

The sample plots of HI versus Tmax also displayed similar trends and identified the kerogen types observed in the plot of HI versus OI for Lynx-1X and Dzata-2A wells (Figs. 6.6, 6.7).

From the above discussion, the ?Turonian-Santonian analysed samples of Lynx-1X and Dzata-2A wells have good potential to generate oil/gas than the Albian-Cenomanian, Campanian-Maastrichtian and Paleocene-Eocene studied intervals.

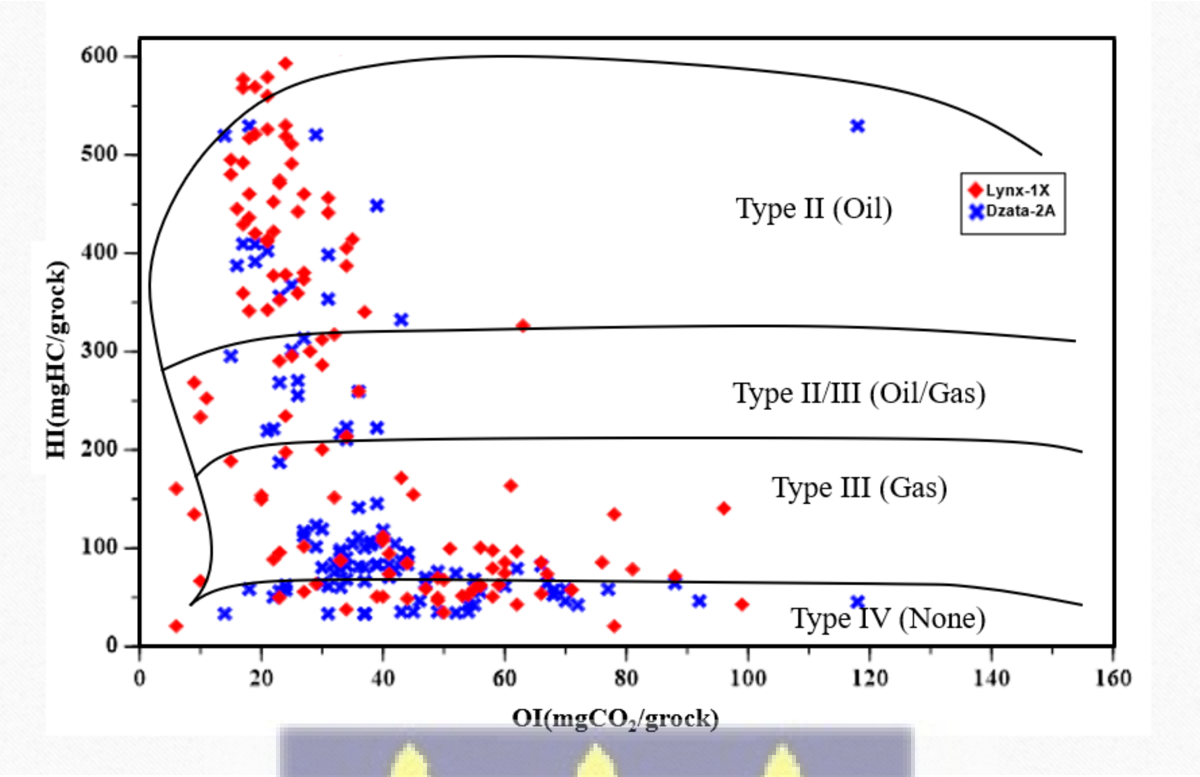

Figure 6.5: Types of kerogens indicated on a modified Van Krevelen diagram

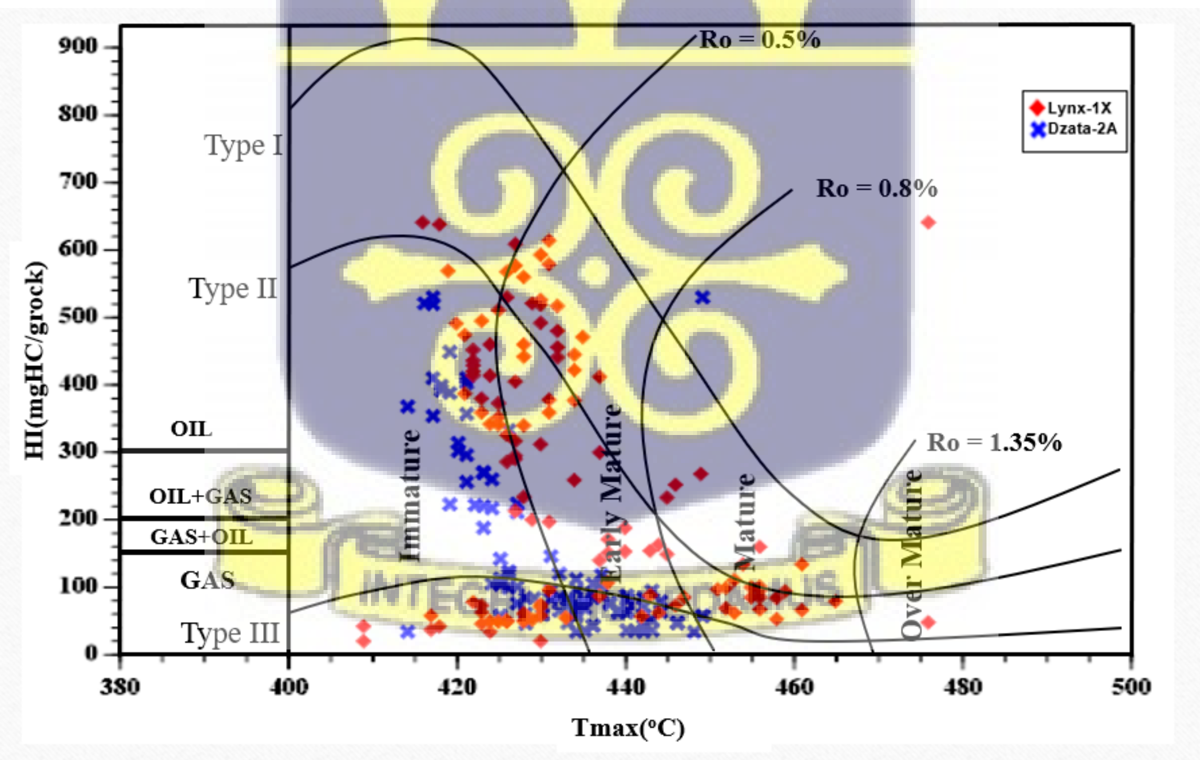

Figure 6.6: Types of kerogen and levels of maturity shown by Hydrogen Index against Tmax

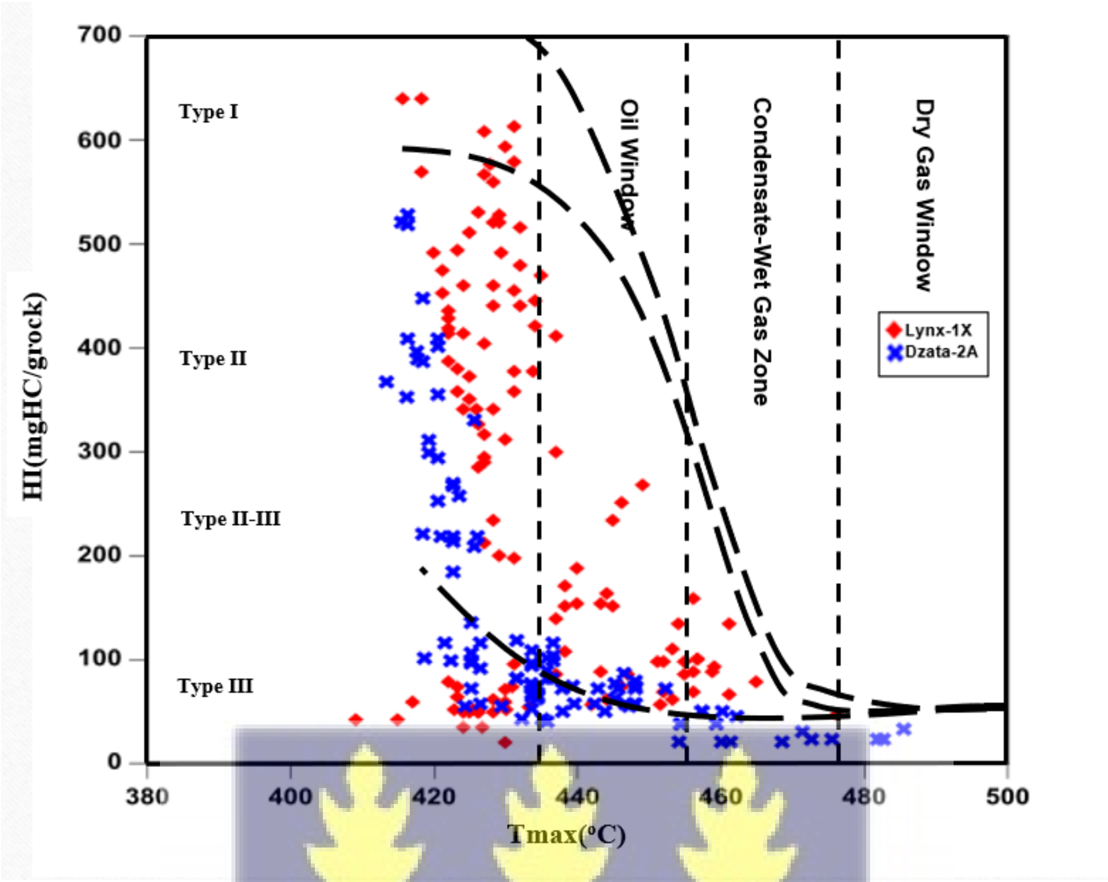

Figure 6.7: Types of kerogen and levels of maturity shown by Hydrogen Index against Tmax

6.3.3 Organic Matter Maturity

The maturity of the source rock is another important factor of source rock evaluation. The level of thermal maturity for the different types of organic matter may be estimated from the T_{max} range and Production Index (Peters and Cassa, 1994; Bacon et al., 2000; El Kammer, 2015). Organic matter maturity is determined by using the level of thermal maturity of organic matter and type of organic matter which influences the type of maturity as well as the presence of free hydrocarbons with other factors which includes content, burial depth, and mineral water (Traverse, 1988). According to Traverse (1988), an increase in maturity level of organic matter corresponds to an increase in T_{max} particularly for immature samples.

The plots of HI/T_{max} from the analysed samples of Lynx-1X and Dzata-2A made it possible to define the kerogen type based on HI only since the variability in T_{max} is confined to 409-476 °C for Lynx-1X well and 416-449 °C for Dzata-2A well.

In the present study, the thermal maturity level of the source rocks was determined by the study of Tmax, production index (PI), and vitrinite reflectance ($R_{calculated}$). According to Peters et al. (2005), $R_{calculated}$ formula (0.018 ⁄ Tmax) 7.16) is applicable for type II and type III kerogen and reasonable when the analysed samples have S_2 values more than 0.5 mg HC/g rock and Tmax <420 °C or >500 °C which is consistent with majority of the analysed samples in this study. According to Peters (1986), oil generation from source rocks began at Tmax 435-465°C, PI values ranging from 0.2-0.4% and vitrinite reflectance (R_o%) greater than 0.6%. Tmax values less than 435°C, PI values less than 0.2% and R_o values less than 0.6% of organic matters are considered to be immature. The gas generation from source rocks started at Tmax 470°C, PI greater than 0.4% and R_o more than 0.8%.

Analysed samples for Lynx-1X and Dzata-2A wells in this study shows majority of the samples have PI values between 0.1 and 0.2 and T_{max} values ranging from 410-460°C, indicating that most of the samples (Tmax < 435°C) are immature with few samples having PI>0.2 and T_{max} > 435°C indicating early mature to mature organic matter (Oil window) (Figs. 6.8, 6.9). Most of the analysed samples have low level of kerogen conversion (Fig. 6.9). A plot of HI/Tmax (Figs. 6.6, 6.7) is also consistent with majority of the analysed samples plotting outside the oil window with few samples constrained in the condensate-wet gas zone (Fig. 6.7). ($R_{calculated}$) values of samples from Lynx-1X and Dzata-2A indicate immature to early mature (Fig. 10), since most of the samples show $R_{calculated}$ values less than 0.6 (Appendix 7 & 8) and increases with depth (Fig. 11). Lynx-1X has most part of the deeper analysed sample intervals to be inconsistent with the decreasing $R_{calculated}$ trend with depth plot (Fig. 11) because most of the samples below 4700 m have S_2 values less than 0.5 mg/g and T_{max} values greater than 420°C and less than 500ºC (Appendix 7). T_{max} and $R_{calculated}$ versus the Hydrogen Index (HI) cross plot after Espitalié (1986) gives an overview of the thermal maturity and variation of organic matter quality. Lynx-1X and Dzata-2A wells have T_{max} values correlates directly with the vitrinite reflectance values (Figs. 6.7, 6.12).

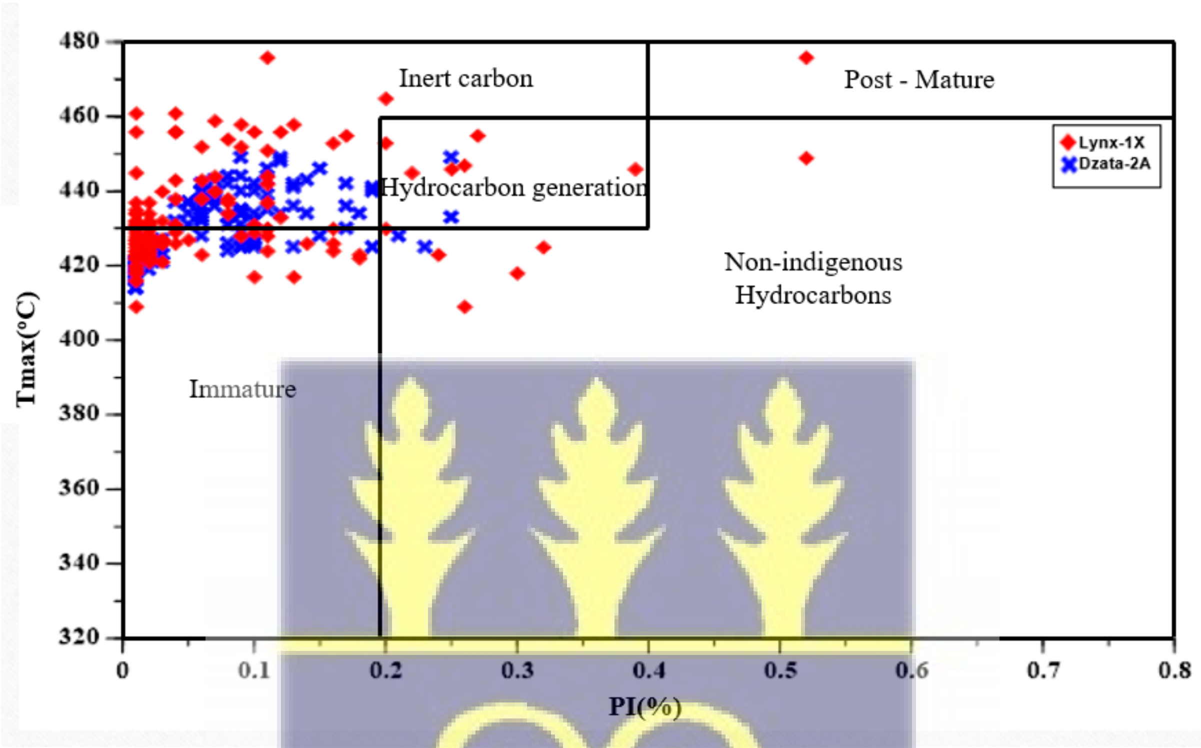

Figure 6.8: Plot of Tmax versus Production Index showing hydrocarbon generation zone.

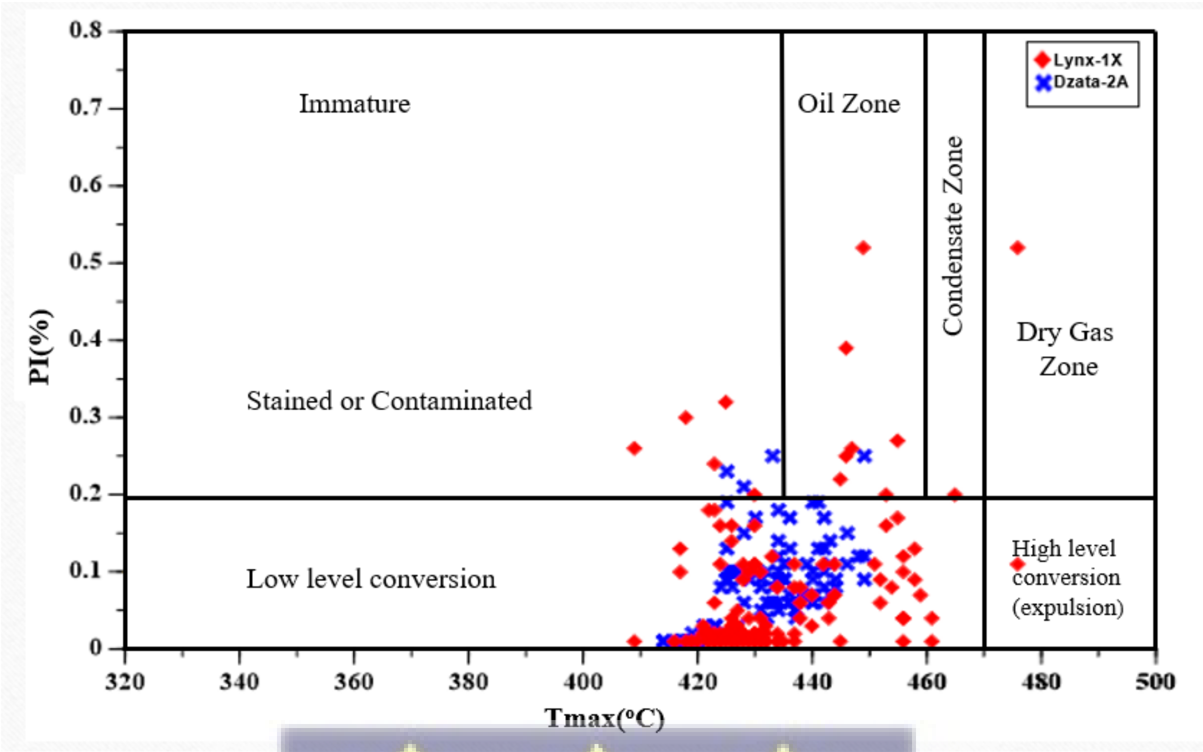

Figure 6.9: Plot of Production Index versus Tmax showing levels of kerogen conversion and maturity

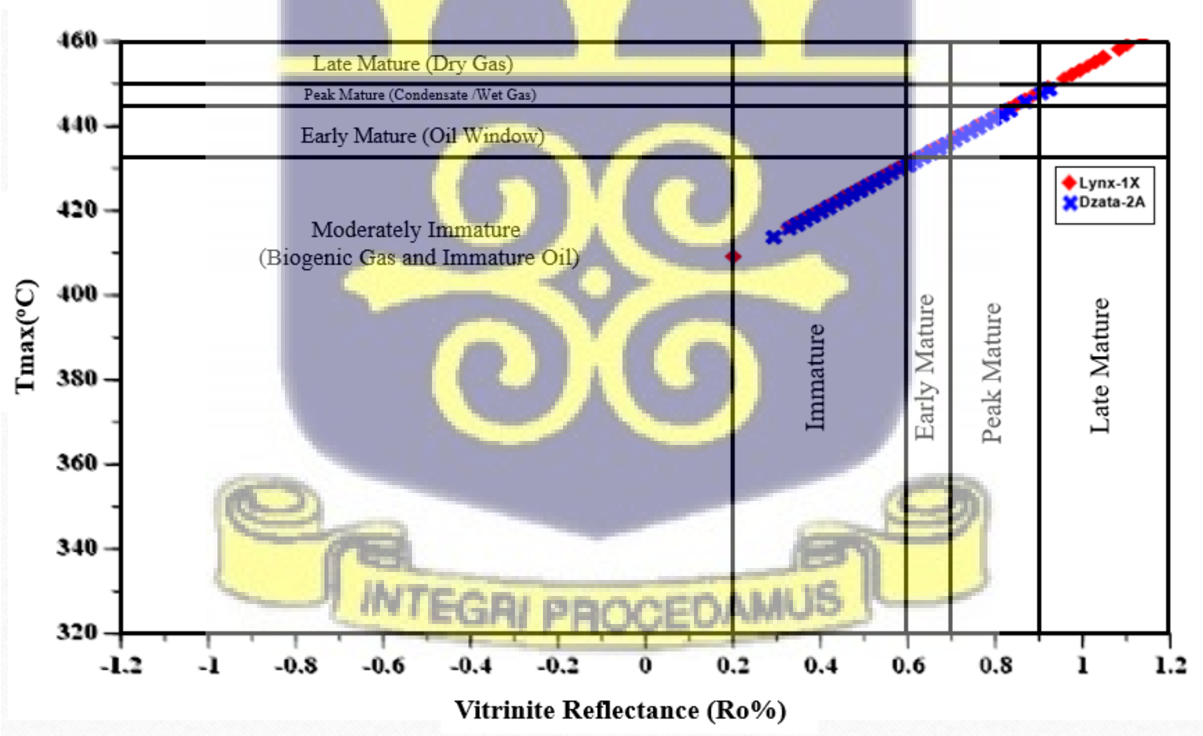

Figure 6.10: Plot of Tmax versus Vitrinite reflectance (Ro) showing maturity levels

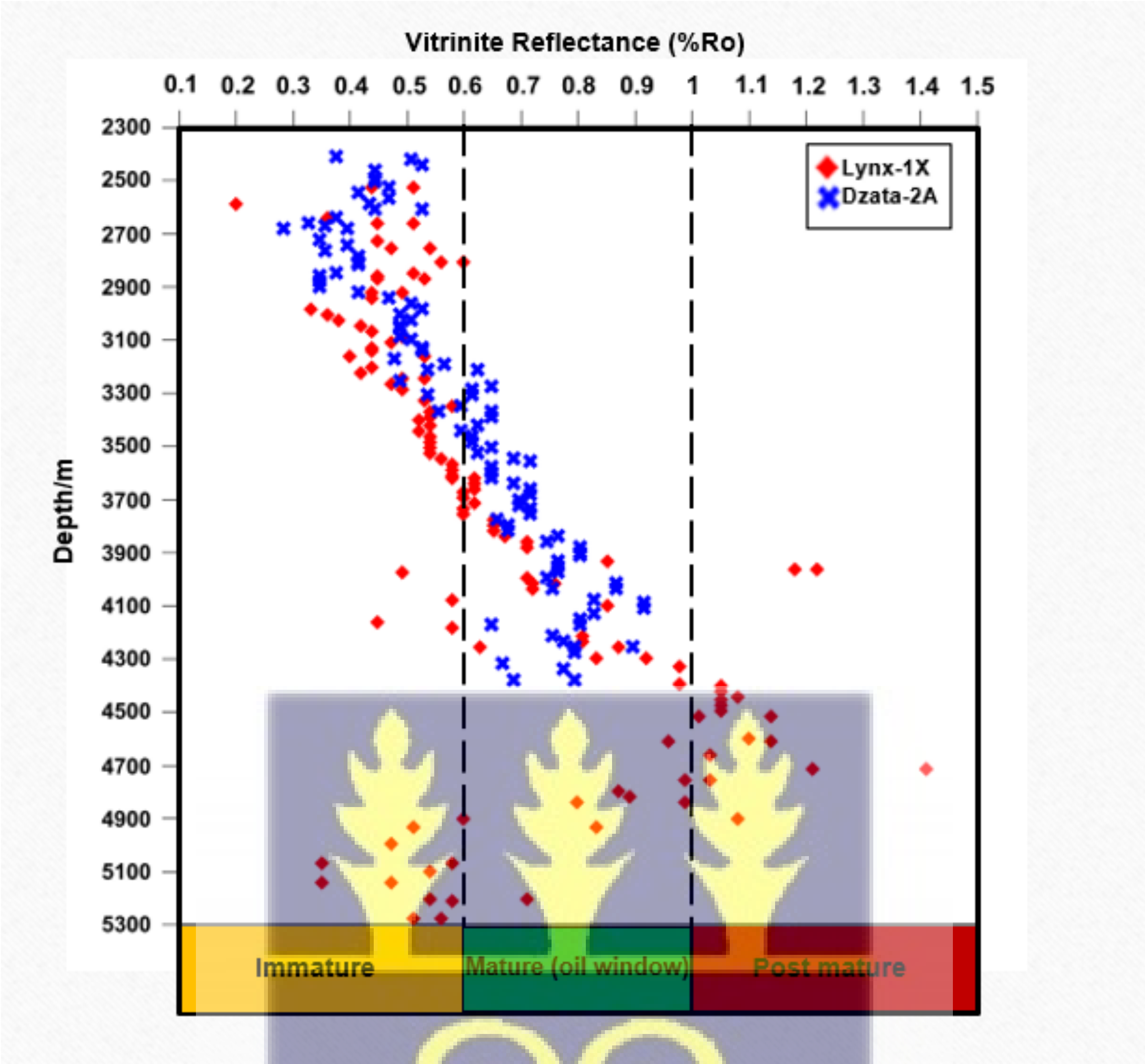

Figure 6.11: Plot of depths versus vitrinite reflectance data ($R_{calculated}$) showing thermal maturity stages of Lynx-1X and Dzata-2A wells.

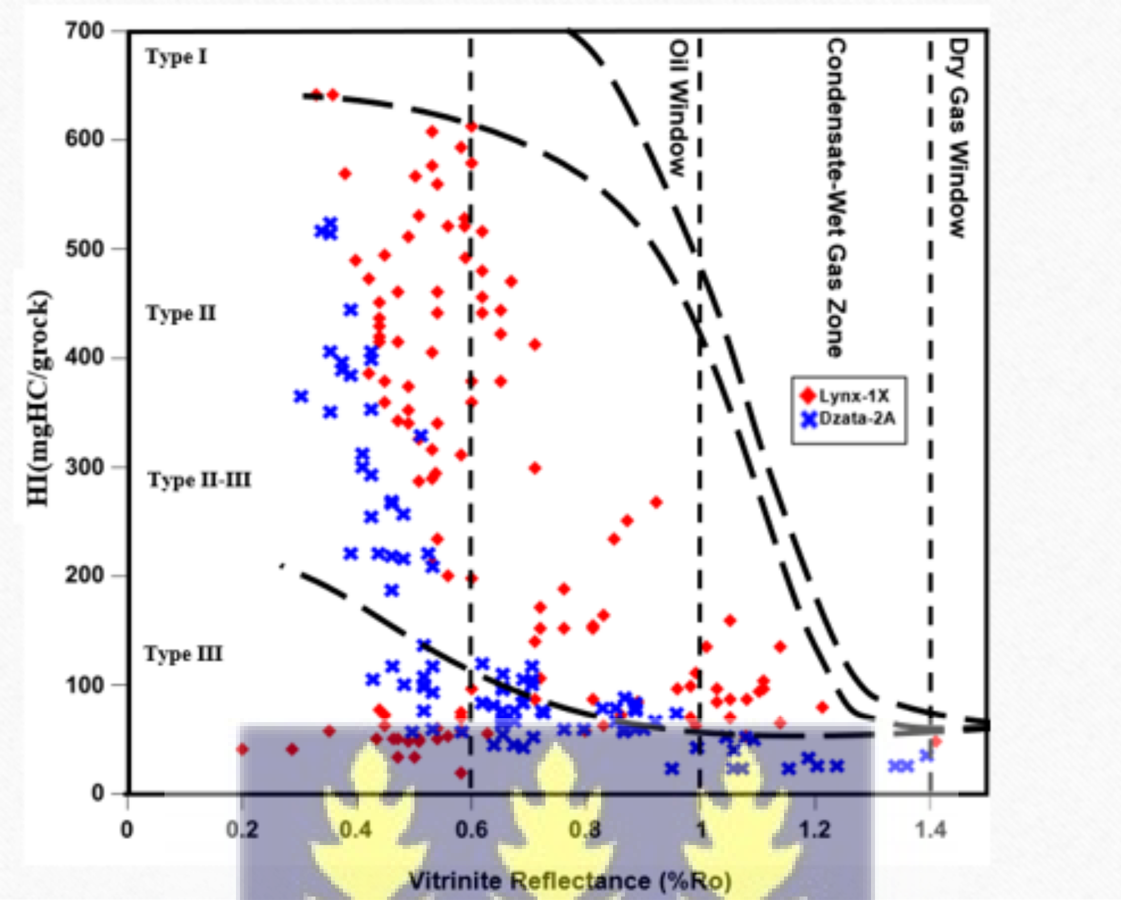

Figure 6.12: Vitrinite reflectance ($R_{calculated}$) versus the Hydrogen Index (HI) showing variation of organic matter quality from Lynx-1X and Dzata-2A wells.

6.3.4 Expulsion Potential

Peters et al., (2006) proposed that the maturity at which the Bituminous Index (BI) = S_1/TOC value begins to decline represents the start of an efficient oil window or indicate efficient oil expulsion. Lewan (1997) proposed that, the compounds generated in the early stages are presumed to be Bitumen or heavy crude oil which later forms lighter oils by partial decomposition at higher maturity. During maturity, S_2 is continuously decomposing, causing a decrease in S_2 and an increase in free Hydrocarbon (S_1) and further increasing BI. According to Hunt (2000), the Ocean Drilling Program used S_1/TOC of 1.5 to determine the presence of indigenous versus migrated or non-indigenous hydrocarbon levels.

S_1 versus Total Organic Carbon (TOC) plot indicates that, part of the source rock contains S_1 hydrocarbons for their given Total Organic Carbon (TOC) making them indigenous (Fig. 6.13), however, in this study very little part of the source rock shows non-indigenous and as such have been expelled from another source (Nady et al., 2014).

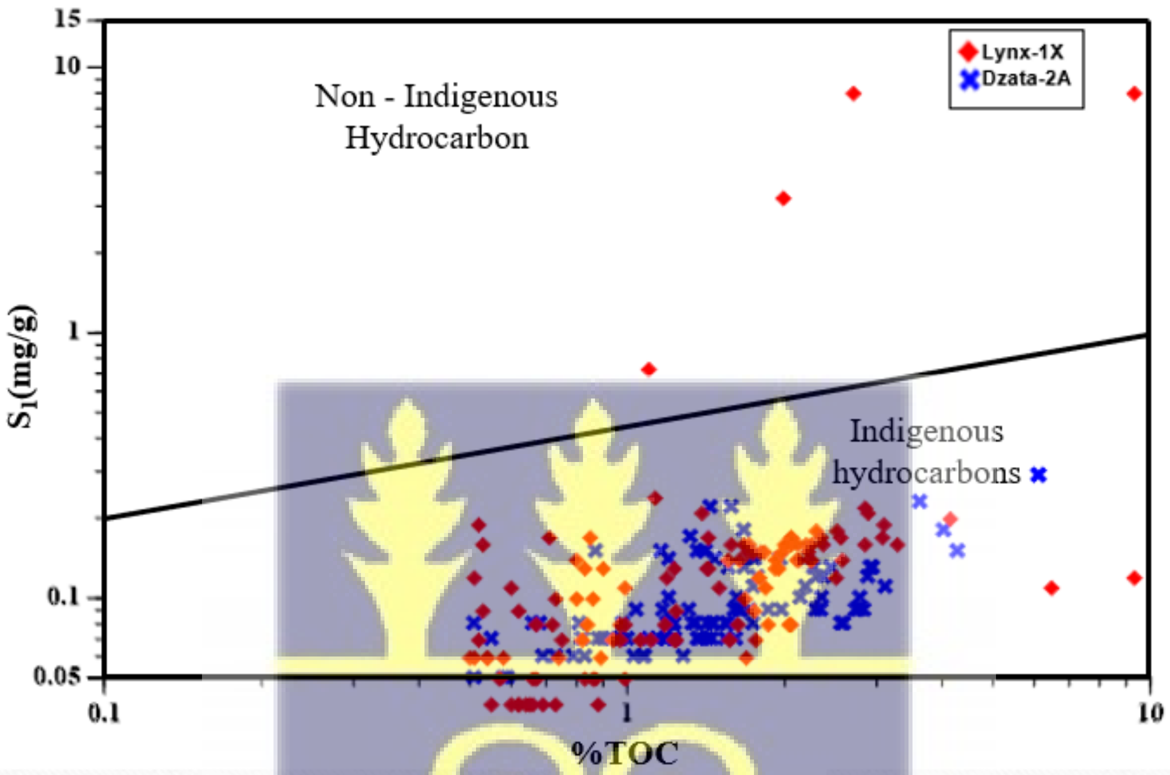

Figure 6.13: S_1 versus TOC as an indicator of indigenous and non-indigenous hydrocarbons

CHAPTER SEVEN

CONCLUSION

Analyzed samples from the Middle Cretaceous to Early Tertiary from three oil wells (Lynx-1X, Dzata-1 & Dzata-2A) in the Deepwater Cape Three Points, offshore Tano, Western Ghana are constituted by rich palynoflora (sporomorphs and dinoflagellate cysts). Based on the First Appearance Datum (FAD) and Last Appearance Datum (LAD) of stratigraphically significant species, four palynozones (PZ-I to PZ-IV) and nine subzones are proposed for the samples. These palynozones and subzones are;

PZ-I: *Afropollis jardinus-Sofrepites legouxae-Elaterocolpites castelaini* Assemblage Zone;

Subzone 1: *Afropollis jardinus-Elaterosporites klaszii* Interval Zone

Subzone 2: *Elaterocolpites castelaini* Interval Zone

Subzone 3: *Elateroplicites africaensis* Interval Zone

Subzone 4: *Galeocornea causea* Interval Zone

PZ-II: *Cretaceaeiporites polygonalis-C. scabratus-Dinogymnium accuminatum* Assemblage Zone

PZ-III: *Trichodinium castanea-Cerodinium diebelli-Dinogymnium acuminatum* Assemblage Zone;

Subzone 1: *Trichodinium castanea* Interval Zone

Subzone 2: *Dinogymnium acuminatum* Interval Zone

PZ-IV: *Cerodinium diebelli-Apectodinium homomorphum- Homotryblium tenuispinosum* Assemblage Zone;

Subzone 1: *Andalusiella polymorpha* Interval Zone

Subzone 2: *Homotryblium tenuispinosum* Interval Zone

Subzone 3: *Apectodinium homomorphum* Interval Zone

Ages proposed for the palynozones are based on similar stratigraphic significant taxa published and recovered by other workers from sediments from other parts of the northern and southern hemispheres which ranges from Albian-Eocene. Lynx-1X is dated from the Albian-Eocene, however Dzata-1 and Dzata-2A wells are dated as Albian-Maastrichtian age.

Distribution of palynomorphs enabled the identification of two major sedimentary facies which are the nearshore and open marine facies. The nearshore facies concentrated at deeper parts of wells are characterized by abundant sporomorphs and peridinoid dinocysts while the open marine facies are dominated by gonyaulacoid dinocysts and are restricted to the shallower parts of the wells. This occurred as a result of marine transgression which flooded the area causing marine sedimentation. The Albian-Cenomanian (PZ-I) sediments reflected arid/semi-arid environment due to the presence of *Classopollis* and Ephedroids. The abundance of peridinoids dinocysts (*Cerodinium*, *Andalusiella*, *Paleocystodinium*, *Phelodinium*) over the gonyaulacoid dinocysts (*Spiniferites*, *Glaphyrocysta*/*Areoligera*, *Cordosphaeridium*) at level 2800-2720m in Lynx-1X and moderate sporomorphs in the Maastrichtian connotes a nearshore/inner neritic environment. The open marine (middle-outer neritic) sediments are constituted by dominant gonyaulacoid dinocysts over peridinoid dinocysts and sporomorphs which is recognized in the Campanian-Maastrichtian of Dzata-1 and Dzata-2A wells and in the Campanian and Paleocene-Eocene of Lynx-1X well which was as a result of transgression in the area that provided conditions favorable for the development of dominant marine palynoflora. The sporomorphs diversity in the Campanian-Eocene sediments indicates variabilities in vegetational zones from mangrove (brackish) water to fresh water environment in a hot tropical climate.

The sporomorphs associations recovered from Lynx-1X, Dzata-1 and Dzata-2A exhibit similarity to Cretaceous Phytogeographic Provinces of African-South America (ASA).

Sporomorphs characteristic of Albian-Cenomanian Elaterate Province for the deeper intervals (PZ-I and II) and of the Senonian Palmae Province for the shallower intervals (PZ-III and IV) have been recognized for all the wells. The Campanian-Eocene peridineacean assemblage (*Cerodinium*, *Andalusiella*, *Paleocystodinium*, *Phelodinium*) has a lot of similarity with those of Malloy or Tropical/Subtropical suite of Lentin and Williams (1980).

Palynofacies analysis revealed Seven (7) palynofacies associations (PF-1 to PF-7) for Lynx-1X well. PF-1 reflects deposition in a fluvio-deltaic/nearshore environment under a marginal dysoxic-anoxic basin condition with sediments typical of kerogen type III-IV (gas prone). PF-2 is deposited under a proximal suboxic-anoxic shelf conditions in a marginal marine/nearshore environment and sediments classified as kerogen type II/III (gas prone). PF-3 suggest a deposition which took place in a marginal marine to shallow marine environment under distal suboxic-anoxic conditions and constituted by kerogen type II>I (highly oil prone). PF-4 is suggested to be deposited under a distal suboxic-anoxic basin condition in a shallow marine environment and sediments characterized by kerogen type II>I (highly oil prone). PF-5 indicates a deposition under a distal dysoxic-oxic shelf conditions in middle-outer neritic environment. PF-5 and sediments constituted by kerogen type II>I (oil prone). PF-6 suggests a deposition in a shelf to basin transition condition in an offshore, most likely from an inner-middle neritic environments and constituted by kerogen type III and II (oil prone). PF-7 supports an outer neritic environment under distal mud-dominated oxic shelf conditions and characterized by kerogen type II/III (gas prone).

In Dzata-1 well, five palynofacies associations (PT-1-PT-5) were recognized. PT-1 suggests a deposition in a nearshore environment under proximal suboxic-anoxic conditions and sediments typical of kerogen type II and III (oil prone). PT-2 indicates a deposition in a dysoxic-suboxic conditions in a nearshore environment and constituted by kerogen type III (gas prone). PT-3 must have been deposited under a marginal dysoxic-anoxic basin condition in a fluvio-deltaic/nearshore environment with kerogens typical of Type III (gas prone). PF-4 suggests an inner-middle neritic environment to an outer neritic environment under distal dysoxic-oxic shelf conditions and kerogens classified as kerogen type II>I (oil prone). In PT-5, a deposition of a nearshore environment under marginal dysoxic-anoxic basin conditions is inferred. It is characterized by kerogen type III (gas prone).

Analyzed samples from Dzata-2A well revealed six palynofacies associations (PT-A-PT-F). PT-A indicates a deposition in a nearshore to shallow marine (inner neritic) environment under a proximal suboxic-anoxic shelf condition with typical Type II/III kerogen (oil prone). PT-B infers an inner neritic/nearshore depositional environment under dysoxic-suboxic conditions with facies characterized by kerogen type III or II (gas prone). PT-C is deposited under a distal dysoxic-oxic shelf conditions in a nearshore/inner neritic to middle-outer neritic environment. This field is characterized by kerogen type II>I (oil prone). PT-D indicates a nearshore/inner neritic depositional environment under marginal dysoxic anoxic basin conditions and facies constituted by kerogen type III (gas prone). PT-E must have been deposited from inner-outer neritic environment under distal suboxic-anoxic basin condition. These facies are characterized by kerogen type II≥I (highly oil prone). PT-F suggests a deposition in a nearshore/shallow marine environment under a distal dysoxic-anoxic shelf environment with facies characterized by kerogen type II/III (oil prone).

Investigation of the hydrocarbon potential for Lynx-1X and Dzata-2A wells indicate that 70-80% of analyzed samples are good to very good potential source rock. However, greater than 50% of the samples have S_2 values less than 10 mg/g which suggest a good hydrocarbon potentiality for Lynx-1X and Dzata-2A wells. Therefore, the ?Turonian-Santonian age samples in the studied wells are considered as better potential source rocks than the Campanian-Eocene and Albian-Cenomanian source rocks.

Analyzed samples from Lynx-1X well in this study have HI values which ranges from 42-326 mg/g and OI values from 24-99 mg/g for the Paleocene-Eocene samples indicates no potential (kerogen type IV) to good source potential for generating oil and gas (type II, III) but mainly gas. The Campanian-Maastrichtian samples have HI values ranging from 197-641 mg/g and OI values from 13-35 mg/g with majority of the samples constituted by type II and III kerogen which reflects potential source for generating oil and gas. Samples analyzed from the ?Turonian-Santonian is represented by HI values (290-614 mg/g) and OI values (14-37 mg/g) where most of the samples belong to types II and III kerogen capable of generating oil and gas. HI values range from 20-471 mg/g and OI values range from 9-88 mg/g for the Albian-Cenomanian analyzed samples which reveals majority of samples are characterized by kerogen types II/III and III which is considered to generate oil and gas but mainly gas.

The Dzata-2A well has HI and OI values ranging from 188-449 mg/g and 15-43 mg/g respectively for the Campanian-Maastrichtian with most of the samples containing more type III than II kerogen which is a good source for generating more gas than oil. Analyzed samples from ?Turonian-Santonian has HI values ranging from 357-530 mg/g and OI values ranging from 14-23 mg/g which is characterized by type II kerogen and considered a good source potential for generating oil. In the Albian-Cenomanian samples, HI values of range (34-256 mg/g) and OI values ranging from 23-118 mg/g with majority of the samples constituted by kerogen type III which is a potential source capable of generating gas with few samples concentrating in kerogen type II/III which indicates potential for generating oil and gas but mainly gas.

Conducting maturity analyses on samples indicates that Lynx-1X and Dzata-2A are considered to have majority of the samples being immature with few being organically matured in both wells and are generally of low kerogen conversion. In this study very little part of the source rock shows non-indigenous and as such have been expelled from another source.

RECOMMENDATION

Complete well log data and seismic data can be incorporated into future research which will further validate palynological results for research and petroleum exploration purposes.

REFERENCES

Abbink, O. A., Van Konijnenburg-Van Cittert, J. H. A., and Visscher, H. (2004). A sporomorph ecogroup model for the Northwest European Jurassic-Lower Cretaceous: concepts and framework. *Netherlands Journal of Geosciences*, *83*(1), 17-31.

ABD EL Ghany, E. S. (1992). Palynological zonation of Abu Roash G member and the upper part of Baharyia Formation in bed well N°. 1-2, Western Desert, Egypt.

Abdel-Kireem, M. R., Schrank, E., Samir, A. M., and Ibrahim, M. I. A. (1996). Cretaceous palaeoecology, palaeogeography and palaeoclimatology of the northern Western Desert, Egypt. *Journal of African Earth Sciences*, *22*(1), 93-112.

Aboul Ela, N., & Mahrous, H. A. (1992). Albian-Cenomanian miospores from the subsurface of the north Western Desert, Egypt. *Neues Jahrbuch für Geologie und Paläontologie-Monatshefte*, 595-613.

Abubakar, M. B., Luterbacher, H. P., Ashraf, A. R., Ziedner, R., and Maigari, A. S. (2011). Late Cretaceous palynostratigraphy in the Gongola Basin (Upper Benue Trough, Nigeria). *Journal of African Earth Sciences*, *60*(1-2), 19-27.

Abubakar, M. B., Obaje, N. G., Luterbacher, H. P., Dike, E. F. C., and Ashraf, A. R. (2006). A report on the occurrence of Albian-Cenomanian elater-bearing pollen in Nasara-1 well, Upper Benue Trough, Nigeria: Biostratigraphic and palaeoclimatological implications. *Journal of African Earth Sciences*, *45*(3), 347-354.

Achaegakwo, C. A. and Atta-Peters, D. (2021). Palynofacies analysis and depositional environments of Upper Cretaceous sediments in the ST-9H well, offshore South Tano Basin, Western Ghana. *Geological Journal*.

Affaton, P. (1975). Etude géologique et structurale du Nord-Ouest Dahomey, du Nord Togo et du Sud-Est de la Haute-Volta. *Marseille, France, Laboratoire Sciences de la Terre (B) 10*, 201.

Affaton, P. (1990). Le bassin des Volta (Afrique de l'Ouest): une marge passive, d'âge protérozoïque supérieur, tectonisée au Panafrican (600 ± 50 Ma). *Editions ORSTOM, Collection Etudes et Thèses, Paris* (pp. 500).

Affaton, P. (2008, March). Litho-stratigraphy of the Volta basin and related structural units. In *The Voltaian Basin, Ghana. Workshop and Excursion Report* (pp. 13-17).

Affaton, P., Rahaman, M. A., Trompette, R., and Sougy, J. (1991). The Dahomeyide Orogen: tectonothermal evolution and relationships with the Volta Basin. In *The West African orogens and circum-Atlantic correlatives* (pp. 107-122). Springer, Berlin, Heidelberg.

Affaton, P., Sougy, J. and Trompette, R. (1980). The tectono-stratigraphic relationships between the upper Precambrian and lower Paleozoic Volta Basin and the pan-african Dahomeyide orogenic belt (West Africa). *American Journal of Science*, *280*(3), 224-248.

Alaug, A. S., Mahmoud, M. S., Deaf, A. S., and AL-Ameri, T. K. (2014). Palynofacies, organic geochemical analyses and hydrocarbon potential of some Upper Jurassic-Lower Cretaceous rocks, the Sabatayn-1 well, Central Yemen. *Arabian Journal of Geosciences*, *7*(6), 2515-2530.

Alberti, G. (1959). Zur Kenntnis der Gattung Deflandrea Eisenack (Dinoflag.) in der Kreide und im Alttertiär Nord-und Mitteldeutschlands. *Mitteilungen aus dem Geologischen Staatsinstitut in Hamburg*, *28*(9), 3-105.

Alberti, G. (1961). Zur Kenntnis mesozoischer und altterti‰ rer Dinoflagellaten und Hystrichosphaerideen von Nord-und Mitteldeutschland sowie einigen anderen europ‰ ischen Gebieten. *Palaeontographica Abteilung A*, 1-58.

Allen, P.A. and Allen, J.R. (1990). Basin Analysis: Principles and Application. Blackwell Sci. Pub., Oxford, London. p. 456.

Annual report on the petroleum funds (2018). Ministry of Finance, Ghana, (appendix 1).

Antolinez, H.J. (2006). Paleocene to Early Eocene Dinoflagellate Cyst Biostratigraphy in Southeast Nigeria and the Côte D'Ivoire-Ghana Transform Margin (ODP Site 959) (Unpublished M.S. thesis). University of Missouri-Rolla, U.S.A., p. 100.

Antolinez-Delgado, H and Oboh-Ikuenobe, F. E. (2007). New species of dinoflagellate cysts from the Paleocene of the Anambra basin, southeast Nigeria. *Palynology*, *31*(1), 53-62.

Antonescu, E. (1973). Quelques donn6es sur la palynologie du Lias sous facies de Gresten de Roumanie. In: A.F. Chlonova (Editor), Palynology of Mesophyte. *Proc. Int. Palynol. Conf., 3rd, Novosibirsk, 1971,* 53-57.

Apaalse, L. A., and Atta-Peters, D. (2013). Cretaceous-Palaeogene palynology of the Keta-1 well offshore Keta basin, southeastern Ghana.

Arai, M., Dias-Brito, D., Ponte, F., De Castro, J., Perinotto, J. A. and Bertini, R. J. (1994). Dinoflagelados do Cretaceo Superior (Turoniano-Maastrichtiano) da Bacia de Campos, Plataforma continental do sudeste brasileiro. *Simpósio sobre o Cretáceo do Brasil*, *3*(1994), 59-61.

Armstrong, H. A and Brasier, M. D. (2005). Microfossils, Oxford, Blackwell Publishing.

Atta-Peters, D and Salami, M. B. (2004a). Late Cretaceous to Early Tertiary pollen grains from Offshore Tano basin, southwestern Ghana. *Revista Española de Micropaleontología*, *36*(3), 451-465.

Atta-Peters, D and Salami, M. B. (2004b). Campanian-Paleocene dinoflagellate cyst Biostratigraphy from offshore sediments in the Tano Basin, southwestern Ghana. *Revista Española de Micropaleontología, 36*(2), 305-321.

Atta-Peters, D. (2013). Occurrences of elaterate pollen from the Lower Cretaceous of Ghana: Implications for biostratigraphy and palaeoclimatology. *International Letters of Natural Sciences*, *4*.

Atta-Peters, D and Achaegakwo, C. A. (2016). Palynofacies and palaeoenvironmental significance of the Albian-Cenomanian succession of the Epunsa-1 well, onshore Tano Basin, western Ghana. *Journal of African Earth Sciences*, *114*, 1-12.

Atta-Peters, D and Garrey, P. (2014). Source rock evaluation and hydrocarbon potential in the Tano basin, South Western Ghana, West Africa. *International journal of oil, gas and coal engineering*, *2*(5), 66-77.

Atta-Peters, D and Kyorku, N. A. (2013). Palynofacies analysis and sedimentary environment of Early Cretaceous sediments from Dixcove 4-2X well, Cape Three Points, offshore Tano Basin, western Ghana. *International Research Journal of Geology and Mining*, *3*(7), 270-281.

Atta-Peters, D and Salami, M. B. (2006). Aptian–Maastrichtian palynomorphs from the offshore Tano Basin, western Ghana. *Journal of African Earth Sciences*, *46*(4), 379-394.

Atta-Peters, D., Achaegakwo, C. A., Kwayisi, D and Garrey, P. (2015). Palynofacies and source rock potential of the ST-7H well, offshore Tano basin, Western Region, Ghana. *Earth Science*, *4*, 1-20.

Atta-Peters, D., Anan-Yorke, R and Anani, C. (2012). Devonian miospores from Atiavi-1 well in the keta basin, southeastern ghana. *Research Journal of Environmental and Earth Sciences*, *4*(12), 1052-1059.

Attoh, K. (1990). Dahomeyides of Southeastern Ghana: Evidence for oceanic closure and crustal imbrication in a Pan-African orogen. *Publication occasionnelle-Centre international pour la formation et les échanges géologiques*, (22), 159-164.

Attoh, K and Nude, P. M. (2008). Tectonic significance of carbonatite and ultrahigh-pressure rocks in the Pan-African Dahomeyide suture zone, southeastern Ghana. *Geological Society, London, Special Publications*, *297*(1), 217-231.

Attoh, K., Dallmeyer, R. D and Affaton, P. (1997). Chronology of nappe assembly in the Pan-African Dahomeyide orogen, West Africa: evidence from 40Ar39Ar mineral ages. *Precambrian research*, *82*(1-2), 153-171.

Awad, W. K and Oboh-Ikuenobe, F. E. (2016). Early Paleogene dinoflagellate cysts from ODP Hole 959D, Côte d'Ivoire-Ghana Transform Margin, West Africa: new species, biostratigraphy and paleoenvironmental implications. *Journal of African Earth Sciences*, *123*, 123-144.

Babinot, J. F., Michaud, L and Flicoteaux-Dupin, F. (1988). Etude micropaléontologique (Ostracodes, palynoflores), et sédimentologiques du Crétacé supérieur des forages de Djifère et Nema-Ding (Sénégal). *Bulletin des centres de recherches exploration-Production Elf-Aquitaine*, *12*(1), 143-163.

Bacon, C. A., Calver, C. R., Boreham, C. J., Leaman, D. E., Morrison, K. C., Revill, A. T and Volkman, J. K. (2000). The petroleum potential of onshore Tasmania: a review. *Geol Surv Bull*, *71*, 1-93.

Balch, W. M., Reid, P. C and Surrey-Gent, S. C. (1983). Spatial and temporal variability of dinoflagellate cyst abundance in a tidal estuary. *Canadian Journal of Fisheries and Aquatic Sciences*, *40*(S1), s244-s261.

Balteş, N. (1973). Catalogue of Fossil Dinoflagellates, Hystorichospheres and Related Microfossils. 1. Dinoflagellates-2nd Supplement: A. Eisenack and Göran Kjellström. Schweizerbart, Stuttgart, 1971, 215 pp., 104 illus., DM. 38.-.

Bankole, S. I., Schrank, E and Erdtmann, B. D. (2007). Palynology of the Paleogene Oshosun formation in the Dahomey Basin, southwestern Nigeria. *Revista española de micropaleontología*, *39*(1), 29-44.

Barnard, P. C., PC, B and BS, C. (1981). Oils and source rocks of the North Sea area.

Barss, M. S., Bujak, J. P and Williams, G. L. (1979). Palynological zonation and correlation of sixty-seven wells, eastern Canada.

Batten, D. J. (1996). Palynofacies and palaeoenvironmental interpretation. *Palynology: principles and applications*, *3*, 1011-1064.

Batten, D. J. (1973). Use of palynological assemblage-types in Wealden correlation. *Palaeontology*, 16, 1-40.

Batten, D. J. (1982a). Palynofacies and salinity in the Purbeck and Wealden of southern England. In Aspects of micropalaeontology (pp. 278-308). Springer, Dordrecht.

Batten, D. J. (1982b). Palynofacies, palaeoenvironments and petroleum. *Journal of Micropalaeontology, 1*(1), 107-114.

Batten, D. J. (1983). Identification of amorphous sedimentary organic matter by transmitted light microscopy. *Geological Society, London, Special Publications*, *12*(1), 275-287.

Batten, D. J and Marshall, K. L. (1991). Palynology of Upper Cretaceous Black Shales from Helgoland, Southern North Sea. *Geologisches Jahrbuch. Reihe A, Allgemeine und regionale Geologie BR Deutschland und Nachbargebiete, Tektonik, Stratigraphie, Paläontologie*, (120), 105-115.

Batten, D. J and Stead, D. T. (2005). Palynofacies analysis and its stratigraphic application. In Applied stratigraphy (pp. 203-226). Springer, Dordrecht.

Batten, D. J and Uwins, P. J. R. (1985). Early-Late Cretaceous (Aptian-Cenomanian) palynomorphs. *Journal of Micropalaeontology*, *4*(1), 151-167.

Begouen, V. (1993). The dinoflagellate cysts of the Late Cretaceous of the Sub-Pyrennes Zone, (France). Biostratigraphy, facies analyses and cladistic approach of the Peridinales. *Strata, 19* (2), 1-257.

Beilstein, U. (1994). Microflora, (sporomorphs, dinoflagellates), from the regressive Upper Cretaceous of Benue-Trough, Nigeria. Geologisches Institut der Universitaet zu Koeln Sonderveroeffentlichungen (Vol. 95, pp. 305).

Benedek, P. N. (1972). Phytoplanktonten aus dem Mittel-und Oberoligozän von Tönisberg (Niederrheingebiet): Phytoplanktons from the middle and upper oligocene of Tönisberg (Lower Rhine Area) (Doctoral dissertation, Schweizerbart).

Benedek, P. N and Sarjeant, W. A. S. (1981). Dinoflagellate cysts from the Middle and Upper Oligocene of Tonisberg (Niederrheingebiet): a morphological and taxonomic restudy. *Nova Hedwigia: Zeitschrift fur Kryptogamenkunde*.

Benson, D. G. (1976). Dinoflagellate taxonomy and biostratigraphy at the Cretaceous-Tertiary boundary, Round Bay, Maryland. Tulane Stud. *Geol. Paleontol., 12*, 169-233.

Benson, J. M. (1990). Palynofacies characteristics and palynological source rock assessment of the Cretaceous sediments of the northern Orange Basin (Kudu 9A-2 and 9A-3 boreholes). *Communications of the Geological Survey of Namibia*, *6*, 31-39.

Bettar, I and Meon, H. (2006). La palynoflore continentale de l'Albien du bassin d'Agadir-Essaouira (Maroc). *Revue de Paléobiologie, 25*(2), 593.

Beurlen, G and Regali, M. D. S. P. (1987). O Cretáceo da plataforma continental do Maranhão e Pará, Brasil: bioestratigrafia e evolucão paleoambiental. *Bol. Geoc. Petrobras*, *1*(2), 135-155.

Boltenhagen, E. (1977). Upper Cretaceous microplankton of Gabon.

Boltenhagen, E. (1980). Palynology of the Upper Cretaceous of Gabon. *Comite Des Travaux Historiques et Scientifiqiues. Mem Sect Sci*, *7*, 1-191.

Boltenhagen, E. (1975). Quelques spores du Crétacé supérieur du Gabon. *Revue de Micropaléontologie*, *18*(2), 69-90.

Bornemann, A., Pross, J., Reichelt, K., Herrle, J. O., Hemleben, C., and Mutterlose, J. (2005). Reconstruction of short-term palaeoceanographic changes during the formation of the Late Albian 'Niveau Breistroffer'black shales (Oceanic Anoxic Event 1d, SE France). *Journal of the Geological Society*, *162*(4), 623-639.

Bostick, N. H. (1971). Thermal alteration of clastic organic particles as an indicator of contact and burial metamorphism in sedimentary rocks. *Geoscience and Man*, *3*(1), 83-92.

Boulter, M. C and Manum, S. B. (1989). The Brito-Arctic igneous province flora around the Paleocene/Eocene boundary. In *Proceedings of the Ocean Drilling Program, Scientific Results* (Vol. 104, pp. 663-680).

Boulter, M. C and Riddick, A. (1986). Classification and analysis of palynodebris from the Palaeocene sediments of the Forties Field. *Sedimentology*, *33*(6), 871-886.

Bozhko, N. A. (1969). Stratigraphy and tectonics of the Voltaian Basin. *Annates: Faculté de Sciences Université de Clermont-Ferrand*, *41*(19), 3-4.

Brenner, G. J. (1976). Middle Cretaceous floral provinces and migrations of angiosperms. *Origin and evolution of angiosperms, Columbia University. Press, New York*, 23-47.

Brenner, G. J. (1968). Middle Cretaceous spores and pollen from northeastern Peru. *Pollen and Spores*, *10*, 341-383.

Brideaux, W. W., WW, B and MJ, F. (1976). Upper Jurassic-Lower Cretaceous dinoflagellate assemblages from Arctic Canada.

Brinkhuis, H and Zachariasse, W. J. (1988). Dinoflagellate cysts, sea level changes and planktonic foraminifers across the Cretaceous-Tertiary boundary at El Haria, northwest Tunisia. *Marine Micropaleontology*, *13*(2), 153-191.

Brinkhuis, H. (1994). Late Eocene to Early Oligocene dinoflagellate cysts from the Priabonian type-area (Northeast Italy): biostratigraphy and paleoenvironmental interpretation. *Palaeogeography, palaeoclimatology, palaeoecology*, *107*(1-2), 121-163.

Brinkhuis, H., Klinkenberg, E., Williams, G. L and Fensome, R. A. (2000). Two unusual new dinoflagellate cyst genera from the Bunde Borehole, Maastrichtian type area, southern Netherlands. *Review of Palaeobotany and Palynology*, *110*(1-2), 93-110.

Brinkhuis, H., Romein, A.J.T., Smit, J., Zachariasse, W.J. (1994). Danian-Selandian dinoflagellate cysts from lower latitudes with special reference to the El Kef section, NW Tunisia. *GFF 116*, 46-48.

Brown, S and Downie, C. (1984). Dinoflagellate cyst biostratigraphy of Late Paleocene and Early Eocene sediments from Holes 551, 552, 553A and 555; Leg 81, Deep Sea Drilling Project (Rockall Plateau). *Deep Sea Drilling Project, Washington, Initial Reports, (U.S. Gov't Print. Office) 81*, 565- 579.

Brownfield, M. E and Charpentier, R. R. (2006). *Geology and total petroleum systems of the west-central coastal province (7203), West Africa* (No. 2207-B). US Geological Survey.

Bujak, J. P and Williams, G. L. (1979). Dinoflagellate diversity through time. *Marine Micropaleontology*, *4*, 1-12.

Bujak, J. P., Brinkhuis, H. E. N. K and Aubry, M. P. (1998). Global warming and dinocyst changes across the Paleocene/Eocene Epoch boundary. *Late Paleocene-early Eocene climatic and biotic events in the marine and terrestrial records*, 277-295.

Bujak, J and Mudge, D. (1994). A high-resolution North Sea Eocene dinocyst zonation. *Journal of the Geological Society*, *151*(3), 449-462.

Bujak, J. P and Williams, G. L. (1977). Jurassic palynostratigraphy of offshore eastern Canada. In *Developments in Palaeontology and Stratigraphy 6*, 321-339.

Bujak, J.P., Barss, M.S., Williams, G.L. (1977). Offshore east Canada's organic type and color and hydrocarbon potential. *The Oil and Gas Journal, 75*, 198-201.

Bujak, J.P., Downie, C., Eaton, G.L and Williams, G.L. (1980). Dinoflagellate cysts and acritarchs from the Eocene of Southern England. *Special Papers in Palaeontology 24*, 1-100.

Burger, D. (1965). Palynology of uppermost Jurassic and lowermost Cretaceous strata in the eastern Netherlands. *Leidse geologische mededelingen*, *35*(1), 209-276.

Burger, D. (1980). Palynology of the Lower Cretaceous of the Surat Basin. *Bureau of Mineral Resources, Geology and Geophysics Australia, Bulletin, 189*, 106.

Cane, R. F. (1976). The origin and formation of oil shale. In *Developments in Petroleum Science* (Vol. 5, pp. 27-60). Elsevier.

Caro, Y., Luterbacher, H., Sanfilippo, A., Riedel, W. R., Premoli-Silva, I and Perch-Neilsen, K. (1975). Oceanic microfossils of the Upper Paleocene and Lower Eocene as an aid to zonation. *Bulletin de la Societe Geologique de France, 7*, 125-147.

Caro, Y. 1973. Contribution a la connaissance des dinoflagellis du Paliochne-Eochne infirieur des Pyrinies espagnoles. *Revista Española de Micropaleontología, 5*, 329-372.

Carvalho, M.A., Ramos, R.R.C., Crud, M.B., Witovisk, L., Kellner, A.W.A., Silva, de P., Grillo, H., Riff, O.N., Romano, D., P.S.R. (2013). Palynofacies as indicators of palaeoenvironmental changes in a cretaceous succession from the larsen basin, james ross island, Antarctica. *Sediment. Geol. 295*, 53-66.

Carvalho, I.S and Pedrão, E. (1998). Brazilian theropods from the Equatorial Atlantic margin: behavior and environmental setting. *Revista Gaia 15*, 369-378.

Chiaghanam, O. I., Chiadikobi, K. C., Ikegwuonu, O. N., Omoboriowo, A. O., Onyemesili, O. C and Acra, E. J. (2013). Palynofacies and kerogen analysis of upper cretaceous (early campanian to Maastrichtian) Enugu shale and Mamu Formation in Anambra basin, south-eastern Nigeria. *International Journal of scientific & technology Research*, *2*(8), 87-97.

Christopher, R. A., Goodman, D. K., Jansonius, J and McGregor, D. C. (1996). Introduction to biostratigraphy and time scales. *Palynology: Principles and Applications. American Association of Stratigraphic Palynologists Foundation*, *2*, 463-492.

Clarke, R. F. A and Verdier, J.-P. (1967). An investigation of microplankton assemblages from the chalk of the Isle of Wight, England. *Verhandelingen der Koninklijke Nederlandse Akademie van Wetenschappen, Afdeeling Natuurkunde, Eerste Reeks, 24*, 1-96.

Cole, J. M., Abdelrahim, O. B., Hunter, A. W., Schrank, E and Ismail, M. S. B. (2017). Late Cretaceous spore-pollen zonation of the Central African Rift System (CARS), Kaikang Trough, Muglad Basin, South Sudan: angiosperm spread and links to the Elaterates Province. *Palynology*, *41*(4), 547-578.

Combaz, A. (1964). Les palynofaciès. *Rev Micropaléont 7*(4), 205-218.

Concheyro, G., Carames, A. A., Rodriguez Amenabar, C., & Lescano, M. A. (2014). Nannofossils, foraminifera and microforaminiferal linings in the Cenozoic diamictites of Cape Lamb, Vega Island, Antarctica.

Cookson, I. C. (1947). Plant microfossils from the lignites of the Kerguelen Archipelago. *BANZ Antarctic Research Expedition, 1929-1931, Reports, Series A*, *2*, 129-142.

Cookson, I. C., Eisenack, A. (1970). Cretaceous microplankton from the Eucla Basin, Western Australia. *Proceedings of the Royal Society of Victoria, 83*, 137-157.

Cookson, I.C. (1956). Additional microplankton from Australian Late Mesozoic and Tertiary sediments. *Austr. Jour. Marine and Freshwater Research 7*, 183-191.

Cookson, I.C. and Eisenack, A. (1967). Some microplankton from the Paleocene Rivernook Bed, Victoria. *Proc. Roy. Soc. of Victoria, 80*(2), 247-257.

Cookson, I.C. and Eisenack, A. (1968). Microplankton from two samples from Gingin Brook No. 4 Borehole, Western Australia. *Journ. of the Royal Soc. of Western Australia, 51*, 110-122.

Cookson, I. C. (1965). Cretaceous and Tertiary microplankton from south-eastern Australia. *Proceedings of the Royal Society of Victoria*, *78*(1), 85-93.

Copestake, P. (1993). Application of micropalaeontology to hydrocarbon exploration in the North Sea Basin. In *Applied Micropalaeontology* (pp. 93-152). Springer, Dordrecht.

Cordani, U. G., D'Agrella-Filho, M. S., Brito-Neves, B. D and Trindade, R. I. F. (2003). Tearing up Rodinia: the Neoproterozoic palaeogeography of South American cratonic fragments. *Terra Nova*, *15*(5), 350-359.

Costa, L.I. and Davey, R.J. (1999). Dinoflagellate cysts from the Cretaceous System. In: Powell, A.J. (Ed.), A Stratigraphic Index of Dinoflagellate Cysts. *British Micropaleontolological Society Publication Series/Kluwer Academic Publishers*, 99-154.

Costa, L.I., Manum, S.B and Meyer, K.-J. (1988). The regional distribution of dinoflagellates; correlation of the interregional zonation with the local zones and with the regional lithostratigraphy. Great Britain-Norway, the Viking Graben. In: Vinken, R. (Ed) *The Northwest European Tertiary Basin. Results of the International*

Geological Correlation Programme, *Project No 124. Geologisches Jahrbuch*, *Reihe A*, *Heft 100*, 330-332.

Costa, L.I. and Davey, R.J. (1992). "Dinoflagellate cysts of the Cretaceous System". In A stratigraphic index of dinoflagellate cysts, *British Micropalaeontological Society Publication Series Edited by*: Powell, A. J. 99-153. London: Chapman and Hall.

Couper, R.A. (1953). Upper Mesozoic and Cainozoic spores and pollen grains from New Zealand. *Bull. N.Z. Geol. Surv. Palaeontol., 22*, 1-77.

Couper, R.A. (1958). British Mesozoic microspores and pollen grains, a systematic and stratigraphic study. *Palaeontographica B, 103*, 75-179.

Cox, L.R. (1952). Cretaceous and Eocene fossils from the Gold Coast. Gold Coast Geological Survey 17, 68.

Crame, J. A., Pirrie, D., Riding, J. B and Thomson, M. R. A. (1991). Campanian–Maastrichtian (Cretaceous) stratigraphy of the James Ross Island area, Antarctica. *Journal of the Geological Society*, *148*(6), 1125-1140.

Crouch, E.M. (2001). Environmental Change at the Time of the Paleocene-Eocene Biotic Turnover (PhD thesis) LPP Contributions Series, 14. Utrecht University, p. 216.

Crouch, E.M and Brinkhuis, H. (2005). Environmental change across the Paleocene-Eocene transition from eastern New Zealand: a marine palynological approach. *Mar. Micropaleontol. 56*, 138-160.

Crouch, E.M., Brinkhuis, H., Visscher, H., Adatte, T. and Bolle, M.P. (2003). Late Paleocene early Eocene dinoflagellate cyst records from the Tethys: further observations on the global distribution of Apectodinium. *Geol. Soc. Am. Spec. Pap. 369*, 113-131.

Crouch, E.M., Bujak, J.P., Brinkhuis, H. (2000). Southern and Northern Hemisphere dinoflagellate cyst assemblage changes in association with the late Paleocene thermal maximum. *Geol. Foren. Stockh. Forh. 122* (1), 40-41.

Crouch, E.M., Willumsen, P.S., Kulhanek, D.K. and Gibbs, S.J. (2014). A revised Paleocene (Teurian) dinoflagellate cyst zonation from eastern New Zealand. *Rev. Palaeobot. Palynol. 202*, 47-79.

Daemon, R.F. (1975). Contribuição à datação da Formação Alter do Chão, Bacia do Amazonas. *Rev Bras Geoci 5*, 78-84.

Dailey, P., Goh, K., Henderson, T., Hudgens, E., Kanschat, K., Lowry, P., Maxted, B. (unpublished). Exploration of the Tano Basin & discovery of the Jubilee Field, Ghana: A new deepwater hydrocarbon play in the transform margin of West Africa, Kosmos Energy, Dallas, Tx.

Dale, B. (1983). Dinoflagellate resting cysts: "benthic plankton". In: Fryxell, G.A. (Ed.), Survival Strategies of the Algae. *Cambridge Univ. Press, Cambridge,* 69-136.

Davey R. J and Verdier J. P. (1973). An investigation of microplankton assemblages from latest Albian (Vraconian) sediments. *Revista Espanola de Micropaleontologia 5*, 173.

Davey, R.J (1969). Non-calcareous microplankton from the Cenomanian of England, northern France and North America, Part I. *Bulletin of the British Museum (Natural History) Geology*, *17*, 103-180.

Davey, R. J. (1970). Non-calcareous microplankton from the Cenomanian of England, northern France and North America Part II. *Bull. British Mus. (Nat. Hist.), Geol.*, 18, 333-397.

Davey, R. J and Williams, G. L. (1966a). The genus Hystrichosphaeridium and its allies. In Davey, R.J., Downie, C., Sarjeant, W.A.S., and Williams, G.L., Studies on Mesozoic and Cainozoic dinoflagellate cysts. *Bull. Brit. Mus. Nat. Hist. (Geol.), Suppl. 3*, 53-106.

Davey, R.J and Williams, G.L. (1966b). The genera Hystrichosphaera and Achomosphaera. In: Davey, R.J., Downie, C., Sarjeant, W.A.S., Williams, G.L. (Eds.), Studies on Mesozoic and Cainozoic Dinoflagellate Cysts, *British Museum (Natural History) Geology, Bull, vol. 3*, 28-52.

Davey, R. J., Williams, G. L., Downie, C and Sarjeant, W. A. S. (1966). The genus Hystrichosphaeridium and its allies. *Studies on Mesozoic and Cainozoic dinoflagellate cysts*, *3*, 53-106.

Davey, R.J. (1969). Some dinoflagellate cysts from the Upper Cretaceous of northern Natal, South Africa. *Palaeontologia Africana*, *12*, 1-23.

Davey, R.J. (1975). A dinoflagellate cyst assemblage from the Late Cretaceous of Ghana. *Proceedings of the 5th West African Colloquium on Micropaleontology, 7*(3), 149-173.

Davey, R.J and Rogers, J. (1975). Palynomorph distribution in recent offshore sediments along two traverses off Southwest Africa. *Mar. Geol. 18*, 213-225.

Davey, R.J., Duxbury, S., Riley, L.A., Fisher, M.J and Denison, C.N. (1977). Stratigraphic range charts, diagnostic dinocysts, Cretaceous. In: Thusu B (Ed), *International Palynological Colloquium*, Distribution of Biostratigraphically Diagnostic Dinoflagellate Cysts and Miospores From Northwest European Continental Shelf and Adjacent Areas. *Continental Shelf Institute*: 17-21.

Davies, D. W. (1986). The Geology and Tectonic Framework of the Republic of Ghana and the Petroleum Geology of the Tano Basin, Southwestern Ghana. Unpublished consultancy report prepared for Petro-Canada International Corporation on behalf of GNPC. p. 24.

Davies, E. H. (1985). The miospore and dinoflagellate cyst Oppel-zonation of the Lias of Portugal. *Palynology*, *9*(1), 105-132.

Davies, E. H and Poulton, T. P. (1986). Upper Jurassic dinoflagellate cysts from strata of northeastern British Columbia. *Current Research, Part B*, 519-537.

Davies, R. W., Linton, L. R and Wrona, F. J. (1982). Passive dispersal of four species of freshwater leeches (Hirudinoidea) by ducks. *Freshwater Invertebrate Biology*, 40- 44.

De Coninck, J. (1977). Organic walled microfossils from the Eocene of the Woensdrecht borehole, southern Netherlands. Mededelingen Rijks Geol. *Dienst, Nieuwe Serie, 28*, 34-63.

de Lima, M.R and Boltenhagen,E. (1981). Comparative study of the evolution of African and South American microfloras. Ii. Upper Cretaceous. Congreso Latinoamericano de Paleontologia, (Porto Alegre),2nd, Anais. 373- 383.

de Lima, M.R and PedrJo, E. (1989). Palynological analysis of the Cretaceous sediments of the Cabo Basin, Pernambuco Stata, Brazil Anais da Academia Brasileira de Ci€ncias. 73-84.

de Lima, M.R. (1978). Palynology of the Santana Formation, (Cretaceous from northeast of Brazil) 1. Geological introduction and systematical descriptions of the spores from the Subtruma Azonotriletes. Ameghiniana. 333-365.

De Vernal, A and Giroux, L. (1991). Distribution of organic-walled microfossils in Recent sediments from the Estuary and Gulf of St. Lawrence: some aspects of the organic matter fluxes. *Canadian Journal of Fisheries and Aquatic Sciences, Special Publication, 113*, 189-199.

Deaf, A.S. (2009). Palynology, Palynofacies and Hydrocarbon Potential of the Cretaceous Rocks of Northern Egypt. *Publ. PhD thesis Uni, Southampton*, 348.

Deaf, A.S., Harding, I.C., Marshall, J.E.A. (2014). Cretaceous (Albian? early Santonian) palynology and stratigraphy of the Abu Tunis 1x borehole, northern Western Desert, Egypt. *Palynology 38*, 51-77.

Deflandre, G. (1935). Biological considerations of the microorganisms of planktonic origin preserved in Flint from Chalk. *Bulletin biologique de la France et de la Belgique 69,* 213-244.

Deflandre, G. (1937). Microfossils from Cretaceous Flints. Second Part. *Annales de Pal©ontologie, 26*, 51-103.

Deflandre, G and Cookson, I.C. (1955). Fossil microplankton from Australian late Mesozoic and tertiary sediments. *Aust. J. Mar. Freshw. Res. 6*, 242-313.

Digbehi, B. Z., Yao, K. R., Tea, Y. J. and Boblai, G. (1996). Contribution à l'étude palynologique et paléoenvironnementale du Campanien et du Maastrichtien du bassin offshore de Côte d'Ivoire. *Géologie méditerranéenne*, *23*(2), 155-171.

Dill, H.G., Kжthe, A., Gramann, F and Botz, R. (1996). A palaeoenvironmental and palaeoecological analysis of fine-grained Paleogene estuarine deposits of North Germany. *Palaeogeography, Palaeoclimatology, Palaeoecology, 124*(3), 273-326.

Dino, R., Pocknall, D.T and Dettman, M.E. (1999). Morphology and ultrastructure of elater-bearing pollen from the Albian to Cenomanian of Brazil and Ecuador: implications for botanical affinity. *Rev. Palaeobot. Palyno. 105*, 201-235.

Doukaga, M. (1980). Etude palynologique dans le Crétacé moyen du bassin sedimentaire du Gabon. *Lille, France: Université des Sciences et Technologies de Lille*, 174.

Dow, W. G and Pearson, D. B. (1975). Organic matter in Gulf coast sediments. Paper presented at Offshore Technology Conference, Dallas, 1975.

Downie, C., Hussain, M.A and Williams, G.L. (1971). Dinoflagellate cyst and the acritarch associations in the Paleogene of southeast England. *Geoscience and Man 3*, 29-35.

Doyle, J.A., Jardine, S and Doerenkamp, A. (1982). Afropollis, a new genus of early angiosperm pollen, with notes on the Cretaceous palynostratigraphy and paleoenvironments of northern Gondwana. *Bull. Centres Recher. Explor. Prod. Elf Aquitaine 6*, 39-117.

Drugg, W. S. (1970). Two new Neogene species of Tuberculodinium and one of Xenicodinium (Pyrrhophyta). *Proceedings of the Biological Society of Washington*, *83*, 115-122.

Drugg, W.S. (1967). Palynology of the Upper Moreno Formation (Late Cretaceous-Paleocene) Escarpado Canyon, California. *Pal¤eontographica Abteilung B, 120*, 1-71.

Duclaux, V., Clanet, C and Quéré, D. (2006). The effects of gravity on the capillary instability in tubes. *Journal of Fluid Mechanics*, *556*, 217-226.

Duringer, P and Doubinger, J. (1985). La palynologie: un outil de caractérisation des faciès marins et continentaux à la limite Muschelkalk supérieur-Lettenkohle. Palynology: a means of characterising marine and continental facies at the Upper Muschelkalk-Lettenkohle boundary. *Sciences Géologiques, bulletins et mémoires*, *38*(1), 19-34.

Duxbury, S. (1980). Barremian phytoplankton from Speeton, east Yorkshire. *Palaeontographica Abteilung B Paläophytologie*, *173*(4-6), 107-146.

Dybkjær, K. (1991). Palynological zonation and palynofacies investigation of the Fjerritslev Formation (Lower Jurassic-basal Middle Jurassic) in the Danish Subbasin. *Danmarks Geologiske Undersøgelse Serie A*, *30*, 1-150.

Eaton, G.L., 1976. Dinoflagellate Cysts from the Bracklesham Beds (Eocene) of the Isle of Wight, Southern England. In: *British Museum (Natural History) Geology. Bull. (Arch. Am. Art) 26*, 227-332.

Edet, J. J. (1992). Palynostratigraphy of Late Cretaceous (late Campanian-early Maastrichtian) sections in the Anambra Basin, Nigeria. *Revista Española de Micropaleontología*, *24*(2), 3-18.

Edet, J. J and Nyong, E. E. 1994. Palynostratigraphy of the Nporo Shale exposures (Late Campanian-Maastrichtian) on the Calabar Flank, S. E. Nigeria. *Review of Paleobotany and Palynology, 80*, 131-147.

Edwards, D. (1996). New insights into early land ecosystems: a glimpse of a Lilliputian world. *Review of Palaeobotany and Palynology*, *90*(3-4), 159-174.

Edwards, L. E. (2001). Dinocyst biostratigraphy of Tertiary sediments from five cores from Screven and Burke Counties, Georgia. Geology and paleontology of five cores from Screven and Burke counties, eastern Georgia. *US Geological Survey Professional Paper*, *1603*, G1-G25.

Edwards, L.E. (1980). Dinoflagellates and the Eocene-Oligocene boundary in Alabama and Mississippi. American Association of Stratigraphic Palynologists, *13th Annual Meeting, Program and Abstracts P*.

Egger, H., Fenner, J., Heilmann-Clausen, C., Rogl, F., Sachsenhofer, R. F., Schmitz, B and Wing, S. L. (2003). Paleoproductivity of the northwestern Tethyan margin (Anthering section, Austria) across the Paleocene-Eocene transition. Special Papers-*Geological Society of America*, 133-146.

Eisenack, A. (1963). Sind die Hystrichosphären Zysten von Dinoflagellaten?. *Neues Jahrbuch für Geologie und Paläontologie Monatschefte*, *1963*, 225-231.

Eisenlohr, B. N and Hirdes, W. (1992). The structural development of the early Proterozoic Birimian and Tarkwaian rocks of southwest Ghana, West Africa. *Journal of African Earth Sciences (and the Middle East)*, *14*(3), 313-325.

El Beialy, S. Y. (1988). Palynostratigraphy of late Tertiary sediments in Kafr El-Dawar Well N. 1, Nile Delta, Egypt. *Revue de Micropaléontologie*, *30*(4), 249-260.

El Beialy, S. Y. (1993). Aptian to Cenomanian palynomorphs from the Qarun 2-1 borehole, Western Desert, Egypt.

El Beialy, S. Y (1994). Palynological evidence for the age and depositional environment of the Cretaceous Bahariya Formation, Northwestern Desert, Egypt. Indications palynologiques pour l'âge et l'environnement sédimentaire de la formation crétacée de Bahariya, Désert Nord-Ouest, Egypte. *Sciences Géologiques, bulletins et mémoires*, *47*(1), 51-65.

El Beialy, S. Y. (1995). Campanian-Maastrichtian palynomorphs from the Duwi (Phosphate) Formation of the Hamrawein and Umm El Hueitat mines, Red Sea Coast, Egypt. *Review of Palaeobotany and Palynology*, *85*(3-4), 303-317.

El Beialy, S. Y., Ayyad, S. N and Kholeif, S. E. (1990). Mesozoic-Tertiary palynomorphs and planktonic foraminifera of the subsurface section of the Sindy-1 well, eastern Nile Delta, Egypt. *Newsletters on Stratigraphy*, 71-85.

El Beialy, S. Y., El Atfy, H. S., Khoriby, E. M., El Khoriby, E. M and Abu-Zied, R. H. (2008). Palynostratigraphy, palynofacies, and the source rock evaluation of the Cenomanian Bahariya Formation, GPTSW-7 Well, north Western Desert, Egypt. *Journal of environmental Sciences*, *36*, 63-88.

El Beialy, S. Y., El Atfy, H. S., Zavada, M. S., El Khoriby, E. M and Abu-Zied, R. H. (2010). Palynological, palynofacies, paleoenvironmental and organic geochemical studies on the Upper Cretaceous succession of the GPTSW-7 well, North Western Desert, Egypt. *Marine and Petroleum Geology*, *27*(2), 370-385.

El Beialy, S., El-Soughier, M., Mohsen, S. A and El Atfy, H. (2011). Palynostratigraphy and paleoenvironmental significance of the Cretaceous succession in the Gebel Rissu-1 well, north Western Desert, Egypt. *Journal of African Earth Sciences*, *59*(2-3), 215-226.

El Kammar, M. M. (2015). Source-rock evaluation of the Dakhla Formation black shale in Gebel Duwi, Quseir area, Egypt. *Journal of African Earth Sciences*, *104*, 19-26.

El-Mehdawi, A. D. (1991). Preliminary palynological study of the Upper Cretaceous Al Hilal Formation, Ra's Al Hilal Area, NE Libya. In *Symposium on the geology of Libya* (pp. 1351-1355).

Epstein, A.G., Epstein, J.B and Harris, L.D. (1977). Conodont color alteration: an index to organic metamorphism: *U.S. Geological Survey Professional Paper, 995*, p. 27.

Eshet, Y., Moshkovitz, S., Habib, D., Benjamini, C and Magaritz, M. (1992). Calcareous nannofossil and dinoflagellate stratigraphy across the Cretaceous/Tertiary boundary at Hor Hahar, Israel. *Marine Micropaleontology*, *18*(3), 199-228.

Espitalié, J., Madec, M., Tissot, B., Mennig, J. J and Leplat, P. (1977, May). Source rock characterization method for petroleum exploration. In *Offshore Technology Conference*. OnePetro.

Espitalié, J., Marquis, F and Barsony, I. (1984). Geochemical logging. In *Analytical pyrolysis* (pp. 276-304). Butterworth-Heinemann.

Evitt, W. R. (1985). *Sporopollenin dinoflagellate cysts: their morphology and interpretation*. Amer Assn of Stratigraphic.

Evitt,W.R., Clarke, R.F.A and Verdier,J.P. (1967). Dinoflagellate studies III. Dinogymnium acuminatum n. gen., n.sp. (Maastrichtian) and other fossils formerly referable to Gymnodinium Stein. *Stanford University Publications, Geological Sciences, 10*, 3-27.

Fauconnier, D and Masure, E. (Eds.). (2004). *Les dinoflagellés fossiles: guide pratique de détermination: les genres à processus et à archéopyle apical*. Editions BRGM.

Federova, V. A. (1977). The significance of the combined use of microphytoplankton, spores, and pollen for differentiation of multi-facies sediments In Samoilovich, SR and Timoshina, NA (Eds.) Questions of Phytostratigraphy. *Leningrad, Trudy Neftyanoinauchno-issledovatelskiigeologorazvedochnyi Institute (VNIGRI)*.

Fensome, R. A., Macrae, R. A and Williams, G. L. (2008). DINOFLAJ2, Version 1. American Association of Stratigraphic Palynologists.

Fensome, R.A., Gocht, H and Williams, G.L. (1995). The Eisenack Catalog of Fossil Dinoflagellates. New Series. Volume 3. E. *Schweizerbart'sche Verlagsbuchhandlung, Stuttgart, Germany, 3*, 1463-2008.

Fensome, R.A., Taylor, F.J.R., Norris, G., Sarjeant, W.A.S., Wharton, D.I. and Williams, G.L. (1993). A Classification of Fossil and Living Dinoflagellates. In: *Micropaleontol. Spec. Publ., 7*

Firth, J. V. (1993). Dinoflagellate assemblages and sea-level fluctuations in the Maastrichtian of southwest Georgia. *Review of Palaeobotany and Palynology*, *79*(3-4), 179-204.

Fisher, M. J. (1980). Kerogen distribution and depositional environments in the Middle Jurassic of Yorkshire UK. In *Proceedings of the 4th International Palynological Conference (Lucknow), 2*, 574-580.

Fowler, M., Snowdon, L and Stasiuk, V. (2005). Applying petroleum geochemistry to hydrocarbon exploration and exploitation. *American Association of Petroleum Geologists Short Course Notes*, 18-19.

Frederiksen, N. O., Edwards, L. E., Ager, T. A and Sheehan, T. P. (2002). Palynology of Eocene strata in the Sagavanirktok and Canning Formations on the North Slope of Alaska. *Palynology*, *26*(1), 59-93.

Gamerro, J. C., Archangelsky, S and Weber, R. (1981). *Bibliografia paleobotanica y palinologica Latinoamericana (1979-1980)*.

Ganz, H. H., Luger, P., Schrank, E., Brooks, P. W and Fowler, M. G. (1990). Facies Evolution of Late Cretaceous Black Shales from Southeast Egypt: Chapter 14.

Garry, P., Atta-Peters, D and Achaegakwo, C. (2016). Source-rock potential of the Lower Cretaceous sediments in SD-1X well, offshore Tano basin, south western Ghana. *Petroleum & Coal*, *58*(4).

Gastaldo, R. A and Huc, A. Y. (1992). Sediment facies, depositional environments, and distribution of phytoclasts in the Recent Mahakam River delta, Kalimantan, Indonesia. *Palaios*, 574-590.

Germeraad, J. H., Hopping, C. A and Muller, J. (1968). Palynology of Tertiary sediments from tropical areas. *Review of palaeobotany and palynology*, *6*(3-4), 189-348.

GNPC (2004). Geological report of the Tano Basin.

GNPC (2010). Ghana Hydrocarbon Potential Report, Tano and Cape Three points, (unpublished). p. 25.

Gocht, H. (1969). Formengemeinschaften alttertiären Mikroplanktons aus Bohrproben des Erdölfeldes Meckelfeld bei Hamburg. *Palaeontographica Abteilung B*, 1-100.

Gohn, G. S., Edwards, L. E., Bybell, L. M., Chirico, P. G., Christopher, R. A., Frederiksen, N. O., ... and Weems, R. E. (2000). *Preliminary Stratigraphic Database for the Subsurface Tertiary and Uppermost Cretaceous Sediments of Dorchester County, South Carolina*. US Department of the Interior, US Geological Survey.

Gohn, G.S., Bybell, L.M., Chirico, P.G., Christopher, R.A., Edwards, L.E., Frederiksen, N.O., Prowell, D.C., Self-Trail, J.M and Weems, R.E. (2000). Drill hole data charts used in the preliminary stratigraphic database for subsurface sediments of Dorchester County, South Carolina. (In: Preliminary stratigraphic database for the subsurface Tertiary and Uppermost Cretaceous sediments of Dorchester County, South Carolina. G.S.Gregory et al, compilers) *United States Geological Survey, Open-File Report*.

Golubić, S and Schneider, J. (1979). Carbonate dissolution. In *Studies in Environmental Science 3*, 107-129. Elsevier.

Goodman, D. K. (1987). Dinoflagellate cysts in ancient and modern sediments. *Botanical Monographs*, *21*, 649-722.

Goodman, D. K and Witmer, R. J. (1985). Archeopyle variation and paratabulation in the dinoflagellate Diphyes colligerum (Deflandre and Cookson 1955) Cookson 1965. *Palynology*, *9*(1), 61-84.

Gorin, G. E and Monteil, E. (1990). Preliminary note on the organic facies, thermal maturity and dinoflagellate cysts of the upper Maastrichtian Wang Formation in the northern Subalpine massifs (western Alps, France). *Eclogae Geologicae Helvetiae*, *83*(2), 265-285.

Gorin, G. E and Steffen, D. (1991). Organic facies as a tool for recording eustatic variations in marine fine-grained carbonates-example of the Berriasian stratotype at Berrias (Ardèche, SE France). *Palaeogeography, Palaeoclimatology, Palaeoecology*, *85*(3-4), 303-320.

Górka, H. (1963). Coccolithophoridés, Dinoflagellés, Hystrichosphaeridés et microfossiles incertae sedis du Crétacé supérieur de Pologne. *Acta Palaeontologica Polonica*, *8*(1).

Gradstein, F. M. (2005). Quantitative methods for applied microfossil biostratigraphy. In *Applied Stratigraphy* (pp. 359-386). Springer, Dordrecht.

Guédé, K. É., Slimani, H., Chekar, M., M'Hamdi, A., Mouah, R and Digbehi, B. Z. (2019). Late Cretaceous to Early Eocene dinoflagellate cysts from the "12 frères" borehole, Fresco, southwestern Côte d'Ivoire: biostratigraphy and paleobiogeographic implication. *Journal of African Earth Sciences*, *150*, 744-756.

Guerstein, G. R., Guler, M. V., Williams, G. L., Fensome, R. A and Chiesa, J. O. (2008). Middle Palaeogene dinoflagellate cysts from Tierra del Fuego, Argentina: biostratigraphy and palaeoenvironments. *Journal of Micropalaeontology*, *27*(1), 75-94.

Guex, J and Edwards, L. E. (1996). Unitary associations and correlation of the Marlboro clay and Nanjemoy Formation (uppermost Paleocene and lower Eocene) of Virginia and Maryland. *Palynology: Principles and Applications*, *3*, 1000-1009.

Guiraud, M., Mascle, J., Benkhelil, J., Basile, C., Mascle, G and Durand, M. (1997). Early Cretaceous deltaic sedimentary environment of the Côte d'Ivoire-Ghana transform margin as deduced from deep dive data. *Geo-Marine Letters*, *17*(1), 79-86.

Guy-Ohlson, D and Norling, E. (1988). Upper Jurassic litho-and biostratigraphy of NW Scania, Sweden. *Sveriges geologiska undersökning. Serie Ca. Avhandlingar och uppsatser I 4: 0*, (72).

Habib, D. (1979). Sedimentology of palynomorphs and palynodebris in Cretaceous carbonaceous facies south of Vigo Seamount. *Initial Reports of the Deep Sea Drilling Project*, *47*(2), 451-65.

Habib, D. (1982). Sedimentary supply origin of Cretaceous black shales. In *Nature and origin of Cretaceous carbon-rich facies. Symposium* (pp. 113-127).

Habib, D. (1983). Sedimentation-Rate-Dependent Distribution of Organic-Matter in the North-Atlantic Jurassic-Cretaceous. *Initial Reports of the Deep Sea Drilling Project*, *76*(NOV), 781-794.

Habib, D and Drugg, W. S. (1987). Palynology of site-603 and site-605, LEG-93, Deep-Sea Drilling Project. *Initial Reports of the Deep Sea Drilling Project*, *93*, 751.

Habib, D and Miller, J. A. (1989). Dinoflagellate species and organic facies evidence of marine transgression and regression in the Atlantic Coastal Plain. *Palaeogeography, Palaeoclimatology, Palaeoecology*, *74*(1-2), 23-47.

Habib, D., Moshkovitz, S and Kramer, C. (1992). Dinoflagellate and calcareous nannofossil response to sea-level change in Cretaceous-Tertiary boundary sections. *Geology*, *20*(2), 165-168.

Hansen, J. M. (1977). Dinoflagellate stratigraphy and echinoid distribution in Upper Maastrichtian and Danian deposits from Denmark. *Bulletin of the Geological Society of Denmark*, *26*, 1-26.

Hansen, J. M. (1979). Palynology of some Danish glacial sediments.

Head, M. J. (1993). Dinoflagellates, sporomorphs, and other palynomorphs from the Upper Pliocene St. Erth Beds of Cornwall, southwestern England. *Memoir (The Paleontological Society)*, 1-62.

Head, M. J., Norris, G., Mudie, P. J and Srivastava, S. P. (1989). New species of dinocysts and a new species of acritarch from the upper Miocene and lowermost Pliocene, ODP Leg 105, Site 646, Labrador Sea. In *Proceedings of the Ocean Drilling Program, Scientific Results* (Vol. 105, pp. 453-466). Ocean Drilling Program Texas A and M University, College Station, Texas.

Heilmann-Clausen, C and Egger, H. (2000). The Anthering outcrop (Austria), a key-section for correlation between Tethys and Northwestern Europe near the Paleocene/Eocene boundary. *GFF*, *122*(1), 69-69.

Helenes, J. (1998). Cretaceous - Tertiary stratigraphy and dinoflagellates from Baja California. *Palynology, 22*, 244-245.

Helenes, J and Somoza, D. (1999). Palynology and sequence stratigraphy of the Cretaceous of eastern Venezuela. *Cretaceous Research*, *20*(4), 447-463.

Helenes, J., De Guerra, C and Vasquez, J. (1998). Palynology and chronostratigraphy of the Upper Cretaceous in the subsurface of the Barinas area, western Venezuela. *AAPG bulletin*, *82*(7), 757-772.

Herngreen, G. F. W. (1973). Palynology of Albian-Cenomanian strata of borehole 1-QS-1-MA, State of Maranhão, Brazil. *Pollen et Spores, 15*, 515-555.

Herngreen, G. F. W. (1975). Palynology of middle and upper Cretaceous strata in Brazil. *Med. R. Geol. D. ns*, *26*, 39-116.

Herngreen, G. F. W. (1980). Cretaceous microfloral provinces. *Berliner Geowissenschaftliche Abhandlungen Reihe A, 19*, 79-82.

Herngreen, G. F. W. (1981). Microfloral relationships between Africa and South America in Middle and Upper Cretaceous time. In *IV International Palynological Conference, 3*, 406-417.

Herngreen, G. F. W. (1998). Cretaceous sporomorph provinces and events in the equatorial region. *Zentralblatt fur Geologie und Paläontolgie, 1, 1996* (11/12), 1313-1323.

Herngreen, G. F. W and Jimenez, H. D. (1990). Dating of the Cretaceous Une Formation, Colombia and the relationship with the Albian-Cenomanian African-South American microfloral province. *Review of Palaeobotany and Palynology*, *66*(3-4), 345-359.

Herngreen, G. F. W., Randrianasolo, A and Verbeek, J. W. (1982). Micropaleontology of Albian to Danian strata in Madagascar. *Micropaleontology*, 97-109.

Herngreen, G.F.W and Chlonova, A.F. (1981). Cretaceous microflora provinces. *Pollen Spore 23*, 241-555.

Herngreen, G.F.W., 1974. Middle Cretaceous palynomorphs from northeastern Brazil. Results of a palynological study of some boreholes and comparison with Africa and the Middle East. *Sci. Geol. Bull. 27* (1-2), 101-116.

Herngreen, G.F.W., Kedves, M., Rovnina, L.V and Smirnova, S.B. (1996). Cretaceous palynofloral provinces: a review. In: Schrank, E. (2001). Paleoecological aspects of Afropollis/ elaterates peaks (Albian-Cenomanian pollen) in the Cretaceous of northern Sudan and Egypt, AASP Foundation, ISBN 0-931871-06-9.

Héroux, Y., Chagnon, A and Bertrand, R. (1979). Compilation and correlation of major thermal maturation indicators. *AAPG Bulletin*, *63*(12), 2128-2144.

Hochuli, P. A. (1981). North Gondwanan floral elements in lower to middle Cretaceous sediments of the southern Alps (southern Switzerland, northern Italy). *Review of Palaeobotany and Palynology*, *35*(2-4), 337-358.

Hochuli, P and Kelts, K. (1980). Palynology of Middle Cretaceous black clay facies from Deep Sea Drilling Project sites 417 and 418 of the western North Atlantic. *Initial Reports of the Deep Sea Drilling Project*, *51*, 897-935.

Hock, R. P., Eshet, Y and Almogi-Labin, A. (1996). Dinoflagellate cyst zonation of Campanian-Maastrichtian sequences in Israel. *Micropaleontology*, 125-150.

Hoffman, P. F. (1991). Did the breakout of Laurentia turn Gondwanaland inside-out?. *Science*, *252*(5011), 1409-1412.

Hubib, D. (1983). Dinoflagellate age of middle Jurassic-early Cretaceous sediments in the Blake Bahama Basin. *Initial Reports of the Deep Sea Drilling Project*, *76*, 623-638.

Hughes, N. F and Moody-Stuart, J. C. (1967). Palynological facies and correlation in the English Wealden. *Review of Palaeobotany and Palynology*, *1*(1-4), 259-268.

Hunt, J.M. (1996). *Petroleum Geochemistry and Geology*, 2nd edn, Freeman, San Francisco, pp. 1-743.

Hutton, A. C. (1988). The lacustrine Condor oil shale sequence. *Geological Society, London, Special Publications*, *40*(1), 329-340.

Iakovleva, A. I., Brinkhuis, H and Cavagnetto, C. (2001). Late Palaeocene-Early Eocene dinoflagellate cysts from the Turgay Strait, Kazakhstan; correlations across ancient seaways. *Palaeogeography, Palaeoclimatology, Palaeoecology*, *172*(3-4), 243-268.

Iakovleva, A. I., Cavagnetto, C and Rousseau, D. D. (2000). Paleocene-Eocene dinoflagellate cysts and continental palynomorphs from borehole no. 4 (vasugan basin, central western Siberia). *Palynology*, *24*(1), 187-200.

Ibrahim, M. I. (1996). Aptian-Turonian palynology of the Ghazalat-1 well (GTX-1), Qattara depression, Egypt. *Review of Palaeobotany and Palynology*, *94*(1-2), 137-168.

Ibrahim, M. I. (2002). Late Albian–middle Cenomanian palynofacies and palynostratigraphy, Abu Gharadig-5 well, western desert, Egypt. *Cretaceous Research*, *23*(6), 775-788.

Ibrahim, M. I. A., Ela, N. A and Kholeif, S. E. (2001). Palynostratigraphy of Jurrasic to Lower Cretaceous sequences from the Eastern Desert of Egypt. *Journal of African Earth Sciences*, *32*(2), 269-297.

Ibrahim, M. I. A., Schrank, E and Abdel-Kireem, M. R. (1995). Cretaceous biostratigraphy and palaeogeography of North Egypt and northeast Libya. *Petroleum Research Journal*, *7*, 75-93.

Ibrahim, M. I., Aboul Ela, N. M and Kholeif, S. E. (2002). Dinoflagellate cyst biostratigraphy of Jurassic-Lower Cretaceous formations of the North Eastern Desert, Egypt. *Neues Jahrbuch für Geologie und Paläontologie-Abhandlungen*, 255-319.

Ioannides, N. S and D. J. McIntyre. (1980). A preliminary palynological study of the Cari- bou Hills outcrop section along the Mackenzie River, District of Mackenzie; pp. 197-208 in Current *Research, Part A, Geological Survey of Canada, Paper* 80-1A.

Islam, M. A. (1983). Dinoflagellate cysts from the Eocene of the London and the Hampshire basins, southern England. *Palynology*, *7*(1), 71-92.

Islam, M. A. (1984). A study of early Eocene palaoenvironments in the Isle of Sheppey as determined from microplankton assemblage composition.

Jain, K.P and Millepied, P. (1973). Cretaceous microplankton from Senegal Basin, West Africa, Part I: Some new genera, species and combinations of dinoflagellates. *Palaeobotanist*, 20:22-32.

Jan Du Chene, R. E and Adediran, S. A. (1984). Late Paleocene to Early Eocene dinoflagellates from Nigeria: Cahierb de Micropaleontologie, editions de centre National de la. *Recherche Scientifique*, *15*.

Jan du Chêne, R. E., De Klasz, I and Archibong, E. E. (1978). Biostratigraphic study of the borehole Ojo-1, SW Nigeria, with special emphasis on the Cretaceous microflora. *Revue de Micropaléontologie*, *21*, 123-139.

Jan Du Chene, R.E. (1988). Etude systematique des Kystes de dinoflagelles de la Formation des Madeleines (Danien du Senegal). In: Cahiers de Micropaleontologie, vol. 2. Centre Nationale de la Recherche Scientifique, pp. 147-174.

Jansonius, J. (1986). Reexamination of Mesozoic Canadian dinoflagellate cysts published by SAJ Pocock (1962, 1972). *Palynology*, *10*(1), 201-223.

Jaramillo, C. A and Oboh-Ikuenobe, F. E. (1999). Sequence stratigraphic interpretations from palynofacies, dinocyst and lithological data of Upper Eocene-Lower Oligocene strata in southern Mississippi and Alabama, US Gulf Coast. *Palaeogeography, Palaeoclimatology, Palaeoecology*, *145*(4), 259-302.

Jardiné, S. (1967). Spores á expansion en forme d'élatéres du crétacé moyen d'afrique occidentale. *Review of Palaeobotany and palynology*, *1*(1-4), 235-258.

Jardiné, S and Magloire, L. (1965). Palynologie et stratigraphie du Crétacé des bassins du Sénégal et de Côte d'Ivoire. *Mémoires du BRGM (Paris)*, (32), 187-245.

Jardiné, S., Combaz, A., Magloire, L., Peniguel, G and Vachey, G. (1974). Distribution stratigraphique des acritarches dans le Paléozoïque du Sahara algérien. *Review of Palaeobotany and Palynology*, *18*(1-2), 99-129.

Jimenez, H. D., Herngreen, G. F. W., (1990). Dating of the Cretaceous Une Formation, Colombia and the relationship with the Albian-Cenomanian African-South American microfloral province. *Review of Palaeobotany and Palynology*, *66*(3-4), 345-359.

Jolley, D. W and Spinner, E. (1989). Some dinoflagellate cysts from the London Clay (Palaeocene-Eocene) near Ipswich, Suffolk, England. *Review of Palaeobotany and Palynology*, *60*(3-4), 361-373.

Junner, N. R. (1940). Geology of the gold coat and Western Togoland. *Bull. Gold Coast Geol. Surv.*, *11*, 40.

Junner, N.R. (1935). Gold in the Gold Coast. *Gold Coast Geol. Surv. Mem.* 4:67 p.

Junner, N.R., Hirst, T., Service, H. (1942). The Tarkwa Goldfield. *Gold Coast Geol. Surv. Mern*. 6:75 p.

Kalsbeek, F., Frei, D and Affaton, P. (2008). Constraints on provenance, stratigraphic correlation and structural context of the Volta basin, Ghana, from detrital zircon geochronology: An Amazonian connection?. *Sedimentary Geology*, *212*(1-4), 86-95.

Kaska, H. V. (1989). A spore and pollen zonation of Early Cretaceous to Tertiary nonmarine sediments of central Sudan. *Palynology*, *13*(1), 79-90.

Kedves, M. (1986). In vitro destruction of the exine of recent palynomorphs I. *Acta Biol. Szeged*, *32*, 49-60.

Keegan, J.B and Stead, D.T. (2007). Late Cretaceous palynofloras from Northeast Libya. In: Subsurface Biostratigraphy of the Cretaceous and Cenozoic of northeast Libya. *Wellstrat Service Ltd., Wrexham*, 85-117.

Kesse, G. O. (1985). The mineral and rock resources of Ghana.

Khan, M.S. (1970). Cretaceous and Tertiary rocks of Ghana with a historical account of oil exploration. *Ghana Geological Survey Bulletin* 40, 43.

Khanna, A.K. (1979). Subathua-stratigraphic status and nomenclature. *Himalayan Geology,* 8(1), 209-223.

Kherngrin, G. F and Khlonova, A. F. (1983). Melovye palinofloristicheskie provintsii mira. *Trudy Instituta geologii i geofiziki (Novosibirsk)*, (556).

Kholeif, S. E. H and Ibrahim, M. I. (2010). Palynofacies analysis of inner continental shelf and middle slope sediments offshore Egypt, south-eastern Mediterranean. *Geobios*, *43*(3), 333-347.

Kieser, G and Du Chêne, R. J. (1979). Periretisyncolpites N. Gen. and Terscissus Tschudy 1970 grands pollen syncolpes du Maastrichtien du Senegal et du Nigeria.

Kitson, A. E. (1928). *Provisional Geological Map of the Gold Coast and Western Togoland with Brief Descriptive Notes Thereon 19 Plates: By Sir Albert E. Kitson*. Benham and Company.

Klement, K. W. (1960). Dinoflagellaten und Hystrichsphaerideen aus dem unteren und mittleren Malm Sudwestdeutschlands. *Palaeontographica, Abteilung A*, *114*, 1-104.

Klumpp, B. (1953). Beitrag zur Kenntnis der Mikrofossilien des mittleren und oberen Eozän. *Palaeontographica Abteilung A*, 377-406.

Kotova, I.Z. (1978). Spores and pollen from Cretaceous deposits of the eastern North Atlantic Ocean, Deep Sea Drilling Project, leg 41, sites 367 and 370. *Initial Report Deep Sea Drilling Project*, U.S. Government Printing Office, Washington, D.C., 41, 841-881.

Kumaran, K. P. N and Rajshekhar, C. (1992). 'Foraminiferal linings' from Late Cretaceous-Palaeocene sediments of Ohafia-Ozu Abam area, Nigeria. *Current Science*, 311-313.

Kurita, H and McIntyre, D. J. (1995). Paleocene dinoflagellates from the turtle mountain formation, southwestern Manitoba, Canada. *Palynology*, *19*(1), 119-136.

Kurita, H., Matsuoka, K and Obuse, A. (1997). Application of organic-walled microfossils (palynomorphs) to sedimentary environmental analyses. *Journal of the Sedimentological Society of Japan*, *44*(44), 59-69.

Lamarche, G., Basile, C and Mascle, J. (1997). The Côte d'Ivoire-Ghana transform margin: Sedimentary and tectonic structure from multichannel seismic data. *Geo-Marine Letters*, *17*(1), 62-69.

Landman, N. H., Johnson, R. O and Edwards, L. E. (2004). Cephalopods from the Cretaceous/Tertiary boundary interval on the Atlantic Coastal Plain, with a description of the highest ammonite zones in North America. Part 2. Northeastern Monmouth County, New Jersey. *Bulletin of the American Museum of Natural History*, *2004*(287), 1-107.

Langenheim, J. H. (1969). Amber: A Botanical Inquiry: Amber provides an evolutionary framework for interdisciplinary studies of resin-secreting plants. *Science*, *163*(3872), 1157-1169.

Larsson, S. G. (1978). *Baltic amber: a palaeobiological study*.

Lawal, O. (1982). *Biostratigraphie palynologique et paléo-environnements des formations crétacées de la Haute-Bénoué, Nigéria nord-oriental* (Doctoral dissertation).

Lawal, O and Moullade, M. (1986). Palynological biostratigraphy of Cretaceous sediments in the upper Benue Basin, NE Nigeria. *Revue de Micropaléontologie*, *29*(1), 61-83.

Lentin, J. K and Williams, G. L. (1977). Taxonomic Note: Fossil dinoflagellate genus Isabelidinium nom. nov.

Lentin, J. K and Williams, G. L. (1987). Status of the fossil dinoflagellate genera Ceratiopsis Vozzhennikova 1963 and Cerodinium Vozzhennikova 1963 emend. *Palynology*, *11*(1), 113-116.

Lentin, J. K andWilliams, G. L. (1989). *Fossil Dinoflagellates: Index to Genera and Species: 1989 Edition*. American Association of Stratigraphic Palynologists Foundation.

Lentin, J.K and Williams, G.L. (1976) A monograph of fossil peridinioid dinoflagellate cysts. *Bedford Institute of Oceanography, Report Series,* BI-R-75-16, 1-237.

Lentin, J.K and Williams, G.L. (1980). Dinoflagellate provincialism with emphasis on Campanian peridiniaceans. *AASP Contribution Series, 7*, 1-47.

Lentin, J.K and Williams, G.L. (1981). Fossil dinoflagellates: index to genera and species, 1981 edition. *Bedford Inst. Oceanogr. Rep. Ser., BI-R-81* (12), 1-345.

Lentin, J.K and Williams, G.L. (1973). Fossil Dinoflagellates: index to genera and species. *Geological Survey of Canada*, Paper no. 73-42 pp.1-176.

Lentin, J.K and Williams, G.L. (1985). Fossil dinoflagellates: Index to genera and species, 1981 edition. *Canadian Technical Report of Hydrography and Ocean Sciences*, *60*, 451-1985.

Leprun, J. C and Trompette, R. (1969). Subdivision du Voltaïen du massif de Godnangou (République de Haute-Volta) en deux séries discordantes séparées par une tillite d'âge éocambrien probable. *Comptes rendus de l'Académie des Sciences. Série D: Sciences Naturelles*, *269*(22), 2187-2190.

Leube, A., Hirdes, W., Mauer, R and Kesse, G. O. (1990). The early Proterozoic Birimian Supergroup of Ghana and some aspects of its associated gold mineralization. *Precambrian research*, *46*(1-2), 139-165.

Lewan, M. D. (1986). Stable carbon isotopes of amorphous kerogens from Phanerozoic sedimentary rocks. *Geochimica et Cosmochimica Acta*, *50*(8), 1583-1591.

Lewan, M. D. (1997). Experiments on the role of water in petroleum formation. *Geochimica et Cosmochimica Acta*, *61*(17), 3691-3723.

Li, H and Habib, D. (1996). Dinoflagellate stratigraphy and its response to sea level change in Cenomanian-Turonian sections of the Western Interior of the United States. *Palaios*, *11*(1), 15-30.

Lima, E. C. (1975). Biostratigraphy of the Barreirinhas Basin. In *Anais do Congresso Brasileiro de Geologia, 26*, 81-91.

Lima, M.R. (1978). Palinologia da Formação Santana (Cretáceo do Nordeste do Brasil) [Tese Doutoramento]. *Inst. Geociênc., Univ. São Paulo*.

Lister, J. K and Batten, D. J. (1988a). Stratigraphic and palaeoenvinronmental distribution of Early Cretaceous dinoflagellate cysts in the Hurlands Farm Borehole, West Sussex, England. *Palaeontographica Abteilung B Paläophytologie*, *210*(1-3), 9-89.

Lister, J. K and Batten, D. J. (1988b). Hurlandsia, a new non-marine Early Cretaceous dinocyst genus. *Neues Jahrbuch für Geologie und Paläontologie-Monatshefte*, 505-516.

Lund, J. J and Pedersen, K. R. (1985). Palynology of the marine Jurassic formations in the Vardekloft ravine, Jameson Land, East Greenland. *Bulletin of the Geological Society of Denmark*, *33*(3-4), 371-399.

M'Hamdi, A., Slimani, H., Ismail-Lattrache, K. B and Ali, W. B. (2014). Dinoflagellate cysts, palynofacies and organic geochemistry of the Cretaceous-Palaeogene (K–Pg) boundary transition at the Ellès section, northeastern Tunisia. In *Annales Societatis Geologorum Poloniae* (Vol. 84).

M'Hamdi, A., Slimani, H., Louwye, S., Soussi, M., Ismail-Lattrache, K. B and Ali, W. B. (2015). Les kystes de dinoflagelles et palynofacies de la transition Maastrichtien–Danien du stratotype El kef (Tunisie). *Comptes Rendus Palevol*, *14*(3), 167-180.

Mah, G. (1987). Geological evaluation of the onshore North Tano Basin. *PCIAC/GNPC report*.

Mahmoud, M. S. (1998). Palynology of Middle Cretaceous-Tertiary sequence of Mersa Matruh-1 well, northern Western Desert, Egypt. *Neues Jahrbuch für Geologie und Paläontologie-Abhandlungen*, 79-104

Mahmoud, M. S and Moawad, A. M. M. (1999). Miospore and dinocyst biostratigraphy and palaeoecology of the Middle Cretaceous (Albian–Early Cenomanian) sequence of the Ghoroud-1X borehole, northern Western Desert, Egypt. In *1st International Conference on the Geology of Africa, Assiut, Egypt, 1*, 1-13.

Mahmoud, M. S and Moawad, A. R. M. (2000). Jurassic-Cretaceous (Bathonian to Cenomanian) palynology and stratigraphy of the West Tiba-1 borehole, northern Western Desert, Egypt. *Journal of African Earth Sciences*, *30*(2), 401-416.

Mahmoud, M. S., Omran, A. M and Ataa, S. A. (1999). Stratigraphy of the Upper Jurassic-Lower Cretaceous sequences from three boreholes, northern Egypt: palynological evidence. *Newsletters on Stratigraphy*, 141-161.

Mansour, A., Mohamed, O., Tahoun, S. S and Elewa, A. M. (2018). Sequence stratigraphy of the Raha Formation, Bakr Oil Field, Gulf of Suez, Egypt: Insights from electrical well log and palynological data. *Journal of African Earth Sciences*, *139*, 205-221.

Mao, S and Mohr, B. A. (1992). Late Cretaceous dinoflagellate cysts (? Santonian-Maestrichtian) from the southern Indian Ocean (hole 748C). In *Proceedings of the Ocean Drilling Program, Scientific Results 120*, 307-341.

Marheinecke, U. (1992). Monographie der dinozysten, acritarcha und chlorophyta des Maastrichtium von hemmoor (Niedersachsen). *Palaeontographica Abteilung B Paläophytologie*, *227*, 1-173.

Marshall, K. L and Batten, D. J. (1988). Dinoflagellate cyst associations in Cenomanian-Turonian "black shale" sequences of northern Europe. *Review of Palaeobotany and Palynology*, *54*(1-2), 85-103.

Masran, T. C and Pocock, S. A. J. (1981). The classification of plantderived particulate organic matter in sedimentary rocks. In J. Brooks (Ed.) Organic maturation studies and fossil fuel exploration (pp. 145-176). London: Academic Press.

Masure, E., Rauscher, R., Dejax, J., Schuler, M and Ferré, B. (1998). 24. Cretaceous-Paleocene Palynology from the Côte D'ivoire-Ghana Transform Margin, Sites 959, 960, 961, AND 9621. In *Proceedings of the Ocean Drilling Program, Scientific Results*, 159, 253-276.

Matsuoka, K. (1983). A new dinoflagellate cyst (Danea heterospinosa) from the eicene of central Java, Indonesia. *Review of palaeobotany and palynology*, *40*(1-2), 115-126.

May, F. E. (1980). Dinoflagellate cysts of the Gymnodiniaceae, Peridiniaceae, and Gonyaulacaceae from the upper Cretaceous Monmouth Group, Atlantic Highlands, New Jersey. *Palaeontographica Abteilung B,* 172**,** 10-116.

Mbesse, C. O., Roche, E and Ngos III, S. (2012). The Paleocene-Eocene boundary in the Douala Basin (Cameroon): Dinocysts biostratigraphy and tentative of Paleoenvironmental reconstruction. *International Journal of Tropical Geology, Geography and Ecology*, *36*, 83-119.

McIntyre, D. J and Brideaux, W. W. (1980). Valanginian miospores and microplankton assemblage from the Northern Richardson Mountains, District of Mackenzie, Canada. Geol. Surv. Canada. *Bull*, *320*.

McNeil, D. H. (1997). Diagenetic regimes and the foraminiferal record in the Beaufort-Mackenzie Basin and adjacent cratonic areas. In *Annales Societatis Geologorum Poloniae*, *67* (2-3), 271-286.

Mehrotra, N. C., Venkatachala, B. S., Swamy, S. N and Kapoor, P. N. (2002). Memoir 48: Palynology in Hydrocarbon Exploration the Indian Scenario (Part I: Category I Basins). *Journal of Geological Society of India (Online archive from Vol 1 to Vol 78)*, *60*(5), 526-526.

Mendonça Filho, J. G. (1999). Aplicação de estudos de palinofácies e fácies orgânica em rochas do Paleozóico Superior da bacia do Paraná, sul do Brasil. *Universidade Federal do Rio Grande do Sul*.

Mendonça Filho, J. G., Menezes, T. R., Mendonça, J. O., Oliveira, A. D., Silva, T. F., Rondon, N. F and Silva, F. S. (2012). Organic Facies: Palynofacies and Organic Geochemistry

Approaches, Geochemistry-Earth's System Processes, Dionisios Panagiotaras (Ed.), ISBN: 978-953-51-0586-2.

Mendonça-Filho, J. G., Menezes, T. R., Mendonça, J. O., Oliveira, A. D., Souza, J. T., Santos, V. S. S and Arienti, L. M. (2010). Aplicação da faciologia orgânica no modelo sedimentológico-estratigráfico do Oligo-Mioceno e Mioceno da Bacia de Campos. *Boletim de Geociências da Petrobras, Rio de Janeiro*, *18*(2), 153-177.

Menéndez, C. A. (1965). Microplancton fósil de sedimentos Terciarios y Cretácicos del norte de Tierra del Fuego (Argentina). *Ameghiniana*, *4*(1), 7-18.

Millioud, M. E. (1969). Dinoflagellates and acritarchs from Western European lower Cretaceous type localities. In Bronnimann, P. and Renz, H. H. (Eds.) *First International Conference on Planktonic Microfossils.* Geneva, Switzerland.

Moawad, A. R. M. M and Mahmoud, M. S. (2002). Cretaceous palynology of the Sanhur-IX Borehole, norhwestern Egypt. *Revista Española de Micropaleontología*, *34*(2), 129-144.

Mohr, B. A. R and Mao, S. (1997). Maastrichtian dinocyst floras from Maud Rise and Georgia Basin (Southern Ocean): their stratigraphic and paleoenvironmental implications. *Palynology*, *21*(1), 41-65.

Morgan, R. (1978). Albian to Senonian palynology of site 364, Angola Basin.

Morgenroth, P. (1966). Mikrofossilien und Konkretionen des nordwesteurop€aischen Untereoz€ans. In: *Palaeontographica, Abteilung, 119*, 1-53.

Moullade, M., Kuhnt, W., Bergen, J. A., Masse, J. P and Tronchetti, G. (1998). Correlation of biostratigraphic and stable isotope events in the Aptian historical stratotype of La Bédoule (southeast France). *Comptes Rendus de l'Académie des Sciences-Series IIA-Earth and Planetary Science*, *327*(10), 693-698.

Mudge, D. C and Bujak, J. P. (1996). Palaeocene biostratigraphy and sequence stratigraphy of the UK central North Sea. *Marine and Petroleum Geology*, *13*(3), 295-312.

Mudie, P. J. (1982). Pollen distribution in recent marine sediments, eastern Canada. *Canadian Journal of Earth Sciences*, *19*(4), 729-747.

Muller, J. (1959). Palynology of Recent Orinoco delta and shelf sediments; reports of the Orinoco shelf expedition, volume 5. *Micropaleontology*, *5*(1), 1-32.

Muller, J. (1966). Montane pollen from the Tertiary of NW. Borneo. *Blumea: Biodiversity, Evolution and Biogeography of Plants*, *14*(1), 231-235.

Muller, J. (1968). Palynology of the Pedawan and plateau sandstone formations (Cretaceous-Eocene) in Sarawak, Malaysia. *Micropaleontology*, 1-37.

Muller, J., de Di Giacomo, E and Van Erve, A. W. (1987). *A palynological zonation for the Cretaceous, Tertiary, and Quaternary of northern South America*. AASP.

Mutterlose, J. Ö. R. G and Harding, I. (1987). Phytoplankton from the anoxic sediments of the Barremian (Lower Cretaceous) of North-West Germany. *Abhandlungen der Geologischen Bendesanstalt Wien*, *39*, 177-215.

Nady M. M., Ramadan S. F., Hammad M. M., Lotfy M. N., (2014); Evaluation of organic matters, hydrocarbon potential and thermal maturity of source rocks based on geochemical and statistical methods: Case study of source rocks in Ras Gharib oilfield, central Gulf of Suez, Egypt. *Egyptian Petroleum Research Institute*, Nasr City, Hei Al-Zehour, 11727 Cairo, Egypt.

Oboh-Ikuenobe, F. E., Antolinez-Delgado, H and Awad, W. K. (2017). Dinoflagellate cyst assemblages, biostratigraphy and paleoenvironment of a Paleocene-Early Eocene sedimentary succession in the northern Niger Delta Basin: comparison with low, mid and high latitude regions. *Palaeogeography, Palaeoclimatology, Palaeoecology*, *481*, 29-43.

Oboh-Ikuenobe, F. E., Hoffmeister, A. P and Chrisfield, R. A. (1999). Cyclical distribution of dispersed organic matter and dinocysts, ODP site 959 (early Oligocene-early Miocene, Côte d'Ivoire-Ghana transform margin). *Palynology*, *23*(1), 87-96.

Oboh-Ikuenobe, F. E., Yepes, O and Gregg, J. M. (1998). 25. Palynostratigraphy, palynofacies, and thermal maturation of Cretaceous-Paleogene sediments from the Côte D'Ivoire-Ghana transform margin. In *Proc Ocean Drill Prog Scient Res*, 159, 277-318.

Odebode, M.O and Salami, M.B. (1984). Palynology of the Odukpani Formation, (Middle Cretaceous) of Southeastern Nigeria. *Nigerian Journal of Science* 18 (1), 83-94.

Ojoh, K. A. (1990). Cretaceous geodynamic evolution of the southern part of the Benue Trough (Nigeria) in the equatorial domain of the South Atlantic. Stratigraphy, basin analysis and paleo-oceanography. *Bulletin des centres de recherches exploration-Production Elf-Aquitaine*, *14*(2), 419-442.

Olivero, E.B., MalumiŶn, N., Palamarczuk, S and Scass, R.A. (2001). The Upper Cretaceous-Paleogene from the Ro Bueno area, Atlantic coast of the Isla Grande de Tierra del Fuego. Revista de la Asociacirn Geolrgica Argentina, p.199-218.

Oloto, I. N. (1989). Maastrichtian dinoflagellate cyst assemblage from the Nkporo Shale on the Benin flank of the Niger Delta. *Review of Palaeobotany and Palynology*, *57*(3-4), 173-186.

Oloto, I. N. (1992). Succession of palynomorphs from the Early Eocene of Gbekebo-1 well in SW Nigeria. *Journal of African Earth Sciences (and the Middle East)*, *15*(3-4), 441-452.

Pearce, M. A., Jarvis, I., Swan, A. R., Murphy, A. M., Tocher, B. A and Edmunds, W. M. (2003). Integrating palynological and geochemical data in a new approach to palaeoecological studies: Upper Cretaceous of the Banterwick Barn Chalk borehole, Berkshire, UK. *Marine Micropaleontology*, *47*(3-4), 271-306.

Pelzer, G., Riegel, W and Wilde, V. (1992). Depositional controls on the Lower Cretaceous Wealden coals of northwest Germany. *Controls on the distribution and quality of Cretaceous coals. Geological Society of America Special Paper*, *267*, 227-244.

Penny, J. H. (1991). Early Cretaceous angiosperm pollen from the borehole Mersa Matruh 1, North West Desert, Egypt. *Palaeontographica Abteilung B Paläophytologie*, *222*, 31-88.

Peters, K. E. (1986). Guidelines for evaluating petroleum source rock using programmed pyrolysis. *AAPG bulletin*, *70*(3), 318-329.

Peters, K. E and Cassa, M. R. (1994). Applied source rock geochemistry: Chapter 5: Part II. Essential elements. In: Ghasemi-Nejad, E., Head, M. J., and Naderi, M. (2009). Palynology and petroleum potential of the Kazhdumi Formation (Cretaceous: Albian–Cenomanian) in the South Pars field, northern Persian Gulf. *Marine and Petroleum Geology*, *26*(6), 805-816.

Peters, K. E., Peters, K. E., Walters, C. C and Moldowan, J. M. (2005). *The biomarker guide* (Vol. 1). Cambridge university press.

Pflug, H.D. (1953). Zur Entsehung und Entwicklung des angiospermiden Pollens in der Erdgeschicte, *Palaeontolographica Abt. B, 95*, 60-171.

Piasecki, S. (1986). Palynological analysis of the organic debris in the Lower Cretaceous Jydegård Formation, Bornholm, Denmark. *Grana*, *25*(2), 119-129.

Pittet, B and Gorin, G. E. (1997). Distribution of sedimentary organic matter in a mixed carbonate-siliciclastic platform environment: Oxfordian of the Swiss Jura Mountains. *Sedimentology*, *44*(5), 915-937.

Playford, G. (1971). Palynology of Lower cretaceous (Swan river) strata of Saskatchewan and Manitoba. *Palaeontology*, *14*(4), 533-565.

Pocklington, R and Leonard, J. D. (1979). Terrigenous organic matter in sediments of the St. Lawrence Estuary and the Saguenay Fjord. *Journal of the Fisheries Board of Canada*, *36*(10), 1250-1255.

Pocknall, D.T., Erlich, R.N., Stein, J.A and Lorente, M.A. (2001). "The palynofloral succession across the Cretaceous to Paleocene transition zone, Mérida Andes, western Venezuela". In *Proceedings of the IX International Palynological Congress, Houston, Texas, USA., 1996*, Edited by: Goodman, D.K. and Clarke, R.T. 171-179. Dallas, Texas: American Association of Stratigraphic Palynologists Foundation.

Pocock, S. A. (1970). Palynology of the Jurassic sediments of western Canada. Part 1. Terrestrial species. *Palaeontographica Abteilung B*, 12-72.

Pocock, S.A.J. (1964). Pollen and spores of Chlamydospermidae and Schizaeaceae from Upper Manville strata of the Saskatoon area of Saskatchwan. *Grana Palynologica*, 5 (2), 129-209.

Pocock, S.A.J., Vasanthy, G and Venkatachala, B.S. (1988). Evolutionary status of columellate Classopollis, Classoidites, Equisetosporites and Cornetipollis *International Palynological Conference, 7th, Abstracts*, 133-133.

Potonie, R. (1970). Synopsis of the genera of the sporae dispersae. Part 5. Supplement to all Groups (Turmae). *Beihefte zum Geologischen Jahrbuch*, 87(5), 1-172.

Powell, A. J. (1992). Dinoflagellate cysts of the Tertiary System. *A Stratigraphic Index of Dinoflagellate Cysts*, 155-251.

Powell, A. J., Brinkhuis, H and Bujak, J. P. (1996). Upper Paleocene-Lower Eocene dinoflagellate cyst sequence biostratigraphy of southeast England. *Geological Society, London, Special Publications*, *101*(1), 145-183.

Powell, A. J., Dodge, J. D and Lewis, J. (1990). 17. Late Neogene to Pleistocene palynological facies of the Peruvian continental margin upwelling, Leg 112. In *Proceedings of the Ocean Drilling Program: Scientific Results* (p. 297). The Program. pp. G1-G25.

Prasad, V., Singh, I. B., Bajpai, S., Garg, R., Thakur, B., Singh, A. and Kapur, V. V. (2013). Palynofacies and sedimentology-based high-resolution sequence stratigraphy of the lignite-bearing muddy coastal deposits (early Eocene) in the Vastan Lignite Mine, Gulf of Cambay, India. *Facies*, *59*(4), 737-761.

Prauss, M. (1989). Dinozysten-stratigraphie und palynofazies im Oberen Lias und Dogger von NW-Deutschland. *Palaeontographica Abteilung B Paläophytologie*, *214*(1-4), 1-124.

Prevot, L., Lucas, J and Doubinger, J. (1979). A note on the palynological contents, mineral composition and chemistry of a sedimentary phosphate series (Ganntour, Maroc). *Sciences Geologiques Bulletin*, *32*(1), 69-90.

Prince, I.M., Jarvis, I. and Tocher, B.A. (1999) High-resolution dinoflagellate cyst biostratigraphy of the Santonian-basal Campanian (Upper Cretaceous): new data from Whitecliff, Isle of Wight, England. *Rev Palaeobot Palynol* 105:143–169

Quadros, L. D. (1975). Organopalinologia na prospecção de petróleo. Rio de Janeiro. *Boletim Técnico da Petrobras*, *18*, 3-11.

Rauscher, R and Doubinger, J. (1981). Palynostratigraphic results in the phosphatic Maestrichtian of Morocco. *Comptes Rendus de l Academie des Sciences Serie II*, *293*(4), 321-324.

Rauscher, R and Doubinger, J. (1982). Les dinokystes du Maestrichtien phosphaté du Maroc. *Sciences Géologiques, bulletins et mémoires*, *35*(3), 97-116.

Rauscher, R., Marhoumi, R., Vanguestaine, M., Hoepffner, C. (1982). Palynological dating of the Moroccan Tazekka Schists: Consequence on the structural evolution of the

Hercynian Basement of the eastern Meseta. *Comptes Rendus de l Academie des Sciences Serie II*, *294*(19), 1203-1206.

Regali, M. S. P. (1989). Tucanopollis, a new genus of early angiosperms. *Boletim Técnico Petrobras*, *3*, 395-402.

Regali, M. S. P., Uesugui, N and Santos, A. S. (1974). Palynology of the Mesozoic-Cenozoic sediments of Brazil. *Boletim Técnico da Petrobras (Rio de Janeiro)*, *17*, 177-301.

Regali, M.S.P., Uesugui, N and Lima, E.C. (1985). Palinoestratigrafia e paleoambiente da Bacia de Barreirinhas Maranhão-Brasil. *Coletânea de trabalhos paleontológicos, DNPM; Rio de Janeiro*, 461-470.

Reyre, Y. (1973) Palynologie du Mésozoique Saharien. Mémoris du Muséum National d'Histoire Naturelle, 27, 1-284.

Riding, J. B. (1992). On the age of the Upper Ostrea Member, Staffin Bay Formation (Middle Jurassic) of north-west Skye. *Scottish Journal of Geology*, *28*(2), 155-158.

Riding, J. B and Hubbard, R. N. (1999). Jurassic (Toarcian to Kimmeridgian) dinoflagellate cysts and paleoclimates. *Palynology*, *23*(1), 15-30.

Riding, J. B., Walton, W and Shaw, D. (1991). Toarcian to Bathonian (Jurassic) palynology of the Inner Hebrides, northwest Scotland. *Palynology*, 15(1), 115-179.

Riegel, W. (1974). New forms of organic-walled microplankton from an Upper Cretaceous assemblage in southern Spain. *Revista Española de Micropaleontología*, *6*(3), 347-366.

Roncaglia, L and Corradini, D. (1997). Upper Campanian to Maastrichtian dinoflagellate zonation in the northern Apennines, Italy. *Cretaceous Research*, *23*, 65-76.

Roncaglia, L. (2002). Lower Maastrichtian dinoflagellates from the Viano Clay Formation at Viano, northern Apennines, Italy. *Cretaceous Research*, *23*(1), 65-76.

Rossignol, M. (1962). Analyse pollinique de sediments Quaternaires en Islael. I: Sediments Pleistocenes. *Pollen et spores*, *4*, 121-148.

Rossignol, M. (1964). Hystrichosphères du Quaternaire en Méditerranée orientale, dans les sédiments Pléistocènes et les boues marines actuelles. *Revue de micropaléontologie*, *7*(2), 83-99.

Saad, S. I. (1978). Palynological studies in the Egyptian Western Desert, Umbarka 1X borehole. *Pollen et Spores*, *20*, 261-301.

Saad, S.I., 1974. Palynological results and their bearing on the theory of continental displacement. *Adv. Pollen Spore Res., 1*, 70-77.

Salami, M. B. (1983). Some Late Cretaceous and Early Tertiary pteridophytic spores from the southern Nigeria sedimentary basin. *Revista española de micropaleontologia*, *15*(2), 257-272.

Salami, M. B. (1986). Some dinoflagellate cysts and acritarchs from the Late Cretaceous and Paleogene sediments of the Benin (Ex Dahomey) Embayment in Southwestern Nigeria. *Ife Journal of Science*, *1*(1), 11-21.

Salami, M.B. (1988). Petrography and palynology of the Upper Maastrichtian Abeokuta formation of southwestern Nigeria. *Nigeria Journal of Science*, *22*(1 and 2), 127-140.

Salard-Cheboldaeff, M. (1991). Intertropical African palynostratigraphy from Cretaceous to Late Quaternary times Journal of African Earth Sciences, 11(1), 1-24.

Sánchez-Pellicer, R., Masure, E and Villier, L. (2017). A new biostratigraphic correlation for Late Cretaceous-Paleocene strata of the Gulf of Guinea: Evidence from dinoflagellate cysts. *Comptes Rendus Geoscience*, *349*(1), 32-41.

Sarjeant, W. A. S. (1970). Xanthidia, Palinospheres and "Hystrix". A review of the study of fossil unicellular microplankton with organic cell walls. *Microscopy*, *31*, 221-253.

Schrank, E. (1984). Organic-geochemical and palynological studies of a Dakhla Shale Profile, (Late Cretaceous), in Southeast Egypt. Part A. Succession of microfloras and depositional environment. *Berliner Geowissenschaftliche Abhandlungen, Reihe A, Geologie und Pal¤ontologie, 50*, 189-207.

Schrank, E. (1987). Paleozoic and Mesozoic palynomorphs from northeast Africa (Egypt and Sudan) with special reference to late Cretaceous pollen and dinoflagellates. *Berliner Geowissenschaftliche Abhandlungen A, 75*(1), 249-310.

Schrank, E. (1988). Effects of chemical processing on the preservation of peridinioid dinoflagellates: a case from the Late Cretaceous of NE Africa. *Review of Palaeobotany and Palynology*, *56*(1-2), 123-140.

Schrank, E. (1990). Palynology of the clastic Cretaceous sediments between Dongola and Wadi Muqaddam, northern Sudan. *Berliner Geowissenschaftliche Abhandlungen, Reihe A*, *120*(1), 149-168.

Schrank, E. (1991). Mesozoic palynology and continental sediments in NE Africa (Egypt and Sudan)-a review. *Journal of African Earth Sciences (and the Middle East)*, *12*(1-2), 363-373.

Schrank, E. (1994). Palynology of the Yesomma Formation in northern Somalia. a study of pollen, spores and associated phytoplankton from the Late Cretaceous Palmae Province. *Palaeontographica Abteilung B Paläophytologie*, *231*, 63-112.

Schrank, E. (2001). Paleoecological aspects of Afropollis/Elaterates peaks (Albian-Cenomanian pollen) in the Cretaceous of northern Sudan and Egypt. *Proceeding of the IX International Palynological Congress, Houston, Texas, USA, 1996, American Association of Stratigraphic Palynologists Foundation.* 201- 210.

Schrank, E and Ibrahim, M. I. A. (1995). Cretaceous (Aptian-Maastrichtian) palynology of foraminifera dated wells (KRM-1, AG-18) in northwestern Egypt. *Berliner Geowissenschaftliche Abhandlungen A*, 177, 1-44.

Schrank, E and Mahmoud, M. S. (1998). Palynology (pollen, spores and dinoflagellates) and Cretaceous stratigraphy of the Dakhla Oasis, central Egypt. *Journal of African Earth Sciences*, *26*(2), 167-193.

Schrank, E and Perch-Nielsen, K. (1985). Late Cretaceous palynostratigraphy in Egypt with comments on Maastrichtian and Early Tertiary calcareous nannofossils. *Newsletters on Stratigraphy*, 81-99.

Sinanoglu, E. (1983). Early Cretaceous palynomorphs from the Zuata area, eastern Venezuela PaleobotŸnica e Palinologa na America do Sul.1983. *Contribuicoes a IV Reuniao de Paleobotanicos e Palinologos Instituto de Geoci€ncias,Universidade de Sao Paulo, 4,* 116-128.

Singh, A., Mahesh, S., Singh, H., Tripathi, S. K and Singh, B. D. (2013). Characterization of Mangrol lignite (Gujarat), India: petrography, palynology, and palynofacies. *International journal of coal geology*, *120*, 82-94.

Singh, G., Opdyke, N. D and Bowler, J. M. (1981). Late Cainozoic stratigraphy, palaeomagnetic chronology and vegetational history from Lake George, NSW. *Journal of the Geological Society of Australia*, *28*(3-4), 435-452.

Singh, C. (1971). Lower Cretaceous microfloras of the Peace River area, Northwestern Canada, (Alberta). *Research Council of Alberta, Bulletin,* 301- 542.

Slimani, H. (2001). Dinoflagellate cysts from Campanian to Danian in the region of Maastricht (Belgium and the Netherlands) and Turnhout (Belgium): biozonation and correlation with other regions in Western Europe. *Geologica and Palaeontologica*, *35*, 161-201.

Slimani, H. (2000). New zonation to dinoflagellate cysts from Campanian to Danian in the North and East of Belgium and in the South-East of the Netherlands. *Memoirs of the Geological Survey of Belgium, 46*, 1-88.

Slimani, H. 1995. The chalk dinocysts from campanian to Danian in Hallembaye and Turnhout (Belgium) and Beutenaken (Netherlands): Biostratigraphy and systematics [Ph.D. thesis]. University of Gent, Gent, Belgium.

Slimani, H., Guédé, K. É., Williams, G. L and Asebriy, L. (2016). Campanian to Eocene dinoflagellate cyst biostratigraphy from the Tahar and Sekada sections at Arba Ayacha, western External Rif, Morocco. *Review of Palaeobotany and Palynology*, *228*, 26-46.

Slimani, H., Louwye, S and Toufiq, A. (2010). Dinoflagellate cysts from the Cretaceous-Paleogene boundary at Ouled Haddou, southeastern Rif, Morocco: biostratigraphy, paleoenvironments and paleobiogeography. *Palynology*, *34*(1), 90-124.

Sluijs, A., Brinkhuis, H., Williams, G. L and Fensome, R. A. (2009). Taxonomic revision of some Cretaceous-Cenozoic spiny organic-walled peridiniacean dinoflagellate cysts. *Review of Palaeobotany and Palynology, 154*(1-4), 34-53.

Smyth, M., Jian, F. X and Ward, C. R. (1992). Potential petroleum source rocks in Triassic lacustrine-delta sediments of the Gunnedah Basin, Eastern Australia. *Journal of Petroleum Geology, 15*, 435-450.

Solai, A., Gandhi, M. S and Sriram, E. (2010). Implications of physical parameters and trace elements in surface water off Pondicherry, Bay of Bengal, South East Coast of India. *International Journal of Environmental Sciences*, *1*(4), 529-542.

Soncini, M. J. (1992). Three new dinoflagellate cysts from the Moroccan Paleocene-Eocene phosphates. *Review of Palaeobotany and Palynology*, *70*(4), 325-338.

Sougy, J. (1971). Remarques sur la stratigraphie du Protérozoique supérieur du basin voltaïen; influence de la paléosurface d'érosion glaciaire de la base du groupe de l'Oti sur le tracé sinueux des Volta et de certains affluents. *C R Acad Sci, Paris, D, 272*, 800-803.

Srivastava, S. K. (1981). Stratigraphic ranges of selected spores and pollen from the Fredericksburg Group (Albian) of the southern United States. *Palynology*, *5*(1), 1-27.

Srivastava, S.K. (1978). *Cretaceous spore-pollen floras Biological Memoirs.* 1-130.

Srivastava, V., Msaky, E. (1999). Albian-Cenomanian micro-floral assemblages from coastal Tanzania. *Palaeoecology of Africa and the Surrounding Islands, 26*, 31-44.

Srivastava, S.C. (1995) Compressed Triassic fructification from India and their usefulness in Gondwanas Plant Cell Biology and Development, 6, 29-29.

Staplin, F.K. (1969). Sedimentary organic matter, organic metamorphism, and oil and gas occurrence. *Bulletin of Canadian Petroleum Geology* 1969;; 17 (1): 47–66. doi: *https://doi.org/10.35767/gscpgbull.17.1.047*

Stout, J. D., Goh, K. M and Rafter, T. A. (1981). Chemistry and turnover of naturally occurring resistant organic compounds in soil. *Soil Biochemistry*, *5*, 1-73.

Stover, L. E and Williams, G. L. (1995). A revision of the Paleogene dinoflagellate genera Areosphaeridium Eaton 1971 and Eatonicysta Stover and Evitt 1978. *Micropaleontology*, 97-141.

Stover, L. E. and Evitt, W. R. (1978). Analyses of pre-Pleistocene organic-walled dinoflagellates. Stanford University Publications, *Geological Sciences*, *15*, 1-300.

Stover, L. E and Partridge, A. D. (1973). Tertiary and Late Cretaceous spores and pollen from the Gippsland Basin, southeastern Australia. *Proceedings of the Royal Society of Victoria*, *85*(2), 237-286.

Stover, L. E., Brinkhuis, H., Damassa, S. P., de Verteuil, L., Helby, R. J., Monteil, E and Williams, G. L. (1996). Mesozoic-Tertiary dinoflagellates, acritarchs and prasinophytes. *In J. Jansonius and D. C. McGregor (Eds.), Palynology: Principles and applications* (Vol. 2, pp. 641-750), Salt Lake City, Utah. American Association of Stratigraphic Palynologists.

Stover, L.E and Williams, G.L. (1987). Analyses of Mesozoic and Cenozoic organic-walled dinoflagellates 1977-1985., Contributions Series, No. 18 243, American Association of Stratigraphic Palynologists.

Sultan, I. Z. (1978). Mid-Cretaceous plant microfossils from the northern part of the Western Desert of Egypt. *Review of Palaeobotany and Palynology*, *25*(3-4), 259-267.

Sultan, I. Z. (1986). Palynostratigraphy of Lower Cretaceous sediments in the Nyle Delta region, Egypt. *Revista española de micropaleontologia*, *18*(1), 55-70.

Sultan, I. Z. (1987). Palynology of Albian-Cenomanian strata in Mersa Matruh well, Western Desert, Egypt. *Journal of African Earth Sciences (1983)*, *6*(5), 665-675.

Summerhayes, C. P. (1983). Sedimentation of organic matter in upwelling regimes. *Coastal upwelling-Its Sediments Record Part B: Sedimentary records of ancient coastal upwelling*, *1*, 29-72.

Tahoun, S. S and Deaf, A. S. (2016). Could the conventionally known Abu Roash "G" reservoir (upper Cenomanian) be a promising active hydrocarbon source in the extreme northwestern part of Egypt? Palynofacies, palaeoenvironmental, and organic geochemical answers. *Marine and Petroleum Geology*, *76*, 231-245.

Tahoun, S. S., Deaf, A., Gentzis, T and Carvajal, H. (2017, April). Exceptional hydrocarbon source rock of the conventional (Albian) Kharita Formation reservoir in Matruh Basin, northern Western Desert of Egypt. In *AAPG Annual Convention and Exhibition*.

Tappan, H. N. (1980). *The paleobiology of plant protists*. WH Freeman.

Tea-Yassi, J., Digbehi, Z. B., Yao, K. R and Boblai, V. (1999). Study of some palynomorphs of Upper Cretaceous in Cote d'Ivoire sedimentary "Offshore" basin. Biostratigraphic and paleoenvironmental implications. *J Afr Earth Sci*, *29*(4), 783-798.

Thusu, B and Van der Eem, J. G. L. A. (1985). Early Cretaceous (Neocomian-Cenomanian) palynomorphs. *Journal of Micropalaeontology*, *4*(1), 131-149.

Tissot, B. P and Welte, D. H. (1984). Diagenesis, catagenesis and metagenesis of organic matter. In *Petroleum formation and occurrence* (pp. 69-73). Springer, Berlin, Heidelberg.

Tissot, B and Pelet, R. (1981). Sources and fate of organic matter in ocean sediments. *Oceanologica Acta, Special Issue*.

Tissot, B., Durand, B., Espitalie, J and Combaz, A. (1974). Influence of nature and diagenesis of organic matter in formation of petroleum. *AAPG Bulletin*, *58*(3), 499-506.

Traverse, A. (2004) Proposal to conserve the fossil pollen morphogeneric name *Classopollis* against *Corollina* and *Circulina*. Taxon, *53*, 847-848.

Traverse, A. (2007). Paleopalynology, Dordrecht, Springer.

Traverse, A. (Ed.), 1994. Sedimentation of Organic Particles. Cambridge University Press, Cambridge.

Traverse, A. (1988). Paleopalynology. Unwin Hyman, Boston, MA, p. 600.

Tschudy, R.H. (1961). Palynomorphs as indicators of facies environments in Upper Cretaceous and Lower Tertiary strata, Colorado and Wyoming Wyoming Geological Association, Guidebook,16th Annual Field Conference,1961. Symposium on Late Cretaceous Rocks. 53-59.

Tucker, M.E. (1988). Sedimentary Petrology: an Introduction. ELBS Edition. *Blackwell Scientific Publications*, p. 252.

Tyson, R. V. (1984). Palynofacies investigation of Callovian (Middle Jurassic) sediments from DSDP Site 534, Blake-Bahama Basin, western Central Atlantic. *Marine and Petroleum Geology*, *1*(1), 3-13.

Tyson, R. V. (1987). The genesis and palynofacies characteristics of marine petroleum source rocks. *Geological Society, London, Special Publications, 26*(1), 47-67.

Tyson, R. V. (1989). Late Jurassic palynofacies trends, Piper and Kimmeridge Clay Formation, UK onshore and offshore. In D. J. Batten and M. C. Keen (Eds.), *Northwest European Micropalaeontology and palynology* (pp. 135-172). Chichester: British Micropalaeontological Society Series.

Tyson, R. V. (1993). Palynofacies analysis. In *Applied micropalaeontology* (pp. 153-191). Springer, Dordrecht. The Netherlands: Kluwer Academic Publishers.

Tyson, R. V. (1995). Abundance of organic matter in sediments: TOC, hydrodynamic equivalence, dilution and flux effects. In *Sedimentary organic matter* (pp. 81-118). Springer, Dordrecht.

Urban, L. L., Moore, L. V and Allen, M. L. (1976). Palynology, thermal alteration and source rock potential of three wells from Alamein area, Western Desert, Egypt. In *5th Exploration Seminar, Egyptian General Petroleum Corporation* (pp. 1-34).

Valdés, J., Sifeddine, A., Ortlieb, L and Pierre, C. (2004). Interplay between sedimentary organic matter and dissolved oxygen availability in a coastal zone of the Humboldt Current System; Mejilones Bay, northern Chile, *Marine Geology*, *265*, 57-166.

Van Hoeken-Klinkenberg, P. M. J. (1964). A palynological investigation of some Upper-Cretaceous sediments in Nigeria. *Pollen et spores*, *6*(1), 209-231.

Van Hoeken-Klinkenberg, P. M. J. (1966). Maastrichtian Paleocene and Eocene pollen and spores from Nigeria. *Leidse Geologische Mededelingen*, *38*(1), 37-44.

Vellekoop, J., Smit, J., van de Schootbrugge, B., Weijers, J. W., Galeotti, S., Damste, J. S. S and Brinkhuis, H. (2015). Palynological evidence for prolonged cooling along the Tunisian continental shelf following the K-Pg boundary impact. *Palaeogeography, Palaeoclimatology, Palaeoecology*, *426*, 216-228.

Verdier, J. P. (1970). Addendum to the memoir of G. Deflandre and IC Cookson. Fossil microplankton from Upper Mesozoic and tertiary sediments of Australia. *Cahiers de Micropaléontologie*, *4*, 1-54.

Volkheimer, W. (1980). Liassic microfloras of the Neuquén Basin (Argentina): relations with other Gondwanic areas. In *Pap. 4th Int. Palynol. Conf., Lucknow, 1976* (Vol. 2) 269-280.

Wall, D., Dale, B., Lohmann, G. P and Smith, W. K. (1977). The environmental and climatic distribution of dinoflagellate cysts in modern marine sediments from regions in the North and South Atlantic Oceans and adjacent seas. *Marine micropaleontology*, *2*, 121-200.

Waples, D. W., Kamata, H and Suizu, M. (1992). The art of maturity modeling, part 1: finding a satisfactory geologic model. *AAPG bulletin*, *76*(1), 31-46.

Warrington, G. (1982). Palynology of cores from the basal lias and the Permian (?)-Triassic sequence of the Winterborne Kingston borehole, Dorset.

Wetzel, O. (1933). The in organic matter obtain microfossils of the Baltic Chalk flint with a sediment-petrographic and stratigraphic appendix. *Palaeontographica*, *Dept. A*, *78*, 1-110.

White, H.H. (1842). On fossil Xanthidia. *Microscopical Journal* (Vol. 11, p. 35-40) Wille, W. (1982). Palynology of upper Liassic bituminous shales. In Cyclic and event stratification (pp. 505-505). Springer, Berlin, Heidelberg.

Williams, G. (1992). Palynology as a palaeoenvironmental indicator in the Brent Group, northern North Sea. *Geological Society, London, Special Publications*, *61*(1), 203-212.

Williams, G. L and Bujak, J. P. (1977). Cenozoic palynostratigraphy of offshore eastern Canada. *American Association of Stratigraphic Palynologists Contribution Series A*, *5*, 14-33.

Williams, G. L and Downie, C. (1966). The genus Hystrichokolpoma. In R. J. Davey, C. Downie, W. A. S. Sargeant and G. L. Williams (Eds.), Studies on the Mesozoic and Cainozoic dinoflagellate cyst (Vol. 3, pp. 176-181). *Bulletin of British Museum (Natural History) Geology*.

Williams, G. L., Brinkhuis, H. M. A. P., Pearce, M. A., Fensome, R. A., Weegink, J. W and Exon, N. F. (2004). Southern Ocean and global dinoflagellate cyst events compared: index events for the Late Cretaceous-Neogene. In *Proceedings of the Ocean Drilling Program, Scientific Results* (Vol. 189, pp. 1-98). College Station, Texas: Ocean Drilling Program.

Williams, G. L., Fensome, R.A and MacRae, R. A. (2017). DINOFLAJ3. American Association of Stratigraphic Palynologists, Data Series no. 2. *World Wide Web: http://dinoflaj. smu. ca/dinoflaj3*.

Williams, G. L., Fensome, R., Miller, M and Bujak, J. (2018). Microfossils, Palynology. *Encyclopedia of Petroleum Geoscience. Springer Encyclopedia of Earth Sciences Series*, 1-15.

Williams, G. L., Jansa, L. F., Clark, D.F. and Ascoli, P. A. (1974). Stratigraphy of the Shell Naskapi N-30 well, Scotia Shelf, Eastern Canada. *Geological Survey of Canada Paper*, 74(50), 1-12.

Williams, G. L., Stover, L.E and Kidson, E. J. (1993). Morphology and stratigraphic ranges of selected Mesozoic-Cenozoic dinoflagellate taxa in the Northern Hemisphere: *Geological Survey of Canada Paper* 92-10, p. 137.

Williams, G.L. (1975). Dinoflagellate and spore stratigraphy of the Mesozoic-Genozoic, offshore eastern Canada *Geological Survey of Canada, Paper*. 107-161.

Wilson, G. J. (1974). *Upper Campanian and Maastrichtian dinoflagellate cysts from the Maastricht region and Denmark* (Doctoral dissertation, University of Nottingham).

Wilson, G. J. (1978). The dinoflagellate species Isabelia druggii (Stover) and I. seelandica (Lange): their association in the Teurian of Woodside Creek, Marlborough, New Zealand. *New Zealand Journal of Geology and Geophysics*, *21*(1), 75-80.

Wilson, G.J. (1974). Upper Campanian and Maastrichtian dinoflagellate cysts from the Maastricht region and Denmark [Ph.D. dissert.]. Nottingham Univ.

Wilson, L.R and Hoffmeister, W. S. (1952). Small foraminifera. *The Micropaleontologist*, *6*(2), 26-28.

Wood, G. D., Miller, M. A., Sorer, Z., Krebs, W.N and Hedlund, R. W. (1997). Palynology, palynofacies, paleoenvironments and geochemistry of the lower cretaceous (pre-salt) Cocobeach group, north Gabon Subbasin, Gabon. *Africa Geoscience Review*, *4*, 481-498.

Yepes, O. (2001). Maastrichtian-Danian dinoflagellate cyst biostratigraphy and biogeography from two equatorial sections in Colombia and Venezuela. *Palynology*, *25*(1), 217-249.

Zobaa, M. K., El Beialy, S. Y., El-Sheikh, H.A and El Beshtawy, M. K. (2013). Jurassic-Cretaceous palynomorphs, palynofacies, and petroleum potential of the Sharib-1X and Ghoroud-1X wells, north Western Desert, Egypt. *Journal of African Earth Sciences*, *78*, 51-65.

APPENDICES

Appendix 1: Distribution chart of the palynomorphs recovered from Lynx-1X well.

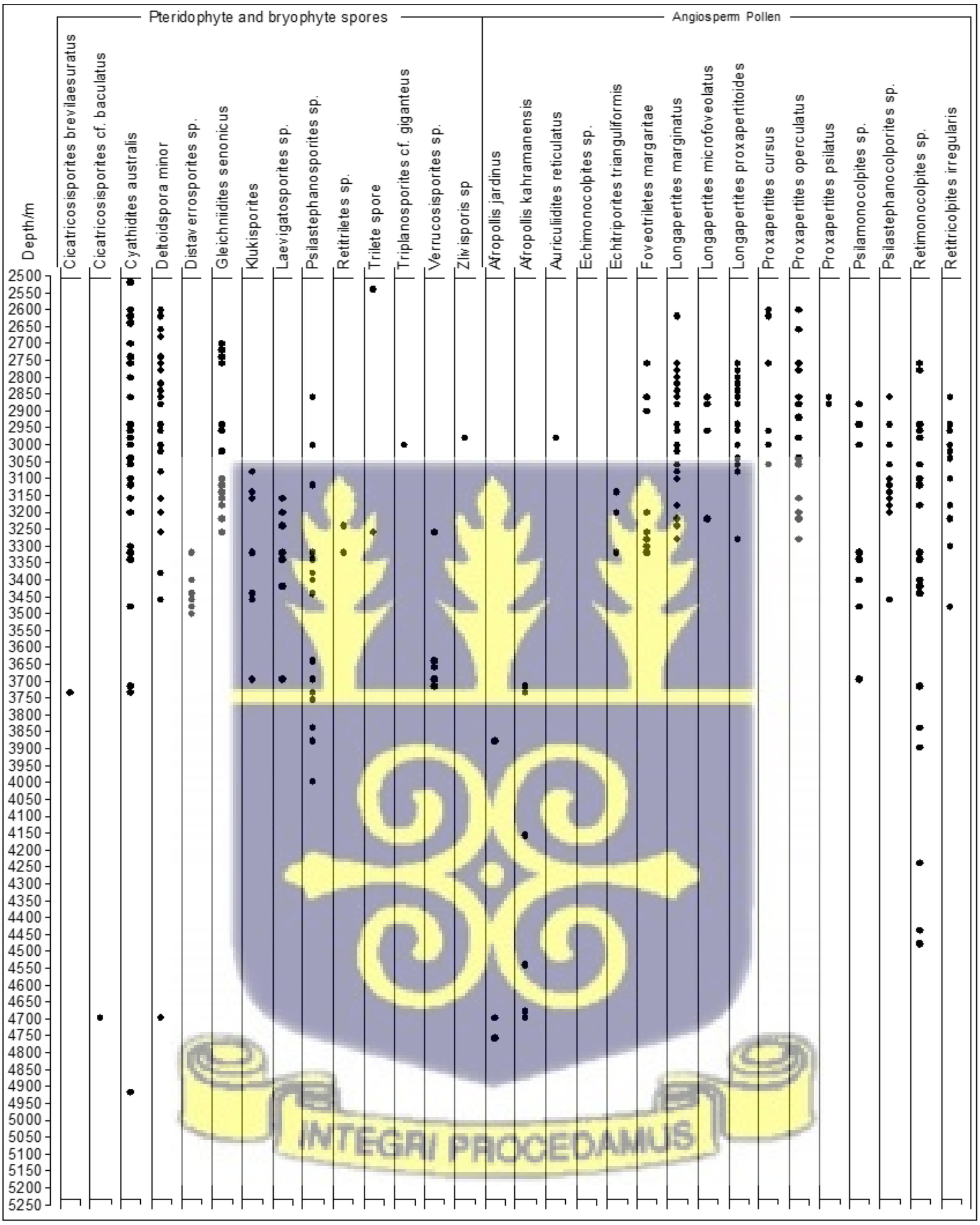

Continued.

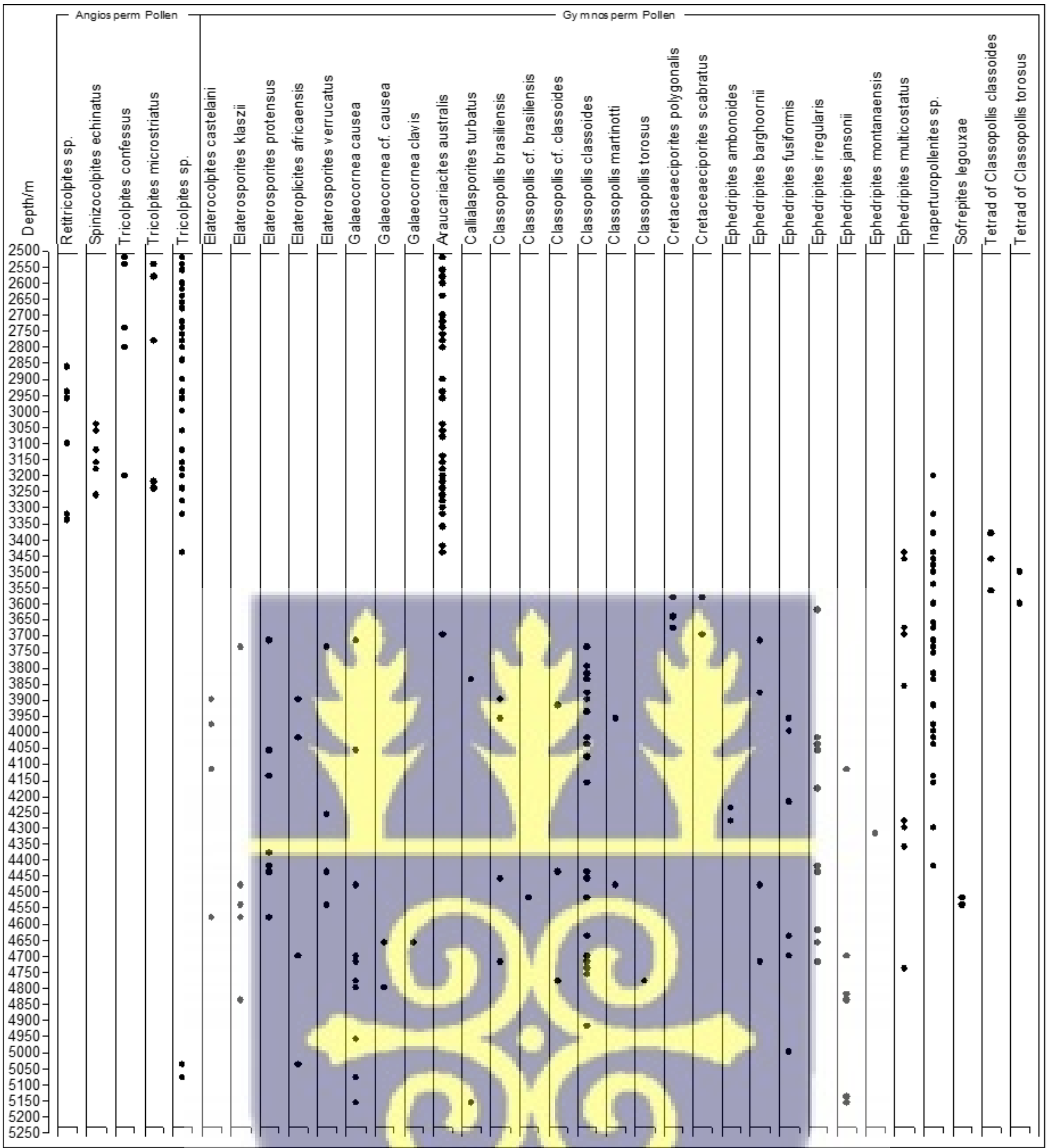

Angiosperm Pollen
Gymnosperm Pollen
Depth/m
Retitricolpites sp.
Spinizocolpites echinatus
Tricolpites confessus
Tricolpites microstriatus
Tricolpites sp.
Elaterocolpites castelaini
Elaterosporites klaszii
Elaterosporites protensus
Elateroplicites africaensis
Elaterosporites verrucatus
Galaeocornea causea
Galaeocornea cf. causea
Galaeocornea clavis
Araucariacites australis
Callialasporites turbatus
Classopollis brasiliensis
Classopollis cf. brasiliensis
Classopollis cf. classoides
Classopollis classoides
Classopollis martinotti
Classopollis torosus
Cretaceaeciporites polygonalis
Cretaceaeciporites scabratus
Ephedripites ambonoides
Ephedripites barghoornii
Ephedripites fusiformis
Ephedripites irregularis
Ephedripites jansonii
Ephedripites montanaensis
Ephedripites multicostatus
Inaperturopollenites sp.
Sofrepites legouxae
Tetrad of Classopollis classoides
Tetrad of Classopollis torosus
2500
2550
2600
2650
2700
2750
2800
2850
2900
2950
3000
3050
3100
3150
3200
3250
3300
3350
3400
3450
3500
3550
3600
3650
3700
3750
3800
3850
3900
3950
4000
4050
4100
4150
4200
4250
4300
4350
4400
4450
4500
4550
4600
4650
4700
4750
4800
4850
4900
4950
5000
5050
5100
5150
5200
5250

Continued.

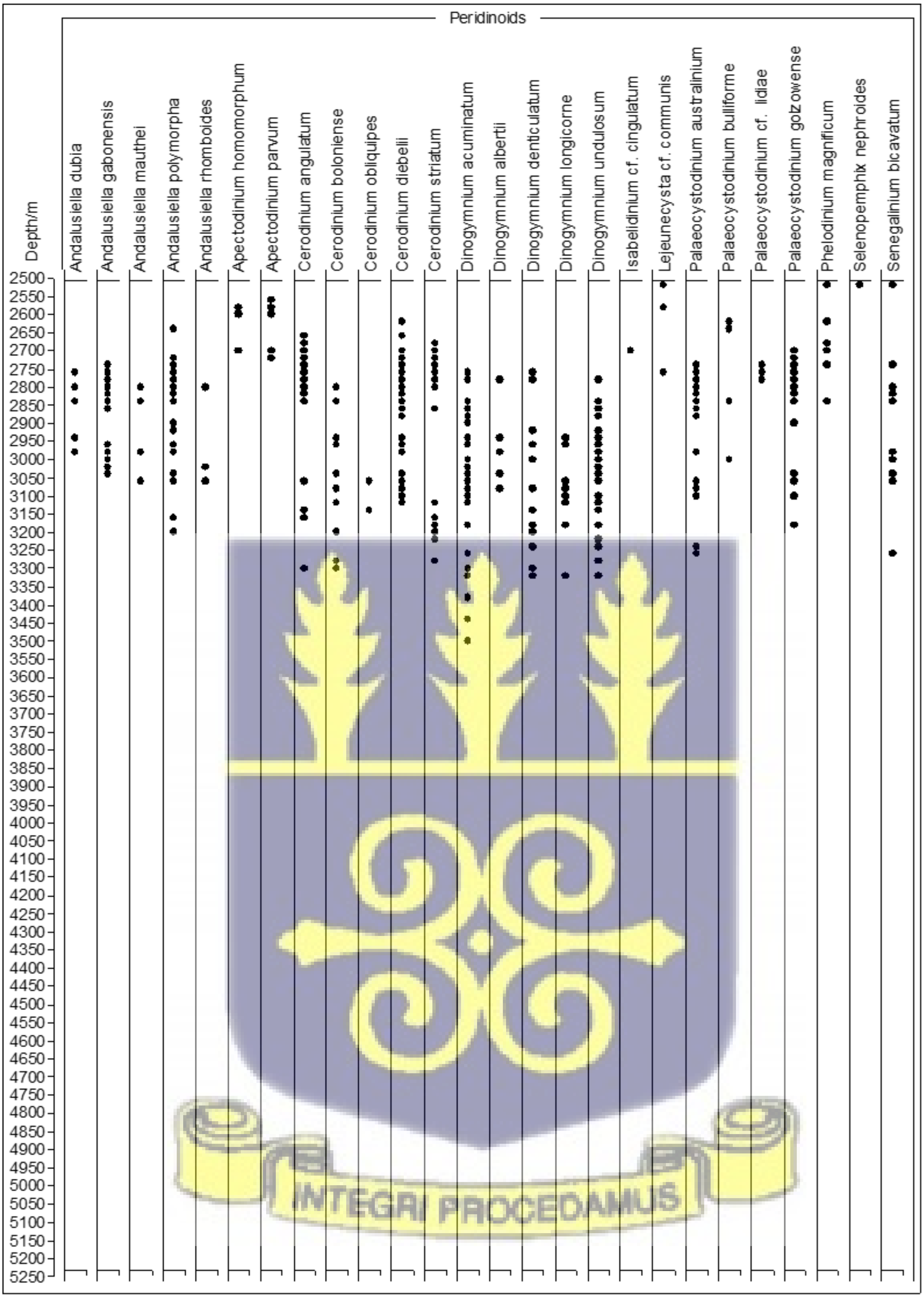
Peridinoids
Depth/m
Andalusiella dubia
Andalusiella gabonensis
Andalusiella mauthei
Andalusiella polymorpha
Andalusiella rhomboides
Apectodinium homomorphum
Apectodinium parvum
Cerodinium angulatum
Cerodinium boloniense
Cerodinium obliquipes
Cerodinium diebelii
Cerodinium striatum
Dinogymnium acuminatum
Dinogymnium albertii
Dinogymnium denticulatum
Dinogymnium longicorne
Dinogymnium undulosum
Isabelidinium cf. cingulatum
Lejeunecysta cf. communis
Palaeocystodinium australinium
Palaeocystodinium bulliforme
Palaeocystodinium cf. lidiae
Palaeocystodinium golzowense
Phelodinium magnificum
Selenopemphix nephroides
Senegalinium bicavatum
2500
2550
2600
2650
2700
2750
2800
2850
2900
2950
3000
3050
3100
3150
3200
3250
3300
3350
3400
3450
3500
3550
3600
3650
3700
3750
3800
3850
3900
3950
4000
4050
4100
4150
4200
4250
4300
4350
4400
4450
4500
4550
4600
4650
4700
4750
4800
4850
4900
4950
5000
5050
5100
5150
5200
5250

Continued.

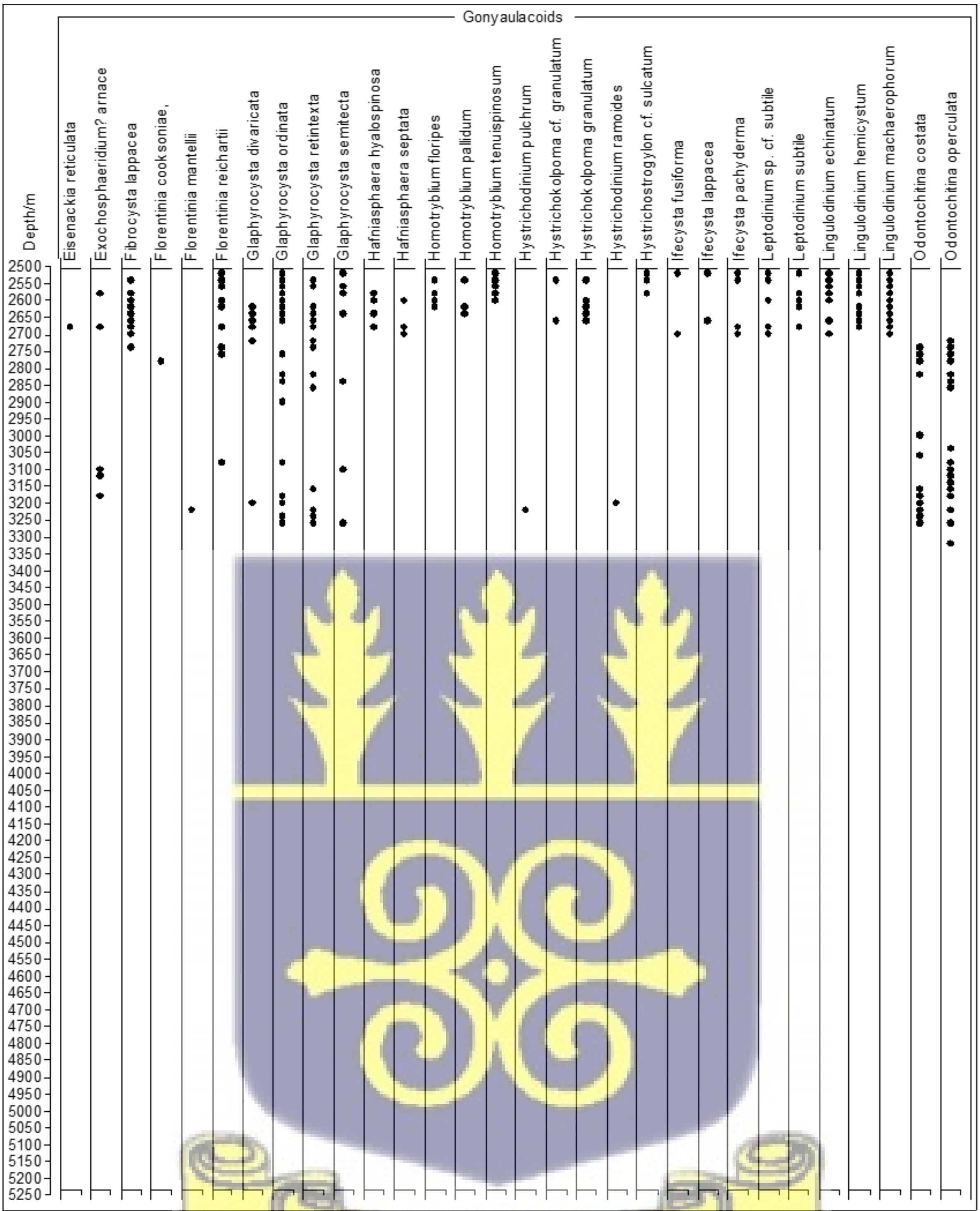
Gonyaulacoids
Depth/m
Eisenackia reticulata
Exochosphaeridium? arnace
Fibrocysta lappacea
Florentinia cooksoniae,
Florentinia mantellii
Florentinia reichartii
Glaphyrocysta divaricata
Glaphyrocysta ordinata
Glaphyrocysta retintexta
Glaphyrocysta semitecta
Hafniasphaera hyalospinosa
Hafniasphaera septata
Homotryblium floripes
Homotryblium pallidum
Homotryblium tenuispinosum
Hystrichodinium pulchrum
Hystrichokolpoma cf. granulatum
Hystrichokolpoma granulatum
Hystrichodinium ramoides
Hystrichostrogylon cf. sulcatum
Ifecysta fusiforma
Ifecysta lappacea
Ifecysta pachyderma
Leptodinium sp. cf. subtile
Leptodinium subtile
Lingulodinium echinatum
Lingulodinium hemicystum
Lingulodinium machaerophorum
Odontochitina costata
Odontochitina operculata
2500
2550
2600
2650
2700
2750
2800
2850
2900
2950
3000
3050
3100
3150
3200
3250
3300
3350
3400
3450
3500
3550
3600
3650
3700
3750
3800
3850
3900
3950
4000
4050
4100
4150
4200
4250
4300
4350
4400
4450
4500
4550
4600
4650
4700
4750
4800
4850
4900
4950
5000
5050
5100
5150
5200
5250

Continued.

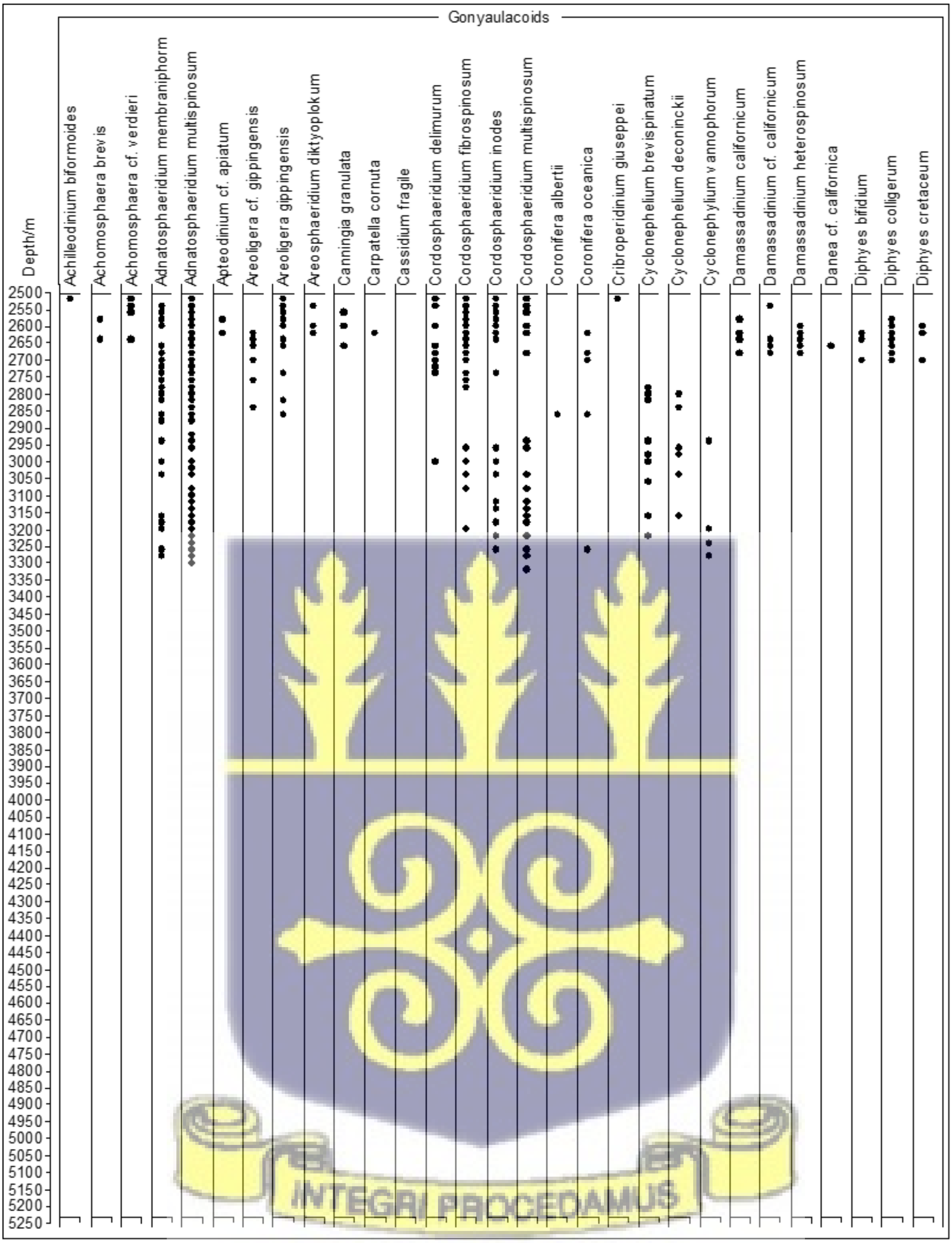
Gonyaulacoids
Depth/m
Achilleodinium biformoides
Achomosphaera brevis
Achomosphaera cf. verdieri
Adnatosphaeridium membraniphorm
Adnatosphaeridium multispinosum
Apteodinium cf. apiatum
Areoligera cf. gippingensis
Areoligera gippingensis
Areosphaeridium diktyoplokum
Canningia granulata
Carpatella cornuta
Cassidium fragile
Cordosphaeridium delimurum
Cordosphaeridium fibrospinosum
Cordosphaeridium inodes
Cordosphaeridium multispinosum
Coronifera albertii
Coronifera oceanica
Cribroperidinium giuseppei
Cyclonephelium brevispinatum
Cyclonephelium deconinckii
Cyclonephylium vannophorum
Damassadinium californicum
Damassadinium cf. californicum
Damassadinium heterospinosum
Danea cf. californica
Diphyes bifidum
Diphyes colligerum
Diphyes cretaceum
2500
2550
2600
2650
2700
2750
2800
2850
2900
2950
3000
3050
3100
3150
3200
3250
3300
3350
3400
3450
3500
3550
3600
3650
3700
3750
3800
3850
3900
3950
4000
4050
4100
4150
4200
4250
4300
4350
4400
4450
4500
4550
4600
4650
4700
4750
4800
4850
4900
4950
5000
5050
5100
5150
5200
5250

Continued.

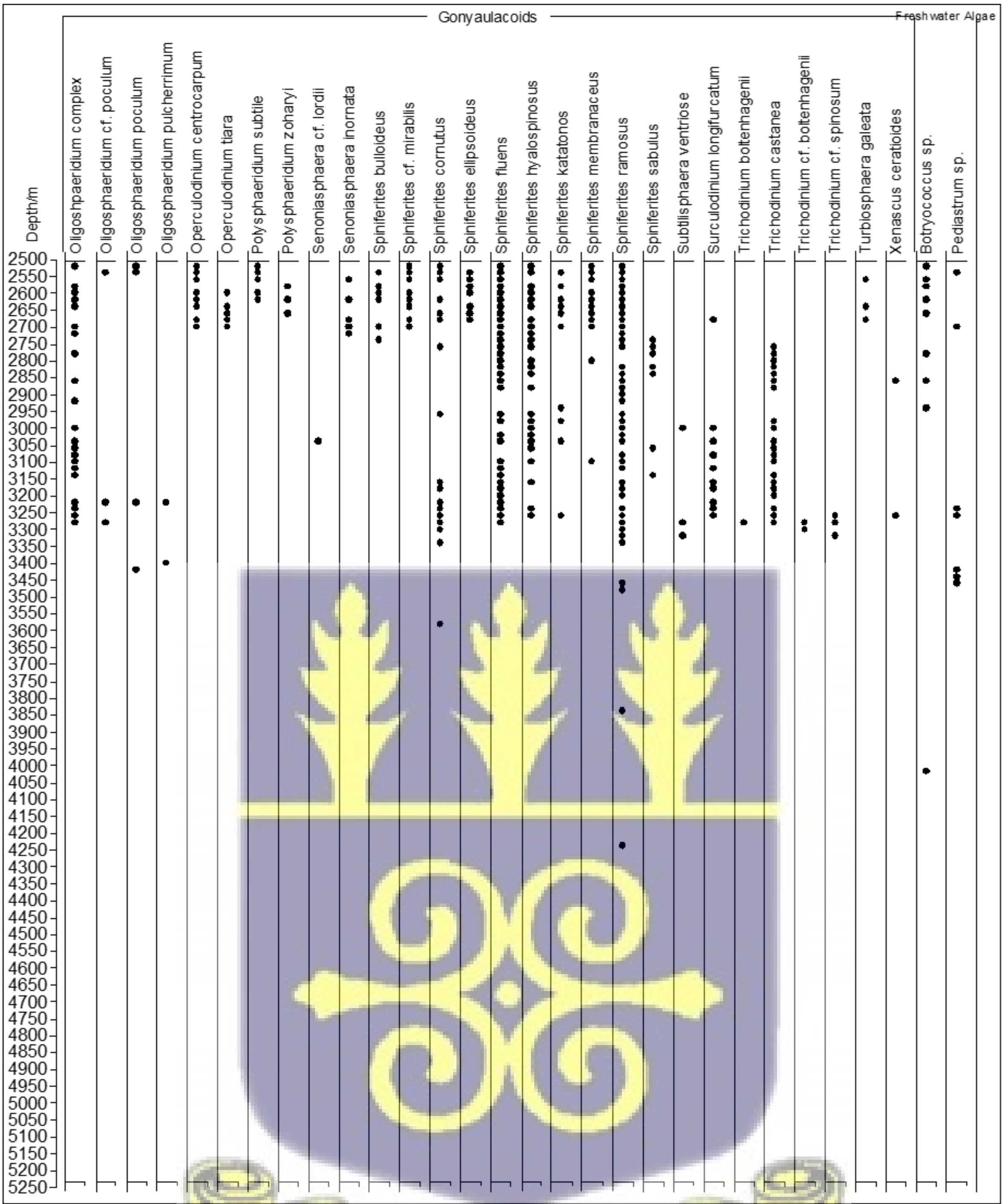

Gonyaulacoids
Freshwater Algae
Depth/m
Oligoshpaeridium complex
Oligosphaeridium cf. poculum
Oligosphaeridium poculum
Oligosphaeridium pulcherrimum
Operculodinium centrocarpum
Operculodinium tiara
Polysphaeridium subtile
Polysphaeridium zoharyi
Senoniasphaera cf. lordii
Senoniasphaera inornata
Spiniferites bulloideus
Spiniferites cf. mirabilis
Spiniferites cornutus
Spiniferites ellipsoideus
Spiniferites fluens
Spiniferites hyalospinosus
Spiniferites katatonos
Spiniferites membranaceus
Spiniferites ramosus
Spiniferites sabulus
Subtilisphaera ventriose
Surculodinium longifurcatum
Trichodinium boltenhagenii
Trichodinium castanea
Trichodinium cf. boltenhagenii
Trichodinium cf. spinosum
Turbiosphaera galeata
Xenascus ceratioides
Botryococcus sp.
Pediastrum sp.
2500
2550
2600
2650
2700
2750
2800
2850
2900
2950
3000
3050
3100
3150
3200
3250
3300
3350
3400
3450
3500
3550
3600
3650
3700
3750
3800
3850
3900
3950
4000
4050
4100
4150
4200
4250
4300
4350
4400
4450
4500
4550
4600
4650
4700
4750
4800
4850
4900
4950
5000
5050
5100
5150
5200
5250

Appendix 2: Distribution chart of the palynomorphs recovered from Dzata-1 well.

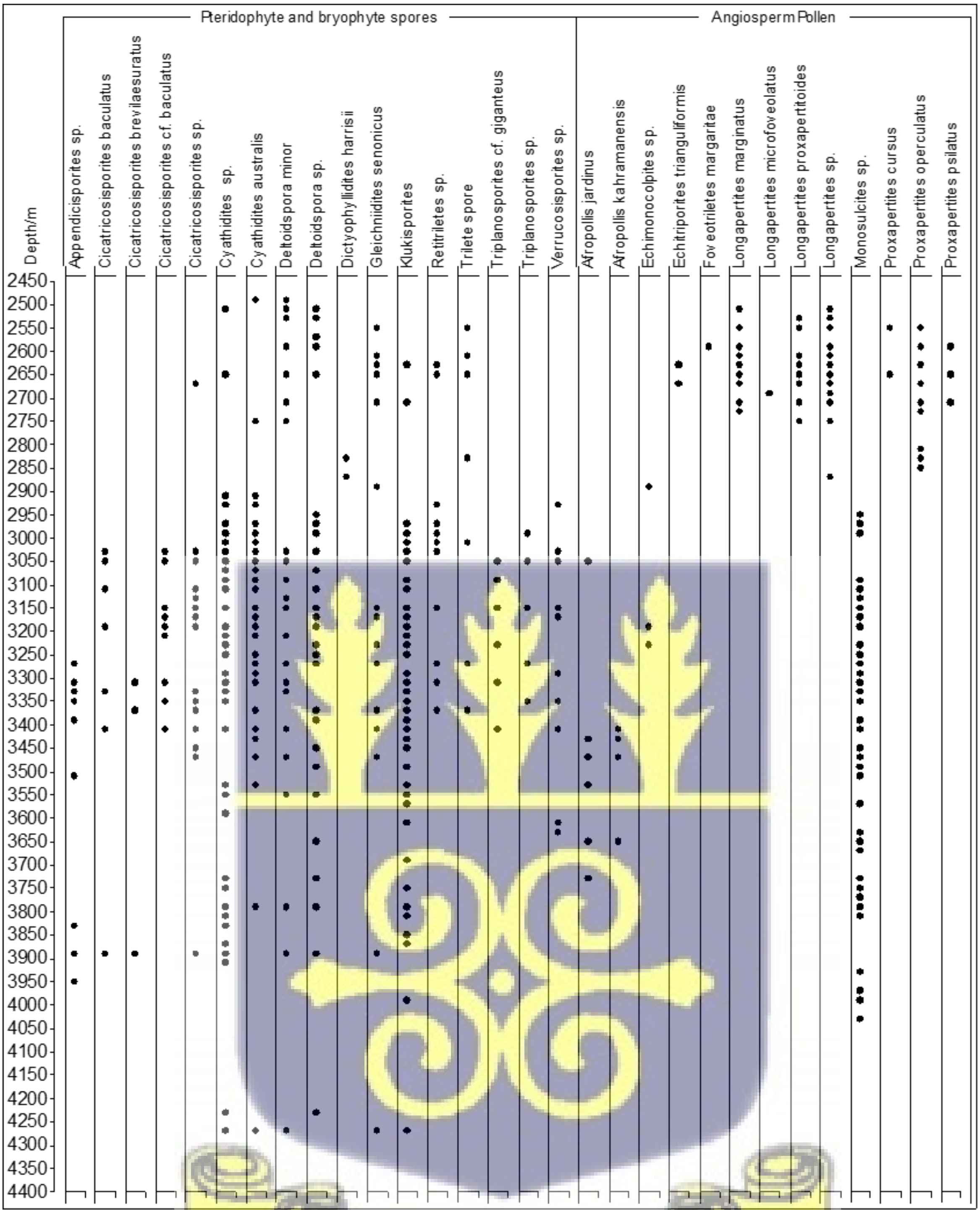

Continued.

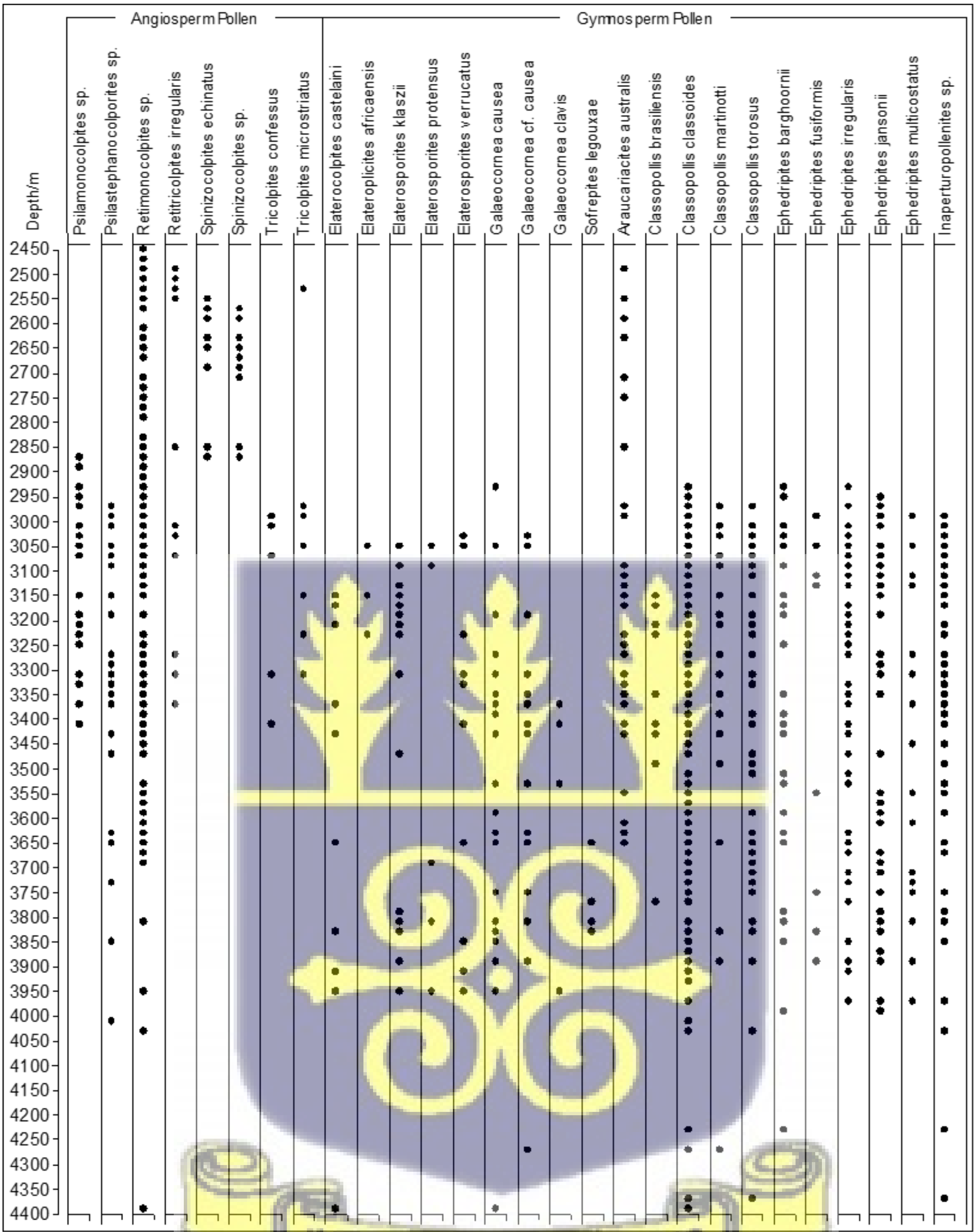
Angiosperm Pollen
Gymnosperm Pollen
Depth/m
Psilamonocolpites sp.
Psilastephanocolporites sp.
Retimonocolpites sp.
Retitricolpites irregularis
Spinizocolpites echinatus
Spinizocolpites sp.
Tricolpites confessus
Tricolpites microstriatus
Elaterocolpites castelaini
Elateroplicites africaensis
Elaterosporites klaszii
Elaterosporites protensus
Elaterosporites verrucatus
Galaeocornea causea
Galaeocornea cf. causea
Galaeocornea clavis
Sofrepites legouxae
Araucariacites australis
Classopollis brasiliensis
Classopollis classoides
Classopollis martinotti
Classopollis torosus
Ephedripites barghoornii
Ephedripites fusiformis
Ephedripites irregularis
Ephedripites jansonii
Ephedripites multicostatus
Inaperturopollenites sp.
2450
2500
2550
2600
2650
2700
2750
2800
2850
2900
2950
3000
3050
3100
3150
3200
3250
3300
3350
3400
3450
3500
3550
3600
3650
3700
3750
3800
3850
3900
3950
4000
4050
4100
4150
4200
4250
4300
4350
4400

Continued.

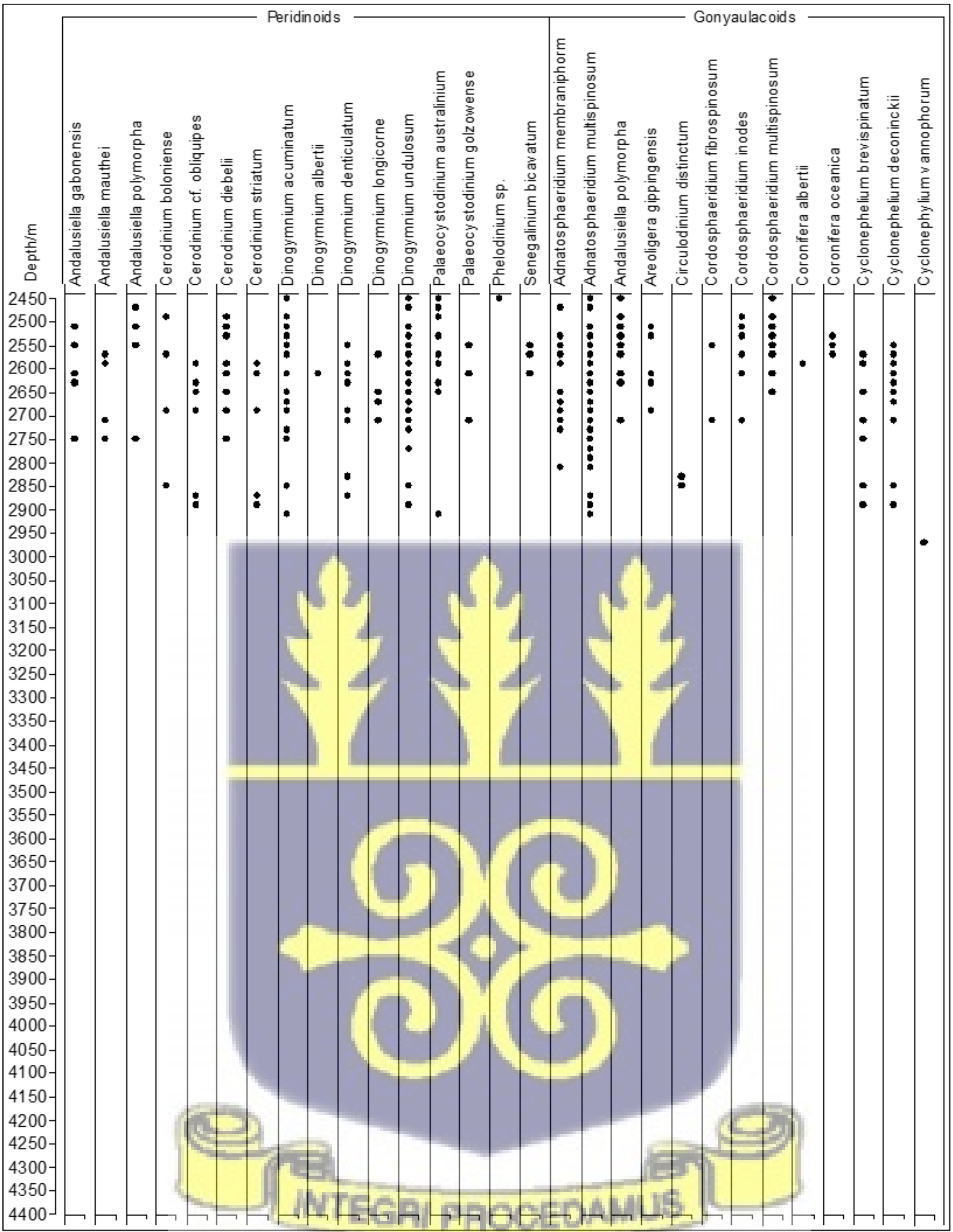
Depth/m
Peridinoids
Gonyaulacoids
Andalusiella gabonensis
Andalusiella mauthei
Andalusiella polymorpha
Cerodinium boloniense
Cerodinium cf. obliquipes
Cerodinium diebelii
Cerodinium striatum
Dinogymnium acuminatum
Dinogymnium albertii
Dinogymnium denticulatum
Dinogymnium longicorne
Dinogymnium undulosum
Palaeocystodinium australinium
Palaeocystodinium golzowense
Phelodinium sp.
Senegalinium bicavatum
Adnatosphaeridium membraniphorm
Adnatosphaeridium multispinosum
Andalusiella polymorpha
Areoligera gippingensis
Circulodinium distinctum
Cordosphaeridium fibrospinosum
Cordosphaeridium inodes
Cordosphaeridium multispinosum
Coronifera albertii
Coronifera oceanica
Cyclonephelium brevispinatum
Cyclonephelium deconinckii
Cyclonephylium vannophorum
2450
2500
2550
2600
2650
2700
2750
2800
2850
2900
2950
3000
3050
3100
3150
3200
3250
3300
3350
3400
3450
3500
3550
3600
3650
3700
3750
3800
3850
3900
3950
4000
4050
4100
4150
4200
4250
4300
4350
4400

Continued.

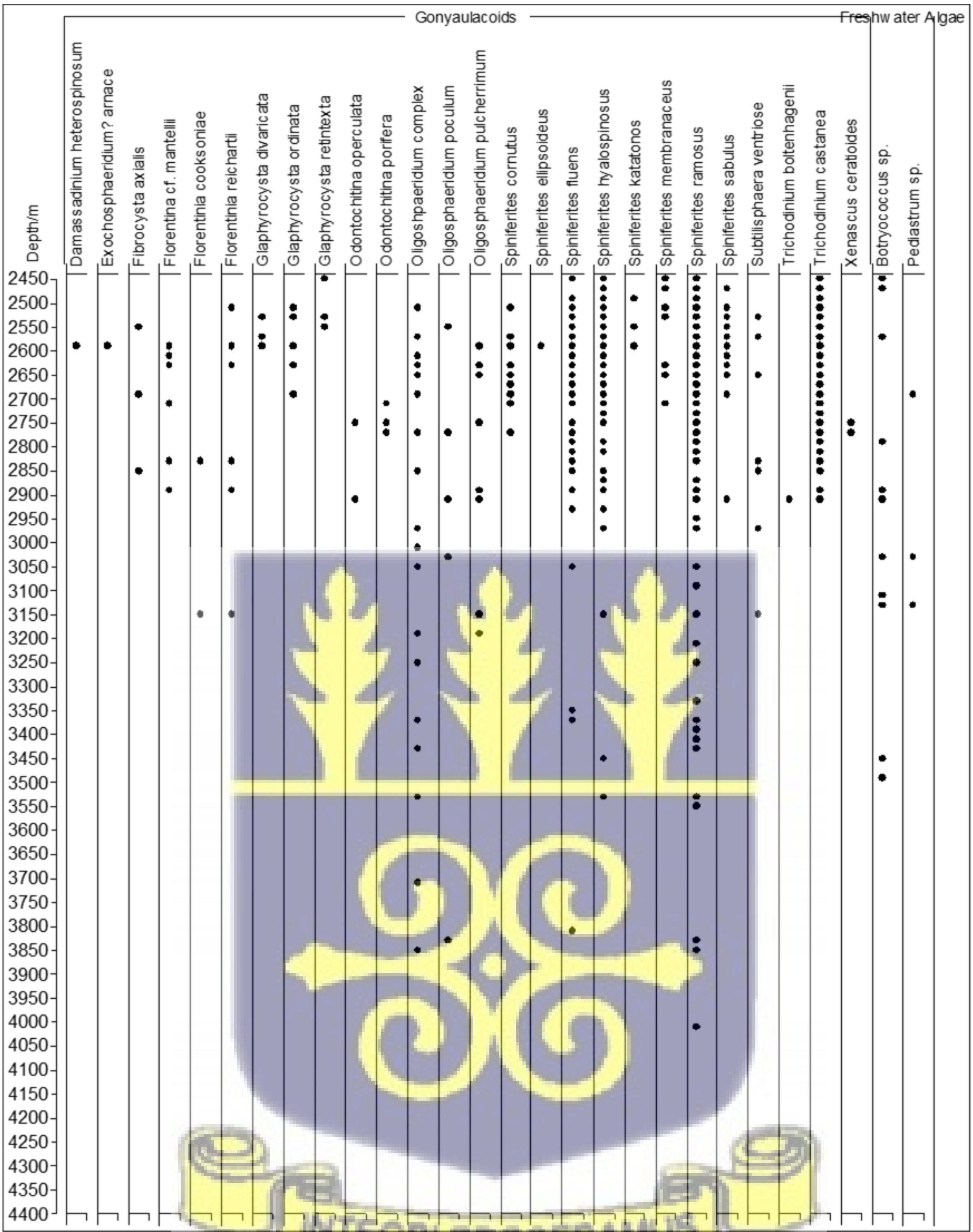

Gonyaulacoids
Freshwater Algae
Depth/m
Damassadinium heterospinosum
Exochosphaeridium ? arnace
Fibrocysta axialis
Florentina cf. mantellii
Florentinia cooksoniae
Florentinia reichartii
Glaphyrocysta divaricata
Glaphyrocysta ordinata
Glaphyrocysta retintexta
Odontochitina operculata
Odontochitina porifera
Oligoshpaeridium complex
Oligosphaeridium poculum
Oligosphaeridium pulcherrimum
Spiniferites cornutus
Spiniferites ellipsoideus
Spiniferites fluens
Spiniferites hyalospinosus
Spiniferites katatonos
Spiniferites membranaceus
Spiniferites ramosus
Spiniferites sabulus
Subtilisphaera ventriose
Trichodinium boltenhagenii
Trichodinium castanea
Xenascus ceratioides
Botryococcus sp.
Pediastrum sp.
2450
2500
2550
2600
2650
2700
2750
2800
2850
2900
2950
3000
3050
3100
3150
3200
3250
3300
3350
3400
3450
3500
3550
3600
3650
3700
3750
3800
3850
3900
3950
4000
4050
4100
4150
4200
4250
4300
4350
4400

Appendix 3: Distribution chart of the palynomorphs recovered from Dzata-2A well.

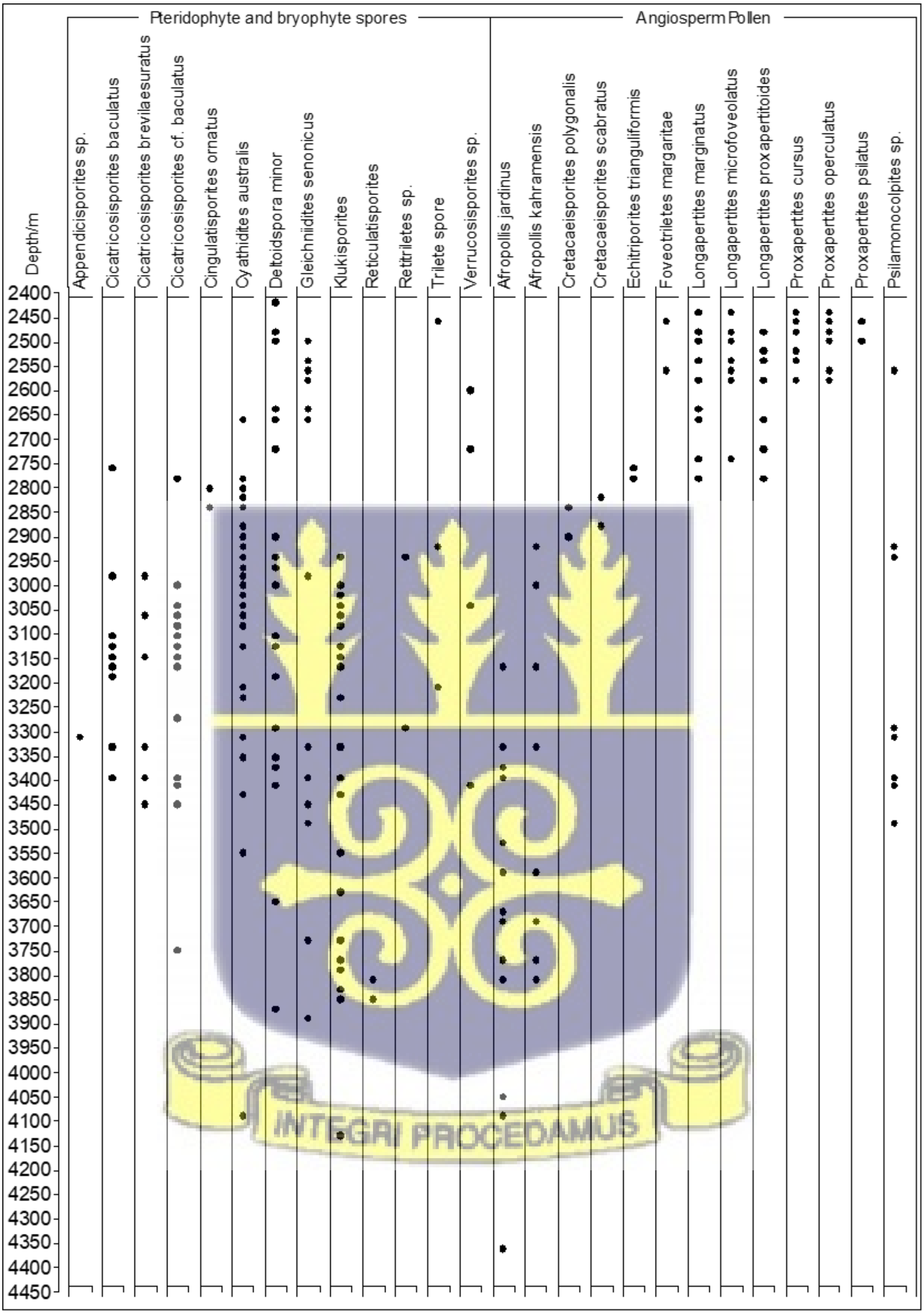

Continued.

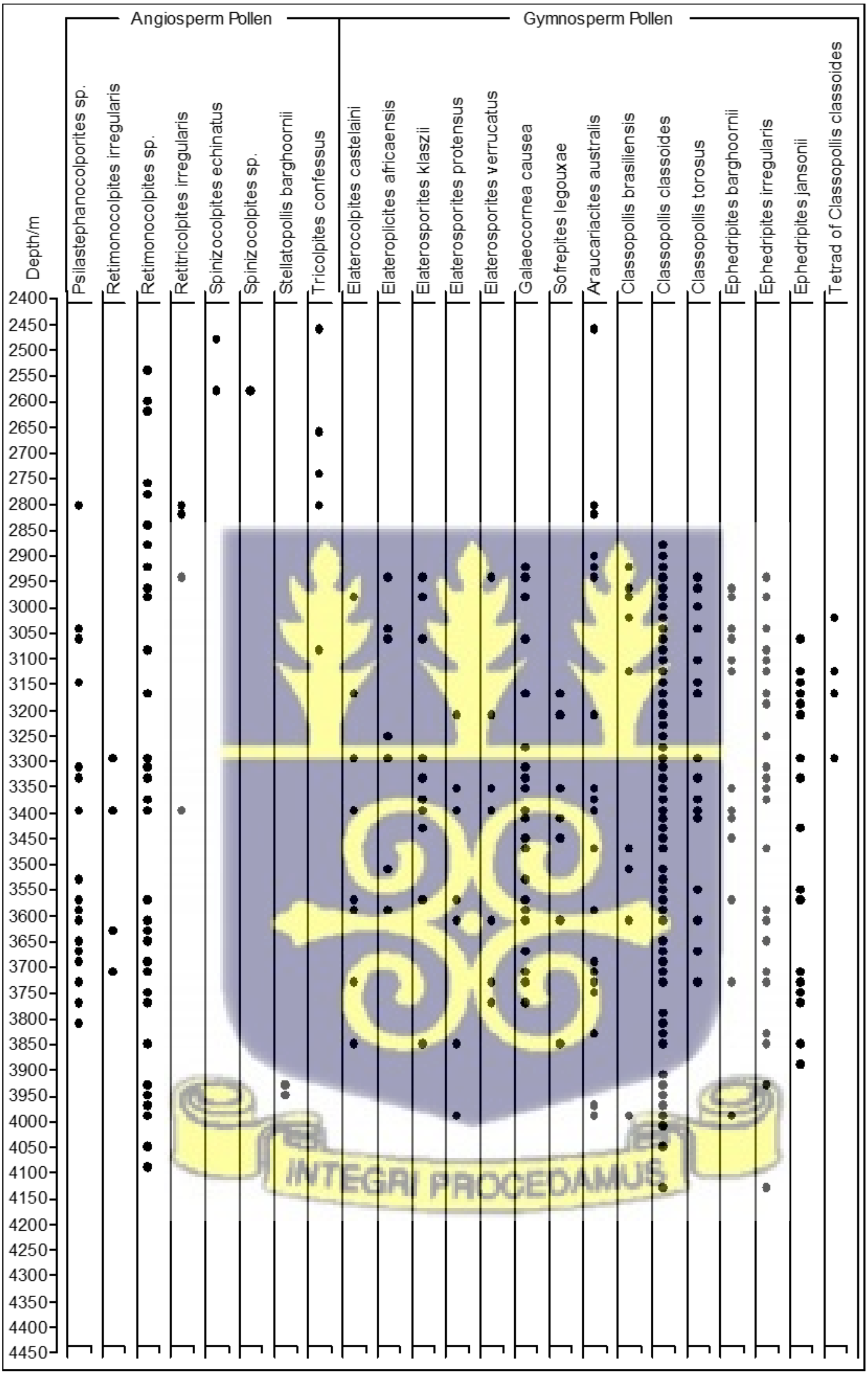

Angiosperm Pollen
Gymnosperm Pollen
Depth/m
Psilastephanocolporites sp.
Retimonocolpites irregularis
Retimonocolpites sp.
Retitricolpites irregularis
Spinizocolpites echinatus
Spinizocolpites sp.
Stellatopollis barghoornii
Tricolpites confessus
Elaterocolpites castelaini
Elateroplicites africaensis
Elaterosporites klaszii
Elaterosporites protensus
Elaterosporites verrucatus
Galaeocornea causea
Sofrepites legouxae
Araucariacites australis
Classopollis brasiliensis
Classopollis classoides
Classopollis torosus
Ephedripites barghoornii
Ephedripites irregularis
Ephedripites jansonii
Tetrad of Classopollis classoides
2400
2450
2500
2550
2600
2650
2700
2750
2800
2850
2900
2950
3000
3050
3100
3150
3200
3250
3300
3350
3400
3450
3500
3550
3600
3650
3700
3750
3800
3850
3900
3950
4000
4050
4100
4150
4200
4250
4300
4350
4400
4450

Continued.

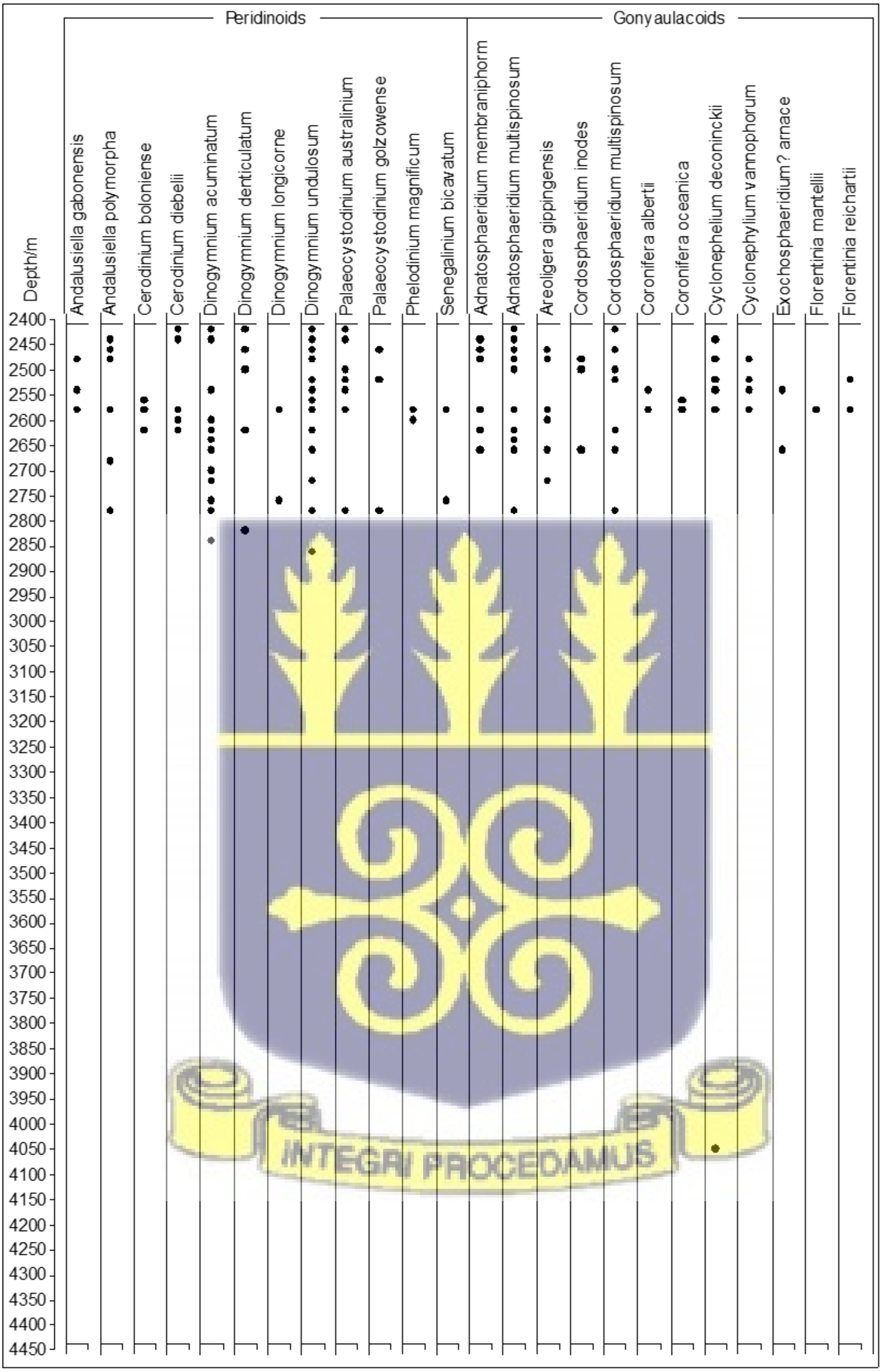
Peridinoids
Gonyaulacoids
Depth/m
Andalusiella gabonensis
Andalusiella polymorpha
Cerodinium boloniense
Cerodinium diebelii
Dinogymnium acuminatum
Dinogymnium denticulatum
Dinogymnium longicorne
Dinogymnium undulosum
Palaeocystodinium australinium
Palaeocystodinium golzowense
Phelodinium magnificum
Senegalinium bicavatum
Adnatosphaeridium membraniphorm
Adnatosphaeridium multispinosum
Areoligera gippingensis
Cordosphaeridium inodes
Cordosphaeridium multispinosum
Coronifera albertii
Coronifera oceanica
Cyclonephelium deconinckii
Cyclonephylium vannophorum
Exochosphaeridium? arnace
Florentinia mantellii
Florentinia reichartii
2400
2450
2500
2550
2600
2650
2700
2750
2800
2850
2900
2950
3000
3050
3100
3150
3200
3250
3300
3350
3400
3450
3500
3550
3600
3650
3700
3750
3800
3850
3900
3950
4000
4050
4100
4150
4200
4250
4300
4350
4400
4450

Continued.

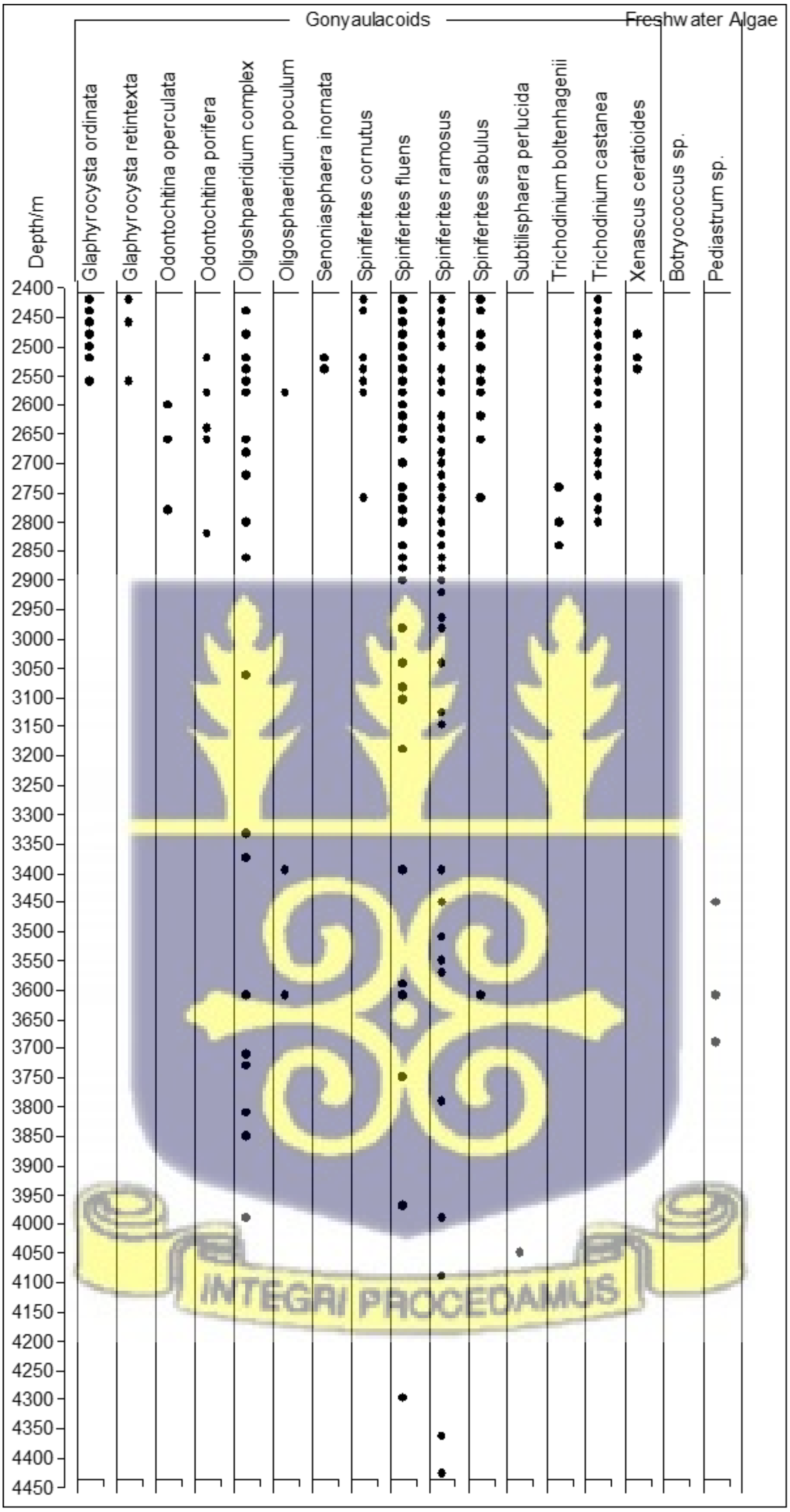

Gonyaulacoids
Freshwater Algae
Depth/m
Glaphyrocysta ordinata
Glaphyrocysta retintexta
Odontochitina operculata
Odontochitina porifera
Oligoshpaeridium complex
Oligosphaeridium poculum
Senoniasphaera inornata
Spiniferites cornutus
Spiniferites fluens
Spiniferites ramosus
Spiniferites sabulus
Subtilisphaera perlucida
Trichodinium boltenhagenii
Trichodinium castanea
Xenascus ceratioides
Botryococcus sp.
Pediastrum sp.
2400
2450
2500
2550
2600
2650
2700
2750
2800
2850
2900
2950
3000
3050
3100
3150
3200
3250
3300
3350
3400
3450
3500
3550
3600
3650
3700
3750
3800
3850
3900
3950
4000
4050
4100
4150
4200
4250
4300
4350
4400
4450

Appendix 4: Relative abundance (%) of POM and palynomorphs in Lynx-1X well

Depth/m	AOM (%)	Opaques (%)	Phytoclasts (%)	Spores (%)	Pollen (%)	Gonyaulacoids (%)	Peridinoids (%)
2520	36	29	6	2	5	19	3
2540	35	25	4	2	6	24	4
2560	34	26	6	1	5	25	3
2580	28	30	4	1	8	25	4
2600	35	33	3	1	4	22	2
2620	30	30	1	2	9	26	2
2640	23	23	6	1	9	33	5
2660	22	28	8	2	6	27	7
2680	20	32	8	1	6	23	10
2700	20	28	10	2	8	23	9
2720	23	29	20	1	8	8	11
2740	19	21	28	2	8	9	13
2760	27	21	28	1	7	5	11
2780	20	26	23	2	9	6	14
2800	23	20	22	3	10	8	14
2820	38	12	26	3	8	7	6
2840	41	10	24	2	8	8	7
2860	45	11	26	2	6	6	4
2880	42	12	22	1	10	7	6
2900	64	10	12	1	5	4	4
2920	58	6	8	1	8	11	8
2940	60	18	4	1	4	9	4
2960	52	8	16	1	8	9	6
2980	54	10	8	1	9	10	8
3000	54	9	12	0	5	13	7
3020	52	12	15	1	5	11	4
3040	55	14	12	1	5	8	5
3060	58	15	7	1	5	9	5
3080	52	18	6	0	6	12	6
3100	57	9	4	2	11	10	7
3120	52	7	7	2	12	14	6
3140	47	10	6	1	10	18	8
3160	58	12	4	2	10	10	4
3180	50	10	5	2	10	18	5
3200	51	7	8	2	8	19	5

Continued.

Depth/m	AOM (%)	Opaques (%)	Phytoclasts (%)	Spores (%)	Pollen (%)	Gonyaulacoids (%)	Peridinoids (%)
3220	53	12	6	2	7	15	5
3240	61	11	5	1	6	13	3
3260	60	13	6	1	7	10	3
3280	62	8	4	1	5	14	6
3300	60	8	8	1	5	13	5
3320	73	19	3	1	4	0	0
3340	72	24	4	0	0	0	0
3360	66	23	7	0	3	0	0
3380	77	20	3	0	0	0	0
3400	73	21	4	1	1	0	0
3420	72	21	7	0	0	0	0
3440	73	20	6	0	1	0	0
3460	66	26	6	0	1	0	0
3480	69	24	5	1	1	0	0
3500	70	22	8	0	0	0	0
3520	70	24	6	0	0	0	0
3540	72	11	16	0	1	0	0
3560	72	13	15	0	0	0	0
3580	64	16	19	0	1	0	0
3600	66	18	13	0	3	0	0
3620	70	17	12	0	1	0	0
3640	67	15	18	0	0	0	0
3656-3660	72	23	5	0	0	0	0
3670-3680	76	20	4	0	0	0	0
3690-3700	75	20	5	0	0	0	0
3710-3720	70	25	5	0	0	0	0
3730-3740	66	29	5	0	0	0	0
3750-3760	67	30	2	0	1	0	0
3770-3780	73	23	4	0	0	0	0
3790-3800	71	20	9	0	0	0	0
3815-3820	74	19	6	0	1	0	0
3835-3840	71	21	7	1	0	0	0
3855-3860	75	22	3	0	0	0	0
3875-3880	48	42	10	0	0	0	0
3895-3900	48	35	14	0	3	0	0
3915-3920	46	44	7	0	3	0	0

Continued.

Depth/m	AOM (%)	Opaques (%)	Phytoclasts (%)	Spores (%)	Pollen (%)	Gonyaulacoids (%)	Peridinoids (%)
3935-3940	41	48	10	0	1	0	0
3955-3960	50	50	0	0	0	0	0
3975-3980	43	56	1	0	0	0	0
3995-4000	40	46	11	0	3	0	0
4015-4020	40	49	8	0	2	0	0
4035-4040	48	44	7	0	1	0	0
4055-4060	22	73	5	0	0	0	0
4075-4080	23	73	3	0	1	0	0
4095-4100	22	70	8	0	0	0	0
4115-4120	25	74	1	0	0	0	0
4135-4140	27	71	2	0	0	0	0
4155-4160	22	76	2	0	0	0	0
4175-4180	22	75	3	0	0	0	0
4195-4200	14	75	10	0	1	0	0
4215-4220	13	79	6	0	2	0	0
4235-4240	18	70	9	0	3	0	0
4255-4260	17	75	7	0	1	0	0
4275-4280	14	80	6	0	0	0	0
4295-4300	11	81	7	0	1	0	0
4315-4320	10	80	8	0	2	0	0
4355-4360	15	83	2	0	0	0	0
4375-4380	12	81	7	0	0	0	0
4395-4400	16	82	1	0	1	0	0
4415-4420	13	79	3	1	4	0	0
4435-4440	10	84	2	1	3	0	0
4455-4460	10	80	3	0	7	0	0
4475-4480	10	86	3	0	1	0	0
4495-4500	11	82	7	0	0	0	0
4515-4520	14	84	2	0	0	0	0
4540	14	85	1	0	0	0	0
4580	40	50	8	0	2	0	0
4595-4600	44	53	3	0	0	0	0
4615-4620	45	48	6	0	1	0	0
4635-4640	51	40	7	0	2	0	0
4655-4660	10	83	7	0	0	0	0
4675-4680	14	80	5	0	1	0	0

Continued.

Depth/m	AOM (%)	Opaques (%)	Phytoclasts (%)	Spores (%)	Pollen (%)	Gonyaulacoids (%)	Peridinoids (%)
4695-4700	10	78	6	0	6	0	0
4715-4720	9	79	4	1	7	0	0
4735-4740	42	48	9	0	1	0	0
4755-4760	43	47	7	0	3	0	0
4775-4780	40	42	15	0	3	0	0
4795-4800	43	51	5	0	1	0	0
4815-4820	44	50	6	0	0	0	0
4835-4840	42	47	10	0	1	0	0
4895-4900	58	28	12	0	2	0	0
4915-5920	53	31	10	1	5	0	0
4955-4960	50	35	12	1	2	0	0
4995-5000	48	42	9	0	1	0	0
5035-5040	9	90	1	0	0	0	0
5075-5080	11	80	9	0	0	0	0
5095-5100	18	78	4	0	0	0	0
5135-5140	20	71	7	0	2	0	0
5155-5160	13	80	4	0	3	0	0
5215-5220	18	80	2	0	0	0	0
5235-5240	12	84	3	0	1	0	0
5275-5280	10	87	1	0	2	0	0
5295-5300	10	85	5	0	0	0	0

Appendix 5: Relative abundance (%) of POM and palynomorphs in Dzata-1 well

Depth/m	AOM (%)	Opaques (%)	Phytoclasts (%)	Spores (%)	Pollen (%)	Gonyaulacoids (%)	Peridinoids (%)
2450	60	8	12	1	1	16	2
2470	67	4	7	2	2	15	3
2490	57	10	10	1	2	16	3
2510	60	8	8	1	3	16	4
2530	61	10	9	0	2	16	1
2550	60	6	12	1	2	17	2
2570	66	5	6	1	2	18	2
2590	60	4	8	0	4	21	3
2610	62	3	5	0	4	24	2
2630	70	2	4	1	2	20	2
2650	68	3	4	0	2	21	2
2670	70	5	6	1	2	15	1
2690	71	3	5	0	2	17	1
2710	68	4	8	1	2	16	1
2730	70	5	6	1	2	15	1
2750	80	2	6	1	1	9	1
2770	82	3	5	0	2	12	2
2790	77	2	3	1	1	15	1
2810	74	4	5	1	2	13	1
2830	76	3	6	2	1	11	1
2850	79	2	6	1	1	9	2
2870	81	3	5	0	1	7	2
2890	78	2	8	1	2	8	1
2910	80	1	4	1	1	13	1
2930	75	4	3	1	1	14	2
2950	74	6	5	0	2	11	2
2970	77	7	6	1	1	8	1
2990	73	5	8	1	2	8	2
3010	76	3	5	1	1	11	3
3030	34	40	17	1	8	0	0
3050	30	45	15	1	9	0	0
3070	40	42	12	0	5	0	0
3090	23	52	18	0	7	0	0
3110	32	44	15	0	8	0	0
3130	40	46	8	1	5	0	1

Continued.

Depth/m	AOM (%)	Opaques (%)	Phytoclasts (%)	Spores (%)	Pollen (%)	Gonyaulacoids (%)	Peridinoids (%)
3150	30	54	9	0	6	0	0
3170	65	13	9	6	7	0	0
3190	71	11	6	4	8	0	0
3210	76	8	5	4	7	0	0
3230	32	30	24	3	11	0	0
3250	22	36	18	4	20	0	0
3270	20	32	20	5	23	0	0
3290	21	30	20	6	23	0	0
3310	20	26	21	6	27	0	0
3330	19	29	25	3	24	0	0
3350	20	32	24	3	20	1	0
3370	30	21	22	3	23	0	0
3390	30	22	28	2	17	0	0
3410	28	23	28	3	18	0	0
3430	27	20	29	3	20	1	0
3450	25	22	30	3	20	0	0
3470	23	23	34	4	16	0	0
3490	22	30	36	2	10	0	0
3510	23	20	35	4	18	0	0
3530	26	13	37	4	19	1	0
3550	29	15	35	4	17	0	0
3570	21	28	32	2	17	0	0
3590	19	31	30	3	17	0	0
3610	27	37	18	2	16	0	0
3630	24	40	18	2	16	0	0
3650	10	80	5	0	4	0	0
3670	3	94	1	0	2	0	0
3690	8	90	0	0	2	0	0
3710	20	23	35	2	20	0	0
3730	21	23	33	4	19	0	0
3750	22	28	30	3	17	0	0
3770	35	30	22	2	11	0	0
3790	25	30	30	2	13	0	0
3810	21	38	21	2	18	0	0
3830	18	35	31	3	13	0	0
3850	30	30	24	2	14	0	0

Continued.

Depth/m	AOM (%)	Opaques (%)	Phytoclasts (%)	Spores (%)	Pollen (%)	Gonyaulacoids (%)	Peridinoids (%)
3870	22	22	36	3	17	0	0
3890	25	25	30	3	17	0	0
3910	22	40	22	4	12	0	0
3930	25	30	25	5	15	0	0
3950	19	28	27	3	23	0	0
3970	18	30	30	3	19	0	0
3990	25	34	22	2	17	0	0
4010	20	35	25	3	17	0	0
4030	54	28	15	1	2	0	0
4230	51	33	10	2	4	0	0
4270	56	38	3	0	3	0	0
4370	55	36	4	1	4	0	0
4390	50	30	10	2	8	0	0

Appendix 6: Relative abundance (%) of POM and palynomorphs in Dzata-2A well

Depth/m	AOM (%)	Opaques (%)	Phytoclasts (%)	Spores (%)	Pollen (%)	Gonyaulacoids (%)	Peridinoids (%)
2420	70	4	10	1	2	10	3
2440	70	3	9	1	2	14	1
2460	66	4	9	0	2	15	4
2480	65	5	7	0	3	19	1
2500	66	4	8	0	3	18	1
2520	70	6	7	0	2	14	1
2540	69	5	9	0	2	12	3
2560	66	3	7	0	3	19	2
2580	68	3	5	1	3	16	5
2600	74	8	10	0	2	3	3
2620	73	10	9	0	1	5	2
2640	78	6	10	0	1	5	0
2660	72	5	19	0	1	3	0
2682	83	3	11	0	0	3	0
2700	86	3	9	0	0	2	0
2721	88	2	7	0	0	2	0
2742	86	5	6	0	1	2	0
2760	83	4	9	0	1	3	0
2781	86	4	6	0	1	2	0
2802	85	4	6	0	1	4	0
2820	78	10	8	0	1	3	0
2841	76	10	9	0	1	3	0
2862	81	9	5	0	1	3	1
2880	82	5	8	0	2	3	0
2901	89	3	5	0	3	0	0
2922	88	2	6	0	4	0	0
2943	85	4	6	0	5	0	0
2964	57	5	20	3	14	1	0
2982	59	7	14	2	18	0	0
3000	58	9	15	3	15	0	0
3021	60	7	15	2	16	0	0
3042	55	8	18	2	17	0	0
3063	58	9	19	2	11	1	0
3084	53	10	20	2	15	0	0
3105	81	5	5	1	8	0	0

Continued.

Depth/m	AOM (%)	Opaques (%)	Phytoclasts (%)	Spores (%)	Pollen (%)	Gonyaulacoids (%)	Peridinoids (%)
3126	77	6	9	1	7	0	0
3147	79	8	6	1	6	0	0
3168	40	30	20	1	9	0	0
3189	37	30	22	1	9	0	0
3210	39	37	20	0	4	0	0
3231	40	34	21	0	5	0	0
3252	34	33	26	0	7	0	0
3273	35	35	22	1	7	0	0
3294	33	28	24	4	11	0	0
3312	30	32	31	0	7	0	0
3333	46	25	23	0	6	0	0
3354	38	34	19	2	8	0	0
3375	40	30	20	1	8	1	0
3396	53	9	10	4	23	1	0
3412	56	6	9	3	26	0	0
3430	64	5	8	2	21	0	0
3450	62	7	9	1	19	1	0
3470	64	8	7	0	21	0	0
3490	63	7	8	5	17	0	0
3510	59	9	9	0	22	1	0
3530	60	8	6	2	23	1	0
3550	61	23	7	0	9	0	0
3570	65	22	8	0	5	0	0
3590	62	21	9	0	8	0	0
3610	65	22	6	0	6	0	0
3630	67	23	5	0	5	0	0
3650	32	19	22	1	26	0	0
3670	25	20	24	1	30	0	0
3690	30	16	29	0	25	0	0
3710	35	18	20	3	24	0	0
3730	29	20	23	3	25	0	0
3750	35	17	23	2	21	3	0
3770	34	19	20	0	25	2	0
3790	31	19	20	3	25	1	1
3810	30	18	27	0	24	1	0
3830	30	14	29	3	23	1	0

Continued.

Depth/m	AOM (%)	Opaques (%)	Phytoclasts (%)	Spores (%)	Pollen (%)	Gonyaulacoids (%)	Peridinoids (%)
3850	40	22	20	0	16	2	0
3870	40	20	24	2	12	1	1
3890	32	19	28	2	17	0	2
3910	35	20	30	3	12	0	0
3930	60	24	12	0	4	0	0
3950	60	28	7	0	5	0	0
3970	55	29	10	0	4	2	0
3990	65	25	7	0	2	1	0
4010	68	23	8	0	1	0	0
4050	62	21	15	0	2	0	0
4090	50	33	14	0	2	1	0
4130	50	37	12	0	1	0	0
4150	58	32	10	0	0	0	0
4297	60	30	10	0	0	0	0
4363	58	32	10	0	0	0	0
4426	60	30	10	0	0	0	0

Appendix 7: Rock-Eval pyrolysis data of rocks of the Albian-Eocene of Lynx-1X well

Age	Depth/m	%TOC	S_1(mg/g)	S_2(mg/g)	S_3(mg/g)	Tmax(◦C)	HI	OI	S_2/S_3	S_1/TOC *100	PI	S_1+S_2(mg/g)	($R_{calculated}$ %)
Early Eocene	2525	0.99	0.11	3.22	0.62	426	326	63	5.18	11.13	0.03	3.33	0.51
Early Eocene	2545	0.53	0.09	0.42	0.43	422	78	81	0.97	16.85	0.18	0.51	0.44
Early Eocene	2585	0.62	0.09	0.26	0.39	409	42	62	0.67	14.45	0.26	0.35	0.20
Paleocene	2645	0.6	0.11	0.25	0.59	418	42	99	0.43	18.3	0.3	0.36	0.36
Paleocene	2665	0.84	0.08	0.43	0.45	426	51	53	0.96	9.49	0.16	0.51	0.51
Paleocene	2685	0.9	0.13	0.41	0.44	423	46	49	0.93	14.46	0.24	0.54	0.45
Paleocene	2735	0.88	0.04	0.64	0.36	423	73	41	1.78	4.55	0.06	0.68	0.45
Maastrichtian	2755	1.63	0.08	3.82	0.39	428	234	24	9.8	4.9	0.02	3.9	0.54
Maastrichtian	2775	2.06	0.08	7.02	0.43	424	342	21	16.33	3.89	0.01	7.1	0.47
Maastrichtian	2805	1.56	0.14	3.07	0.38	431	197	24	8.11	8.97	0.04	3.21	0.60
Maastrichtian	2825	1.42	0.13	2.85	0.42	429	200	30	6.73	9.15	0.04	2.98	0.56
Maastrichtian	2845	1.71	0.16	4.91	0.52	426	286	30	9.41	9.33	0.03	5.07	0.51
Maastrichtian	2865	1.74	0.15	5.13	0.43	427	295	25	11.88	8.61	0.03	5.28	0.53
Maastrichtian	2885	2.37	0.16	9.02	0.63	423	380	27	14.31	6.74	0.02	9.18	0.45
Maastrichtian	2905	2.58	0.14	9.28	0.43	423	359	17	21.48	5.42	0.01	9.42	0.45
Maastrichtian	2925	2.25	0.14	7.68	0.41	425	341	18	18.97	6.22	0.02	7.82	0.49
Maastrichtian	2945	3.1	0.19	13	0.59	422	420	19	22.22	6.14	0.01	13.19	0.44
Maastrichtian	2965	2.3	0.18	9.88	0.4	422	429	17	24.94	7.81	0.02	10.06	0.44
Maastrichtian	2985	4.15	0.2	26.58	0.54	416	641	13	49.22	4.82	0.01	26.78	0.33
Maastrichtian	3005	2.89	0.21	18.4	0.51	418	638	18	35.86	7.28	0.01	18.61	0.36
Maastrichtian	3025	2.85	0.22	16.24	0.54	419	569	19	30.07	7.71	0.01	16.46	0.38
Maastrichtian	3045	2.06	0.17	9.77	0.47	421	474	23	20.89	8.24	0.02	9.94	0.42
Maastrichtian	3065	2	0.16	9.02	0.43	422	452	22	20.88	8.01	0.02	9.18	0.44
Maastrichtian	3085	1.83	0.15	6.84	0.49	425	373	27	14.07	8.18	0.02	6.99	0.49
Maastrichtian	3105	2.2	0.16	9.11	0.46	424	414	21	19.86	7.27	0.02	9.27	0.47
Campanian	3125	2.85	0.16	12.44	0.5	422	436	18	24.69	5.61	0.01	12.6	0.44
Campanian	3145	3.29	0.16	16.32	0.5	423	495	15	32.38	4.86	0.01	16.48	0.45
Campanian	3165	1.43	0.13	4.53	0.45	427	317	32	10.06	9.1	0.03	4.66	0.53
Campanian	3185	1.92	0.13	9.44	0.48	420	491	25	19.78	6.76	0.01	9.57	0.40
Campanian	3205	2.13	0.14	8.82	0.74	422	414	35	11.92	6.58	0.02	8.96	0.44
Campanian	3225	1.23	0.13	4.78	0.42	421	387	34	11.37	10.53	0.03	4.91	0.42
Campanian	3245	1.19	0.12	2.54	0.4	427	213	34	6.35	10.08	0.05	2.66	0.53
Campanian	3265	2.24	0.14	7.87	0.51	425	352	23	15.43	6.26	0.02	8.01	0.49
Campanian	3285	2.51	0.12	11.52	0.46	424	460	18	25.05	4.79	0.01	11.64	0.47
Campanian	3305	2.25	0.16	11.51	0.57	425	511	25	20.19	7.11	0.01	11.67	0.49

Continued.

Age	Depth/m	%TOC	S_1(mg/g)	S_2(mg/g)	S_3(mg/g)	Tmax(°C)	HI	OI	S_2/S_3	S_1/TOC *100	PI	S_1+S_2(mg/g)	($R_{calculated}$ %)
?Turonian-Santonian	3325	1.79	0.12	5.18	0.41	427	290	23	12.63	6.71	0.02	5.3	0.53
?Turonian-Santonian	3345	1.5	0.11	4.67	0.45	430	312	30	10.38	7.34	0.02	4.78	0.58
?Turonian-Santonian	3365	1.64	0.14	5.57	0.61	428	340	37	9.14	8.54	0.02	5.71	0.54
?Turonian-Santonian	3385	1.58	0.16	6.38	0.53	427	405	34	12.04	10.15	0.02	6.54	0.53
?Turonian-Santonian	3405	2.06	0.16	10.91	0.5	426	530	24	21.83	7.77	0.01	11.07	0.51
?Turonian-Santonian	3425	2.06	0.17	12.58	0.68	427	609	33	18.5	8.24	0.01	12.75	0.53
?Turonian-Santonian	3445	2.35	0.17	13.32	0.41	426	568	17	32.49	7.25	0.01	13.49	0.51
?Turonian-Santonian	3465	2.22	0.15	12.79	0.37	427	577	17	34.58	6.76	0.01	12.94	0.53
?Turonian-Santonian	3485	1.7	0.15	7.81	0.45	428	460	27	17.36	8.83	0.02	7.96	0.54
?Turonian-Santonian	3505	1.67	0.16	7.39	0.44	428	442	26	16.79	9.56	0.02	7.55	0.54
?Turonian-Santonian	3525	1.92	0.14	10.76	0.4	428	560	21	26.91	7.29	0.01	10.9	0.54
?Turonian-Santonian	3545	1.95	0.13	10.16	0.38	429	521	19	26.74	6.67	0.01	10.29	0.56
?Turonian-Santonian	3565	1.8	0.15	9.33	0.44	430	519	24	21.21	8.33	0.02	9.48	0.58
?Turonian-Santonian	3585	1.98	0.15	10.4	0.42	430	526	21	24.75	7.59	0.01	10.55	0.58
?Turonian-Santonian	3605	2.11	0.14	12.5	0.51	430	593	24	24.51	6.64	0.01	12.64	0.58
?Turonian-Santonian	3615	1.86	0.08	9.63	0.34	432	517	18	28.32	4.3	0.01	9.71	0.62
?Turonian-Santonian	3625	2.12	0.16	10.41	0.37	430	492	17	28.12	7.57	0.02	10.57	0.58
?Turonian-Santonian	3635	1.84	0.11	8.83	0.27	432	480	15	32.7	5.98	0.01	8.94	0.62
?Turonian-Santonian	3658	2.52	0.18	11.11	0.79	432	441	31	14.06	7.15	0.02	11.29	0.62
?Turonian-Santonian	3675	2.56	0.17	14.81	0.53	431	579	21	27.94	6.64	0.01	14.98	0.60
?Turonian-Santonian	3695	3.08	0.17	18.93	0.42	431	614	14	45.07	5.51	0.01	19.1	0.60
Cenomanian	3715	1.43	0.17	6.52	0.44	432	456	31	14.82	11.89	0.03	6.69	0.62
Cenomanian	3735	0.97	0.08	3.47	0.25	431	359	26	13.88	8.27	0.02	3.55	0.60
Cenomanian	3755	0.97	0.07	3.68	0.23	431	378	24	16	7.19	0.02	3.75	0.60
Cenomanian	3775	1.23	0.07	4.65	0.27	434	377	22	17.22	5.68	0.01	4.72	0.65
Cenomanian	3795	1.18	0.08	4.98	0.26	434	422	22	19.15	6.79	0.02	5.06	0.65
Cenomanian	3817.5	1.69	0.06	7.52	0.27	434	445	16	27.85	3.55	0.01	7.58	0.65
Cenomanian	3837.5	1.68	0.1	7.92	0.39	435	471	23	20.31	5.95	0.01	8.02	0.67
Cenomanian	3857.5	2.04	0.08	8.4	0.42	437	412	21	20	3.92	0.01	8.48	0.71
Cenomanian	3877.5	1.75	0.09	5.25	0.49	437	300	28	10.71	5.14	0.02	5.34	0.71
Cenomanian	3897.5	1.24	0.07	2.33	0.19	440	188	15	12.26	5.65	0.03	2.4	0.76
Cenomanian	3917.5	0.87	0.05	1.32	0.28	438	151	32	4.71	5.72	0.04	1.37	0.72
Cenomanian	3937	0.91	0.01	1.36	0.18	445	149	20	7.56	1.09	0.01	1.37	0.85
Cenomanian	3977.5	0.51	0.12	0.25	0.25	425	49	49	1	23.53	0.32	0.37	0.49
Cenomanian	3997.5	0.54	0.06	0.47	0.18	437	87	33	2.61	11.05	0.11	0.53	0.71
Cenomanian	4017.5	0.86	0.1	1.31	0.17	440	153	20	7.71	11.66	0.07	1.41	0.76
Cenomanian	4037.5	0.75	0.07	0.81	0.3	438	107	40	2.7	9.28	0.08	0.88	0.72
Cenomanian	4057.5	0.54	0.06	0.92	0.23	438	171	43	4	11.15	0.06	0.98	0.72
Cenomanian	4077.5	0.52	0.07	0.37	0.46	430	71	88	0.8	13.44	0.16	0.44	0.58
Cenomanian	4098	1.1	0.73	2.57	0.11	445	233	10	23.36	66.24	0.22	3.3	0.85

Continued.

Age	Depth/m	%TOC	S_1(mg/g)	S_2(mg/g)	S_3(mg/g)	Tmax(◦C)	HI	OI	S_2/S_3	S_1/TOC *100	PI	S_1+S_2(mg/g)	($R_{calculated}$ %)
Cenomanian	4157.5	0.73	0.1	0.46	0.21	423	63	29	2.19	13.66	0.18	0.56	0.45
Cenomanian	4177.5	0.99	0.05	0.2	0.78	430	20	78	0.26	5.03	0.2	0.25	0.58
Cenomanian	4217.5	0.86	0.05	0.76	0.19	443	88	22	4	5.82	0.06	0.81	0.81
Cenomanian	4237.5	1.11	0.07	1.71	0.5	443	154	45	3.42	6.3	0.04	1.78	0.81
Cenomanian	4257	1.99	3.22	5.02	0.21	446	252	11	23.9	161.73	0.39	8.24	0.87
Cenomanian	4277.5	1.24	0.09	0.68	0.33	433	55	27	2.06	7.26	0.12	0.77	0.63
Cenomanian	4296	2.71	7.98	7.25	0.25	449	268	9	29	294.9	0.52	15.23	0.92
Cenomanian	4317.5	0.8	0.1	1.31	0.49	444	163	61	2.67	12.44	0.07	1.41	0.83
Cenomanian	4332.5	0.69	0.04	0.68	0.35	452	99	51	1.94	5.8	0.06	0.72	0.98
Cenomanian	4377.5	1.06	0.07	0.73	0.52	452	69	49	1.4	6.58	0.09	0.8	0.98
Cenomanian	4397.5	0.94	0.07	0.63	0.47	456	67	50	1.34	7.47	0.1	0.7	1.05
Cenomanian	4417.5	0.67	0.08	0.57	0.44	456	85	66	1.3	11.99	0.12	0.65	1.05
Cenomanian	4437.5	0.82	0.07	0.69	0.36	458	84	44	1.92	8.56	0.09	0.76	1.08
Cenomanian	4457.5	1.76	0.07	1.68	0.4	456	95	23	4.2	3.97	0.04	1.75	1.05
Cenomanian	4477.5	1.57	0.07	1.59	0.43	456	101	27	3.7	4.46	0.04	1.66	1.05
Cenomanian	4517.5	6.48	0.11	8.68	0.6	461	134	9	14.47	1.7	0.01	8.79	1.14
Albian	4537.5	0.72	0.08	0.96	0.56	454	134	78	1.71	11.17	0.08	1.04	1.01
Albian	4597.5	0.89	0.06	0.84	0.37	459	94	41	2.27	6.72	0.07	0.9	1.10
Albian	4612.5	0.81	0.02	0.53	0.08	461	66	10	6.31	2.47	0.04	0.55	1.14
Albian	4637.5	0.5	0.06	0.48	0.29	451	97	58	1.66	12.07	0.11	0.54	0.96
Albian	4657.5	0.52	0.19	0.52	0.29	455	100	56	1.79	36.61	0.27	0.71	1.03
Albian	4717.5	0.66	0.04	0.32	0.29	476	48	44	1.1	6.06	0.11	0.36	1.41
Albian	4737.5	0.85	0.17	0.67	0.49	465	79	58	1.37	20.09	0.2	0.84	1.21
Albian	4757.5	0.8	0.14	0.68	0.48	455	85	60	1.42	17.54	0.17	0.82	1.03
Albian	4777.5	1.13	0.24	1.25	0.45	453	111	40	2.78	21.33	0.16	1.49	0.99
Albian	4797.5	0.71	0.17	0.52	0.48	446	73	67	1.08	23.81	0.25	0.69	0.87
Albian	4817.5	0.53	0.16	0.45	0.4	447	85	76	1.13	30.3	0.26	0.61	0.89
Albian	4837.5	0.83	0.13	0.51	0.49	453	62	59	1.04	15.76	0.2	0.64	0.99
Albian	4862.5	0.55	0.04	0.31	0.39	442	57	71	0.79	7.31	0.11	0.35	0.80
Albian	4902.5	0.74	0.06	0.39	0.49	458	53	66	0.8	8.13	0.13	0.45	1.08
Albian	4922.5	0.58	0.06	0.56	0.36	431	96	62	1.56	10.27	0.1	0.62	0.60
Albian	4932.5	0.66	0.05	0.41	0.37	444	62	56	1.11	7.61	0.11	0.46	0.83
Albian	4955	0.49	0.01	0.24	0.11	426	49	23	2.18	2.05	0.04	0.25	0.51
Albian	4997.5	0.65	0.04	0.32	0.25	424	50	39	1.28	6.19	0.11	0.36	0.47
Albian	5067.5	0.67	0.05	0.39	0.37	430	58	55	1.05	7.47	0.11	0.44	0.58
Albian	5077.5	0.6	0.04	0.35	0.28	417	58	47	1.25	6.68	0.1	0.39	0.35

Continued.

Age	Depth/ m	%TOC	S_1(mg/g)	S_2(mg/g)	S_3(mg/g)	Tmax(◦C)	HI	OI	S_2/S_3	S_1/TOC *100	PI	S_1+S_2(mg/g)	($R_{calculated}$ %)
Albian	5097.5	0.62	0.04	0.31	0.25	428	50	40	1.24	6.47	0.11	0.35	0.54
Albian	5137.5	0.62	0.04	0.21	0.31	424	34	50	0.68	6.44	0.16	0.25	0.47
Albian	5157.5	0.73	0.04	0.27	0.25	417	37	34	1.08	5.51	0.13	0.31	0.35
Albian	5207.5	0.51	0.06	0.72	0.49	437	140	96	1.47	11.7	0.08	0.78	0.71
Albian	5227.5	0.64	0.04	0.39	0.36	428	61	56	1.08	6.24	0.09	0.43	0.54
Albian	5237.5	0.57	0.05	0.42	0.34	430	74	60	1.24	8.83	0.11	0.47	0.58
Albian	5277.5	0.83	0.05	0.43	0.45	429	52	54	0.96	6.02	0.1	0.48	0.56
Albian	5297.5	0.99	0.08	0.49	0.57	426	50	58	0.86	8.09	0.14	0.57	0.51

Appendix 8: Rock-Eval pyrolysis data of rocks of the Albian-Maastrichtian of Dzata-2A well

Age	Depth/m	%TOC	S_1(mg/g)	S_2(mg/g)	S_3(mg/g)	Tmax (°C)	HI	OI	S_2/S_3	S_1/TOC*100	PI	S_1+S_2(mg/g)	$R_{calculated}$
Maastrichtian	2418-2420	6.1	0.29	27.37	2.4	419	449	39	11.4	5	0.01	27.66	0.38
Maastrichtian	2430-2440	3.62	0.23	12.04	1.56	426	333	43	7.7	6	0.02	12.27	0.51
Maastrichtian	2450-2460	1.96	0.14	4.13	0.66	427	211	34	6.3	7	0.03	4.27	0.53
Maastrichtian	2470-2480	1.67	0.13	4.53	0.44	423	271	26	10.3	8	0.03	4.66	0.45
Maastrichtian	2500-2510	2.37	0.12	5.22	0.51	423	220	21	10.2	5	0.02	5.34	0.45
Maastrichtian	2520-2530	2.88	0.12	7.74	0.65	423	269	23	11.9	4	0.02	7.86	0.45
Maastrichtian	2540-2550	2.45	0.13	5.32	0.81	424	217	33	6.6	5	0.02	5.45	0.47
Maastrichtian	2560-2570	2.91	0.13	8.62	0.44	421	296	15	19.6	4	0.01	8.75	0.42
Maastrichtian	2580-2590	2.3	0.12	5.98	0.82	424	260	36	7.3	5	0.02	6.1	0.47
Maastrichtian	2600-2610	2.19	0.11	4.87	0.48	422	222	22	10.1	5	0.02	4.98	0.44
Maastrichtian	2620-2630	2.14	0.1	4.79	0.73	427	224	34	6.6	5	0.02	4.89	0.53
Campanian	2630-2640	1.77	0.12	3.33	0.4	423	188	23	8.3	7	0.03	3.45	0.45
Campanian	2650-2660	2.27	0.13	5.07	0.89	419	223	39	5.7	6	0.02	5.2	0.38
Campanian	2673-2676	4.27	0.15	22.27	1.26	416	521	29	17.7	4	0.01	22.42	0.33
Campanian	2682-2685	3.11	0.11	12.42	0.95	418	399	31	13.1	4	0.01	12.53	0.36
Campanian	2700-2703	2.78	0.1	8.42	0.7	420	302	25	12	4	0.01	8.52	0.40
Campanian	2721-2724	2.73	0.09	10.07	0.67	414	368	25	15	3	0.01	10.16	0.29
Campanian	2742-2745	2.34	0.09	8.29	0.72	417	354	31	11.5	4	0.01	8.38	0.35
Campanian	2760-2763	2.94	0.13	9.23	0.78	420	314	27	11.8	4	0.01	9.36	0.40
Campanian	2781-2784	2.77	0.09	10.87	0.54	418	392	19	20.1	3	0.01	10.96	0.36
?Turonian-Santonian	2799-2802	1.97	0.09	7.94	0.41	421	403	21	19.4	5	0.01	8.03	0.42
?Turonian-Santonian	2820-2823	2.35	0.1	9.64	0.45	421	410	19	21.4	4	0.01	9.74	0.42
?Turonian-Santonian	2838-2841	2.29	0.09	8.16	0.53	421	357	23	15.4	4	0.01	8.25	0.42
?Turonian-Santonian	2862-2865	2.56	0.08	9.94	0.41	419	388	16	24.2	3	0.01	10.02	0.38
?Turonian-Santonian	2880-2883	2.59	0.08	10.62	0.43	417	410	17	24.7	3	0.01	10.7	0.35
?Turonian-Santonian	2901-2904	2.83	0.09	14.72	0.41	417	520	14	35.9	3	0.01	14.81	0.35
?Turonian-Santonian	2919-2922	4.02	0.18	21.28	0.72	417	530	18	29.6	4	0.01	21.46	0.35
Cenomanian	2940-2943	1.75	0.14	4.48	0.45	421	256	26	10	8	0.03	4.62	0.42
Cenomanian	2961-2964	1.47	0.14	1.54	0.52	424	105	35	3	10	0.08	1.68	0.47
Cenomanian	2979-2982	1.16	0.15	1.39	0.47	426	119	40	3	13	0.1	1.54	0.51
Cenomanian	3000-3003	1.2	0.14	1.21	0.45	427	101	37	2.7	12	0.1	1.35	0.53
Cenomanian	3021-3024	1.36	0.15	1.45	0.51	425	107	38	2.8	11	0.09	1.6	0.49
Cenomanian	3042-3045	1.67	0.18	2.08	0.49	426	124	29	4.2	11	0.08	2.26	0.51
Cenomanian	3066-3069	1.58	0.22	2.25	0.57	425	142	36	3.9	14	0.09	2.47	0.49
Cenomanian	3081-3084	1.44	0.22	1.5	0.55	425	104	38	2.7	15	0.13	1.72	0.49
Cenomanian	3105-3108	1.32	0.17	1.49	0.36	425	113	27	4.1	13	0.1	1.66	0.49
Cenomanian	3123-3126	1.41	0.15	1.4	0.47	426	99	33	3	11	0.1	1.55	0.51

Continued.

Age	Depth/m	%TOC	S_1(mg/g)	S_2(mg/g)	S_3(mg/g)	Tmax (°C)	HI	OI	S_2/S_3	S_1/TOC*100	PI	S_1+S_2(mg/g)	$R_{calculated}$
Cenomanian	3147-3150	1.56	0.13	1.18	0.5	427	76	32	2.4	8	0.1	1.31	0.53
Cenomanian	3165-3168	1.4	0.15	0.86	0.47	428	61	33	1.8	11	0.15	1.01	0.54
Cenomanian	3189-3192	0.87	0.15	0.5	0.59	425	58	68	0.8	17	0.23	0.65	0.49
Cenomanian	3210-3213	0.66	0.08	0.39	0.46	430	59	70	0.8	12	0.17	0.47	0.58
Cenomanian	3231-3234	0.51	0.08	0.24	0.47	433	47	92	0.5	16	0.25	0.32	0.63
Cenomanian	3252-3255	0.68	0.08	0.31	0.8	428	46	118	0.4	12	0.21	0.39	0.54
Cenomanian	3273-3276	0.55	0.07	0.29	0.37	425	53	68	0.8	13	0.19	0.36	0.49
Cenomanian	3294-3297	0.81	0.08	0.48	0.62	434	59	77	0.8	10	0.14	0.56	0.65
Cenomanian	3312-3315	1	0.07	0.65	0.47	432	65	47	1.4	7	0.1	0.72	0.62
Cenomanian	3333-3336	1.35	0.08	0.96	0.55	433	71	41	1.7	6	0.08	1.04	0.63
Cenomanian	3351-3354	1.23	0.07	1.03	0.5	428	84	41	2.1	6	0.06	1.1	0.54
Albian	3375-3378	1.04	0.09	0.86	0.69	431	83	66	1.2	9	0.09	0.95	0.60
Albian	3396-3399	1.21	0.08	1.36	0.44	434	112	36	3.1	7	0.06	1.44	0.65
Albian	3412-3420	1.46	0.08	1.41	0.65	434	96	44	2.2	5	0.05	1.49	0.65
Albian	3430-3440	1.2	0.1	1.01	0.47	429	84	39	2.1	8	0.09	1.11	0.56
Albian	3450-3460	1.71	0.09	1.41	0.61	433	82	36	2.3	5	0.06	1.5	0.63
Albian	3470-3480	1.74	0.08	1.67	0.57	431	96	33	2.9	5	0.05	1.75	0.60
Albian	3490-3500	1.86	0.09	2.24	0.56	432	120	30	4	5	0.04	2.33	0.62
Albian	3510-3520	1.64	0.09	1.39	0.53	432	85	32	2.6	5	0.06	1.48	0.62
Albian	3530-3540	0.83	0.06	0.54	0.73	434	65	88	0.7	7	0.1	0.6	0.65
Albian	3550-3560	1.42	0.07	1.15	0.43	433	81	30	2.7	5	0.06	1.22	0.63
Albian	3570-3580	1.2	0.08	0.52	0.65	436	43	54	0.8	7	0.13	0.6	0.69
Albian	3590-3600	1.07	0.06	0.8	0.56	438	75	52	1.4	6	0.07	0.86	0.72
Albian	3610-3620	0.97	0.07	0.67	0.53	434	69	55	1.3	7	0.09	0.74	0.65
Albian	3630-3640	0.93	0.07	0.52	0.52	434	56	56	1	8	0.12	0.59	0.65
Albian	3650-3660	0.96	0.07	0.74	0.47	434	77	49	1.6	7	0.09	0.81	0.65
Albian	3670-3680	1.14	0.07	0.95	0.5	436	84	44	1.9	6	0.07	1.02	0.69
Albian	3690-3700	1.08	0.06	0.84	0.45	438	78	42	1.9	6	0.07	0.9	0.72
Albian	3710-3720	1.42	0.08	1.52	0.55	437	107	39	2.8	6	0.05	1.6	0.71
Albian	3730-3740	1.45	0.08	1.32	0.49	436	91	34	2.7	6	0.06	1.4	0.69
Albian	3750-3760	1.22	0.08	1.28	0.51	436	105	42	2.5	7	0.06	1.36	0.69
Albian	3770-3780	1.64	0.09	1.93	0.45	437	118	27	4.3	5	0.04	2.02	0.71
Albian	3790-3800	1.6	0.09	1.64	0.47	437	102	29	3.5	6	0.05	1.73	0.71
Albian	3810-3820	1.23	0.08	0.82	0.46	434	67	37	1.8	7	0.09	0.9	0.65
Albian	3830-3840	1.31	0.09	0.91	0.45	435	69	34	2	7	0.09	1	0.67
Albian	3850-3860	0.9	0.07	0.72	0.56	435	80	62	1.3	8	0.09	0.79	0.67
Albian	3870-3880	0.97	0.07	0.6	0.58	440	62	60	1	7	0.1	0.67	0.76
Albian	3890-3900	0.88	0.07	0.57	0.59	439	65	67	1	8	0.11	0.64	0.74
Albian	3910-3920	1.36	0.07	1.14	0.53	442	84	39	2.2	5	0.06	1.21	0.80
Albian	3930-3940	1.19	0.08	1.13	0.53	443	95	44	2.1	7	0.07	1.21	0.81
Albian	3950-3960	1.1	0.07	0.78	0.51	442	71	47	1.5	6	0.08	0.85	0.80
Albian	3970-3980	1.23	0.07	1	0.45	440	81	37	2.2	6	0.07	1.07	0.76

Continued.

Age	Depth/m	%TOC	S_1(mg/g)	S_2(mg/g)	S_3(mg/g)	Tmax (°C)	HI	OI	S_2/S_3	S_1/TOC*100	PI	S_1+S_2(mg/g)	$R_{calculated}$
Albian	3990-4000	1.61	0.07	1.04	0.48	440	65	30	2.2	4	0.06	1.11	0.76
Albian	4010-4020	1.38	0.07	1.14	0.47	440	83	34	2.4	5	0.06	1.21	0.76
Albian	4030-4040	1.45	0.07	0.89	0.45	439	62	31	2	5	0.07	0.96	0.74
Albian	4050-4060	0.73	0.06	0.34	0.51	446	47	70	0.7	8	0.15	0.4	0.87
Albian	4070-4080	1.33	0.08	0.63	0.61	446	47	46	1	6	0.11	0.71	0.87
Albian	4090-4100	0.98	0.08	0.86	0.42	440	88	43	2	8	0.09	0.94	0.76
Albian	4110-4120	1.22	0.08	0.96	0.4	444	79	33	2.4	7	0.08	1.04	0.83
Albian	4130-4140	1.18	0.07	0.67	0.27	449	57	23	2.5	6	0.09	0.74	0.92
Albian	4150-4160	1.17	0.09	0.67	0.28	449	58	24	2.4	8	0.12	0.76	0.92
Albian	4170-4180	1.19	0.07	0.75	0.28	444	63	24	2.7	6	0.09	0.82	0.83
Albian	4192-4195	1.21	0.08	0.62	0.27	443	51	22	2.3	7	0.11	0.7	0.81
Albian	4213-4216	1.74	0.11	1.02	0.32	442	59	18	3.2	6	0.1	1.13	0.80
Albian	4234-4237	0.79	0.06	0.27	0.29	434	34	37	0.9	8	0.18	0.33	0.65
Albian	4255-4258	0.69	0.06	0.25	0.34	440	36	49	0.7	9	0.19	0.31	0.76
Albian	4276-4279	0.59	0.05	0.21	0.31	441	35	52	0.7	8	0.19	0.26	0.78
Albian	4297-4300	1.28	0.06	0.44	0.4	448	34	31	1.1	5	0.12	0.5	0.90
Albian	4321-4324	0.58	0.05	0.25	0.32	442	43	55	0.8	9	0.17	0.3	0.80
Albian	4342-4345	1.03	0.06	0.37	0.55	443	36	54	0.7	6	0.14	0.43	0.81
Albian	4363-4366	1.54	0.07	0.55	0.69	435	36	45	0.8	5	0.11	0.62	0.67
Albian	4384-4387	1.54	0.08	0.56	0.66	441	36	43	0.8	5	0.13	0.64	0.78
Albian	4423-4426	1.56	0.08	0.53	0.57	442	34	37	0.9	5	0.13	0.61	0.80
Albian	4447-4450	0.82	0.07	0.35	0.59	436	43	72	0.6	9	0.17	0.42	0.69